AN EVALUATION OF LIBERATION MODELS FOR THE PREDICTION OF DIAGNOSTIC LEACHING RESULTS

GIDEON JOHANNES ANNANDALE

A thesis submitted in partial fulfilment of the requirements
for the degree of
Master
in Engineering

at the University of Stellenbosch

Supervisors: Prof. L. Lorenzen
Prof. J.S.J. van Deventer

STELLENBOSCH

APRIL 1995

" And science, we should insist, better than any other discipline, can hold up to its students and followers an ideal of patient devotion to the search for objective truth, with vision unclouded by personal or political motive, not tolerating any lapse from precision or neglect of any anomaly, fearing only prejudice and preconception, accepting nature's answers humbly and with courage, and giving them to the world with unflinching fidelity. The world cannot afford to lose such a contribution to the moral framework of its civilisation."

- Sir Henry Dale

DECLARATION

I hereby certify that this thesis is my own original work, except where specifically acknowledged in the text. Neither the present dissertation nor any part thereof, has previously been submitted for a degree to any other University.

G.J. ANNANDALE
20 April 1995

ACKNOWLEDGEMENTS

The work described in this thesis was carried out in the Department of Chemical Engineering at the University of Stellenbosch.

I wish to express my sincere appreciation to:

- God who grants wisdom to anyone who asks in faith. James 1:5

- Prof. L. Lorenzen and Prof J.S.J. van Deventer for their supervision, assistance and financial support (by arranging the necessary funds), throughout the length of the project.

- Dr. C. Aldrich for his contribution and supervision in the analysis of the data by neural networks.

- To Gencor for their sponsorship of the project.

- The technical personnel of the Department of Chemical Engineering for their varied and valuable contributions, in particular Mr Vincent Carolissen, Mr Charles Atkins, Mr James Olin, Mr Aubrey Atkins, Mr Leander Brand, Mr Jannie Barnard and Mrs Leonie Strydom.

- Retief de Villiers for his assistance in performing analysis on the AA

- Personnel at the various GENCOR mines, St. Helena, Beatrix, Leslie, Kinross and Barberton, for their support in taking and delivering of the different ore samples.

- My parents and Mia for their long distance support.

SYNOPSIS

The interrelationship between mineral liberation and leaching behaviour of a gold ore is ill defined and lacks understanding, mainly due to the complexity of the individually processes, i.e. leaching and mineral liberation. An understanding of this relationship could result in lower costs, since an increase in the efficiency of gold dissolution and a decrease in costs related to the crushing and grinding operations, could be expected.

Diagnostic leaching was used as the analytical method to investigate the mineralogy (gold deportment) of various gold-bearing ores designating from different goldfields in South Africa. A thorough literature survey was also conducted to determine the availibility of theoretical models which could describe the relationship between liberation and leaching behaviour.

From the experimental results obtained, it was concluded that the leachability of an ore is not only dependent on the degree of liberation of that ore when comminuted, but that it is also very much dependent on the degree of exposure of gold grains throughout the whole of the ore. It was found that all the theoretical liberation and exposure models underestimated the amount of leachable gold in each particle size fraction, mainly due to the neglecting of exposed gold grains situated in minor cracks and fractures.

It became evident in this research, that in order to model the leachability of gold fundamentally, the data obtained from diagnostic leaching tests alone are insufficient. Data concerning the amounts of gold bearing minerals, present in the ores as well as SEM data of the gold grains, are needed together with diagnostic leaching results.

However, an empirical model was developed that predicts the degree of liberation (leachability) of an ore milled to 70% -75µm fairly accurately as a first attempt to model this highly complex process. The degree of liberation (leachability) was found to be a function of the particle size and the gold deportment of the unmilled ore. It was decided to extend the King liberation model and the exposure model developed by Hsih and co-workers empirically to provide for the fraction of gold not directly related to liberation. Both the models showed good agreements with the experimental results. Neural network analysis of the diagnostic leaching results were done with partial success, but unfortunately more data is still needed to assist in the development of an accurate leaching or liberation model.

OPSOMMING

Weens die komplekse aard van die mineraalvrystelling- en logings prosesse, word die verwantskap tussen mineraal vrystelling en die logingsgedrag van 'n goud erts nie goed verstaan nie. Aangesien hoë kostes verbonde is aan die vergruising- en die maalproses van die ertse, is dit belangrik om hierdie verwantskap goed te verstaan . Dit kan ook tot gevolg hê dat die effektiwiteit waarmee die goud opgelos word,.verhoog word, wat op sy beurt tot laer kostes sal lei.

Die analitiese metode, diagnostiese loging, is gebruik om die mineralogie (goud verspreiding relatief tot die verskillende minerale, in die erts) van ertse uit verskeie Suid-Afrikaanse goudvelde te bepaal. 'n Deeglike literatuurstudie het die verskillende teoretiese mineraal vrystellings modelle getoon, wat vrystelling met logingsgedrag in verband probeer bring.

Die eksperimentele resultate het getoon dat die loogbaarheid van 'n erts nie slegs afhanklik is van die graad van vrystelling nie, maar ook van die mate waartoe die goudkorrels aan die logingsvloeistof blootgestel is. Daar is tot die gevolgtrekking gekom dat al die teoretiese mineraal vrystellingsmodelle, die hoeveelheid goud in elke partikelgrootte fraksie totaal en al onderskat. Dit kan hoofsaaklik toegeskryf word aan die hoeveelheid goud wat barste en krake in die erts vul, wat nie so seer vrygestel is nie, maar wel loogbaar is.

Dit blyk duidelik uit die navorsing, dat die diagnostiese logingsdata alleen, onvoldoende is om die loogbaarheid van goud fundamenteel te modelleer. Data in verband met die hoeveelheid van elke mineraal wat in die erts teenwoordig is asook SEM data van die goudkorrels in die verskillende minerale, word ook sodanig benodig.

Desnieteenstaande, is daar as 'n eerste probeerslag, 'n empiriese model voorgestel wat die loogbaarheid van 'n gemaalde erts (gemaal tot 70% -75 µm) redelik goed voorspel. Die graad waartoe die goud loogbaar is (mineraal-vrystelling), is 'n funksie van die partikelgrootte en die goudverdeling in die ongemaalde erts. Twee teoretiese modelle, nl die King vrystellingsmodel en die Hsih en ander-model is ook empiries aangepas om sekere tekortkominge te oorbrug. Die modelle hot goed met die eksperimentele waardes ooreengestem. Analises van die diagnostiese logings resultate is met behulp van neurale netwerke gedoen. Alhoewel dit gedeeltelik suksesvol was, word heelwat meer data benodig om die loogbaarheid van goud akkuraat te voorspel.

TABLE OF CONTENTS

APPENDICES

LIST OF FIGURES

FIGURES

FIGURES PAGE

CHAPTER 6

FIGURES PAGE

CHAPTER 7

FIGURES PAGE

CHAPTER 8

FIGURES PAGE

FIGURES

PAGE

LIST OF TABLES

TABLES **PAGE**

TABLES

PAGE

CHAPTER 5

TABLES PAGE

CHAPTER 6

TABLES **PAGE**

CHAPTER 7

TABLES

PAGE

CHAPTER 8

TABLES

PAGE

APPENDIX B

TABLES **PAGE**

TABLES

PAGE

CHAPTER 1

INTRODUCTION

CHAPTER 1

INTRODUCTION

Grinding and milling operations are used to liberate minerals prior to further upgrading by subsequent ore-dressing operations. The degree to which the minerals are liberated has a definite effect on the efficiency of the concentrating procedure. A concentrate of sufficiently high grade is normally required in the feed to finishing operations. The choice of fineness of grind is an important decision, not only due to the need for a concentrate of adequately high grade, but also due to the high costs of the grinding operations.

A model that can be used for the quantitative estimation of mineral liberation or the leachability of an ore, as a function of fineness of grind and the mineralogical texture of the ore will be of great practical use such as in the design and simulation of plants when combined with other quantitative models for concentrating operations, for example models describing operations such as flotation.

An accurate liberation (leaching) model would also be of a great help to the plant metallurgist whenever the question of "How fine must the ore be ground to liberate the gold?" or "Is it economically viable to grind the ore to such an extent, for example does an ore milled to 70% -100µm yields the same liberation as an ore milled to 70% -75µm?", arises. A proper liberation (leaching) model is thus required to answer these questions in an expeditious and accurate fashion.

The first attempt to develop a liberation model came from Gaudin in 1939. This, however, was a highly simplified model with no significant use for quantitative predictions. Wiegel developed this model to a greater extent but unfortunately the predictions deviate considerably from reality (Klimpel and Austin, 1983). This was also the tendency of other approaches such as those of Andrews and Mika and Wiegel (Meloy and Gotoh, 1985).

King (1979) however, has taken a different approach by measuring the intercept lengths of an occluded mineral in a line traversing a polished section of the ore. This was the first realistic liberation model which gave reasonable predictions. Finch and Petruk (1984) proposed different distribution functions for the model developed by King and thus broaden its general applicability.

Meloy and Gotoh (1985) used a similar approach as King (1979) by considering line intercepts to derive an equation for a multi-component ore. Klimpel and Austin (1983) developed a simple model of liberation and by assuming a random fracture mechanism, simulations were conducted by using the Monte Carlo technique. They simplified this model at a later stage to provide an analytical solution.

Barbery (1991) proposed a model which considers liberation in space dimensionality of 1,2 and 3. The degree of liberation is a function of the particle size, and of the particle size at which the degree of liberation is 50%. Gaudin's model was recently extended by Hsih and Wen (1994) by incorporating a detachment factor in addition to the mineral grain size distribution.

Lorenzen (1992a) used leaching experimental results with the liberation model of King to predict the liberation of gold from complex ores. Diagnostic leaches were conducted on various complex ores, thus explaining the deportment of gold in various minerals in these ores. The free or leachable gold in an ore obtained from such an experiment would be similar to the gold liberated by crushing and/ or milling.

Lorenzen modified King's model by adding a term to the equation because no provision was made for the amount of leachable gold in the various particle size fractions that is not related to the liberation of gold due to comminution. Lorenzen concluded that the model gives reasonable predictions and that the model is only a preliminary one which still needs some refinement. However, there are currently no models available for the accurate prediction of leachable gold as a function of particle size.

The greatest drawback of all the liberation models until now is that it is very tedious to obtain the parameters of the models, such as intercept lengths, the particle size at which the liberation is 50%, the diameter of the gold particles, etc. in order to predict the liberation of the valuable mineral (gold). Lorenzen with his new approach conducted an easy and swift way to determine the mineralogy of a gold ore, by using the diagnostic leaching procedure.

The main objectives of this thesis is thus:

- To compare the available liberation models to determine which model(s) could be extended in order to predict leachable gold as a function of particle size;
- The development of a model which predicts the leachable (liberated) gold in the milled ore by using the leachable (liberated) gold or gold deportment of the specific unmilled ore;
- Usage of neural network methods to model the liberation or leachability of gold from various South African gold ores;
- To furnish a more accurate model for the design and simulation of plants;
- To assist the metallurgist in the effective operation of a gold plant;
- An improved understanding of the interrelationship between liberation and leaching behaviour to set a framework for future work.

CHAPTER 2

LITERATURE SURVEY AND THEORETICAL CONSIDERATIONS

CHAPTER 2

LITERATURE SURVEY AND THEORETICAL CONSIDERATIONS

In section 2.1 the historical background of gold recovery in South Africa is discussed. The mineralogy, especially the deportment of gold in the various minerals, of the principal goldfields in South Africa are under discussion in section 2.2. In section 2.3, 2.4 and 2.5 mineral liberation, leaching and diagnostic leaching are defined, respectively. Mineral liberation models since Gaudin (1939) until now, are the subject of section 2.6. In section 2.7 the models which predict leachable gold related to particle size, are discussed.

2.1 HISTORICAL BACKGROUND OF GOLD RECOVERY IN SOUTH AFRICA

The earliest reference to gold in South Africa dates back to 1806 and came from John Barrow, Secretary to the Governor of the Cape. He reported a gold locality roughly between the Witwatersrand and the Magaliesberg. Reports of gold findings came with sporadic intervals over the next century from different people designated at various locations (G.G. Stanley, 1987), such as;

1836 - Soutpansberg - J.G.S. Bronkhorst (gold mining by native population)

1850 - Prince Albert district - local farmers (gold nuggets in Gamka River)

1868 - Olifants River (Transvaal) - Carl Mauch

1868 - Murchison Range - Button and Sutherland

1872 - Sabie-Pelgrim's Rest Area (alluvial gold)

1874 - Blaauwbank area (near Magaliesberg) - Henry Lewis (alluvial gold)

1875 - Kaapsehoop (near Barberton) (alluvial gold)

1877 - Streams traversing the Barberton Mountain Land

1881 - Kromdraai (the first gold in quartz veins)

1883 - Sheba Valley (vein gold)

1884 - Confidence Reef west of Johannesburg - Struben (vein gold)

The first organised gold mining in South Africa began on the farm Eersteling, south of Pietersburg. The mine was opened in 1871 by Button and Goodwin, which exploited the gold from a quartz lode.

However, the first payable discovery in an exposed conglomerate was made by George Harrison in February 1886. He was the first to report officially the presence of gold in a reef, known at present as the Main Reef. Prospecting and then mining spread rapidly eastwards and westwards along the outcrops of the Witwatersrand sediments.

In March 1939, six years after the drilling of the first prospecting borehole in the Orange Free State, the Basal Reef, which is the major contributor of gold and uranium in the Orange Free State Goldfield, was intersected and led to the foundation of the St. Helena Gold mine.

The broad outline of the main basin had been established by 1952 and the subsidiary basin at the north-eastern extent by the mid-fifties on which the Evander goldfield is located. The Leslie and Kinross goldmines, located on the Evander goldfield, were opened on 1962 and 1968 respectively.

As a result of continuous exploration in the Free State, the Unisel and Beatrix Gold mines originated in 1979 and 1983 respectively. The Harmony and Free State Geduld mine, also positioned on the Orange Free State Goldfields, have been in operation since the midfifties. The Hartebeesfontein mine (Harties), which is part of the Klerksdorp goldfield, started production in July 1955.

The gold and uranium bearing [illegible] Witwatersrand, which occupies roughly an oval area of app[illegible]420 00 km² in the Transvaal and Orange Free State, has becom[illegible] known and largest contributor of gold in the world. During the period 1884 to 1985 a total of 40 000 tons of fine gold was produced in South Africa (G.G. Stanley, 1987).

2.2 MINERALOGY OF THE PRINCIPAL GOLDFIELDS IN SOUTH AFRICA

2.2.1 Gold in the Witwatersrand Triad

The geology of the Witwatersrand depository (West, Central and East Rand; West Wits Line (Carletonville); Klerksdorp; Evander and Orange Free State Gold Fields) is well documented in many books and papers and therefore only a broad outline is given below.

Gold occurs throughout the Witwatersrand in placers, which range from coarse conglomerates in the more proximal depositional zones to coarse arsenites in the more distal zones. However, conglomerates which are greyish metamorphosed sedimentary rocks, predominate in the Witwatersrand depository.

The conglomerates are greyish metamorphosed sedimentary rocks which consist mainly of vein quartz pebbles. It is sometimes accompanied by pebbles of other minerals such as quartzite, chert and red jasper. These pebbles are cemented by a fine-grained matrix consisting mainly of recrystallized quartz, accompanied by phyllosilicates (mixture of muscovite and chlorite), pyrite and other sulphides such as pyrrhotite, pentlandite, galena, etc.

Liebenberg (G.G. Stanley, 1987) showed that gold and uranium bearing conglomerates consists essentially of the following minerals (percentages by mass):

(a) quartz, primary as well as secondary (70 to 90%)

(b) muscovite, with variable amounts of chlorite, pyrophyllite and chloritiod (10 to 30%)

(c) pyrite (3 to 4%)

(d) other sulphides such as pyrrhotite, chalcopyrite, arsenopyrite, galena, sphalerite, cobaltite, gersdorffite and pentlandite (1 to 2%).

(e) grains of primary minerals such as uraninite, leuxocene, rutile, etc. (1 to 2%)

(f) uraniferous kerogen (1%)

From microscopic examinations of the conglomerates, it was found that most of the gold are confined to the matrix and occur as hackly grains exhibiting serrated outlines and as filamentous gold occupying fissures

and minute cracks in the different minerals of the groundmass. Gold sometimes occupies interstitial spaces between the minerals of the matrix where it welds these minerals together. This phenomenon occurs however as irregular patches in the matrix. The gold particles are extremely variable in shape with the most being of an irregular or jagged form.

Hallbauer (G.G. Stanley, 1987) differentiated five major types of gold in the Witwatersrand deposits, namely:

(a) Detrital gold as inclusions of sphalerite, linneite, gersdorffite, cobaltite and chalcopyrite

(b) Biochemically redistributed gold, intimately intergrown with carbonaceous material.

(c) Gold recrystallized or redistributed by metamorphic processes within the reef such as crack filling in various minerals

(d) Primary gold in detrital allogenic sulphides, mostly in pyrite (rare in arsenopyrite)

(e) Gold in secondary quartz veins

Liebenberg (G.G. Stanley, 1987) indicated that the gold in the Witwatersrand conglomerate is alloyed with silver and more recently Erasmus et al found (G.G. Stanley, 1987) small quantities of mercury and trace metals. Other metals found with the Witwatersrand ore include copper, nickel and iron.

As previously mentioned, gold in the Witwatersrand depository is associated with a number of different minerals. It was therefore decided to distinguish between these minerals on the basis of the amount of gold associated with those minerals, and to divide them into the following classes.

1. Free Gold.

2. Gold associated with Pyrite.

3. Gold associated with Base Metal Sulphides.

4. Gold associated with Carbonaceous material.

5. Gold associated with Silicates

2.2.2 Gold in the Barberton Mountain Land

De Villiers (G.G. Stanley, 1987) provided the first mineralogical details of 21 mines in the Barberton greenstone belt and described 27 ore minerals, as well as various associations of gold with sulphide minerals. He concluded that the ores in the Barberton region could be devided into four main types:

(a) ore containing arsenopyrite and pyrrhotite,

(b) pyrite ore,

(c) lead-bearing ore,

(d) antimonial ore.

It was further concluded that the ores containing pyrite, arsenopyrite and pyrrhotite are the most abundant, whereas lead and antimonial ores are sparsely distributed in the region.

Most of the gold in the major gold deposits in the district is associated with sulphide minerals (arsenopyrite, pyrite) and does not respond to conventional cyanidation techniques. The gold ores of this region are therefore classified as refractory.

Schweigart and Liebenberg (G.G. Stanley, 1987) identified a further 28 ore minerals in their study. Viljoen et al (G.G. Stanley, 1987), however, extended the list from the 55 to 65 ore minerals found in this region. Gold is associated with 28 of these known minerals. The most important gold-bearing sulphide in the Barberton ores is pyrite followed by arsenopyrite which occurs commonly with pyrrhotite.

From further investigations by Schweigart and Liebenberg (G.G. Stanley, 1987), they concluded that the division of the Barberton gold ores into four categories as done by De Villiers (G.G. Stanley, 1987), is not strictly correct. The reason being that the ores contain a large number of minerals. They proposed the following classification of the Barberton ores:

(a) unoxidised, complex sulphide ore that is the main ore type present,

(b) gold-bearing quartz veins which contain only negligible amounts of sulphide minerals,

(c) weathered ore (oxidised ore) that represents the main gold supplier in historical times.

Gay (G.G. Stanley, 1987) investigated the minor and trace elements of samples of visible gold and reported traces of Be, Bi, Co, Mn, Hg, Mo, Pd, Pt, Ag, Sn, V, Sb, Cu, Fe, Pb, Ni, Ti and Zn with the gold. It was suggested that these elements were present as alloy constituents in solid solutions with gold. However Liebenberg (G.G. Stanley, 1987) indicated that large gold particles contain inclusions of sulphides. Due to the difficulty to separate these sulphide inclusions from the gold, he suggested that the trace elements reported by Gay (G.G. Stanley, 1987) were probably derived mainly from inclusions in the gold.

Various researchers, Schweigart and Liebenberg (G.G. Stanley, 1987), Liebenberg (G.G. Stanley, 1987) and Viljoen (G.G. Stanley, 1987) showed from microprobe analyses of gold from the Barberton area that silver, copper, nickel and iron were the only gold alloying elements.

2.3 MINERAL LIBERATION

The two basic reasons for comminuting an ore are:

(1) to provide a more manageable ore, simply by reduction of its particle size;

(2) to liberate one component from another in the ore to permit subsequent separation of the valuable component from the gangue.

As a result of the extremely small proportion of the ore volume being occupied by gold particles, the latter applies to the comminution of gold ores.

The liberation of a mineral in a specific ore is essentially the percentage of that mineral that is present as free particles. To predict the degree of liberation of a mineral in an ore successfully, the following parameters need to be considered, and their interaction during liberation well understood:

1. grain size
2. the shape of the grains
3. types of intergrowths
4. cohesion along grain boundaries
5. internal cohesion in the grains
6. mineral association
7. abundance of each of these associated minerals

8. amount of the valuable mineral present
9. structural characteristics of the ore; fractures and cavities present
10. relative milling properties
11. processing factors such as fineness of grind, milling and separation methods.

2.4 LEACHING

Leaching is the dissolution of a metal or mineral in a liquid to produce metal ions or complexes which can then be extracted selectively from the solution. In this study the dissolution of gold in aqueous solution is of primary concern.

Many leaching reagents can be used but the choice normally depends on the following criteria:

1. It must dissolve the mineral to such an extent to make commercial extraction possible.
2. It must be inexpensive and readily obtainable.
3. If possible, it should be regenerated in subsequent processes.

Leaching methods bear direct relevance to the nature of the mineral deposit. The various leaching techniques which are of commercial importance, are as follows:

1. *In situ* Leaching - the ore is not mined, but is leached where it occurs.
2. Heap Leaching - the uncrushed ore is carefully piled, followed by the spraying of the leaching solution onto the pile.
3. Dump leaching - it is very similar to heap leaching except that dump leaching is used predominantly for sulphide-bearing ores and heap leaching for oxide-bearing ores.
4. Vat leaching - the ore, confined to a vat, is treated with increasing concentrations of leach solution
5. Agitated leaching - the solids are dispersed in the liquid, which contains the leach solution, either by gas injection or rotating impeller. This method is mostly used in the South African gold industry
6. Bacterial leaching - is a chemical liberation process and is followed by a cyanide leaching step (mostly used with refractory

ores, containing arsenopyrite such as Barberton gold ores).

It is important to note the difference between liberated gold and leachable gold. Grinding or milling is used to liberate or expose the gold to the reagents in the solution and thus, the gold is leached. Gold particles situated in minor cracks or fractures are not liberated as such, but they remain leachable whenever in contact with the leaching solutions.

2.5 DIAGNOSTIC LEACHING

Lorenzen et al (1986) developed diagnostic leaching as an analytical method to examine the deportment of gold in an ore. The concept of diagnostic leaching is very simple and produces, when carried out on representative samples, easily interpreted results.

The approach of diagnostic leaching is to eliminate firstly, the least stable mineral present in the matrix of the sample in aqueous media, by using a selective oxidative leach. The gold (or any other precious mineral which furnishes it to leaching) liberated by this action is then extracted by using subsequent cyanidation. The gold extracted can then easily be measured in solution (by usage of the Atomic Absorption apparatus (AA) or the Ion Conductively coupled Plasma (ICP) apparatus) and thus represents the amount of gold associated with that mineral. The residue from this first stage can then be subjected to a more oxidative acid leach and the process repeated. The procedure can be varied to suit the mineralogy of the matrix material. At the end of such a diagnostic leach, the researcher is left with an almost complete record of the deportment of gold in the ore.

The development of the diagnostic leaching concept was done at Anglo American Research Laboratories (AARL) in 1985. Until then, other researchers had used acid pre-treatment as a means to liberate and examine the shape and size of goldparticles. Due to gold's nobleness and resistance to attacks to most acids, oxygen and sulphur (Puddephatt 1978) at any temperature (except aqua regia), it lends itself to this type of analysis. Some guidelines to the design of a diagnostic leaching experiment (Lorenzen, 1995) is presented in Appendix A.

2.6 MINERAL LIBERATION MODELS

Since the first attempt by Gaudin in 1939 to develop a liberation model, many researchers such as Wiegel (1976), King (1979), Meloy and Gotoh (1985), Klimpel and Austin (1983), Barbery (1991) and Hsih and Wen (1994) contributed to the field of mineral liberation. Unfortunately, despite all these attempts, mineral liberation is still a complex problem which lacks understanding. The attempts by these researchers will be discussed briefly below.

2.6.1 Gaudin liberation model

Gaudin (1939) conceptually represented an ore as a uniform distribution of cubical mineral grains in a matrix of rock. He considered two phases, A and B of the same size α, in which A is *n* times more abundant than B. The phases are arranged in such a manner that the various B's are on the average as far apart as possible. It is further assumed that a fracturing lattice of parameter β such that $\alpha=k\times\beta$ is superimposed upon the grain lattice and parallel to it.

Thus, the degree of liberation of B is:

$$f_B = \left(\frac{k-1}{k}\right)^3 \qquad (2.1)$$

and of A (n>4) is:

$$f_A = \frac{nk^2 - 3k - 2}{nk^2} \qquad (2.2)$$

Gaudin concluded that:

1. the less abundant phase is not liberated at all, unless the particles are finer than the grain size.
2. the more abundant phase is always more liberated than the less abundant phase.

This model, however, is too idealised and not realistic enough to be very useful in predicting mineral liberation.

2.6.2 Wiegel liberation model

Wiegel and Li (1977) proposed a liberation model for an idealised binary mineral system. They found that the degree to which a certain component is liberated, is a function of the ratio of the volumetric abundance of the two mineral components and the ratio of the mineral grain size to particle size. The proposed model is an extension to the liberation model proposed by Gaudin (1939) with the only difference being the arrangements of the mineral grains. The proposed model is based on a completely random arrangement of mineral grains, while Gaudin (1939) chose to place the grains of the least abundant mineral as far apart as possible.

The model is based on the following assumptions:

1. the grains of both mineral species are cubic and are of the same uniform size (α),
2. the grains are aligned so that the grain surfaces form continuous planes,
3. the grains of the two mineral species are randomly arranged throughout the aggregate,
4. the aggregate, when comminuted, is broken into particles of uniform size (β) by a cubic fracture lattice which is superimposed randomly on the aggregate parallel to the grain lattice.

In deriving the liberation model the following parameters were defined, namely:

1. k is the ratio of grain to particle size (α/β), and
2. n is the volumetric abundance ratio, defined as the ratio of the volume of A to that of B in the aggregate.

The following two cases were discussed by the authors:

1. k≥1: The probability of occurrence of a liberated particle of A and that of B are respectively as follows:

$$P_A = \frac{(k-1)^3}{k^3}\left(\frac{n}{n+1}\right) + \frac{3(k-1)^2}{k^3}\left(\frac{n}{n+1}\right)^2 + \frac{3(k-1)}{k^3}\left(\frac{n}{n+1}\right)^4 + \frac{1}{k^3}\left(\frac{n}{n+1}\right)^8 \tag{2.3a}$$

$$P_B = \frac{(k-1)^3}{k^3}\left(\frac{1}{n+1}\right) + \frac{3(k-1)^2}{k^3}\left(\frac{1}{n+1}\right)^2 + \frac{3(k-1)}{k^3}\left(\frac{1}{n+1}\right)^4 + \frac{1}{k^3}\left(\frac{1}{n+1}\right)^8 \tag{2.3b}$$

The probability of occurrence of a locked particle containing both A and B is given by

$$P_{AB} = 1 - (P_A + P_B) \tag{2.4}$$

2. k<1: The probability of occurrence of a liberated particle of A and that of B are:

$$P_A = (1-\varepsilon)^3\left(\frac{n}{n+1}\right)^{(t+1)^3} + 3\varepsilon(1-\varepsilon)^2\left(\frac{n}{n+1}\right)^{(t+2)(t+1)^2} + 3\varepsilon^2(1-\varepsilon)\left(\frac{n}{n+1}\right)^{(t+2)^2(t+1)} + \varepsilon^3\left(\frac{n}{n+1}\right)^{(t+2)^3} \tag{2.5a}$$

$$P_B = (1-\varepsilon)^3\left(\frac{1}{n+1}\right)^{(t+1)^3} + 3\varepsilon(1-\varepsilon)^2\left(\frac{1}{n+1}\right)^{(t+2)(t+1)^2} + 3\varepsilon^2(1-\varepsilon)\left(\frac{1}{n+1}\right)^{(t+2)^2(t+1)} + \varepsilon^3\left(\frac{1}{n+1}\right)^{(t+2)^3} \tag{2.5b}$$

where t is defined as the largest integer contained in $1/k$ and ε as the fractional remainder so that $1/k = t + \varepsilon$

The probability of occurrence of a locked particle containing both A and B is given by

$$P_{AB} = 1 - (P_A + P_B) \tag{2.4}$$

The degree of liberation is thus:

$$L_A = \frac{n+1}{n} P_A \tag{2.6a}$$

$$L_B = (n+1)P_B \tag{2.6b}$$

2.6.3 The King liberation model

The King liberation model (King ,1979) is an exact expression that is derived for the fraction of particle size D, that contains less than a prescribed fraction of any particular mineral. The expression is obtained entirely in terms of the distributions of linear intercept lengths of the minerals in the ore. The theory predicts that the fractional liberation of mineral at particle size D is given by:

$$L(D) = 1 - \frac{1}{\mu}\int_{0}^{D_u} \{1 - N(l/D)\}\{1 - F(l)\}dl \qquad (2.7)$$

where F(*l*) - distribution of linear intercept lengths of mineral

μ - mean linear intercept length [μm]

N(*l*/*D*) - linear intercept distribution function for particles of particle size D

D_u - the largest intercept length across any particle of particle size D [μm]

l - linear intercept length

King's model is based on the following assumptions:

1. The ore is considered to be a random assemblage of mineral grains with distinct boundaries between adjacent grains.
2. The grains are random in size, shape and orientation but each grain is a distinct mineral species.
3. It is developed for binary isotopic assemblies (the mineral and gangue).
4. The ore does not fracture preferentially along grain boundaries nor do small fragments of one material "fall out" of larger particles of the other material.
5. Equivalence between the fraction of a line through the ore to the volumetric fraction in the ore as a whole is assumed.
6. A particle has a size "D" when it just passes through a square opening of side D

Assumption five is the main assumption on which the model is based. Although it is regularly used in modal analysis and its validity has been critically, though inadequately, examined by Chayes (King 1979), it does not seem to be possible to prove or disprove its validity theoretically and the usefulness of the model can therefore be established only by appeal to experiment.

To solve equation (2.7) analytically, a relationship between F(*l*) and *l* and N(*l*/*D*) and *l* is essential.

King (Finch & Petruk, 1984) suggested the following relationships:

$$F(l) = 1 - \exp(-l/\mu_m) \qquad (2.8)$$

and

$$N(l/D) = l^2/D^2 \qquad (2.9a)$$

with the latter being derived by Underwood (1970) for spherical particles.

Finlayson (1980) suggested the following expression for the function N(*l*/*D*), namely:

$$N(l/D) = 1 - (1 - \frac{1}{\sqrt{2}Du})\exp(-\frac{R^2 l}{\sqrt{2}Du}) \qquad (2.9b)$$

where R is the ratio of upper to lower size of the screen interval.

Equation (2.9b) fits Finlayson data fairly well, although for $l > \sqrt{2Du}$, N(*l*/*D*) becomes greater than 1, which is ,however, impossible.

It is furthermore suggested by Finch & Petruk (1984) that N(*l*/*D*) could be of the form :

$$N(l/D) = 1 - \exp(-kl/D) \qquad (2.9c)$$

where k = constant (value = 2 ± 0.4(i.e. 20%))

It was found by Finch & Petruk (1984) that eq. (2.9b) gives as good a fit as eq (2.9c) to King's data.

When equation (2.8) is combined with equations (2.9a), (2.9b) or (2.9c) and integrated, it yields the following expressions, respectively (assumingly that D = D_u):

$$L(D)=\frac{2\mu_m^2}{D^2}[1-(1+\frac{D}{\mu_m})\exp(\frac{-D}{\mu_m})] \qquad (2.10a)$$

$$L(D)=1+\frac{\sqrt{2}Du}{\mu_m B^2}[1-B-\exp(-B)] \qquad (2.10b)$$

where $B=R^2+\frac{\sqrt{2}Du}{\mu_m}$

$$L(D)=1-\frac{D}{2\mu_m+D}[1-\exp-(\frac{2\mu_m+D}{\mu_m})] \qquad (2.10c)$$

2.6.4 The Klimpel and Austin model

The model (Klimpel and Austin, 1983), programmed for Monte Carlo simulation, is based on a simple binary system of component B occluded in a matrix of A. An analytical solution was also proposed after some additional assumptions were made. Their liberation model was based on the following assumptions:

1. Fracture planes can pass with equal ease through A or B.
2. The volume fraction of B in the AB matrix is small.
3. The grains of B are randomly dispersed in AB.
4. The primogeniture material is reduced in size to an experimentally determined size distribution, without preferential grinding of one component with respect to another.
5. The ore does not fracture preferentially along the grain boundaries.
6. An amount of zero or one mineral fragment per particle was assumed in deriving the analytical solution.

The analytical solution is of the following form:

$$f(V_{AB},V_B') = (1-\phi)\exp(-\alpha * V_{AB}) \quad \ldots\ldots r = 0$$

$$= \phi[2\int_{V_B'}^{\infty}\frac{g(V_B)}{V_B}dV_B + V_{AB} * (1-r) * \frac{g(V_B')}{V_B'}]dV_B' \quad \ldots 0 < r < \quad (2.11)$$

$$= \phi\int_{V_{AB}}^{\infty}(V_B - V_{AB})\frac{g(V_B)}{V_B}dV_B \quad \ldots\ldots r = 1$$

$f(V_{AB}, V_B')$ - final joint partial differential function which gives the fraction of unit volume having particle size (volume) between V_{AB} and $V_{AB} + dV_{AB}$ and containing a volume of component B of V_B' to $V_B' + dV_B'$, where $0 \leq V_B' \leq V_{AB}$

$g(V_B)$ - size distribution of grains in B

$g(V_B)dV_B$ - fraction of volume B which lies in the grain volume size range of V_B to V_B+dV_B

ϕ - overall fraction of B in AB

$p(V_{AB})$ - size distribution of fragments of the ore (AB)

α - number of B grains per unit volume of A

N_B - number of B grains

V_B' - a specific size which contains a specific volume of component B

where α and r are defined as

$$\alpha = \frac{N_B}{(1-\phi)} \quad (2.11a)$$

$$r = \frac{V_B'}{V_{AB}} \quad (2.11b)$$

Klimpel solved equation (2.11) for three starting grain size distributions of B in AB, in a later paper (Klimpel, 1984). The equation was solved for the following cases:

1. A single B grain size
2. A rectangular (uniform) B grain distribution
3. Schuhmann B grain distribution

2.6.5 Liberation model developed by Meloy and Gotoh

The model proposed by the authors (Meloy and Gotoh, 1985) considers comminution independently of the spatial positions of the inclusions. This means that the reduction of the matrix (phase B) and the inclusions (phase A) is the same, that there is no preferential cracking between the grains, and that the position of a given particle is independent of the positions of the inclusions. Meloy and Gotoh also assumed the following:

1. All phases have the same size distribution.
2. The shape of the particles and the inclusions are spherical.
3. The inclusions are randomly distributed.
4. Locked particles contain target material from one inclusion only.
5. Particle sizes are equal to or smaller than inclusion sizes.

In deriving the model, a spherical particle of diameter x and composed of pure phase A, which is entirely within a spherical inclusion (composed of A) of diameter y, is considered. After deriving an expression for the expected probability of the particle being inside all the inclusions, of size y, it was multiplied by the probability of having a particle of size x to obtain the probability of having a particle composed of pure A and of size x and being in the proper volume region of an inclusion of size y.

The total volume of free (unlocked) particles was obtained after the double integration of the above mentioned function, by integrating first over y to obtain the frequency number distribution function (of particles of size x) which was multiplied by the volume of a particle of diameter x to obtain the volume frequency distribution function and then over all sizes of particles.

The degree of liberation (the fraction of the material A that was in the inclusions that is now liberated) is thus the total volume of free particles (V_A) divided by the total volume of inclusions (V_I):

$$L_A = \frac{\pi}{6 * V_0 * V_I} \int_0^{X_0} \int_x^{Y_0} f(x)(y-x)^3 g(y) dy dx \qquad (2.12)$$

L_A - the degree of liberation.

V_o - total volume of the sample (total volume of phases A and B).

V_i - total volume of inclusions composed of phase A.

y - the inclusion diameter.

Y_m - the largest inclusion diameter.

x - the particle diameter.

X_m - the largest particle diameter.

$f(x)$ - particle volume frequency distribution.

$g(y)$ - inclusion number frequency distribution.

Due to the lack of experimentally determined functions for g(y) and f(x) the authors assumed the following distributions:

$$f(x) = \frac{nV_o}{Y_m} \qquad (2.13a)$$

$$g(y) = \frac{24V_o}{1000Y_m^4\pi} \qquad (2.13b)$$

with n - a positive integer

After the substitution of equations (2.13a) and (2.13b) into equation (2.12) and integration, the degree of liberation is given by the following expression:

$$L_A = \frac{-nV_i}{5Y_m^5}\left(\left(Y_m - \frac{Y_m}{n}\right)^5 - Y_m^5\right) \qquad (2.14)$$

The validity of this theoretical model still has to be proved since the distribution functions, g(y) and f(x), have not yet been determined experimentally.

2.6.6 Liberation model developed by Barbery

In deriving a model for mineral liberation by size reduction, mathematical morphology and integral geometry methods were used by Barbery (1991). The derivation was made for space dimensionalities of 1, 2 and 3. The model was developed for ore textures which correspond to Boolean schemes with primary Poisson polyhedra and Poisson polyhedral textures. The solutions are, however, mathematically complex and the derivation of the solution is difficult to follow, due to intricacies of geometrical probability and integral geometry.

The results obtained were plotted and fitted empirically to obtain the following simple exponential function which relates the degree of liberation to the screen size, D measured in d dimensions:

$$L(D) = \exp[-0.693(\frac{D}{D_{50,d}})] \qquad (2.15)$$

L(D) - degree of liberation at particle size D in space dimension "d"

D - particle screen size

$D_{50,d}$ - particle size at which the degree of liberation is 0.5 in space dimension "d"

The following assumptions were made in deriving the model:

1. A particle has a size D when it just passes through a square opening of side D.

2. The random intercept lengths and the distribution of random section areas across a particle with size D, are known.

3. The intercept length density distribution and the area density distribution have been measured.

4. The ore texture corresponds to Boolean schemes with primary Poisson polyhedra and Poisson polyhedral textures.

2.6.7 Liberation model developed by Hsih and Wen

Hsih and Wen (1994) extended Gaudin's liberation model by incorporating a detachment factor and taking variations in grain size into account. The basic idea of the detachment factor is simply to incorporate breakage along grain boundaries. According to Gaudin's model none of the grains of the valuable or target mineral breaks at the mineral-gangue boundaries. The proposed model is as follows:

$$L_m(D_i) = \frac{\sum_{i=1}^{J} PK_i^3 V_m(G_i) + \sum_{i=1}^{J} (1-P)(K_i - 1)^3 V_m(G_i)}{\sum_{i=1}^{N} K_i^3 V_m(G_i)} \quad \ldots\ldots K \geq 1 \qquad (2.16)$$

$$= 0 \quad \ldots\ldots K < 1$$

where $0 \leq P \leq 1$

$$K_i = G_i/D_i$$

$L_m(D_i)$ - degree of liberation of the ore in the ith interval

P - detachment factor

D_i - the particle size in the interval i of the crushed ore

G_i - grain size of mineral m in the interval *i* in the uncrushed ore

$V_m(G_i)$ - volume fraction of the ith interval

N - amount of grain size intervals

The average degree of liberation over all particle sizes can be evaluated by summation over all size intervals:

$$L_m = \sum_{j=1}^{N} L_m(D_j) W_j \qquad (2.17)$$

where W_j represents the weight fraction of the comminution product belonging to size interval j

2.7 LEACHING LIBERATION MODELS

The models which predict leachable gold as a function of particle size will now be discussed. Since this is a fairly new field, only two models are available.

2.7.1 Model proposed by Lorenzen

Lorenzen and Van Deventer (1994) and Lorenzen (1992a) tested the King liberation model on their experimental data (the leachable gold of three different gold ores was determined by diagnostic leaching, see Chapter 3) and the results predicted by the model were compared to the experimental results. The mean linear intercept length of the mineral in the ore was not known and it was not possible to determine it by using SEM.

Equation (2.10a), obtained from King's model, was fitted against the experimental data and it was found that the model underestimates the amount of free leachable gold in each particle size fraction entirely.

Lorenzen modified equation (2.10a) by adding a term to provide for the amount of leachable gold in various particle size fractions that is not related to the liberation of gold due to comminution. The modified model, which gave reasonable predictions, has the following form:

$$L_m(D) = \frac{2\mu_m}{D^2}[\mu_m - (\mu_m + D)\exp(-\frac{D}{\mu_m})] + [A\exp(\frac{1}{D})] \qquad (2.13)$$

where:

$L_m(D)$ - fraction of leachable gold for particle size (D),

A - empirical constant for the specific ore,

$\{A\exp(1/D)\}$ - fraction of leachable gold for particle size (D) not related to liberation

D - geometric mean of the screen interval (μm)

μ_m - mean linear intercept length of gold in the ore (μm);

2.7.2 Exposure model developed by Hsih and co-workers

Hsih and co-workers (Wen et al, 1995) derived an exposure model that predicts the degree to which precious mineral grains are exposed to the particle's surface. The model is based on cubical particle and grain sizes and on the same principles as their liberation model (Hsih and Wen, 1994). The major differences of the exposure model to the liberation model, is:

1. G < D, thus where the grain size of the precious mineral, gold, is smaller than the particle size of the comminuted ore.
2. The detachment factor in the liberation model is a function of the differences in the physical properties of the target mineral and the matrix gangue, while the intergranular fracturing factor is only determined by the physical properties of the matrix gangue.

Their exposure model (Wen et al, 1995) for gold ores is as follows:

$$L_m(K) = P\left(\frac{K^3-(K-2)^3}{K^3}\right)+(1-P)*\left(\frac{K^3-(K-1)^3}{K^3}\right) \qquad (2.19)$$

where $K=D/d$

$L_m(K)$ - degree of the liberation

P - intergranular fracturing factor (P=1 - only fracture along grain boundaries; P=0 - only transgranular fracture)

d - grain size of the gold (μm)

D - particle size of the ore (μm)

The first term of equation (2.19) anticipates the case where fracture along grain boundaries occur while the second term predicts the exposure of grains when transgranular fracture occurs. The authors extended this model to provide for variation in grain and particle size and the average degree of liberation is thus;

$$L_m(K_{ij}) = \sum_{j=1}^{n}\{\sum_{i=1}^{m} L_m(K_{ij})*W_i\}*W_j \qquad (2.20)$$

where $K_{ij} = D_i/d_j$

2.8 SUMMARY

From the literature survey as presented in this chapter it is evident that although many researchers have contributed to the field of mineral liberation, it is still a complex problem and more research is still needed to assist in the understanding of not only the interrelationship between the different factors, such as particle size, the texture and mineralogy of a specific ore, fracture mechanisms, etc. and liberation, but also the interrelationship between mineral liberation and leaching behaviour.

CHAPTER 3

EXPERIMENTAL

CHAPTER 3

EXPERIMENTAL

3.1 ORES USED IN EXPERIMENTAL WORK

Seven ores were used in the experiments, with one being refractory. An ore is regarded refractory, whenever it does not respond well to conventional cyanidation techniques, due to the intergrowth of gold grains mainly with sulphide minerals (arsenopyrite and pyrite). A large representative sample (300 kg), obviously only representative of the specific conditions at the stage when the sample was taken, due to the immense variation in mineral content in the feed to the mine, was taken from each mine. The conveyor feedbelt to the mine was stopped and the ore over a 5 meter strip was taken. The different ores that are under investigation, are as follows:

1. Beatrix gold ore
2. St. Helena gold ore
3. Unisel gold ore
4. Harmony gold ore
5. Kinross gold ore
6. Leslie gold ore
7. Barberton gold ore.

All the ores, except the Barberton ore, were uncrushed because they are fed to autogeneous mills. The Barberton ore was crushed to -2000 mm. The deportment of gold in the different ores is described in the following paragraphs:

3.1.1 Beatrix gold ore

The Beatrix reef is situated in the Orange Free State gold fields (see Figure 3.1) with an average headgrade of 6 g/ton (1994). From mineralogical analysis (report from the Beatrix mine), gold occurs in four main forms in the Beatrix reef:

1. Free gold

2. Gold associated with quartz and other silicates

3. Gold associated with pyrite

4. Gold associated with hydrocarbons.

About 70% of the gold in the Beatrix reef occurs as free gold interstitially with quartz. Gold grains observed in studies varied in size from 210x75 microns to 5x2 microns, with a median size of 38x14 microns.

Gold locked-up in quartz and other silicates, such as chlorite, comprises 10% of the Beatrix gold. The median size of the gold grains is 32x10 microns.

Gold associated with pyrite comprises roughly of 5% of the gold in the ore. The gold grains are generally smaller than the free gold grains and those associated with silicates with a median size of 15x6 microns.

Almost 15% of the gold is associated with hydrocarbons. The median size is 8x3 microns.

3.1.2 St. Helena -and Unisel gold ores

The mineralisation of both the St. Helena and Unisel gold ores is discussed here, since they are only two separate feedstreams to the St. Helena gold mine. The St. Helena gold ore is mined from the Basal reef with an average head grade of between 4 to 5 g/ton. The Unisel gold ore comprises of two-thirds from the Basal reef and one-third from the Leader reef. The average head grade amounts to 5.5 g/ton. The gold mineralisation of only the Basal reef is available (report from St. Helena) and thus only a general description of the St. Helena gold ore is given. Gold occurs in the following forms:

1. Free Gold

2. Gold attached to pyrite

3. Gold included in pyrite

4. Gold associated with hydrocarbons.

It is estimated that 50% of all the gold occurs as free gold grains. The sizes of hackly (sharp angular) gold grains vary considerably from a few millimetres in diameter to a few microns.

Approximately 10% of the gold occurs as gold attached to pyrite grains, usually pyrite grains which also occlude gold. It was found to be 100% extractable by cyanidation.

Gold included in pyrite is estimated at 35% of the total gold. The average diameter of gold grains is approximately 10 microns. The estimated recoverability by cyanidation of these gold grains with a size greater than 20 microns is 80%, a size smaller than 20 microns but larger than 5 microns is 50% and a size smaller than 5 microns is approximately 10%.

An estimated 5-10% of gold is associated with hydrocarbons. The gold grains are extremely small with the average being 2 microns.

3.1.3 Harmony gold ore

The Harmony gold mine is situated on the south eastern part of the Orange Free State goldfields (see Figure 3.1). Unfortunately, no other information is available.

3.1.4 Kinross and Leslie gold ore

The Kinross and Leslie gold mines are situated on the eastern and western part of the Evander goldfield, respectively (Figure 3.1). Due to their extreme location relative to each other and to the other goldfields, their gold mineralogy is thus different, with an average head grade of 7 g/ton (1994) for the Kinross gold ore and between 5 to 6 g/ton (1994) for the Leslie gold ore.

The Leslie gold ore, different to the other gold ores which is milled to 70% -75µm, is milled to 90% -75µm due to the large occurrence of shales in this region which interfere with the extraction of gold by cyanidation.

3.1.5 Barberton gold ore

The Barberton gold mine is situated in the Barberton region and due to the occurrence of large amounts of pyrite and arsenopyrite in the gold ore, the extraction of gold by means of the normal cyanidation procedure is unsuccessful. The gold from this refractory ore is however, liberated by bacterial leaching and then recovered in the subsequent cyanide leaching process.

3.1.6 WDL, FSG and Harties gold ores

The Western Deep Level (WDL), Free State Geduld (FSG) and Harties (Hartebeesfontein) gold ores were investigated by Lorenzen (Lorenzen 1992a).

Because the same experimental methods were used, Lorenzen's data were thus used with the ores under investigation in achieving the main goals of this thesis.

The WDL, FSG and Harties gold mines are situated on the West Wits Line, Orange Free State and Klerksdorp gold fields, respectively (see Figure 3.1).

3.2 EXPERIMENTAL PROCEDURE

3.2.1 Taking of representative samples.

A sample of approximately 150 kg (half the original sample) was taken as a first attempt to reduce the large sample taken at the different mines. The sampling procedure was the same for all the different ores and it could be summarised as follows:

1. The original sample was scooped out of the container onto a clean working space.
2. After the heap of ore was thoroughly mixed with a spade, the ore was split into two heaps by taking smaller samples at random from the original heap.
3. One of these heaps was then taken as the new sample for further processing.

3.2.2 The distribution of the representative sample

Since the ore contained a lot of moisture, the ore sample had to be wet screened (washed) to retrieve all the fine material from the coarser lumps. The ore sample was first screened into three size intervals, namely

1. +6700 µm fraction
2. +1500 -6700 µm fraction
3. -1500 µm fraction

The -1500 µm fraction (residue from the first wet screening), now a slurry, was wet screened (washed) further into six intervals:

1. +300 -1500 µm fraction
2. +150 - 300 µm fraction
3. +106 -150 µm fraction
4. +75 -106 µm fraction
5. +53 -75 µm fraction
6. -53 µm fraction

The -53 µm fraction was filtered in a pressure filter to remove the excess water. The filter cake was then dried with the other particle size fractions. The dry particle size fractions were then screened dried on a vibrating sieve shaker (Fritsch Analysette type 03.502) at an amplitude of 7 for a period of 45 minutes.

These eight particle size fractions represent the unmilled ore. A representative sample was then taken from the unmilled sample: the -53 µm up to the +1500 - 6700 µm was split by even chance with a splitter and a rotary sample splitter (Hi-Vi vibratory equipment from Eriez magnetics, model 15A) and the +6700 µm was split randomly by hand. This representative sample, about one eighth of the unmilled sample, was used for further processing, namely crushing and milling.

The +1500 µm -6700µm and the +6700 µm particle size fractions were then crushed, first by a jaw crusher and then by a cone crusher, to -1500 µm. This crushed sample was screened using the same

technique as mentioned above. The size fractions -53 µm up to the +150 -300µm fraction represent the crushed sample.

The size fractions -53 µm up to the +300 -1500 µm fraction of the representative sample taken from the unmilled sample, combined with the +300 -1500 fraction from the crushers, were used in a laboratory ball mill with a size distribution of iron balls, to produce the milled sample of 70% -75 µm. This milled sample was also screened into the above mentioned size fractions.

3.2.3 Diagnostic Leaching Technique (Lorenzen et al, 1986 and Lorenzen 1995)

The concept of diagnostic leaching, as already mentioned, is very simple. The least stable mineral present in the matrix of the ore sample is first destroyed over a period of time by using the least oxidative acid. The residue is filtered, washed with water and/or dilute acid, cyanided to extract the gold liberated and washed with a dilute cyanide solution and water. The process is repeated with a more oxidative acid leach until all the minerals with which the gold is associated with, are destroyed. A record of the gold deportment of the specific ore is then available. According to Tumilty et al (1987) an overlap of the extent of leaching does occur, but it is generally limited to 90% of the required mineral and 10% of the next most stable mineral. Before the design of a diagnostic leaching procedure, the mineralogy of the ore treated should first be determined.

The diagnostic leaching procedure was performed once on each of the particle size fractions (-53 µm; +53 -75 µm; +75 -106µm; +106 -150 µm; +150 -300 µm; +300µm) of the unmilled and milled samples of each ore and on the crushed samples of some ores. The results obtained is given in chapter 4.

A summary of the pre-treatments and cyanidations as conducted in the experiments is given below. A more general detailed diagnostic leaching procedure is presented in Appendix A.

3.2.3.1 Pre-treatments

The various stages of acid pre-treatment that can be used and the minerals it will most likely destroy are presented in Table 3.1. As a result of the absence of major amounts of pyrrhotites, calcines, galena, ferrites, etc. in the ores, the HCl and $FeCl_3$ pre-treatments were abandoned. Due to the occurrence of pyrite, labile base metal sulphides and carbonaceous material in the different gold-bearing ores, the following pre-treatments were used in conducting the experiments:

1. Sulphuric acid
2. Nitric acid
3. Carbon burn-off

The potential (± 500 mV) during sulphuric acid (98 %) pre-treatment stages was controlled with H_2O_2 via a 16 channel automatic titrator unit (computer, interface, titrator, magnetic valves, electrodes and pH-meter).

Two pre-treatment methods exist to destroy carbon or carbonaceous material, namely

1. By using acetonitrile elution
2. Carbon burn-off

Both methods were at first used and it was found that the carbon burn-off seemed to be the most effective. The carbon burn-off was performed at a temperature of 700 °C over a period of 18 hours. The ore sample was spread out to ensure the largest possible exposed area. During the 18 hour period, the ore sample was thoroughly mixed at times.

3.2.3.2 Cyanidation

The cyanidation between pre-treatment stages was performed in agitated vessels (1/ beakers with variable speed overhead stirrers) except the +300 fraction of each ore where roiling bottles were used. The rotating speed was set to keep the ore in

suspension. In all the experiments 2000 ppm KCN was used at a pH of 10 to 12 and a temperature of 20 to 25 °C.

3.2.4 Analysis of samples

The gold dissolved in each sample was analysed on the Atomic Absorption Apparatus, at the Department of Chemical Engineering, University of Stellenbosch. The dried residue after the completion of the diagnostic leaching procedure was sent to the Gencor Research Laboratory at Springs for the required gold assays.

TABLE 3.1:

STAGES OF SELECTIVE PRE-TREATMENT FOLLOWED BY LEACHING, AND THE MINERALS DESTROYED

	Pre-treatment stage	Minerals likely to be destroyed
1.	NaCN washes	Precipitated gold
2.	NaCN	Free gold
3.	HCl	Pyrrhotite, Calcite, Ferittes, Dolomite, Galena, Haematite, Goethite, Calcium, Carbonate
4.	H_2SO_4	Uraninite, Sphalerite, Labile Copper Sulphides, Labile Base Metal Sulphides, Labile Pyrite
5.	HNO_3	Pyrite, Arsenopyrite, Marcasite
6.	Na_2CO_3	Gypsum and Arsenates
7.	$FeCl_3$	Sphalerite, Galena, Labile Sulphides, Tetrahedrite
8.	Oxalic Acid Washes	Oxide Coatings
9.	HF	Silicates
10.	Acetonitrile elution	Gold adsorbed on carbon, Kerogen, Coal

Note: All the abovementioned pre-treatment stages can be modified according to the matrix of the material. Temperature, potential, concentration, treating time, etc. all determine the desired pre-treatment stages.

Reference: Lorenzen, 1992a

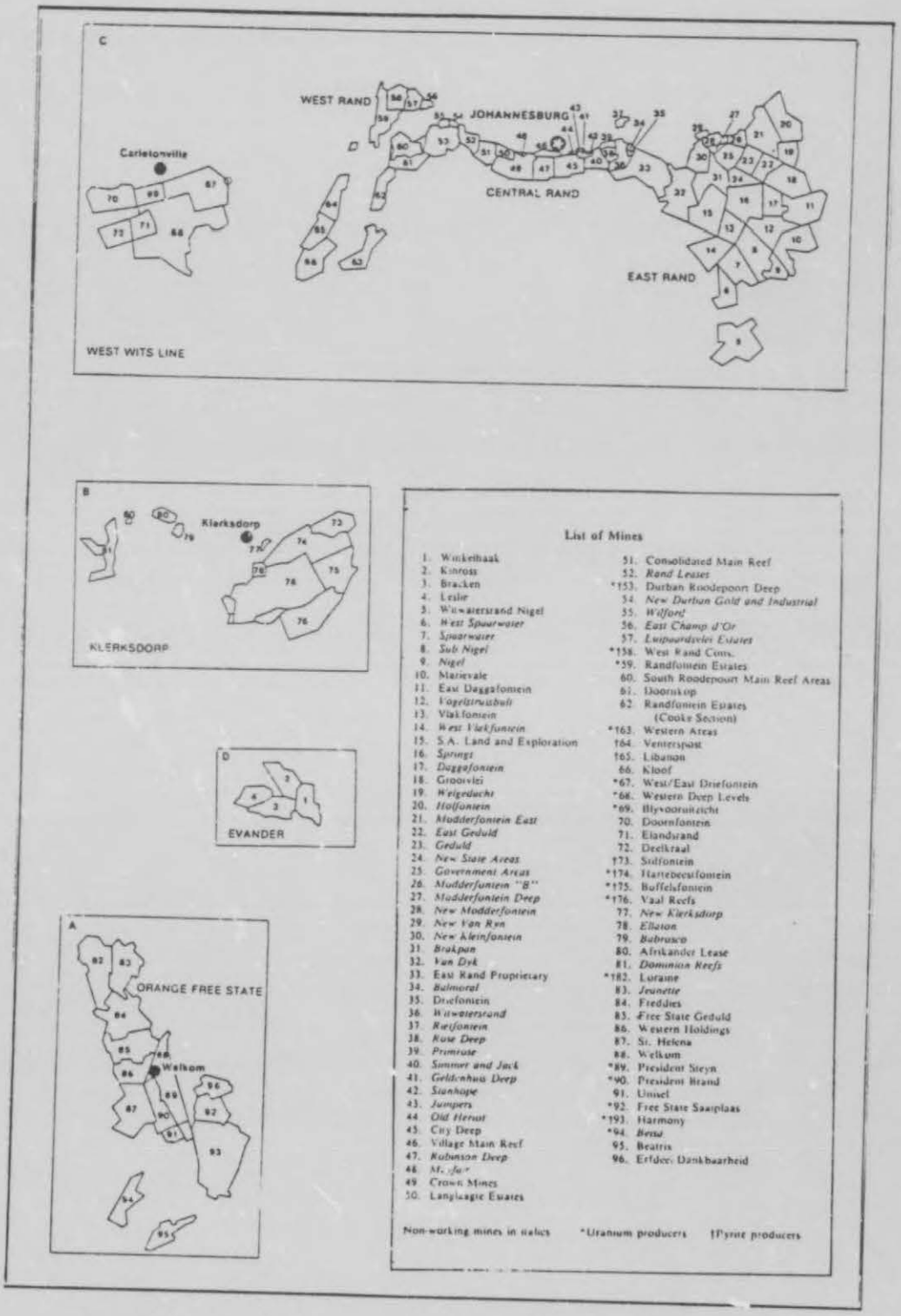

FIGURE 3.1 : THE LOCATION OF THE GOLDBEARING MINES IN SA (Reference: G.G. Stanley, p9)

CHAPTER 4

DIAGNOSTIC LEACHING RESULTS

CHAPTER 4

DIAGNOSTIC LEACHING RESULTS

In this chapter, the results obtained from diagnostic leaching tests, performed on the different ores, are presented. The fluctuations in the gold deportment (mineralogy) of the different ores are discussed and some qualitative conclusions are drawn from the results. The results obtained are presented in Tables 4.1 to 4.22 and Figures 4.1 to 4.10. The liberation (free gold as a function of particle size) trends of the different ores are presented in Figures 4.11 to 4.20.

4.1 ORES FROM THE EVANDER GOLDFIELDS

It is evident from Tables 4.1 to 4.5 and Figures 4.1 to 4.2 that when the gold deportments of the different unmilled ores are compared, that the gold ores from the Evander area, Kinross and Leslie gold ores, have the highest amount of free gold, namely 36.49 % and 32.08% of the total amount of gold, respectively. The gold associated with BMS amounts to 13.31% and 8.25%, gold associated with pyrite to 6.93% and 11.02%, gold associated with silicates to 38.87% and 46.03% and gold associated with carbonaceous material to 4.40% and 2.62% of the total gold for the Kinross and Leslie gold ores, respectively. When these ores are milled to 70% -75 µm, the degree of liberation is higher than 90% for the smaller particle size fractions.

4.2 ORES FROM THE ORANGE FREE STATE GOLDFIELDS

Five ores from different parts of the Orange Free State goldfields were used in this study. It is evident from Tables 4.6 to 4.8 (St. Helena ore), 4.9 to 4.10 (Beatrix ore), 4.11 to 4.12 (Harmony ore), 4.13 to 4.14 (Unisel) and 4.15 to 4.16 (FSG ore) that the mineralogy (gold deportment) of the ores differ quite considerably, although being mined from the same goldfield. However, the free gold for most of the ores, except the Unisel ore, is constant, being in the order of 20% of the total gold. The gold associated with pyrite varies from 6% to 29%, gold associated with BMS for the non-refractory ores is quite constant in the order of 8% with the refractory ore (FSG) being 35% , the gold associated with silicates varies from 10% to 55% and the gold associated with carbonaceous material varies from 7% to 33% of the total gold.

It is thus evident that the mineralogy of a gold ore is quite dependent on the location of the ore, even within a specific goldfield (Figures 4.3 to 4.7).

4.3 ORES FROM THE CARLETONVILLE GOLDFIELDS

Lorenzen (1992) used the diagnostic leaching technique to determine the mineralogy (gold deportment) of only one ore from this region. In the WDL ore 30% of the total gold is associated with BMS, 46% with pyrite, 16% with the silicates and the remainder, 8%, is free gold (Tables 4.17 to 4.18 and Figure 4.8).

4.4 ORES FROM THE BARBERTON GOLDFIELDS

Diagnostic leaching was performed on the gold ore from the Barberton gold mine (owned by Gencor). The mineralogy (gold deportment) of this ore, varies considerably compared to the other gold-bearing ores; the degree of liberation is constant for particle sizes between 100 and 200 µm. From Tables 4.19 and 4.20 it is evident that 14.5% of the total gold is associated with the BMS, 65.6% with pyrite including arsenopyrite, 4.5% with silicates and 7.4% is free gold (Figure 4.9).

4.5 ORES FROM THE KLERKSDORP GOLDFIELDS

The Harties ore is the only ore from this region that was diagnostically leached. The gold deportment (mineralogy) of each size fraction of the unmilled and milled ore was unfortunately not determined by Lorenzen (1992). Nevertheless, it was established that with the above mentioned analytical technique, 45.7% of the total gold is free, 8.3% is associated with the BMS, 8.3% is associated with pyrite and 37.7 % is associated with the silicates (Tables 4.21 to 4.22 and Figure 4.10).

4.6 GENERAL DISCUSSION

It is evident from the results presented in Tables 4.1 to 4.22 and Figures 4.1 to 4.20, that the gold liberation increases with a corresponding decrease in particle size, as expected. Quite unexpected, however, is the slight decrease in the degree of gold liberation for the particle size fraction -53 µm for some of the ores under investigation. One would rather anticipate the degree of liberation to be constant or to show a slight increase. This unnatural behaviour is most probably due to experimental error. In performing the diagnostic leaching tests, the ore samples have to be repulped and filtered twice after each cyanidation (see Appendix A). Due to the small ore particles in the -53 µm fraction, more liquid is captured intergranularly than in the coarser particles. Thus, although the ore sample was thoroughly washed twice, some of the gold-cyanide-complex remained intergranular, resulting in a much higher gold content in the next stage. It must be noted that the results in Tables 4.1 to 4.22 are relative to the total amount of gold in each particle size fraction. Thus, the cumulative error is reflected in the amount of free gold, resulting in the unexpected decrease in the degree of liberation:

$$Err_{Total} = Err_{Au-Pyrite} + Err_{Au-BMS} + Err_{Au-Silicates} + Err_{Au-Carbon} \qquad (4.1)$$

$$FreeAu(\%) = \frac{FreeAu(g/ton)}{TotalAu(g/ton) + Err_{Total}} \qquad (4.2)$$

Kiss and Schonert (1980) made a two-phase composite material from quartz particles and Portland cement, comminuted it and found that the degree of liberation was only affected by the degree of size reduction and not the method of breakage.

Malvik (1982) milled two ores, a pyrite ore from Skorovass and a galena ore from Mofjellet, to different fineness of grind and showed from his experimental results that liberation is dependent on the fineness of grind. This means that the liberation in one particular sieve fraction of a specific mineral is not constant, but varies depending on the fineness of grind. Lorenzen, (1992) also showed this phenomenon in his study of the FSG (Free State Geduld) gold ore.

When the results of the unmilled, crushed and milled ore samples of a specific ore are compared, there is a variation in the degree of liberation for a specific particle size fraction. The smaller particle size fractions of the unmilled, crushed and milled ore samples are due to the breakage of the ore in the

mine (explosives, handling, etc.), in the jaw- and conecrushers and in the mills, respectively. Different methods of breakage were thus used and it resulted in different fineness of grind. The validity of Kiss and Schonert findings could thus not be proved.

However, various researchers (King 1979, Klimpel and Austin 1984, Meloy 1985) in deriving theories of liberation, made use of the assumption that an ore breaks randomly when milled. Laslett et al (1990), investigated the validity of the assumption and found that random breakage does not always occur. He concluded from his investigation of a simple copper ore that fracturing along grain boundary was occurring. Random breakage means that the breakage is independent of the fracturing mechanism and the ore texture. The fracturing mechanism is, however, very much dependent on the method of breakage. Therefore, the assumption of random breakage permits the concept that the method of breakage does not affect the liberation of the valuable material.

It is further noticeable from the experimental results that most of the gold in the +300 µm fraction for all the different ores is associated with the silicates and that only a small amount of the total gold is liberated. King (1979) found in his study of pyrite in Witwatersrand quartzite that the measured liberation decreases very rapidly at the large size fraction, +415 µm -833 µm. An increase in the degree of liberation of approximately 1% for the +415 µm -833 µm fraction to approximately 47% for the +295 µm -415 µm fraction was detected. King believed it to be a real effect and that it is not due to experimental error.

The fluctuations in the gold values associated with the different minerals are probably due to the inaccuracy of the AA (Atomic absorption) apparatus when gold values with a concentration of under 1 ppm have to be detected; since this was the case for most of the gold values associated with the different minerals.

When the liberation trends of the different ores are compared (see Figures 4.11 to 4.20) it is evident that the degree of liberation increases exponentially with a decrease in particle size. This phenomenon is evident from all the different ores except for the Barberton gold ore. It seems that the degree of liberation of the Barberton ore is constant for particle sizes between 100 and 200 µm. This behaviour could be explained when the minerals of which the Barberton gold ore is composed of, are taken into account. The Barberton

gold ore contains large amounts of arsenopyrite and pyrite (Paragraph 2.2.2) which is not the case for the other gold bearing ores.

It is evident from Figures 4.18 and 4.19 that although the liberation trends of the WDL and FSG gold ores are the same as the other ores (except the Barberton gold ore), the degree of liberation of the smaller particle size fractions is much lower. This is due to the unique mineral composition of the ores. It seems that the gold grains are either very small or intergrown with the gold-bearing minerals, to such an extent that the liberation process, due to comminution, is hindered.

When the experimental (diagnostic leaching) procedure was performed, no distinction was made between gold associated with pyrite and gold associated with arsenopyrite. The reason is that, both pyrite and arsenopyrite are destroyed by nitric acid (Jones and Flemming) (diagnostic leaching procedure - Appendix A) and sulphuric acid destroys arsenopyrite only partially at potentials of 200 to 600 mV (Lorenzen, 1992, p 535 -535) (diagnostic leaching procedure - Appendix A); thus gold associated with arsenopyrite could not distinctly be determined.

4.7 SUMMARY

It was established that ores from different regions and even different locations within a specific region, yield different liberation characteristics, due to the different mineralogies (distribution of different gold bearing minerals in different ores) of the ores. It is evident that although the mineralogies of the ores differ, that the degree of liberation (leachability) increases exponentially with a decrease in particle size. This phenomenon is valid for all the ores, even the Barberton gold ore (for particle sizes smaller than 100 µm). It will thus be possible to model this phenomenon and the properties of the function that describes it, will be a function of the mineralogy of the specific ore.

TABLE 4.1

GOLD DEPORTMENT VS SIZE FRACTION (KINROSS UNMILLED ORE)

Size Fraction [µm]	Mass [%]	Head grade [g/ton]	Free Gold [%]	Gold in BMS [%]	Gold in Pyrite [%]	Gold in Carbon [%]	Gold in Silicate [%]
+300	94.31	3.09	33.29	13.78	7.31	4.62	41.00
-300 +150	1.76	7.63	79.5	9.91	0.23	1.31	9.06
-150 +106	0.71	12.57	85.53	9.03	1.47	0.94	3.03
-106 +75	0.51	14.35	90.55	6.07	0.61	0.93	1.83
-75 +53	0.4	21.76	95.79	2.98	0.38	0.15	0.70
-53	2.32	19.90	97.09	1.36	0.89	0.14	0.52
Total	**100.00**	**3.76**	**36.49**	**13.31**	**6.93**	**4.4**	**38.87**

TABLE 4.2

GOLD DEPORTMENT VS SIZE FRACTION (KINROSS CRUSHED ORE)

Size Fraction [µm]	Mass [%]	Head grade [g/ton]	Free Gold [%]	Gold in BMS [%]	Gold in Pyrite [%]	Gold in Carbon [%]	Gold in Silicate [%]
+300	92.6	3.09	33.29	13.78	7.31	4.62	41.00
-300 +150	3.1	2.92	69.80	16.08	3.75	1.82	8.56
-150 +106	1.0	4.50	84.40	6.00	2.88	3.46	3.27
-106 +75	0.6	4.68	91.68	3.52	0.60	0.56	3.64
-75 +53	0.5	6.68	86.57	2.95	5.17	1.40	3.92
-53	2.2	6.62	89.21	2.95	6.29	1.06	0.50
Total	**100.0**	**3.20**	**36.77**	**13.42**	**7.08**	**4.40**	**38.33**

TABLE 4.3

GOLD DEPORTMENT VS SIZE FRACTION (KINROSS 70% -75µm)

Size Fraction [µm]	Mass [%]	Head grade [g/ton]	Free Gold [%]	Gold in BMS [%]	Gold in Pyrite [%]	Gold in Carbon [%]	Gold in Silicate [%]
+300	4.1	4.2	23.85	8.34	20.55	5.24	42.02
-300 +150	2.2	3.76	76.46	6.80	4.46	5.21	7.07
-150 +106	8.0	3.18	75.20	7.76	4.01	4	9.04
-106 +75	14.4	3.92	79.90	5.08	4.28	6.91	3.83
-75 +53	13.6	3.73	89.00	3.78	2.19	2.33	2.71
-53	57.6	3.52	91.25	2.21	2.87	0.72	2.95
Total	**100**	**3.61**	**84.91**	**3.64**	**3.84**	**2.38**	**5.24**

TABLE 4.4

GOLD DEPORTMENT VS SIZE FRACTION (LESLIE UNMILLED ORE)

Size Fraction [µm]	Mass [%]	Head grade [g/ton]	Free Gold [%]	Gold in BMS [%]	Gold in Pyrite [%]	Gold in Carbon [%]	Gold in Silicate [%]
+300	92.6	8.05	27.87	8.14	11.77	2.81	49.41
-300 +150	2.6	8.60	69.58	19.76	2.44	0.00	8.22
-150 +106	1.2	12.44	81.60	11.76	2.84	0.92	2.88
-106 +75	0.9	36.05	93.42	4.66	0.98	0.36	0.58
-75 +53	0.7	74.88	97.57	1.84	0.21	0.15	0.22
-53	2.0	38.30	98.22	0.78	0.59	0.25	0.17
Total	**100.0**	**9.46**	**32.08**	**8.25**	**11.02**	**2.62**	**46.03**

TABLE 4.5

GOLD DEPORTMENT VS SIZE FRACTION (LESLIE 70% -75µm)

Size Fraction [µm]	Mass [%]	Head grade [g/ton]	Free Gold [%]	Gold in BMS [%]	Gold in Pyrite [%]	Gold in Carbon [%]	Gold in Silicate [%]
+300	18.9	7.12	12.67	6.43	6.21	5.08	69.61
-300 +150	2.0	7.36	79.48	9.70	5.71	1.45	3.70
-150 +106	3.7	10.53	88.85	6.35	2.47	0.52	1.81
-106 +75	7.8	9.48	92.44	5.15	0.53	0.66	1.22
-75 +53	10.2	15.45	96.36	2.24	0.57	0.23	0.60
-53	57.4	5.09	89.74	4.89	3.04	1.66	0.67
Total	**100**	**7.12**	**75.82**	**5.08**	**3.23**	**2.04**	**13.83**

TABLE 4.6

GOLD DEPORTMENT VS SIZE FRACTION (St HELENA UNMILLED ORE)

Size Fraction [µm]	Mass [%]	Head grade [g/ton]	Free Gold [%]	Gold in BMS [%]	Gold in Pyrite [%]	Gold in Carbon [%]	Gold in Silicate [%]
+300	85.0	12.91	13.24	5.79	6.79	11.78	62.41
-300 +150	4.3	10.81	73.25	8.01	3.79	3.78	11.16
-150 +106	2.0	15.19	81.64	5.10	4.54	3.27	5.45
-106 +75	1.5	8.97	59.00	29.85	7.19	1.39	2.57
-75 +53	1.2	16.58	91.76	3.27	1.87	2.58	0.51
-53	6.0	16.72	85.82	7.79	4.86	0.45	1.08
Total	**100**	**13.08**	**23.21**	**6.31**	**6.44**	**10.31**	**53.72**

TABLE 4.7

GOLD DEPORTMENT VS SIZE FRACTION (St HELENA CRUSHED ORE)

Size Fraction [µm]	Mass [%]	Head grade [g/ton]	Free Gold [%]	Gold in BMS [%]	Gold in Pyrite [%]	Gold in Carbon [%]	Gold in Silicate [%]
+300	93.1	12.91	13.24	5.79	6.79	11.78	62.41
-300 +150	2.9	8.47	58.19	25.27	6.96	3.26	6.32
-150 +106	0.8	7.75	71.43	17.14	5.09	3.88	2.45
-106 +75	0.7	11.17	84.90	9.88	1.72	1.37	2.13
-75 +53	0.5	7.00	77.20	9.33	3.03	0.50	4.69
-53	2	3.66	92.64	1.68	0.98	1.31	3.39
Total	**100**	**12.51**	**17.42**	**6.40**	**6.61**	**11.13**	**58.41**

TABLE 4.8

GOLD DEPORTMENT VS SIZE FRACTION (St HELENA 70% -75 µm)

Size Fraction [µm]	Mass [%]	Head grade [g/ton]	Free Gold [%]	Gold in BMS [%]	Gold in Pyrite [%]	Gold in Carbon [%]	Gold in Silicate [%]
+300	19.9	5.24	18.84	8.99	26.45	9.15	36.56
-300 +150	1.6	36.75	85.49	12.15	1.14	0.80	0.41
-150 +106	2.9	30.15	86.14	10.29	2.33	0.83	0.40
-106 +75	5.8	16.55	88.71	7.98	1.69	0.83	0.79
-75 +53	9.0	9.80	78.98	11.14	2.32	6.64	0.92
-53	60.8	5.95	80.36	10.24	2.81	5.55	1.04
Total	**100**	**7.96**	**68.76**	**9.97**	**7.36**	**5.88**	**8.04**

TABLE 4.9

GOLD DEPORTMENT VS SIZE FRACTION (BEATRIX UNMILLED ORE)

Size Fraction [µm]	Mass [%]	Head grade [g/ton]	Free Gold [%]	Gold in BMS [%]	Gold in Pyrite [%]	Gold in Carbon [%]	Gold in Silicate [%]
+300	94.4	7.02	13.39	10.47	10.15	7.49	58.50
-300 +150	1.6	14.62	72.26	11.59	10.32	1.96	3.87
-150 +106	0.6	20.73	83.50	5.12	7.89	2.09	1.41
-106 +75	0.5	26.45	95.50	1.51	2.07	0.87	0.05
-75 +53	0.4	18.61	91.87	4.32	1.91	0.66	1.25
-53	2.5	11.95	89.91	3.63	4.96	0.82	0.69
Total	**100**	**7.49**	**17.40**	**10.22**	**9.33**	**7.14**	**55.30**

TABLE 4.10

GOLD DEPORTMENT VS SIZE FRACTION (BEATRIX 70% -75µm)

Size Fraction [µm]	Mass [%]	Head grade [g/ton]	Free Gold [%]	Gold in BMS [%]	Gold in Pyrite [%]	Gold in Carbon [%]	Gold in Silicate [%]
+300	20.9	6.94	9.66	7.84	14.43	15.12	52.95
-300 +150	0.4	11.89	82.88	4.87	7.43	3.11	1.70
-150 +106	1.1	23.42	88.31	4.30	3.68	1.77	1.94
-106 +75	4.1	17.35	86.96	4.19	3.68	4.77	0.40
-75 +53	8.0	11.52	84.54	4.86	5.74	4.52	0.34
-53	65.4	6.57	76.97	8.80	7.45	6.32	0.46
Total	**100**	**7.70**	**64.05**	**8.03**	**8.58**	**7.89**	**11.45**

TABLE 4.11

GOLD DEPORTMENT VS SIZE FRACTION (HARMONY UNMILLED ORE)

Size Fraction [µm]	Mass [%]	Head grade [g/ton]	Free Gold [%]	Gold in BMS [%]	Gold in Pyrite [%]	Gold in Carbon [%]	Gold in Silicate [%]
+300	98.4	2.62	17.6	6.5	4.6	33.9	37.4
-300 +150	0.8	2.62	77.5	5.8	4.2	6.9	5.6
-150 +106	0.1	6.90	76.9	10.1	7.5	3.0	2.4
-106 +75	0.1	16.32	94.0	1.6	0.6	3.5	0.3
-75 +53	0.1	13.30	36.7	11.7	8.5	14.1	29.0
-53	0.5	4.46	92.0	0.8	0.4	5.6	1.1
Total	**100**	**2.65**	**18.58**	**6.47**	**4.56**	**33.45**	**36.94**

TABLE 4.12

GOLD DEPORTMENT VS SIZE FRACTION (HARMONY 70% -75µm)

Size Fraction [µm]	Mass [%]	Head grade [g/ton]	Free Gold [%]	Gold in BMS [%]	Gold in Pyrite [%]	Gold in Carbon [%]	Gold in Silicate [%]
+300	1.0	2.24	7.22	1.53	3.61	9.8	77.81
-300 +150	7.2	5.77	72.11	20.92	4.52	1.1	1.36
-150 +106	12.1	3.92	92.28	4.20	1.03	1.5	0.97
-106 +75	8.6	3.81	92.35	3.54	0.03	3.1	0.94
-75 +53	11.8	4.51	94.99	3.69	0.49	1.3	0.51
-53	58.3	1.69	92.37	3.70	1.29	1.2	1.45
Total	**100**	**2.76**	**89.43**	**4.81**	**1.30**	**0.54**	**1.98**

TABLE 4.13

GOLD DEPORTMENT VS SIZE FRACTION (UNISEL UNMILLED ORE)

Size Fraction [µm]	Mass [%]	Head grade [g/ton]	Free Gold [%]	Gold in BMS [%]	Gold in Pyrite [%]	Gold in Carbon [%]	Gold in Silicate [%]
+300	92.29	7.65	38.18	8.99	17.26	12.21	23.36
-300 +150	2.12	14.17	72.12	12.17	6.77	1.12	7.83
-150 +106	0.94	18.65	76.82	11.92	8.19	0.46	2.61
-106 +75	0.73	23.75	79.13	14.35	3.29	0.43	2.80
-75 +53	0.60	16.49	74.33	15.78	6.77	0.62	2.50
-53	3.31	12.09	66.87	8.22	5.46	0.64	18.80
Total	**100**	**8.21**	**40.73**	**9.14**	**16.40**	**11.32**	**22.41**

TABLE 4.14

GOLD DEPORTMENT VS SIZE FRACTION (UNISEL 70% -75µm)

Size Fraction [µm]	Mass [%]	Head grade [g/ton]	Free Gold [%]	Gold in BMS [%]	Gold in Pyrite [%]	Gold in Carbon [%]	Gold in Silicate [%]
+300	12.3	9.92	22.95	17.64	25.05	18.21	16.15
-300 +150	3.3	27.14	81.16	10.90	4.67	0.96	2.30
-150 +106	5.8	15.45	87.93	5.96	4.80	0.17	1.14
-106 +75	8.1	15.30	68.08	19.28	10.01	1.67	0.96
-75 +53	10.3	9.39	80.51	6.52	9.88	1.14	1.95
-53	60.2	6.60	82.55	5.81	8.03	1.55	2.06
Total	**100**	**9.20**	**74.09**	**8.62**	**10.18**	**3.47**	**3.65**

TABLE 4.15 (Lorenzen, 1992)

GOLD DEPORTMENT VS SIZE FRACTION (FSG UNMILLED ORE)

Size Fraction [µm]	Mass [%]	Head grade [g/ton]	Free Gold [%]	Gold in BMS [%]	Gold in Pyrite [%]	Gold in Silicate [%]
+300	80.1	4.38	23.0	35.5	31.0	10.5
-300 +150	11.8	10.63	24.6	36.8	28.5	10.1
-150 +106	2.1	8.63	23.8	33.5	25.3	17.4
-106 +75	0.9	15.75	31.2	31.9	24.4	12.5
-75 +53	1.5	18.81	34.5	31.1	21.7	12.3
-53	3.6	14.35	30.4	34.8	31.7	3.1
Total	**100.0**	**5.88**	**25.2**	**35.3**	**29.4**	**10.1**

TABLE 4.16 (Lorenzen, 1992)

GOLD DEPORTMENT VS SIZE FRACTION (FSG 70% -75µm)

Size Fraction [µm]	Mass [%]	Head grade [g/ton]	Free Gold [%]	Gold in BMS [%]	Gold in Pyrite [%]	Gold in Silicate [%]
+300	6.6	2.91	18.1	42.7	34.1	5.1
-300 +150	6.8	3.03	18.2	40.6	32.9	8.3
-150 +106	12.1	3.50	25.6	36.1	31.8	8.1
-106 +75	10.5	5.20	46.0	20.0	22.1	11.1
-75 +53	9.7	6.23	55.1	18.6	20.5	5.8
-53	60.3	6.20	54.2	20.6	23.4	1.8
Total	**100.0**	**5.52**	**47.4**	**23.8**	**24.8**	**4.0**

TABLE 4.17 (Lorenzen, 1992)

GOLD DEPORTMENT VS SIZE FRACTION (WDL UNMILLED ORE)

Size Fraction [µm]	Mass [%]	Head grade [g/ton]	Free Gold [%]	Gold in BMS [%]	Gold in Pyrite [%]	Gold in Silicate [%]
+300	78.0	2.98	7.4	30.5	47.0	15.1
-300 +150	11.7	5.96	7.9	30.0	46.1	16.0
-150 +106	4.4	6.21	8.4	30.6	43.6	17.4
-106 +75	1.0	6.70	10.1	27.2	45.2	17.5
-75 +53	0.8	9.87	12.1	30.5	42.0	15.4
-53	4.1	8.29	11.8	25.8	44.2	18.2
Total	**100.0**	**3.78**	**8.3**	**29.9**	**46.1**	**15.7**

TABLE 4.18 (Lorenzen, 1992)

GOLD DEPORTMENT VS SIZE FRACTION (WDL 70% -75 µm)

Size Fraction [µm]	Mass [%]	Head grade [g/ton]	Free Gold [%]	Gold in BMS [%]	Gold in Pyrite [%]	Gold in Silicate [%]
+300	1.2	1.85	5.9	39.5	49.2	5.4
-300 +150	5.3	2.20	6.8	34.6	53.6	5.0
-150 +106	12.8	2.60	11.2	33.1	49.6	6.2
-106 +75	9.7	3.41	18.5	32.3	43.1	6.2
-75 +53	9.1	4.70	21.3	29.6	39.8	9.4
-53	61.9	4.30	22.8	29.3	10.5	7.4
Total	**100.0**	**3.86**	**20.2**	**30.1**	**42.1**	**7.5**

TABLE 4.19

GOLD DEPORTMENT VS SIZE FRACTION (BARBERTON UNMILLED ORE)

Size Fraction [µm]	Mass [%]	Head grade [g/ton]	Free Gold [%]	Gold in BMS [%]	Gold in Pyrite [%]	Gold in Carbon [%]	Gold in Silicate [%]
+300	86.2	8.70	4.01	10.66	71.70	8.70	4.94
-300 +150	2.5	9.76	16.09	30.06	49.34	2.70	1.80
-150 +106	1.4	19.08	15.08	54.48	24.75	5.20	0.49
-106 +75	1.2	30.07	18.00	36.43	43.19	1.88	0.49
-75 +53	0.9	35.21	24.04	43.21	25.83	6.65	0.27
-53	7.9	7.83	36.39	38.20	19.66	4.11	1.64
Total	**100**	**9.29**	**7.36**	**14.51**	**65.65**	**8.04**	**4.45**

TABLE 4.20

GOLD DEPORTMENT VS SIZE FRACTION (BARBERTON 70% -75µm)

Size Fraction [µm]	Mass [%]	Head grade [g/ton]	Free Gold [%]	Gold in BMS [%]	Gold in Pyrite [%]	Gold in Carbon [%]	Gold in Silicate [%]
+300	9.9	5.75	7.89	8.20	68.23	10.98	4.71
-300 +150	3.6	6.46	24.67	36.87	35.97	1.21	1.28
-150 +106	5.4	9.53	24.62	23.35	48.49	2.89	0.65
-106 +75	8.4	15.33	22.68	16.79	57.07	2.93	0.53
-75 +53	9.1	22.92	24.46	32.55	38.24	4.36	0.39
-53	63.7	9.84	29.51	33.30	33.51	2.78	0.90
Total	**100**	**10.94**	**25.90**	**28.96**	**40.24**	**3.70**	**1.20**

TABLE 4.21 (Lorenzen, 1992)

GOLD DEPORTMENT VS SIZE FRACTION (HARTIES UNMILLED ORE)

Size Fraction [µm]	Mass [%]	Head grade [g/ton]	Free Gold [%]	Gold in BMS [%]	Gold in Pyrite [%]	Gold in Silicate [%]
+300	72.5	11.5	40.9			
-300 +150	13.3	14.1	51.2			
-150 +106	6.0	12.8	55.4			
-106 +75	1.8	14.9	65.6			
-75 +53	2.8	18.1	73.1			
-53	3.8	16.9	69.8			
Total	**100.0**	**12.4**	**45.7**	**8.3**	**8.3**	**37.7**

TABLE 4.22 (Lorenzen, 1992)

GOLD DEPORTMENT VS SIZE FRACTION (HARTIES 70% -75 µm)

Size Fraction [µm]	Mass [%]	Head grade [g/ton]	Free Gold [%]	Gold in BMS [%]	Gold in Pyrite [%]	Gold in Silicate [%]
+300	1.0	8.5	25			
-300 +150	7.2	10.6	2[illegible]			
-150 +106	12.1	10.7	32.8			
-106 +75	8.6	11.8	54.6			
-75 +53	11.8	13.3	75.8			
-53	58.3	12.8	77.0			
Total	**100.0**	**12.23**	**67.4**	**7.7**	**4.9**	**20.0**

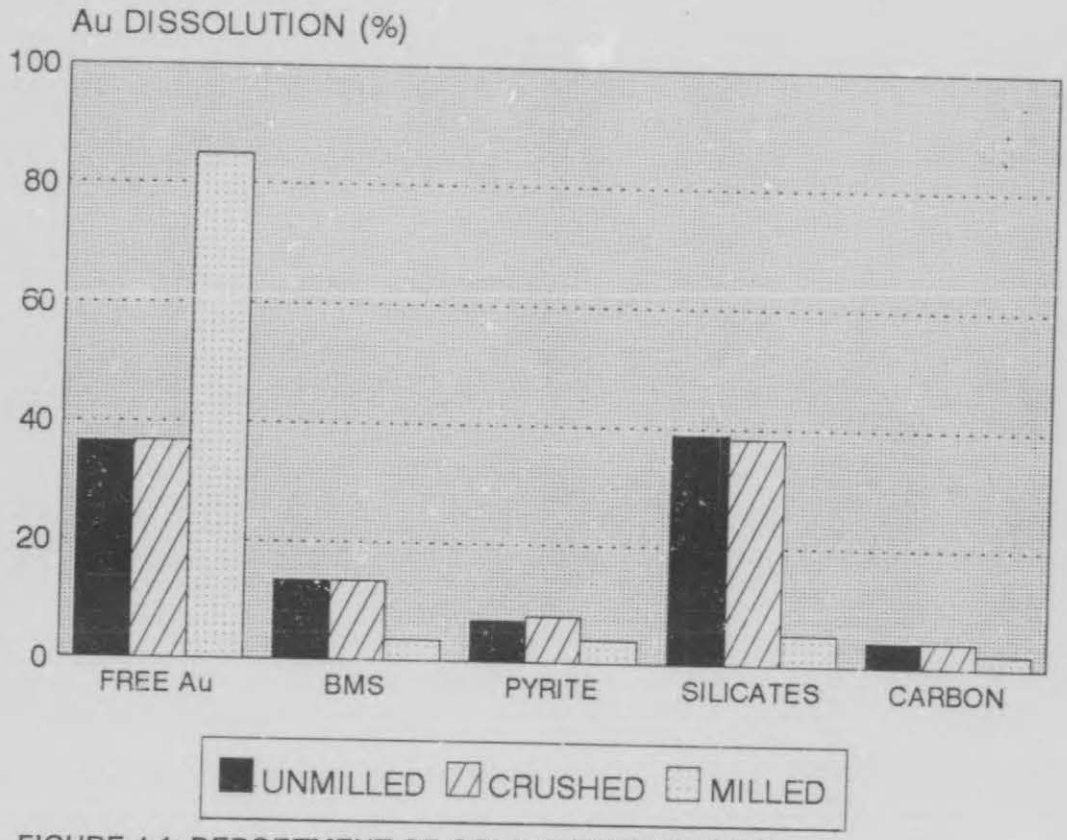

FIGURE 4.1: DEPORTMENT OF GOLD IN KINROSS ORE.

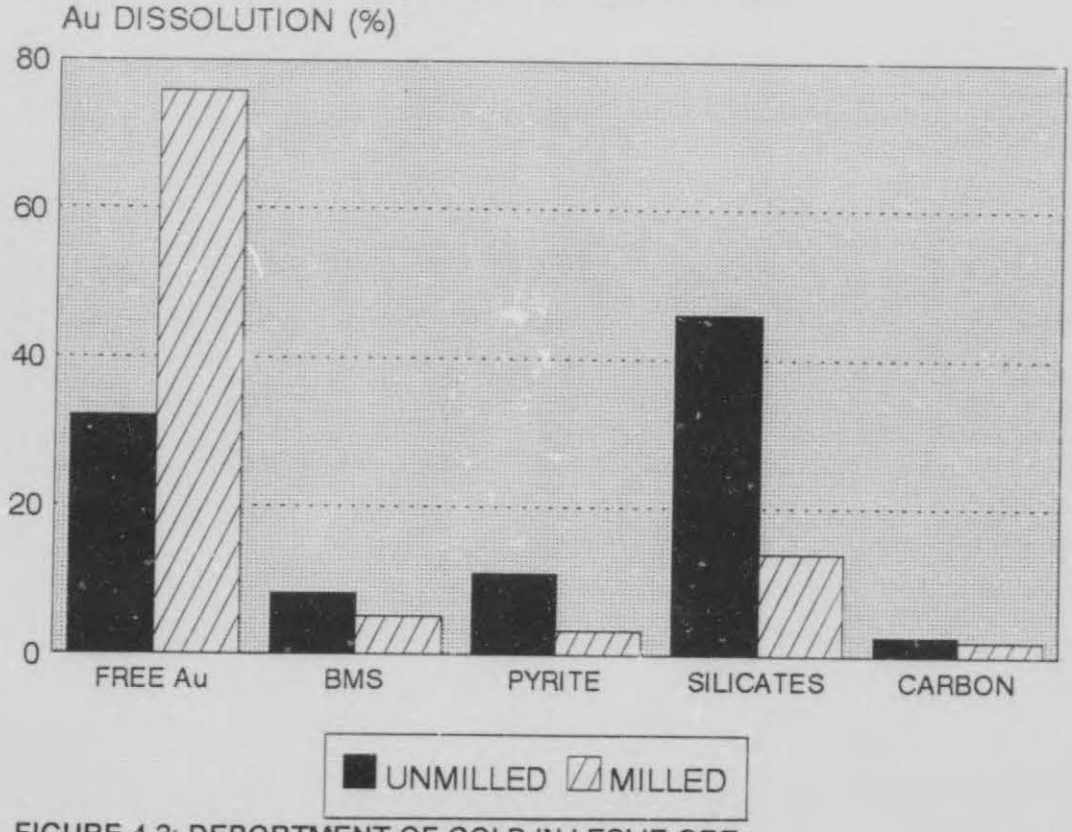

FIGURE 4.2: DEPORTMENT OF GOLD IN LESLIE ORE.

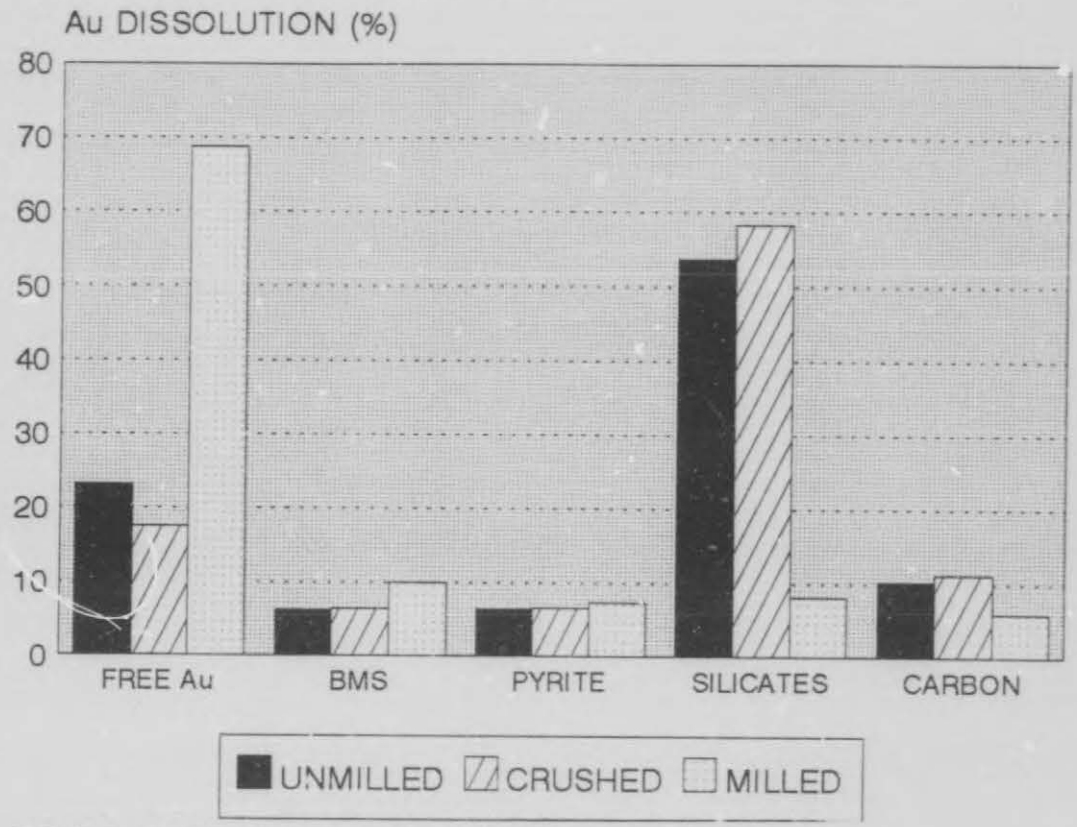

FIGURE 4.3: DEPORTMENT OF GOLD IN St. HELENA ORE.

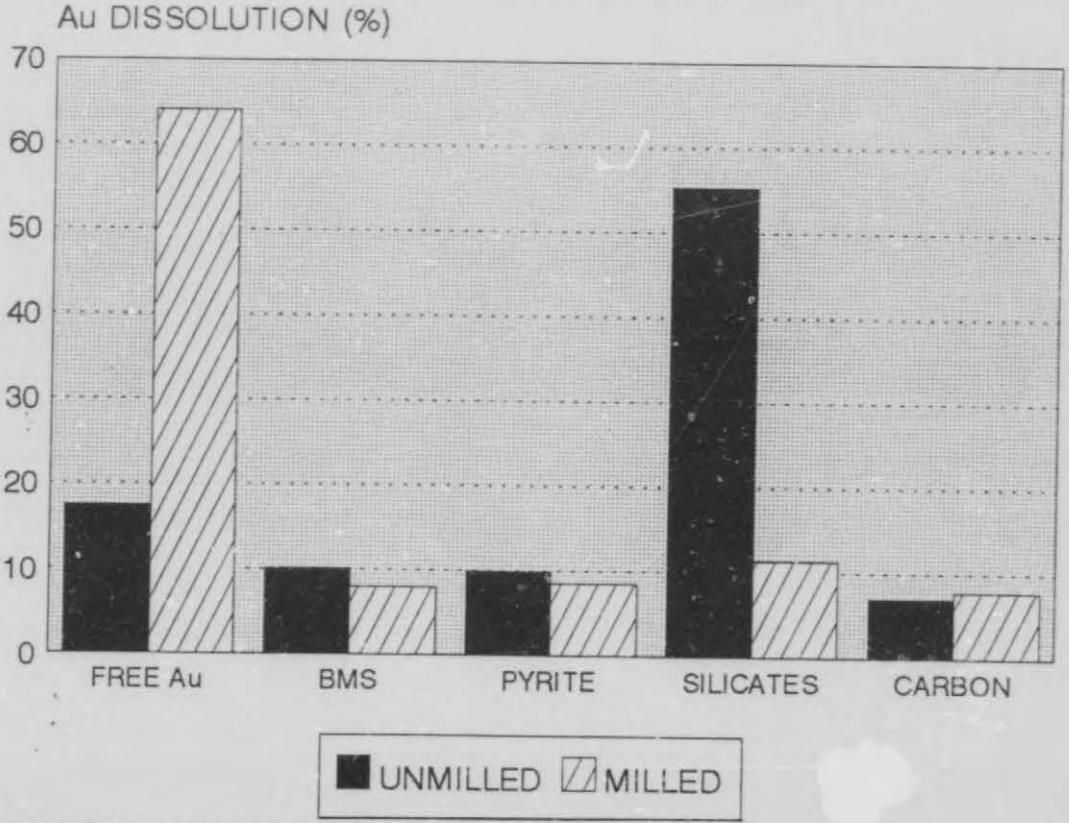

FIGURE 4.4: DEPORTMENT OF GOLD IN BEATRIX ORE.

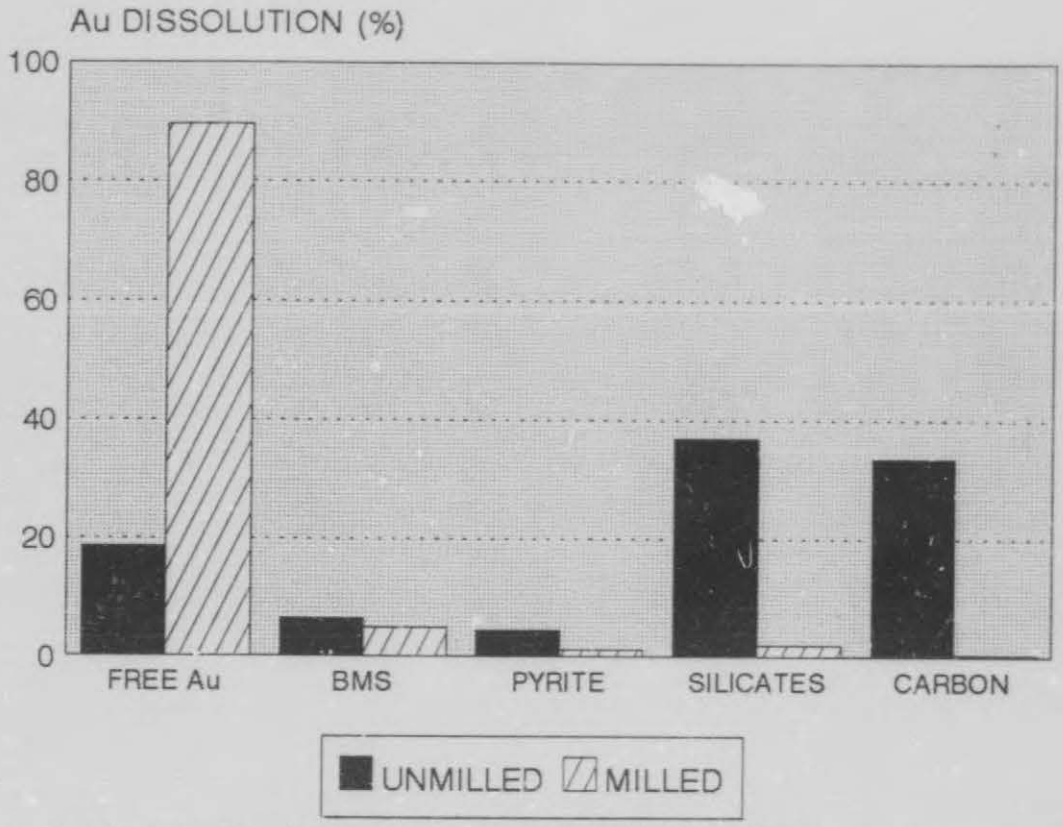

FIGURE 4.5: DEPORTMENT OF GOLD IN HARMONY ORE.

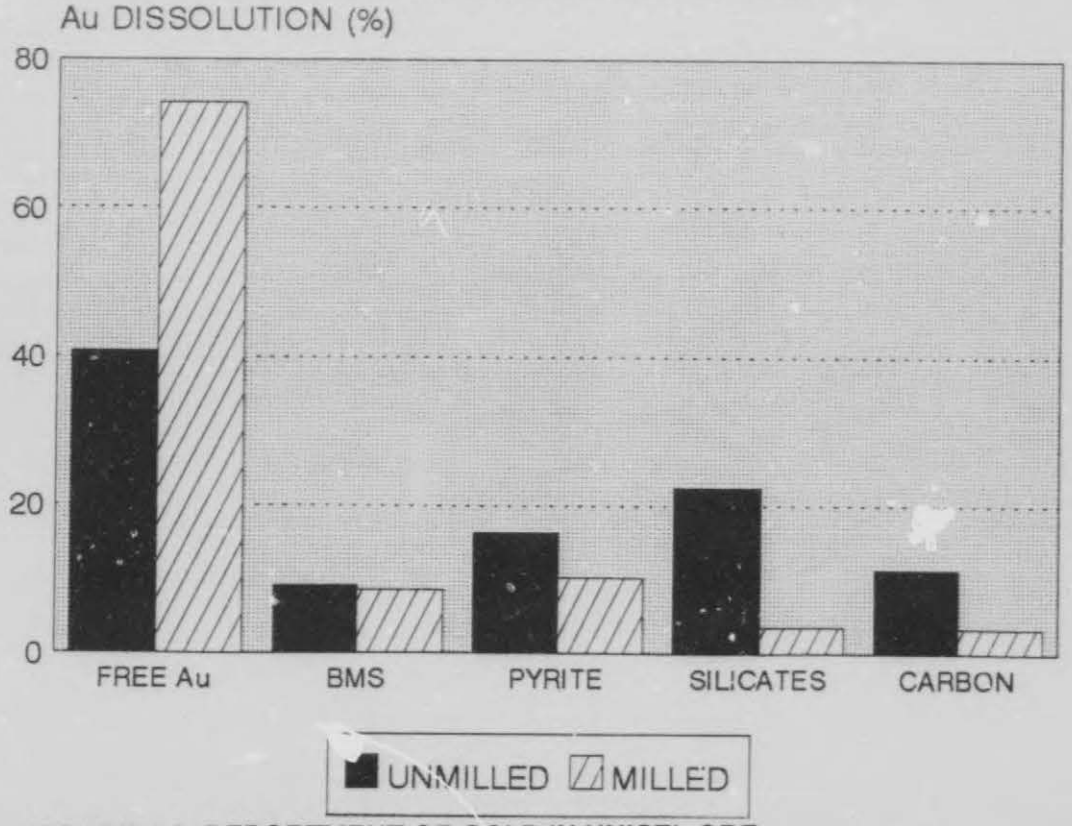

FIGURE 4.6: DEPORTMENT OF GOLD IN UNISEL ORE.

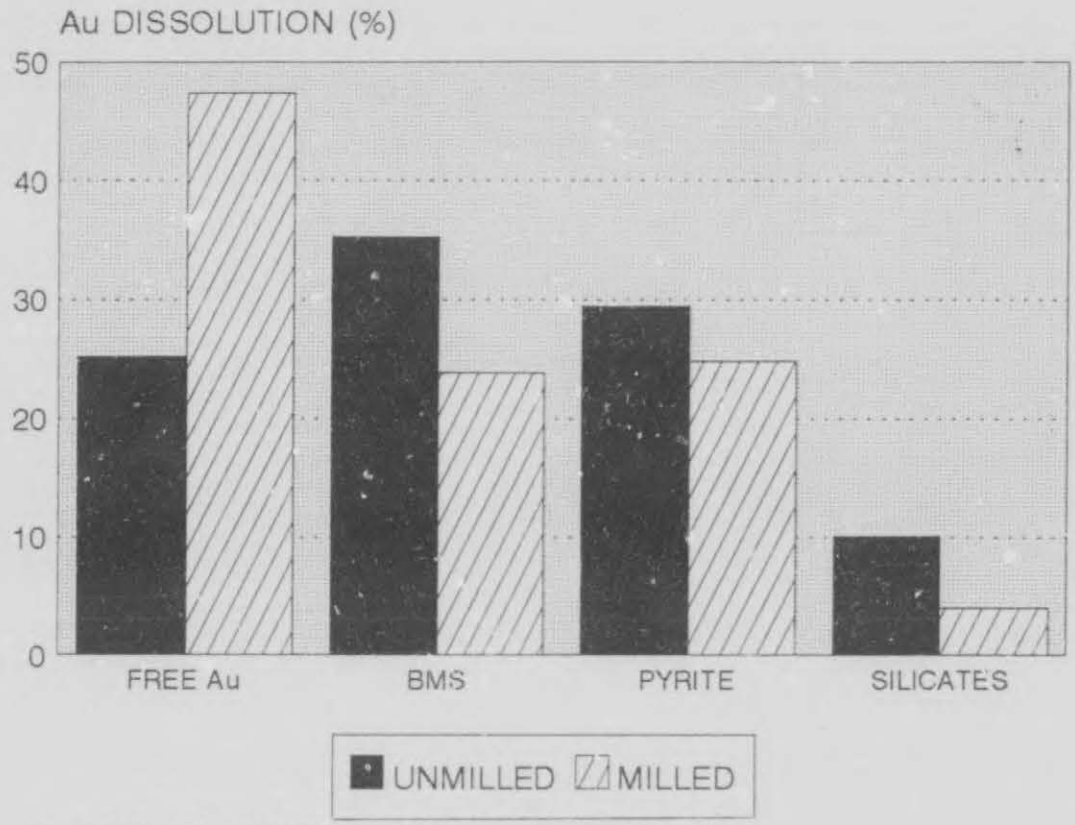

FIGURE 4.7: DEPORTMENT OF GOLD IN FSG ORE.

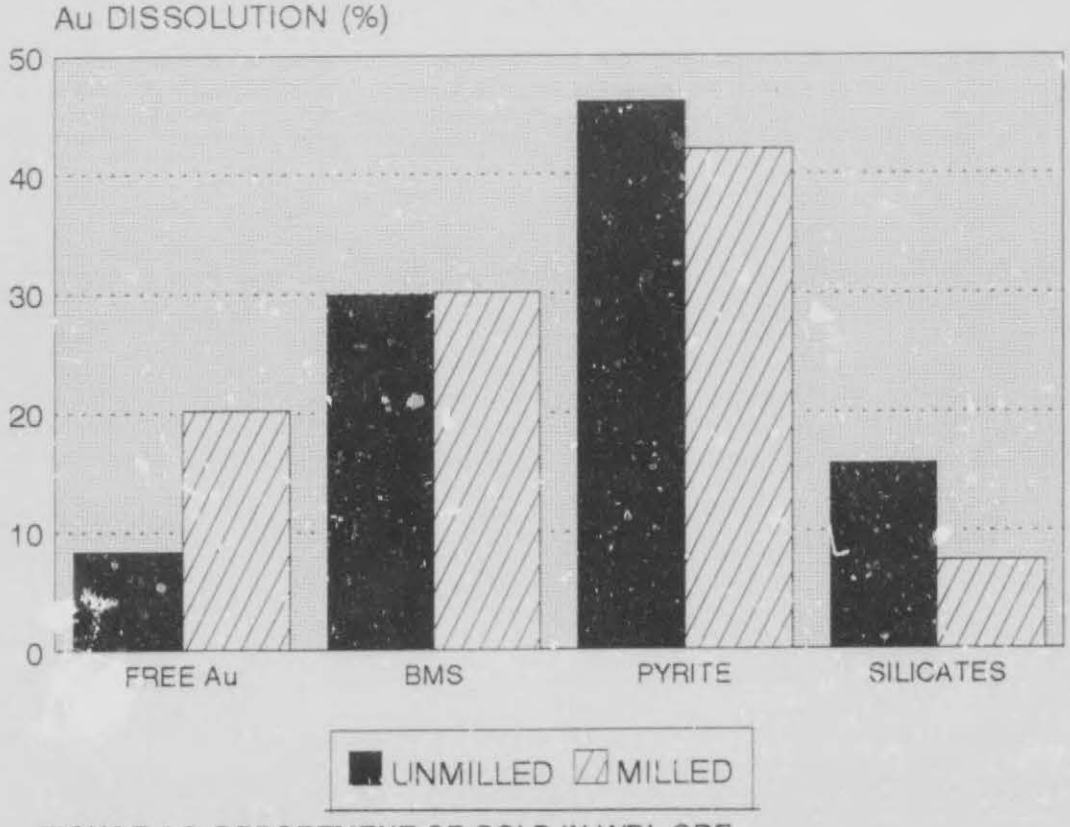

FIGURE 4.8: DEPORTMENT OF GOLD IN WDL ORE.

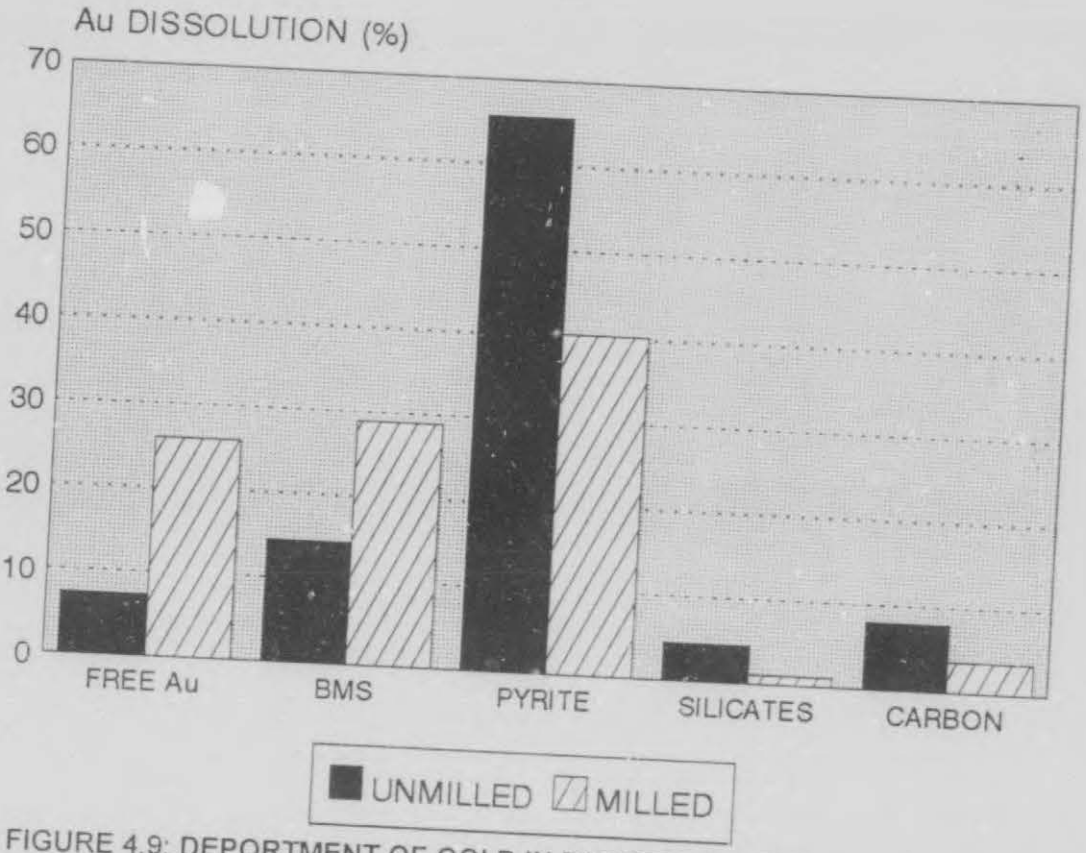

FIGURE 4.9: DEPORTMENT OF GOLD IN BARBERTON ORE.

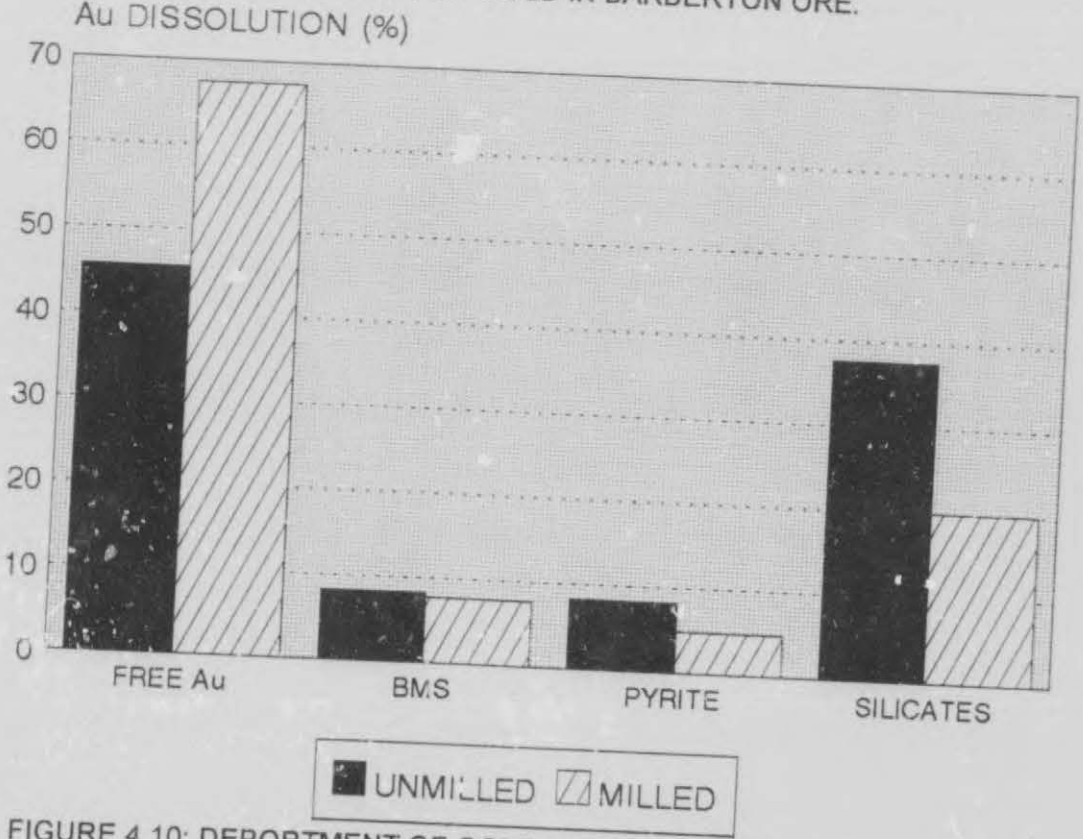

FIGURE 4.10: DEPORTMENT OF GOLD IN HARTIES ORE.

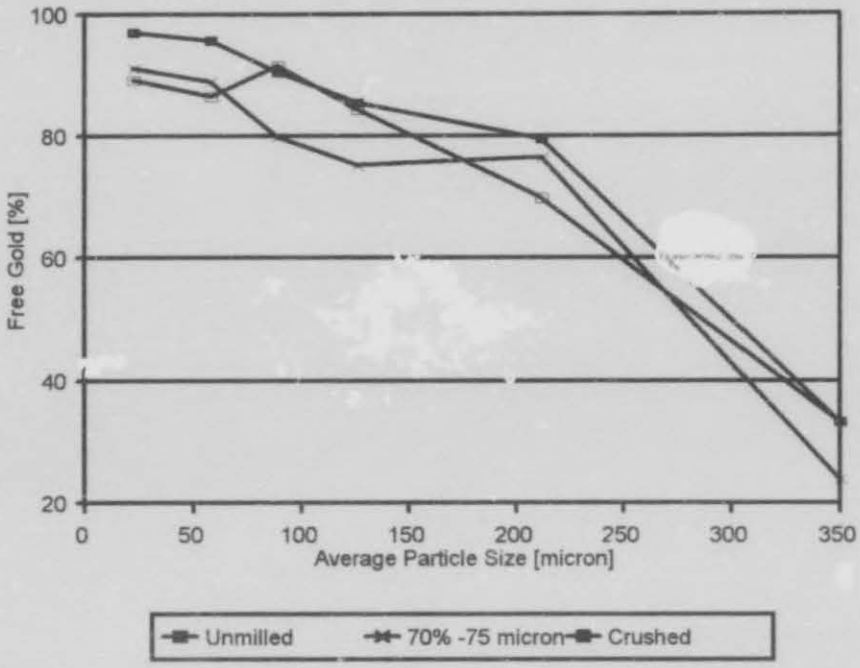

FIGURE 4:11:FREE GOLD AS A FUNCTION OF PARTICLE SIZE (KINROSS).

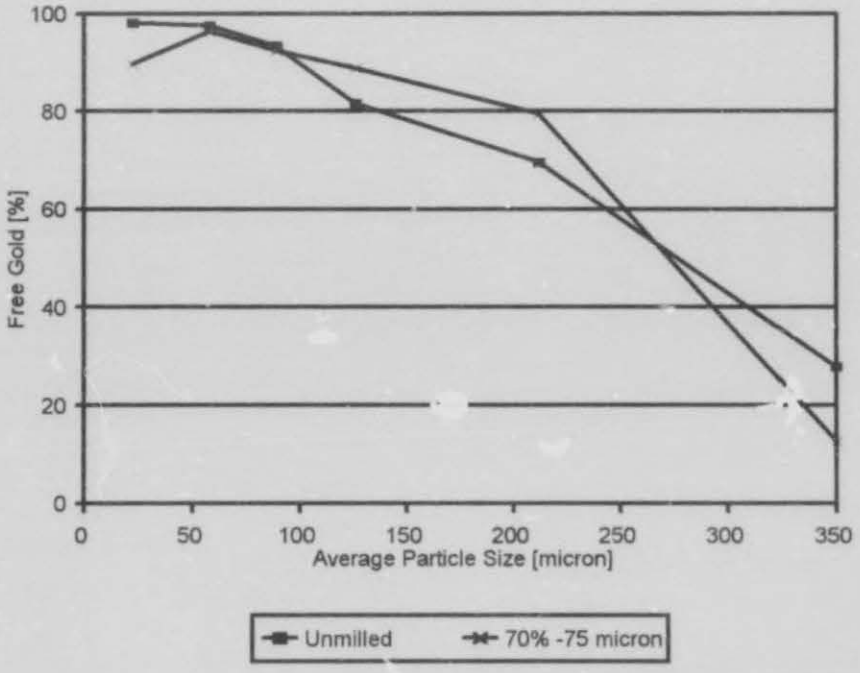

FIGURE 4:12:FREE GOLD AS A FUNCTION OF PARTICLE SIZE (LESLIE).

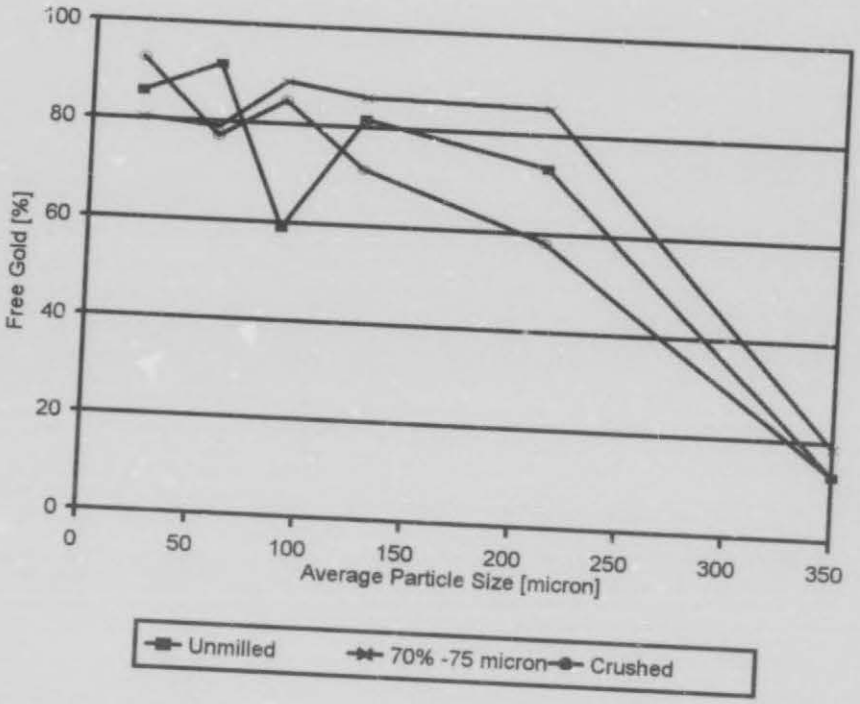

FIGURE 4:13:FREE GOLD AS A FUNCTION OF PARTICLE SIZE (St. HELENA).

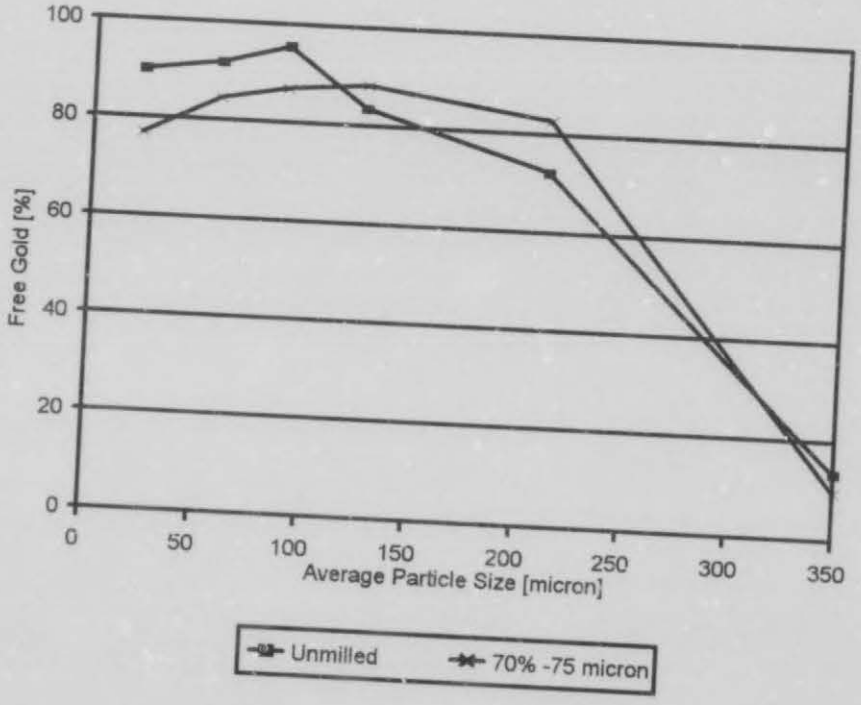

FIGURE 4:14:FREE GOLD AS A FUNCTION OF PARTICLE SIZE (BEATRIX).

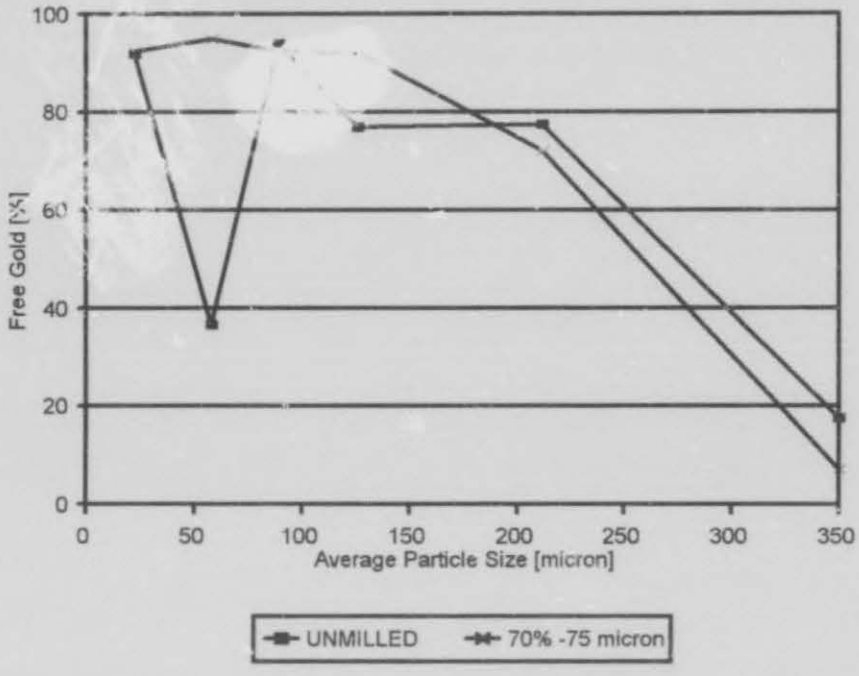

FIGURE 4:15:FREE GOLD AS A FUNCTION OF PARTICLE SIZE (HARMONY).

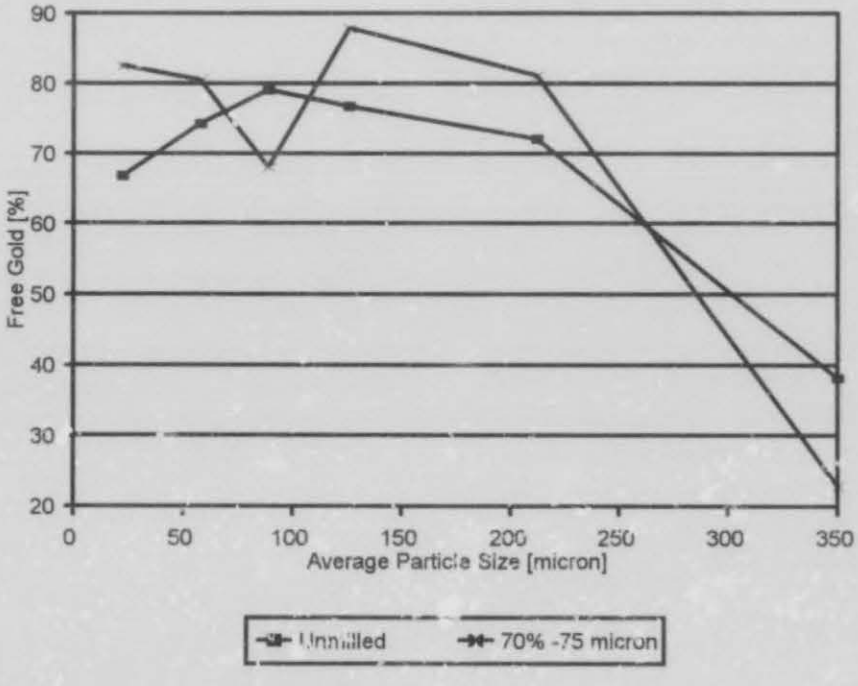

FIGURE 4:16:FREE GOLD AS A FUNCTION OF PARTICLE SIZE (UNISEL).

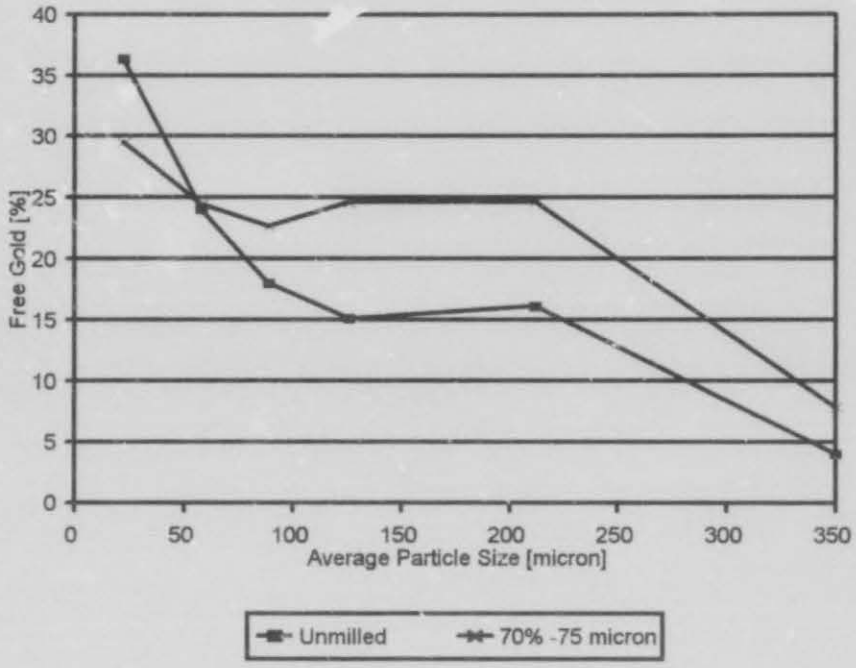

FIGURE 4:17:FREE GOLD AS A FUNCTION OF PARTICLE SIZE (BARBERTON)

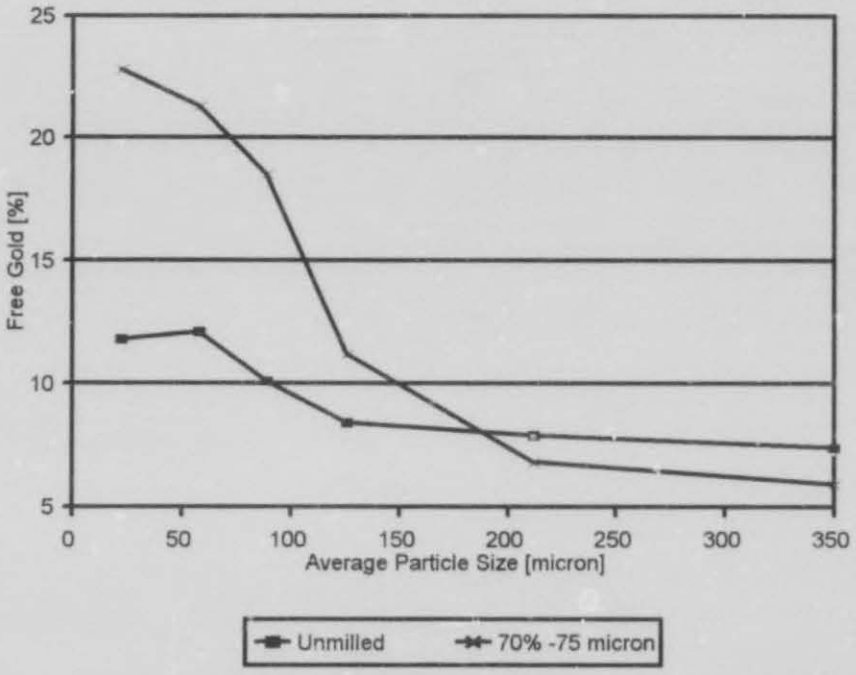

FIGURE 4:18:FREE GOLD AS A FUNCTION OF PARTICLE SIZE (WDL).

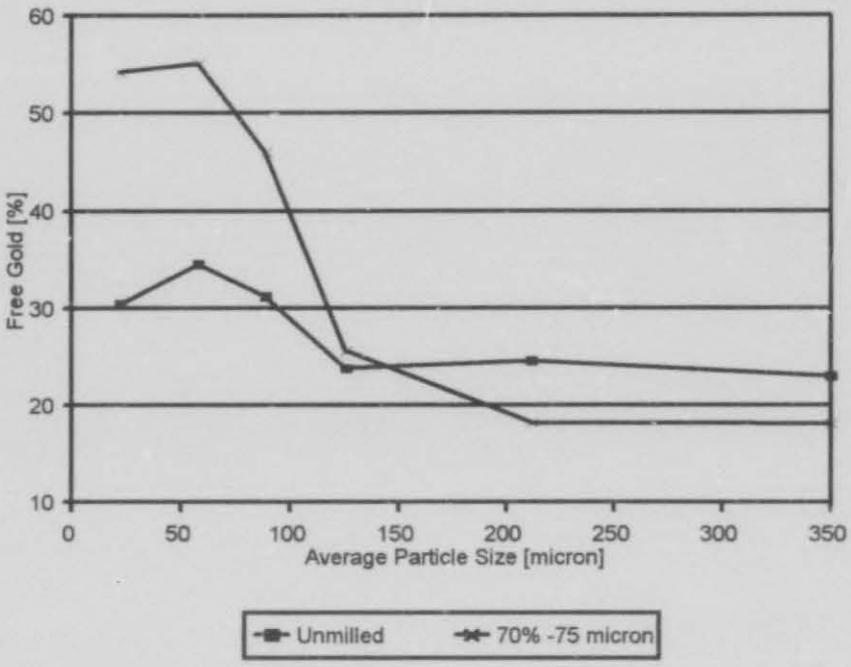

FIGURE 4:19:FREE GOLD AS A FUNCTION OF PARTICLE SIZE (FSG)

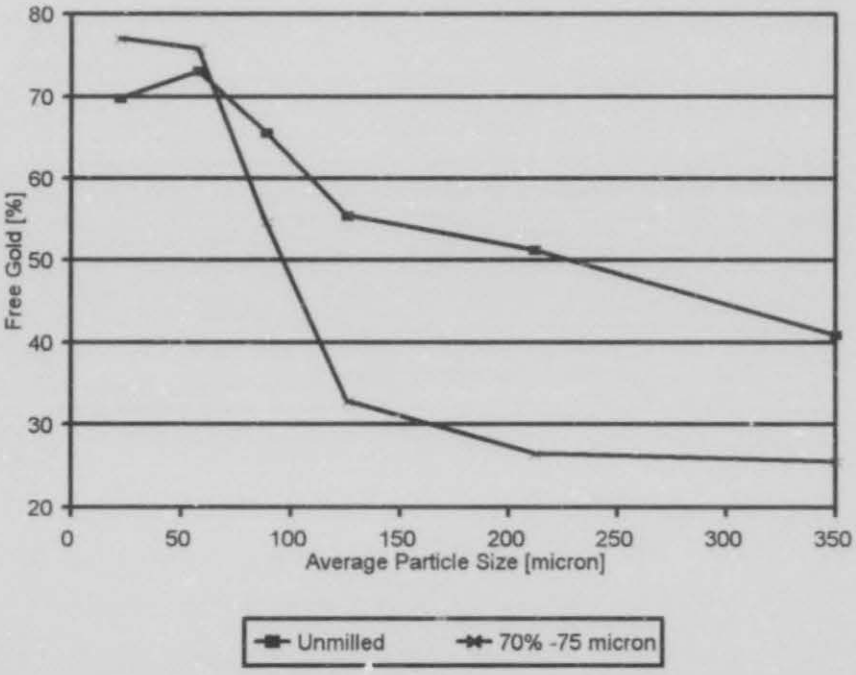

FIGURE 4:20:FREE GOLD AS A FUNCTION OF PARTICLE SIZE (HARTIES).

CHAPTER 5

DISCUSSION OF THE LIBERATION MODELS

CHAPTER 5

DISCUSSION OF LIBERATION MODELS

In this chapter, the applicability of the different liberation models (chapter 2) in predicting leachable gold as a function of particle size, is discussed. As stated earlier, liberated gold is always leachable but the inverse is not always true, due to for example, the leachability of gold particles situated in minor cracks. It is thus evident that the liberation models as discussed in chapter 2 would probably underestimate the amount of leachable gold in each particle size fraction. Lorenzen and Van Deventer (1994) found this to be true when they investigated King's liberation model as a possible model to predict leachable gold as a function of particle size.

Some of the liberation models discussed in chapter 2 are very inaccurate in predicting the degree of liberation due to certain assumptions and other factors which are addressed in the following sections.

5.1 SHORTCOMINGS IN GENERAL

5.1.1 Random breakage

The assumption of random breakage was critically reviewed by Laslett et al (1990) and it was concluded from the investigation of a chalcopyrite bearing ore that random breakage did not occur, but that fracturing along grain boundaries was occurring. According to G.G. Stanley (1987) small irregular masses of gold occupy interstitial spaces between grains and pebbles of quartz. Mineralogical analysis (report from Beatrix Gold Mine) of the Beatrix reef was done and it was found that most of the gold (70%) occurs as free gold interstitially to quartz. Since most of the gold in the unmilled ore samples was associated with the silicates (see Tables 4.1 to 4.20 - chapter 4), one would expect to some extend that grain boundary fracture was occurring when the ores were comminuted.

Recrystalized gold or gold distributed by metaphoric processes within the reef makes up 5 to 40% of the total gold in an ore, depending on the local conditions (GG. Stanley, 1987). Hallbauer (G.G. Stanley, 1987) found that this type of gold occurs either as epitaxial growth on pyrite or as crack filling in various minerals. Cracks (macro or microscopic) in an ore are

defects which result in fracture propagation whenever the ore tolerates strain in operations such as crushing and milling.

It is thus evident, although not quantitatively, that when a gold ore is comminuted, the assumption of random breakage is not always valid.

5.1.2 Steriology

Some researchers attempt to predict the degree of liberation by assuming one or two dimensions instead of addressing a three dimensional problem in three dimensions. Chayes (King, 1979) examined the validity of assuming equivalence between the fraction of a line through the ore to the volumetric fraction in the ore as a whole, critically, though inadequately. According to G.G. Stanley (1987) most gold particles occur as hackly grains exhibiting serrated outlines. Rounded and oval grains of gold that are perfectly preserved are encountered only rarely in the matrix of the Witwatersrand banket. Single grains of gold are relatively common in some areas of the matrix, but more often the grains occur in clusters. It is thus evident that spherical gold particles are a rare phenomenon and a distribution of different shapes is generally encountered. The mentioned assumption is thus not valid since the linear intercept lengths (a one dimensional measurement) are determined from cross sections of the ore and a different orientation of a gold particle will result in a different measure for the linear intercept length.

5.1.3 Particle shape

Assumptions regarding the shape of a particle are commonly made by researchers. Theories are derived for particles of simple geometry such as spherical, cubic, rectangular, etc. It is important to remember that this is very idealistic and could result in inaccurate predictions by such models.

5.1.4 Interrelationship of texture and particle production

Barbery and Le Roux (1988) found when they compared liberation models, published up to 1988, that all researchers agree on the assumption that particle production and texture are not related. Only Davy (1984) makes a

presentation for the possibility of deriving a solution in the important practical case where texture and particle production are related, that is for intergranular fracture and preferential breakage of one phase. Unfortunately, Davy (1984) could not provide a clear outline or a solution to the question at hand. From the results presented in Table 4.1 to 4.20 it is evident that the liberation of gold from the silicates is quite expeditious compared to the other minerals. It appears that the silicates break preferentially to set the locked gold free. As earlier discussed, it is believed that intergranular breakage does occur when the gold ores are comminuted. It is thus believed that the interrelationship between texture and particle production does exist.

5.1.5 Mineralogy

In most of the liberation models the degree of liberation is a function of particle size and some measurement to account for the mineralogy of the ore. These measurements are either difficult or impossible to obtain. The measurements include linear intercept lengths, the size distribution of the valuable mineral in the ore, the particle size at which the degree of liberation is 50%, etc. All these measurements are impractical for the everyday use on a plant due to excessive time usage and high costs in determining these measurements.

The different factors as discussed above for the different liberation models, are presented in Tables 5.1 and 5.2.

5.2 SHORTCOMINGS OF THE DIFFERENT MODELS

The major shortcomings of the different models are summarised in the following sections.

5.2.1 Gaudin model

Gaudin (1939) considered a two-phase ore to be distributed as cubical mineral grains in the matrix of the host rock. Despite this unrealistic assumption with respect to the grain structure of the minerals in the ore, the fracture pattern resulting from crushing and milling is also assumed to be perfectly cubical and the fracture planes parallel to the edges of the mineral grains. The model is also based on the size ratio between the cubical grain structure and that of the cubical fracture pattern that is not amenable to precise measurement. It must be noted that only transgranular breakage was considered and no provision was made for intergranular breakage of the ore. This model is thus highly idealistic and of no practical importance.

5.2.2 The Wiegel liberation model

The liberation model proposed by Wiegel (1967) is just an extension of the Gaudin model (1939). The only difference between the two models is that Wiegel provides for the random arrangement of mineral grains and thus describes the haphazard appearance of a real mineral system more realistically. Apart from this improvement, all the other shortcomings of the Gaudin model also apply to the model developed by Wiegel.

5.2.3 The King liberation model (King, 1979)

Although the model is free of any empirical constants and no assumptions were made about the shape of the grains or particles, the model is based on the distribution of one dimensional intercept lengths that could be measured under the microscope. Equivalence between the fraction of a line through the ore to the volumetric fraction of the ore as a whole is assumed. King assumed in deriving the model that the ore is a random assemblage of mineral grains with distinct boundaries between adjacent grains and that fracture does not occur preferentially along grain boundaries; nor do small fragments of one material "fall out" of larger particles of the other.

Despite these shortcomings, the model could be extended to predict leachable gold as a function of particle size.

5.2.4 The Klimpel and Austin model

The model (Klimpel and Austin, 1983) is based on a simple binary system of component B occluded in a matrix of A, with the volume fraction of B being very small in the matrix. The grains of B are randomly dispersed in the matrix with no preferential fracture through A or B. It is assumed that random fracture occurs. The model is mathematical solved using a Monte Carlo simulation. However, Klimpel (1984) derived analytical solutions to the model by assuming several grain size distributions of the minor component and that only one grain of B is occluded in the formation of an AB particle. Thus, the approach used by the authors only has limited practical utility.

5.2.5 Liberation model developed by Meloy and Gotoh

The authors (Meloy and Gotoh, 1985) assumed apart from the fact that there is no preferential breakage between the grains, that the shapes of the particles and the inclusions are spherical and that the inclusions are randomly distributed. The greatest drawback of the algorithm is the need for the inclusion size distribution in order to integrate over the set boundaries.

5.2.6 Liberation model developed by G. Barbery

The model (Barbery, 1991) was developed only for ore textures that correspond to Boolean schemes with primary Poisson polyhedra and Poisson polyhedral textures. The model predicts the degree of liberation from the particle size (D) of the ore and the particle size at which the degree of liberation is 0.5 (D_{50}). The measurement of D_{50} is very tedious and impractical and is thus the greatest drawback of this model.

5.2.7 Liberation model developed by Hsih and Wen

The model developed by Hsih and Wen (1994) is the first to incorporate intergranular fracture and thus realising that random breakage does not always occur. They extended the Gaudin model by incorporating a detachment factor. The authors also assumed the ore to consist of cubical

grains but provided for a variation in grain and particle sizes in the derivation of their model. In order to calculate the degree of liberation from the proposed model, one needs not only the grain sizes and particle sizes, but unfortunately also the detachment factor that is difficult to obtain. The authors provided a graph (Hsih and Wen, 1994) relating the detachment factor to the difference in hardness (Mohs hardness) of the adjacent minerals.

The model was derived for the case where the particle sizes are smaller than the grain sizes. Since the particles are in the most cases coarser than the gold grains, the model does not apply to this investigation.

5.2.8 Model proposed by Lorenzen

The model proposed by Lorenzen and Van Deventer (1994) is the first and at this stage, the only model that predicts leachable gold as a function of particle size. They extended the King liberation model as described in section 2.7.1 to accommodate the amount of gold that is not related to liberation due to comminution. Besides the shortcomings of the King liberation model the proposed model has some additional shortcomings, namely:

1. The addition of an empirical constant
2. The term that was added to the King model is mathematically incorrect, since the exponent of a non-dimensionless variable, particle diameter, was taken. The only way to rectify this problem is by
   (a) giving the empirical constant a unit of exp(μm), or
   (b) giving the numerator a unit of μm, or
   (c) add a mathematically correct term

   Solutions (a) and (b) are however, trivial, leaving solution (c) as the only option.
3. The King liberation model was derived for a binary assembly of minerals only. However, Lorenzen did not consider the different mineral species in the ores individually, resulting only in reasonable predictions. The accuracy of the predictions could be improved when the binary analysis is performed on each mineral in turn.

5.2.9 Exposure model developed by Hsih and co-workers

Hsih and co-workers (Wen et al, 1995) developed an exposure model for gold ores by assuming the mineral grains to be cubical. They incorporated an intergranular fracturing factor in their model, to provide for exposure (liberation) due to detachment (intergranular fracture). Despite the assumptions regarding the shapes of particles and grains, the model developed by Hsih and co-workers with few alterations applies to the current investigation.

5.3 SUMMARY

From the above discussion it is evident that the model developed by Hsih and co-workers and the model extended by Lorenzen are the only models suitable for the development of an accurate model that predicts the leachable gold as a function of particle size. It is, however, expected at this stage, that the exposure model developed by Hsih and co-workers might give more accurate predictions than the model extended by Lorenzen since the former provided for the amount of gold liberated by detachment in the derivation of their model.

TABLE 5.1

TEXTURE CHARACTERISATION METHODS PRESENTED BY VARIOUS RESEARCHERS

Researchers	Grain shape	Grain dimensions	Phases relationships
Gaudin	Square	Monosize	Checkerboard
Wiegel	Cubic	Monosize	Cube
Bodziony	Any	Any	Regular pattern
Steiner	Any	Any	Any
King	Any	Any	Any
Klimpel & Austin	Any	Various cases	One minor, small constituent
Meloy & Gotoh	Ball	Monosize	Hard spheres in a matrix
Serra/Davy/Barbery	Any	Any	Any
Lorenzen(1992,1994)	Any	Any	Any
Hsih et al (1994,1995)	Cubic	Monosize	Cube

Reference: Barbery and Le Roux, 1988 except Lorenzen and Hsih et al

TABLE 5.2

PARTICLE PRODUCTION CHARACTERISATION METHODS USED BY VARIOUS RESEARCHERS

Researchers	Dimen-sionality	Particle shape	Breakage method	Practical significance
Gaudin	Two	Square	Random	None
Wiegel	Three	Cubic	Random	None
Bodziony	Three	Any (convex)	Random	Some
Steiner	Three	Any	Random	Some
King	One	Segments	Random	Some
Klimpel & Austin	One	Segments	Random	Some
Meloy & Gotoh	Three	Ball	Random	None
Serra/Davy/ Barbery	Three	Any (convex)	Random	Some
Lorenzen (1992, 1994)	One	Segments	Random	Some
Hsih et al (1994, 1995)	Three	Cubic	Trans- and intergranular	Some

Reference: Barbery and Le Roux, 1988 except Lorenzen and Hsih et al

CHAPTER 6

EMPIRICAL MODEL

CHAPTER 6

EMPIRICAL MODEL

Due to the complex nature of the liberation (leaching) process, it was decided to fit the obtained liberation data to the corresponding particle size as a first attempt to model, mineral liberation. The computer package, TBL Curve, was used to model this highly complex phenomenon. As a first attempt only the non-refractory ores were considered in modelling the liberation data. After the liberation of the refractory ores was modelled, a general model for both refractory and non-refractory ores was constructed which was partially successful, due to reasons that will be discussed in subsequent sections.

The proposed models calculate the fraction of gold liberated (exposed) from each individual mineral with the corresponding reduction in the particle size of the ore. The gold enclosed by each mineral versus the geometric mean of the particle size fraction was fitted empirically. It was found that the liberation pattern of gold enclosed by a specific mineral, is the same for all the ores when the ores are comminuted. General expressions for the different liberation patterns were thus determined and found to be functions of not only the particle size but also of two parameters (constants for a specific ore). The sum of the fractions of gold enclosed by each mineral is thus the total amount of unliberated (unexposed) gold, and the degree of liberation (leachability) can easily be determined.

$$\mathrm{Au}_{\substack{Liberated/\\Leachable}} = 100 - (\mathrm{Au}_{Silicates} + \mathrm{Au}_{BMS} + \mathrm{Au}_{Pyrite} + \mathrm{Au}_{\substack{Carbonaceous\\material}}) \qquad (6.1)$$

where

$$Au_{BMS} = a_1 + b_1\sqrt{d} \qquad (6.2)$$

$$Au_{Pyrite} = e^{a_2 + b_2\sqrt{d}} \qquad (6.3)$$

$$Au_{\substack{Carbonaceous\\material}} = a_3 + b_3 \ln d \qquad (6.4)$$

$$Au_{Silicates} = e^{a_4 + b_4 d} \qquad (6.5)$$

where d - particle size in μm

$a_1, b_1 \ldots a_4, b_4$ - constants for an ore with a specific mineralogy.

Au - percentage of gold associated with a specific mineral [%].

Thus, the general equation for the amount of gold liberated (leachable) in a specific ore, is as follows:

$$\mathrm{Au}_{\substack{\text{Liberated/}\\ \text{Leachable}}} = 100 - \left((a_1 + a_3) + b_1\sqrt{d} + b_3 \ln d + e^{a_2 + b_2\sqrt{d}} + e^{a_4 + b_4 d}\right) \qquad (6.6)$$

It was found that the above relations (the amount of gold enclosed in a specific mineral as a function of particle size) were applicable to both the refractory and non-refractory ores, as would be expected. The constants namely, $a_1, b_1 \ldots b_4$, were found to differ depending on the mineralogy (gold deportment) of the ore. The constants were found to be functions of the total grade of gold in the different mineral species in the unmilled ore. In determining the functions for the different constants only three ores were used. The remaining ores were than used to test the validity of these functions.

The different functions obtained for the non-refractory and refractory ores are discussed in the following sections.

6.1 AN EMPIRICAL MODEL FOR THE NON-REFRACTORY ORES

Different ores were used to determine the functions for the different constants. They are as follows:

1. for constants a_1 and b_1 the Kinross, St. Helena and Beatrix gold ores,
2. for constants a_2 and b_2 the Unisel, Kinross and Leslie gold ores,
3. for constants a_3 and b_3 the Unisel, Kinross, Leslie and Beatrix gold ores
4. for constants a_4 and b_4 the Unisel, Kinross and Beatrix gold ores were used.

Model 1:

$$a_1 = 0.305 + 3640.2\exp(-B)$$
$$b_1 = 0.335 + 3.594\times10^{-7}\exp(B) \qquad (6.7a)$$

$$a_2 = \exp\left(1.644 - \frac{15.42}{P}\right)$$
$$b_2 = 0.0664 - 3.993\times10^{-9}\exp(P) \qquad (6.7b)$$

$$a_3 = -1.044 - 3.750\exp\left[\frac{-(C-7.14)^2}{4.594}\right]$$

$$b_3 = 0.324 + 1.128\exp\left[\frac{-(C-4.4)^2}{4.594}\right] \qquad (6.7c)$$

$$a_4 = 1.167 - 1.576\times10^{-5}S^3$$

$$b_4 = \exp(-2.689 - \frac{93.935}{S}) \qquad (6.7d)$$

where $a_1, b_1 \ldots a_4, b_4$ - constants for an ore with a specific mineralogy

B - amount of gold(%) in the unmilled ore associated with the BMS.

C - amount of gold(%) in theunmilled ore associated with carbonaceous material

P - amount of gold(%) in the unmilled ore associated with pyrite.

S - amount of gold(%) in the unmilled ore associated with silicates.

Equations (6.7a) to (6.7d) could be used with confidence in expectancy of fairly accurate results whenever the mineralogy of the ore under investigation satisfies the following constraints:

1. $6\% < B < 14\%$
2. $6\% < P < 17\%$
3. $2\% < C < 12\%$
4. $22\% < S < 56\%$

6.2 AN EMPIRICAL MODEL FOR THE REFRACTORY ORES

A full data summary of only three refractory ores was available, namely the Barberton, WDL and FSG gold ores. The validity of the proposed model could thus not be proven. It must be noted that the fraction of gold associated with carbonaceous material was not determined by Lorenzen (1992a) for the WDL and FSG gold ores. The constants for equation (6.4) could thus not be determined. The functions for the remaining constants have the following form:

Model 2:

$$a_1 = 28.791 - 1.274 \times 10^{-14} \exp(B)$$
$$b_1 = 0.486 + 1.006 \times 10^{-15} \exp(B) \quad (6.8a)$$

$$a_2 = 3.391 - 4.375 \times 10^{12} \exp(-P)$$
$$b_2 = 0.040 + 1.164 \times 10^{11} \exp(-P) \quad (6.8b)$$

$$a_4 = 1.544 - 249.387 \exp(-S)$$
$$b_4 = \exp(-4.299 - 0.134 \times S) \quad (6.8c)$$

Equations (6.8a) to (6.8c) are valid when the following constraints are satisfied:

1. $14\% < B < 36\%$
2. $29\% < P < 66\%$
3. $8\% < S < 15\%$

6.3 A GENERAL EMPIRICAL MODEL

As previously stated, an empirical model was developed for both the non-refractory and refractory ores, thus taking the mineralogy of a wide range of ores into account. The functions for the different constants were determined by using mostly five ores:

1. constants a_1 and b_1 the Kinross, Leslie, Beatrix, St. Helena, Barberton, WDL and FSG gold ores,
2. constants a_2 and b_2 the Unisel, Kinross, Beatrix, Barberton and FSG gold ores,
3. constants a_3 and b_3 the Unisel, Kinross, Leslie, Beatrix and Barberton gold ores,
4. constants a_4 and b_4 the Leslie, Unisel, Beatrix, Barberton and WDL gold ores were used.

Model 3:

$$a_1 = -429.614 - 65.526B - 924.426 \ln B + 1016.42\sqrt{b}$$
$$b_1 = 0.372 + 0.007B - \frac{4.481}{B^2} + 9.441 \times 10^{-8} \exp(B) \quad (6.9a)$$

$$a_2 = (1.928 - \frac{8.372}{P})^2$$
$$b_2 = \exp(-2.714 - 9.810 \times 10^{-5} P^2) \quad (6.9b)$$

$$a_3 = -1.043 + 3.960 \exp\left[\frac{-(C-7.14)^2}{4.594}\right]$$
$$b_3 = 0.287 + 1.171 \exp\left[\frac{-(C-4.4)^2}{4.594}\right] \quad (6.9c)$$

$$a_4 = 1.256 - 1.723 \times 10^{-5} S^3 - 224.586 \exp(-S)$$
$$b_4 = 0.021 + 6.330 \times 10^{-4} S - 0.011 \ln(S) \quad (6.9d)$$

with the variables being the same as defined in equations (6.7) and (6.8).

The following constraints apply to equations (6.9a), (6.9b), (6.9c) and (6.9d).

1. $6\% < B < 36\%$
2. $6\% < P < 66\%$
3. $2\% < C < 12\%$
4. $8\% < S < 56\%$

6.4 DISCUSSION

The results obtained from the non-refractory ore-model (model 1 - equations 6.6 and 6.7) compared to the experimental results, are shown in Tables 6.1 to 6.6. The results of the refractory ore-model (model 2 - equations 6.6 and 6.8) and those of the general model (model 3 - equation 6.6 and 6.9) are shown in Tables 6.7 to 6.10 and Tables 6.11 to 6.20, respectively. The average percentage error was used as criterion to which the accuracy of the models was tested.

The percentage error for each particle size fraction, was calculated from the experimentally determined free gold values and those predicted by the models. The average percentage error was thus calculated from the following function:

$$\%\,\text{error} = \frac{(\text{Experimental value} - \text{Predicted value})}{\text{Experimental value}} \times 100$$

$$\%\,\text{average error} = \frac{\sum_{1}^{5} |\%\,\text{error}_i|}{5} \qquad (6.10)$$

where i - different size fractions

Although the gold deportment of the +300 µm particle size fraction of the milled ore samples was predicted by the empirical models (see Tables 6.1 to 6.20), the percentage error of that particle size fraction was not calculated, since the empirical models were only fitted on the gold deportment data that corresponded to particle size fractions smaller than 300 µm.

From Figures 6.1 to 6.6 and Tables 6.1 to 6.6 it is evident that model 1 gives good predictions for all non-refractory ores, with an average error within boundaries of experimental error (average error being smaller than 10% in most cases, except for the Unisel gold ore with an average error of 11.6%).

This, however, is not the case for model 2 (the refractory ore-model) when Figures 6.7 to 6.10 and Tables 6.7 to 6.10 are studied. The average error differs from 17% to 27%. The experimentally determined degree of liberation (leachability) for the Barberton gold ore differs quite substantially from the predicted values especially for particle sizes greater than 70 µm. The reason for the underestimation of the degree of liberation (leachability) is evident when the liberation (leachability) trends of the different refractory ores are compared. It seems that the degree of liberation (leachability) of the Barberton ore is constant for particle sizes between 100 and 200 µm, while that is not the case for the WDL and FSG gold ores, where the degree of liberation (leachability) decreases with increase in particle size. The reason for this phenomenon is discussed in Chapter 4.

Figures 6.1 to 6.10 and Tables 6.11 to 6.20 present the results obtained from model 3 (general model). It is noticeable that the model in some cases predicts the degree of liberation (leachability) slightly more accurately than model 1 and 2, for example the Harmony, Unisel and FSG gold ores, but unfortunately in other cases, such as WDL, Kinross and Barberton gold ores even more inaccurate predictions are made. When the results from models 1 and 2 are compared with the results of model 3, it is evident from Figures 6.1 to 6.10 that the degree of liberation (leachability) predicted by models 1 and 2 differ only with a fairly constant value from the predictions made by model 3.

A summary of the average errors encountered with the different models for each ore is given in Table 6.21.

When the prediction of the gold, enclosed by the individual minerals, is considered in general, it is quite evident from Tables 6.1 to 6.20 that the predictions of the unliberated gold associated with the base metal sulphides (BMS) are the most inaccurate. This is because the base metal sulphides include a number of different minerals, such as uraninite, sphalerite, labile copper sulphides, etc. each having its own characteristics and texture and thus, liberating gold differently when the specific mineral is fragmented. The liberation (leachabilty) of gold from pyrite, silicates and carbonaceous material, in general, is predicted fairly accurately by the different models, as expected.

Although diagnostic leaching was not performed by Lorenzen (1992) on the individual size fractions of the Harties gold ore (only the gold deportment of the unmilled and milled ore as a whole is known), the empirical models were still used to predict the degree of liberation (leachabilty). Unfortunately, none of the models was capable of predicting the degree of liberation (leachability) accurately. This was due to inaccurate predictions of the gold enclosed by the silicates. It is evident from the other gold-bearing ores that the gold enclosed by the silicates is normally easily liberated when the ore is milled. This occurrence, however, was not found when the Harties gold ore was comminuted. The general model (model 3) predicts that ±5% of the total amount of gold will still be enclosed by the silicates after the ore had been milled to 70% -75µm. The experimentally determined fraction, however, was 20% of the total amount of gold. The only explanation for this phenomenon is that the gold associated with the silicates was not only associated with the silicates, but also associated with other minerals such as kerogen and carbon.

6.5 SUMMARY

In this chapter empirical models are proposed for non-refractory and/or refractory ores as a first attempt to model mineral liberation or the leachability of gold from different minerals. The degree of liberation (leachability) is found to be a function of particle size and the mineralogy (gold deportment of the unmilled ore) of the ore. The models in general predict the degree of liberation (leachability) of an ore milled to 70% -75µm fairly well. It is recommended that the models are used only if the specified constraints are satisfied. Furthermore, is it advisable that model 1 (non-refractory ore model)

and model 2 (refractory ore model) rather than model 3 (general model) should be used in the prediction of the degree of liberation (leachability) of a milled ore.

TABLE 6.1

GOLD DEPORTMENT (EXPERIMENTAL AND MODEL 1 PREDICTIONS) VS SIZE FRACTION (KINROSS 70% -75 µm)

Size Fraction [µm]	Mass [%]	Free Gold [%].		Au in BMS [%]		Au in Pyrite [%]	
		Exp.	Predict.	Exp.	Predict.	Exp.	Predict.
+300	4.1	23.85	65.65	8.34	10.63	20.55	4.90
+150-300	2.2	76.46	75.87	6.80	8.35	4.46	3.72
+106-150	8.0	75.20	81.07	7.76	6.50	4.01	2.98
+75 -106	14.4	79.90	83.45	5.08	5.52	4.28	2.64
+53 -75	13.6	89.00	85.75	3.78	4.51	2.19	2.34
-53	57.6	91.25	89.39	2.21	2.96	2.87	1.94
Total	**100**	**84.91**		**3.64**		**3.84**	

TABLE 6.1 (continue)

Size Fraction [µm]	Mass [%]	Au in carbon [%]		Au in Silicates [%]		Error [%]
		Exp.	Predict.	Exp.	Predict.	
+300	4.1	5.24	8.20	42.02	10.63	-
+150-300	2.2	5.21	7.47	7.07	4.60	0.78
+106-150	8.0	4.00	6.71	9.04	2.73	7.81
+75-106	14.4	6.91	6.21	3.83	2.18	4.44
+53-75	13.6	2.33	5.59	2.71	1.81	3.66
-53	57.6	0.72	4.24	2.95	1.46	2.04
Total	**100**	**2.38**		**5.24**		**3.74**

TABLE 6.2

GOLD DEPORTMENT (EXPERIMENTAL AND MODEL 1 PREDICTIONS) VS SIZE FRACTION (LESLIE 70% -75 µm)

Size Fraction [µm]	Mass [%]	Free Gold [%].		Au in BMS [%]		Au in Pyrite [%]	
		Exp.	Predict.	Exp.	Predict.	Exp.	Predict.
+300	18.9	12.67	67.69	6.43	7.55	6.21	7.60
+150-300	2.0	79.48	81.86	9.67	6.15	5.71	5.78
+106-150	3.7	88.85	86.78	6.35	5.03	2.47	4.63
+75 -106	7.8	92.44	88.66	5.15	4.43	0.53	4.12
+53 -75	10.2	96.36	90.32	2.24	3.82	0.57	3.65
-53	57.4	89.74	92.66	4.89	2.87	3.04	3.03
Total	**100**	**75.82**		**5.08**		**3.23**	

TABLE 6.2 (continue)

Size Fraction [µm]	Mass [%]	Au in carbon [%]		Au in Silicates [%]		Error [%]
		Exp.	Predict.	Exp.	Predict.	
+300	18.9	5.08	1.98	69.91	15.18	-
+150-300	2.0	1.45	1.72	3.70	4.49	3.00
+106-150	3.7	0.52	1.46	1.81	2.10	2.33
+75-106	7.8	0.66	1.28	1.22	1.52	4.09
+53-75	10.2	0.23	1.06	0.60	1.15	6.27
-53	57.4	1.66	0.59	0.67	0.85	3.26
Total		**2.04**		**13.83**		**3.79**

TABLE 6.3

GOLD DEPORTMENT (EXPERIMENTAL AND MODEL 1 PREDICTIONS) VS SIZE FRACTION (BEATRIX 70% -75 µm)

Size Fraction [µm]	Mass [%]	Free Gold [%].		Au in BMS [%]		Au in Pyrite [%]	
		Exp.	Predict.	Exp.	Predict.	Exp.	Predict.
+300	20.9	9.66	64.28	7.84	6.89	14.43	6.81
+150-300	0.4	82.88	81.73	4.87	5.46	7.43	5.17
+106-150	1.1	88.31	86.13	4.30	4.31	3.68	4.15
+75 -106	4.1	86.96	87.72	4.19	3.69	3.68	3.68
+53 -75	8.0	84.54	89.13	4.86	3.06	5.74	3.26
-53	65.4	76.97	91.13	8.80	2.09	7.45	2.71
Total	**100**	**64.05**		**8.03**		**8.58**	

TABLE 6.3 (continue)

Size Fraction [µm]	Mass [%]	Au in carbon [%]		Au in Silicates [%]		Error [%]
		Exp.	Predict.	Exp.	Predict.	
+300	20.9	15.12	4.69	52.95	17.33	-
+150-300	0.4	3.11	4.52	1.70	3.12	1.40
+106-150	1.1	1.77	4.35	1.94	1.07	2.48
+75-106	4.1	4.77	4.23	0.40	0.68	0.88
+53-75	8.0	4.52	4.08	0.34	0.46	5.43
-53	65.4	6.32	3.77	0.46	0.30	18.40
Total		**7.89**		**8.58**		**5.72**

TABLE 6.4

GOLD DEPORTMENT (EXPERIMENTAL AND MODEL 1 PREDICTIONS) VS SIZE FRACTION (St. HELENA 70% -75 µm)

Size Fraction [µm]	Mass [%]	Free Gold [%].		Au in BMS [%]		Au in Pyrite [%]	
		Exp.	Predict.	Exp.	Predict.	Exp.	Predict.
+300	19.9	18.84	63.39	8.99	13.19	26.45	4.64
+150-300	1.6	85.49	80.14	12.15	11.80	1.14	3.52
+106-150	2.9	86.14	84.31	10.29	10.69	2.33	2.82
+75 -106	5.8	88.71	85.78	7.98	10.09	1.69	2.51
+53 -75	9.0	78.98	87.05	11.14	9.48	2.32	2.22
-53	60.8	80.36	88.87	10.24	8.53	2.81	1.84
Total	**100**	**68.76**		**9.97**		**7.36**	

TABLE 6.4 (continue)

Size Fraction [µm]	Mass [%]	Au in carbon [%]		Au in Silicates [%]		Error [%]
		Exp.	Predict.	Exp.	Predict.	
+300	19.9	9.15	1.28	36.56	17.50	-
+150-300	1.6	0.80	1.12	0.41	3.42	6.26
+106-150	2.9	0.83	0.95	0.40	1.24	2.13
+75-106	5.8	0.83	0.83	0.79	0.80	3.31
+53-75	9.0	6.64	0.70	0.92	0.55	10.23
-53	60.8	5.55	0.40	1.04	0.37	10.58
Total	**100**	**5.88**		**8.04**		**6.50**

TABLE 6.5

GOLD DEPORTMENT (EXPERIMENTAL AND MODEL 1 PREDICTIONS) VS SIZE FRACTION (HARMONY 70% -75 µm)

Size Fraction [µm]	Mass [%]	Free Gold [%].		Au in BMS [%]		Au in Pyrite [%]	
		Exp.	Predict.	Exp.	Predict.	Exp.	Predict.
+300	2.0	7.22	66.66	1.53	12.22	3.61	3.86
+150-300	7.2	72.11	80.19	20.92	10.83	4.52	2.93
+106-150	12.1	92.28	83.17	4.20	9.71	1.03	2.35
+75 -106	8.6	92.35	84.35	3.54	9.11	0.03	2.09
+53 -75	11.8	94.99	85.48	2.69	8.50	0.49	1.85
-53	58.3	92.37	87.17	3.70	7.55	1.29	1.53
Total	**100**	**89.43**		**4.81**		**1.30**	

TABLE 6.5 (continue)

Size Fraction [µm]	Mass [%]	Au in carbon [%]		Au in Silicates [%]		Error [%]
		Exp.	Predict.	Exp.	Predict.	
+300	2.0	9.8	4.83	77.81	12.43	-
+150-300	7.2	1.1	4.62	1.36	1.44	11.20
+106-150	12.1	1.5	4.40	0.97	0.37	9.87
+75-106	8.6	3.1	4.25	0.94	0.21	8.67
+53-75	11.8	1.3	4.07.	0.51	0.13	10.03
-53	58.3	1.2	3.67	1.45	0.07	5.63
Total	**100**	**0.54**		**1.98**		**9.08**

TABLE 6.6

GOLD DEPORTMENT (EXPERIMENTAL AND MODEL 1 PREDICTIONS) VS SIZE FRACTION (UNISEL 70% -75 µm)

Size Fraction [µm]	Mass [%]	Free Gold [%].		Au in BMS [%]		Au in Pyrite [%]	
		Exp.	Predict.	Exp.	Predict.	Exp.	Predict.
+300	12.3	22.95	83.68	17.64	7.03	25.05	4.50
+150-300	3.3	81.16	86.00	10.90	5.62	4.67	4.25
+106-150	5.8	87.93	87.77	5.96	4.49	4.80	4.07
+75 -106	8.1	68.08	88.70	19.28	3.89	10.01	3.97
+53 -75	10.3	80.51	89.64	6.52	3.27	9.88	3.87
-53	60.2	82.55	91.14	5.81	2.32	8.03	3.73
Total	**100**	**74.09**		**8.62**		**10.18**	

TABLE 6.6 (continue)

Size Fraction [µm]	Mass [%]	Au in carbon [%]		Au in Silicates [%]		Error [%]
		Exp.	Predict.	Exp.	Predict.	
+300	12.3	18.21	0.94	16.15	3.85	-
+150-300	3.3	0.96	0.78	2.30	3.34	5.96
+106-150	5.8	0.17	0.61	1.14	3.06	0.18
+75-106	8.1	1.67	0.50	0.96	2.95	30.28
+53-75	10.3	1.14	0.36	1.95	2.86	11.34
-53	60.2	1.55	0.06	2.06	2.75	10.40
Total	**100**	**3.47**		**3.65**		**11.63**

TABLE 6.7

GOLD DEPORTMENT (EXPERIMENTAL AND MODEL 2 PREDICTIONS) VS SIZE FRACTION (BARBERTON 70% -75 µm)

Size Fraction [µm]	Mass [%]	Free Gold [%].		Au in BMS [%]		Au in Pyrite [%]	
		Exp.	Predict.	Exp.	Predict.	Exp.	Predict.
+300	9.9	7.89	-7.98	8.20	37.88	68.23	62.64
+150-300	3.6	24.67	5.98	36.87	35.87	35.97	53.09
+106-150	5.4	24.62	14.97	23.35	34.25	48.49	46.47
+75 -106	8.4	22.68	19.31	16.79	33.38	57.07	43.27
+53 -75	9.1	24.46	23.46	32.55	32.49	38.24	40.24
-53	63.7	29.51	29.51	33.30	31.12	33.51	35.96
Total	**100**	**25.90**		**28.96**		**40.24**	

TABLE 6.7 (continue)

Size Fraction [µm]	Mass [%]	Au in carbon [%]		Au in Silicates [%]		Error [%]
		Exp.	Predict.	Exp.	Predict.	
+300	9.9	10.98	4.00	4.71	3.45	-
+150-300	3.6	1.21	3.84	1.28	1.23	75.76
+106-150	5.4	2.89	3.67	0.65	0.64	39.20
+75-106	8.4	2.93	3.56	0.53	0.49	14.85
+53-75	9.1	4.36	3.42	0.39	0.39	4.08
-53	63.7	2.78	3.12	0.90	0.30	0.02
Total	**100**	**3.70**		**1.20**		**26.78**

TABLE 6.8

GOLD DEPORTMENT (EXPERIMENTAL AND MODEL 2 PREDICTIONS) VS SIZE FRACTION (WDL 70% -75 µm)

Size Fraction [µm]	Mass [%]	Free Gold [%].		Au in BMS [%]		Au in Pyrite [%]	
		Exp.	Predict.	Exp.	Predict.	Exp.	Predict.
+300	1.2	5.9	-8.95	39.5	37.94	49.2	62.64
+150-300	5.3	6.8	4.4	34.6	35.9	53.6	53.1
+106-150	12.8	11.2	13.5	33.1	34.2	49.6	46.5
+75 -106	9.7	18.5	18.00	32.3	33.3	43.1	43.3
+53 -75	9.1	21.3	22.2	29.6	32.4	39.8	40.2
-53	61.9	22.8	28.1	29.3	31.1	40.5	36.00
Total	**100**	**20.2**		**30.1**		**42.1**	

TABLE 6.8 (continue)

Size Fraction [µm]	Mass [%]	Au in Silicates [%]		Error [%]
		Exp.	Predict.	
+300	1.2	5.4	8.36	-
+150-300	5.3	5.0	6.7	35.7
+106-150	12.8	6.2	5.8	20.75
+75-106	9.7	6.2	5.4	2.92
+53-75	9.1	9.4	5.2	4.04
-53	61.9	7.4	4.9	23.38
Total	**100**	**7.5**		**17.36**

TABLE 6.9

GOLD DEPORTMENT (EXPERIMENTAL AND MODEL 2 PREDICTIONS) VS SIZE FRACTION (FSG 70% -75 µm)

Size Fraction [µm]	Mass [%]	Free Gold [%].		Au in BMS [%]		Au in Pyrite [%]	
		Exp.	Predict.	Exp.	Predict.	Exp.	Predict.
+300	0.6	18.1	-15.55	42.7	52.26	34.1	47.46
+150-300	6.8	18.2	12.0	40.6	40.4	32.9	37.8
+106-150	12.1	25.6	30.4	36.1	30.8	31.8	31.5
+75 -106	10.5	46.0	39.4	20.0	25.7	22.1	28.6
+53 -75	9.7	55.1	48.0	18.6	20.5	20.5	25.9
-53	60.3	54.2	60.4	20.6	12.4	23.4	22.2
Total	**100**	**47.4**		**23.8**		**24.8**	

TABLE 6.9 (continue)

Size Fraction [µm]	Mass [%]	Au in Silicates [%]		Error [%]
		Exp.	Predict.	
+300	0.6	5.1	15.83	-
+150-300	6.8	8.3	9.8	33.9
+106-150	12.1	8.1	7.2	18.9
+75-106	10.5	11.1	6.3	14.4
+53-75	9.7	5.8	5.7	13.0
-53	60.3	1.8	5.0	11.4
Total		**4.0**		**18.3**

TABLE 6.10

GOLD DEPORTMENT (EXPERIMENTAL AND MODEL 2 PREDICTIONS) VS SIZE FRACTION (HARTIES 70% -75 µm)

Size Fraction [µm]	Mass [%]	Free Gold [%].		Au in BMS [%]		Au in Pyrite [%]	
		Exp.	Predict.	Exp.	Predict.	Exp.	Predict.
+300	1.0	25.6	57.29		37.88		0
+150-300	7.2	26.5	59.36		35.87		0
+106-150	12.1	32.8	61.02		34.25		0
+75 -106	8.6	54.6	61.90		33.38		0
+53 -75	11.8	75.8	62.80		32.49		0
-53	58.3	77.0	64.19		31.12		0
Total	**100**	**67.4**		**7.7**		**4.9**	

TABLE 6.10 (continue)

Size Fraction [µm]	Mass [%]	Au in Silicates [%]		Error [%]
		Exp.	Predict.	
+300	1.0		4.83	-
+150-300	7.2		4.77	124.0
+106-150	12.1		4.73	86.0
+75-106	8.6		4.72	13.4
+53-75	11.8		4.71	17.2
-53	58.3		4.69	16.6
Total	**100**	**20.0**		**51.4**

TABLE 6.11

GOLD DEPORTMENT (EXPERIMENTAL AND MODEL 3 PREDICTIONS) VS SIZE FRACTION (KINROSS 70% -75 µm)

Size Fraction [µm]	Mass [%]	Free Gold [%].		Au in BMS [%]		Au in Pyrite [%]	
		Exp.	Predict.	Exp.	Predict.	Exp.	Predict.
+300	4.1	23.85	48.51	8.34	21.78	20.55	5.77
+150-300	2.2	76.46	62.20	6.80	19.95	4.46	4.39
+106-150	8.0	75.20	67.97	7.76	18.48	4.01	3.52
+75 -106	14.4	79.90	70.39	5.08	17.69	4.28	3.13
+53 -75	13.6	89.00	72.66	3.78	16.89	2.19	2.77
-53	57.6	91.25	76.17	2.21	15.65	2.87	2.30
Total	**100**	**84.91**		**3.64**		**3.84**	

TABLE 6.11 (continue)

Size Fraction [µm]	Mass [%]	Au in carbon [%]		Au in Silicates [%]		Error [%]
		Exp.	Predict.	Exp.	Predict.	
+300	4.1	5.24	8.41	42.02	15.54	-
+150-300	2.2	5.21	7.66	7.07	5.80	18.65
+106-150	8.0	4.00	6.89	9.04	3.14	9.62
+75-106	14.4	6.91	6.38	3.83	2.41	11.90
+53-75	13.6	2.33	5.74	2.71	1.93	18.36
-53	57.6	0.72	4.37	2.95	1.50	16.53
Total	**100**	**2.38**		**5.24**		**15.01**

TABLE 6.12

GOLD DEPORTMENT (EXPERIMENTAL AND MODEL 3 PREDICTIONS) VS SIZE FRACTION (LESLIE 70% -75 µm)

Size Fraction [µm]	Mass [%]	Free Gold [%].		Au in BMS [%]		Au in Pyrite [%]	
		Exp.	Predict.	Exp.	Predict.	Exp.	Predict.
+300	18.9	12.67	57.28	6.43	5.32	6.21	13.33
+150-300	2.0	79.48	78.83	9.67	3.81	5.71	10.16
+106-150	3.7	88.85	85.49	6.35	2.60	2.47	8.17
+75 -106	7.8	92.44	87.94	5.15	1.94	0.53	7.26
+53 -75	10.2	96.36	90.07	2.24	1.28	0.57	6.45
-53	57.4	89.74	92.99	4.89	0.25	3.04	5.36
Total	**100**	**75.82**		**5.08**		**3.23**	

TABLE 6.12 (continue)

Size Fraction [µm]	Mass [%]	Au in carbon [%]		Au in Silicates [%]		Error [%]
		Exp.	Predict.	Exp.	Predict.	
+300	18.9	5.08	1.93	69.91	22.13	-
+150-300	2.0	1.45	1.68	3.70	5.52	0.82
+106-150	3.7	0.52	1.42	1.81	2.32	3.78
+75-106	7.8	0.66	1.25	1.22	1.60	4.87
+53-75	10.2	0.23	1.03	0.60	1.17	6.53
-53	57.4	1.66	0.57	0.67	0.82	3.62
Total		**2.04**		**13.83**		**3.92**

TABLE 6.13

GOLD DEPORTMENT (EXPERIMENTAL AND MODEL 3 PREDICTIONS) VS SIZE FRACTION (BEATRIX 70% -75 µm)

Size Fraction [µm]	Mass [%]	Free Gold [%].		Au in BMS [%]		Au in Pyrite [%]	
		Exp.	Predict.	Exp.	Predict.	Exp.	Predict.
+300	20.9	9.66	47.51	7.84	8.90	14.43	11.08
+150-300	0.4	82.88	75.78	4.87	7.23	7.43	8.44
+106-150	1.1	88.31	81.69	4.30	5.89	3.68	6.78
+75 -106	4.1	86.96	83.74	4.19	5.18	3.68	6.03
+53 -75	8.0	84.54	85.53	4.86	4.45	5.74	5.35
-53	65.4	76.97	88.04	8.80	3.31	7.45	4.44
Total	**100**	**64.05**		8.03		**8.58**	

TABLE 6.13 (continue)

Size Fraction [µm]	Mass [%]	Au in carbon [%]		Au in Silicates [%]		Error [%]
		Exp.	Predict.	Exp.	Predict.	
+300	20.9	15.12	4.82	52.95	27.70	-
+150-300	0.4	3.11	4.66	1.70	3.89	8.57
+106-150	1.1	1.77	4.49	1.94	1.14	7.50
+75-106	4.1	4.77	4.38	0.40	0.68	3.69
+53-75	8.0	4.52	4.24	0.34	0.43	1.18
-53	65.4	6.32	3.94	0.46	0.26	14.38
Total		**7.89**		**8.58**		**7.06**

TABLE 6.14

GOLD DEPORTMENT (EXPERIMENTAL AND MODEL 3 PREDICTIONS) VS SIZE FRACTION (St. HELENA 70% -75 µm)

Size Fraction [µm]	Mass [%]	Free Gold [%].		Au in BMS [%]		Au in Pyrite [%]	
		Exp.	Predict.	Exp.	Predict.	Exp.	Predict.
+300	19.9	18.84	53.48	8.99	12.90	26.45	5.10
+150-300	1.6	85.49	79.18	12.15	11.64	1.14	3.88
+106-150	2.9	86.14	84.03	10.29	10.63	2.33	3.11
+75 -106	5.8	88.71	85.55	7.98	10.08	1.69	2.77
+53 -75	9.0	78.98	86.83	11.14	9.53	2.32	2.45
-53	60.8	80.36	88.59	10.24	8.67	2.81	2.04
Total	**100**	**68.76**		**9.97**		**7.36**	

TABLE 6.14 (continue)

Size Fraction [µm]	Mass [%]	Au in carbon [%]		Au in Silicates [%]		Error [%]
		Exp.	Predict.	Exp.	Predict.	
+300	19.9	9.15	1.22	36.56	27.30	-
+150-300	1.6	0.80	1.06	0.41	4.24	7.39
+106-150	2.9	0.83	0.90	0.40	1.33	2.45
+75-106	5.8	0.83	0.79	0.79	0.81	3.57
+53-75	9.0	6.64	0.66	0.92	0.53	9.94
-53	60.8	5.55	0.37	1.04	0.33	10.23
Total	**100**	**5.88**		**8.04**		**6.71**

TABLE 6.15

GOLD DEPORTMENT (EXPERIMENTAL AND MODEL 3 PREDICTIONS) VS SIZE FRACTION (HARMONY 70% -75 µm)

Size Fraction [µm]	Mass [%]	Free Gold [%].		Au in BMS [%]		Au in Pyrite [%]	
		Exp.	Predict.	Exp.	Predict.	Exp.	Predict.
+300	2.0	7.22	55.78	1.53	11.56	3.61	3.48
+150-300	7.2	72.11	80.42	20.92	10.28	4.52	2.64
+106-150	12.1	92.28	83.71	4.20	9.24	1.03	2.12
+75 -106	8.6	92.35	84.84	3.54	8.68	0.03	1.88
+53 -75	11.8	94.99	85.89	2.69	8.12	0.49	1.67
-53	58.3	92.37	87.48	3.70	7.24	1.29	1.38
Total	**100**	**89.43**		**4.81**		**1.30**	

TABLE 6.15 (continue)

Size Fraction [µm]	Mass [%]	Au in carbon [%]		Au in Silicates [%]		Error [%]
		Exp.	Predict.	Exp.	Predict.	
+300	2.0	9.8	4.96	77.81	24.22	-
+150-300	7.2	1.1	4.75	1.36	1.92	11.51
+106-150	12.1	1.5	4.54	0.97	0.39	9.29
+75-106	8.6	3.1	4.39	0.94	0.20	8.13
+53-75	11.8	1.3	4.21.	0.51	0.11	9.58
-53	58.3	1.2	3.83	1.45	0.06	5.29
Total	**100**	**0.54**		**1.98**		**8.76**

TABLE 6.16

GOLD DEPORTMENT (EXPERIMENTAL AND MODEL 3 PREDICTIONS) VS SIZE FRACTION (UNISEL 70% -75 µm)

Size Fraction [µm]	Mass [%]	Free Gold [%].		Au in BMS [%]		Au in Pyrite [%]	
		Exp.	Predict.	Exp.	Predict.	Exp.	Predict.
+300	12.3	22.95	61.96	17.64	6.09	25.05	24.95
+150-300	3.3	81.16	71.12	10.90	4.50	4.67	19.09
+106-150	5.8	87.93	77.04	5.96	3.22	4.80	15.39
+75 -106	8.1	68.08	79.81	19.28	2.53	10.01	13.71
+53 -75	10.3	80.51	82.38	6.52	1.84	9.88	12.19
-53	60.2	82.55	86.02	5.81	0.76	8.03	10.16
Total	**100**	**74.09**		**8.62**		**10.18**	

TABLE 6.16 (continue)

Size Fraction [µm]	Mass [%]	Au in carbon [%]		Au in Silicates [%]		Error [%]
		Exp.	Predict.	Exp.	Predict.	
+300	12.3	18.21	0.86	16.15	6.19	-
+150-300	3.3	0.96	0.70	2.30	4.59	12.37
+106-150	5.8	0.17	0.54	1.14	3.80	12.38
+75-106	8.1	1.67	0.44	0.96	3.51	17.22
+53-75	10.3	1.14	0.30	1.95	3.28	2.33
-53	60.2	1.55	0.02	2.06	3.04	4.20
Total	**100**	**3.47**		**3.65**		**9.70**

TABLE 6.17

GOLD DEPORTMENT (EXPERIMENTAL AND MODEL 3 PREDICTIONS) VS SIZE FRACTION (BARBERTON 70% -75 µm)

Size Fraction [µm]	Mass [%]	Free Gold [%].		Au in BMS [%]		Au in Pyrite [%]	
		Exp.	Predict.	Exp.	Predict.	Exp.	Predict.
+300	9.9	7.89	7.39	8.20	27.12	68.23	57.63
+150-300	3.6	24.67	21.40	36.87	25.24	35.97	48.13
+106-150	5.4	24.62	30.19	23.35	23.73	48.49	41.64
+75 -106	8.4	22.68	34.39	16.79	22.92	57.07	38.53
+53 -75	9.1	24.46	38.38	32.55	22.09	38.24	35.60
-53	63.7	29.51	44.14	33.30	20.82	33.51	31.50
Total	**100**	**25.90**		**28.96**		**40.24**	

TABLE 6.17 (continue)

Size Fraction [µm]	Mass [%]	Au in carbon [%]		Au in Silicates [%]		Error [%]
		Exp.	Predict.	Exp.	Predict.	
+300	9.9	10.98	4.09	4.71	3.77	-
+150-300	3.6	1.21	3.94	1.28	1.30	13.27
+106-150	5.4	2.89	3.77	0.65	0.67	22.63
+75-106	8.4	2.93	3.67	0.53	0.50	51.63
+53-75	9.1	4.36	3.53	0.39	0.39	56.90
-53	63.7	2.78	3.25	0.90	0.30	49.56
Total	**100**	**3.70**		**1.20**		**38.79**

TABLE 6.18

GOLD DEPORTMENT (EXPERIMENTAL AND MODEL 3 PREDICTIONS) VS SIZE FRACTION (WDL 70% -75 µm)

Size Fraction [µm]	Mass [%]	Free Gold [%].		Au in BMS [%]		Au in Pyrite [%]	
		Exp.	Predict.	Exp.	Predict.	Exp.	Predict.
+300	1.2	5.9	-2.41	39.5	38.95	49.2	57.77
+150-300	5.3	6.8	12.7	34.6	36.5	53.6	46.2
+106-150	12.8	11.2	22.8	33.1	34.6	49.6	38.6
+75 -106	9.7	18.5	27.6	32.3	33.5	43.1	35.1
+53 -75	9.1	21.3	32.2	29.6	32.4	39.8	31.8
-53	61.9	22.8	38.5	29.3	30.8	40.5	27.3
Total	**100**	**20.2**		**30.1**		**42.1**	

TABLE 6.18 (continue)

Size Fraction [µm]	Mass [%]	Au in Silicates [%]		Error [%]
		Exp.	Predict.	
+300	1.2	5.4	5.69	-
+150-300	5.3	5.0	4.6	86.6
+106-150	12.8	6.2	4.0	103.7
+75-106	9.7	6.2	3.8	49.4
+53-75	9.1	9.4	3.6	51.0
-53	61.9	7.4	3.4	68.9
Total	**100**	**7.5**		**71.4**

TABLE 6.19

GOLD DEPORTMENT (EXPERIMENTAL AND MODEL 3 PREDICTIONS) VS SIZE FRACTION (FSG 70% -75 µm)

Size Fraction [µm]	Mass [%]	Free Gold [%].		Au in BMS [%]		Au in Pyrite [%]	
		Exp.	Predict.	Exp.	Predict.	Exp.	Predict.
+300	0.6	18.1	-9.84	42.7	54.45	34.1	46.84
+150-300	6.8	18.2	15.0	40.6	42.6	32.9	36.4
+106-150	12.1	25.6	32.4	36.1	33.1	31.8	29.7
+75 -106	10.5	46.0	41.0	20.0	28.0	22.1	26.7
+53 -75	9.7	55.1	49.3	18.6	22.8	20.5	23.9
-53	60.3	54.2	61.5	20.6	14.8	23.4	20.1
Total	100	**47.4**		**23.8**		**24.8**	

TABLE 6.19 (continue)

Size Fraction [µm]	Mass [%]	Au in Silicates [%]		
		Exp.	Pre	
+300	0.6	5.1	8.55	-
+150-300	6.8	8.3	6.0	17.5
+106-150	12.1	8.1	4.8	26.6
+75-106	10.5	11.1	4.3	10.8
+53-75	9.7	5.8	4.0	10 5
-53	60.3	1.8	3.6	13.5
Total		**4.0**		**15.8**

TABLE 6.20

GOLD DEPORTMENT (EXPERIMENTAL AND MODEL 3 PREDICTIONS) VS SIZE FRACTION (HARTIES 70% -75 µm)

Size Fraction [µm]	Mass [%]	Free Gold [%].		Au in BMS [%]		Au in Pyrite [%]	
		Exp.	Predict.	Exp.	Predict.	Exp.	Predict.
+300	1.0	25.6	72.18		5.32		7.98
+150-300	7.2	26.5	84.36		3.80		6.07
+106-150	12.1	32.8	89.30		2.58		4.87
+75 -106	8.6	54.6	91.21		1.92		4.33
+53 -75	11.8	75.8	92.84		1.26		3.84
-53	58.3	77.0	94.95		0.23		3.19
Total	**100**	**67.4**		**7.7**		**4.9**	

TABLE 6.20 (continue)

Size Fraction [µm]	Mass [%]	Au in Silicates [%]		Error [%]
		Exp.	Predict.	
+300	1.0		14.53	-
+150-300	7.2		5.77	218.4
+106-150	12.1		3.24	172.3
+75-106	8.6		2.53	67.1
+53-75	11.8		2.06	22.5
-53	58.3		1.63	23.3
Total	**100**	**20.0**		**100.7**

TABLE 6.21

AVERAGE ERRORS ENCOUNTERED WITH THE DIFFERENT EMPIRICAL MODELS

Ore sample	Model 1	Model 2	Model 3
Kinross	3.74		15.01
Leslie	3.79		3.92
Beatrix	5.72		7.06
St. Helena	6.50		6.71
Harmony	9.08		8.76
Unisel	11.63		9.70
Barberton		26.78	38.79
WDL		17.36	71.4
FSG		18.3	15.8
Harties		51.4	100.7

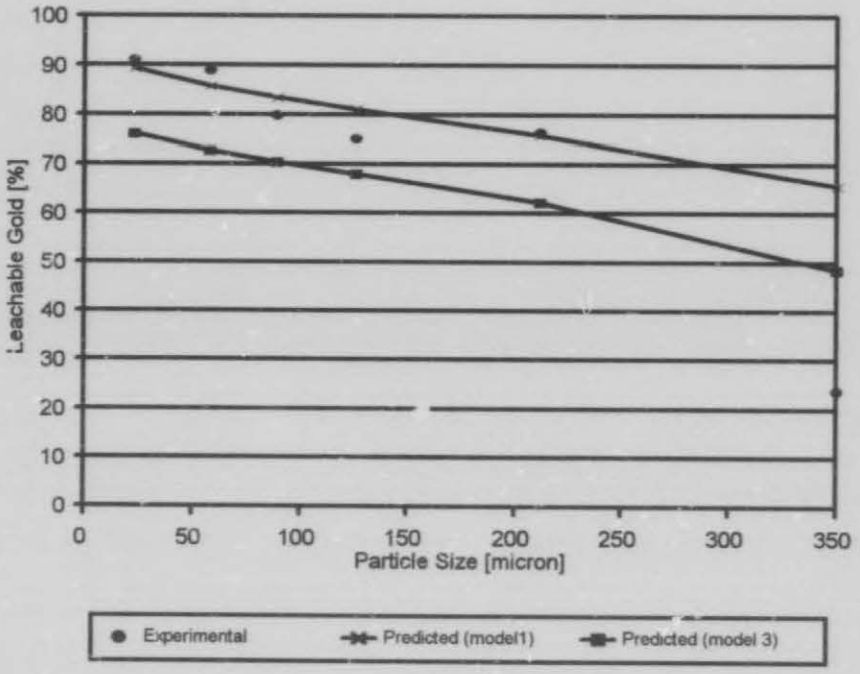

FIGURE 6.1: LEACHABLE GOLD AS A FUNCTION OF PARTICLE SIZE FOR MILLED KINROSS ORE WITH APPLICATION OF MODEL 1 & 3

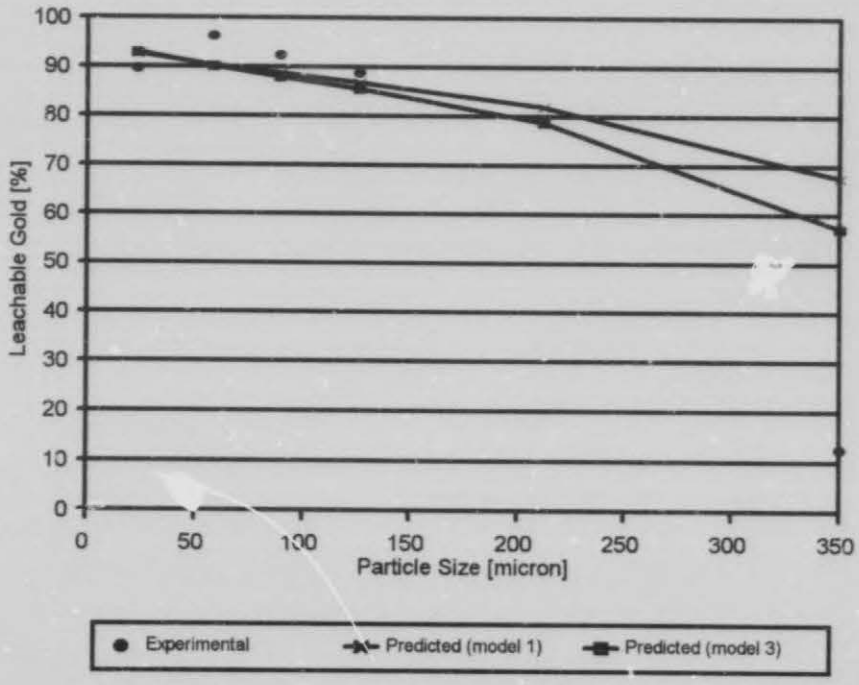

FIGURE 6.2: LEACHABLE GOLD AS A FUNCTION OF PARTICLE SIZE FOR MILLED LESLIE ORE WITH APPLICATION OF MODEL 1 & 3

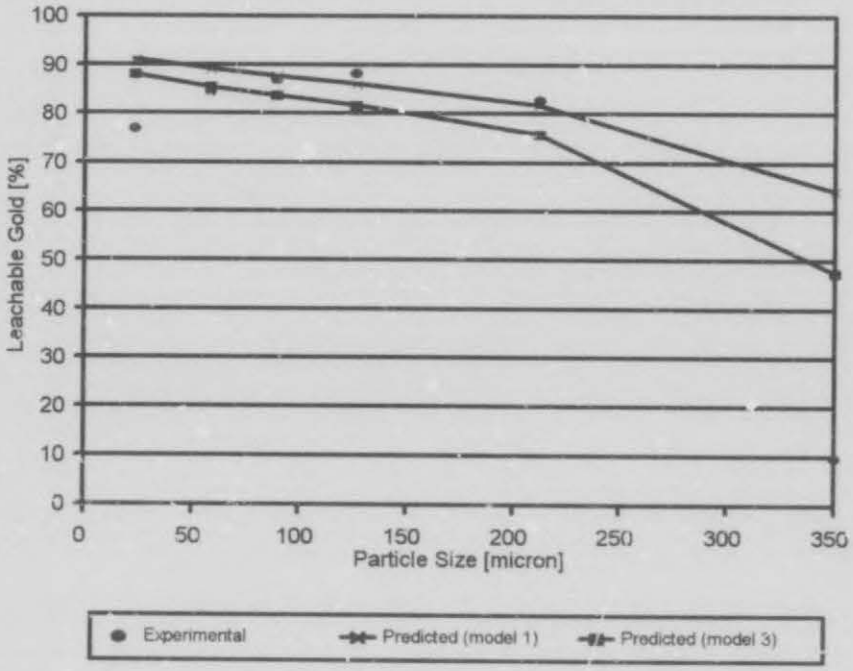

FIGURE 6.3: LEACHABLE GOLD AS A FUNCTION OF PARTICLE SIZE FOR MILLED BEATRIX ORE WITH APPLICATION OF MODEL 1 & 3

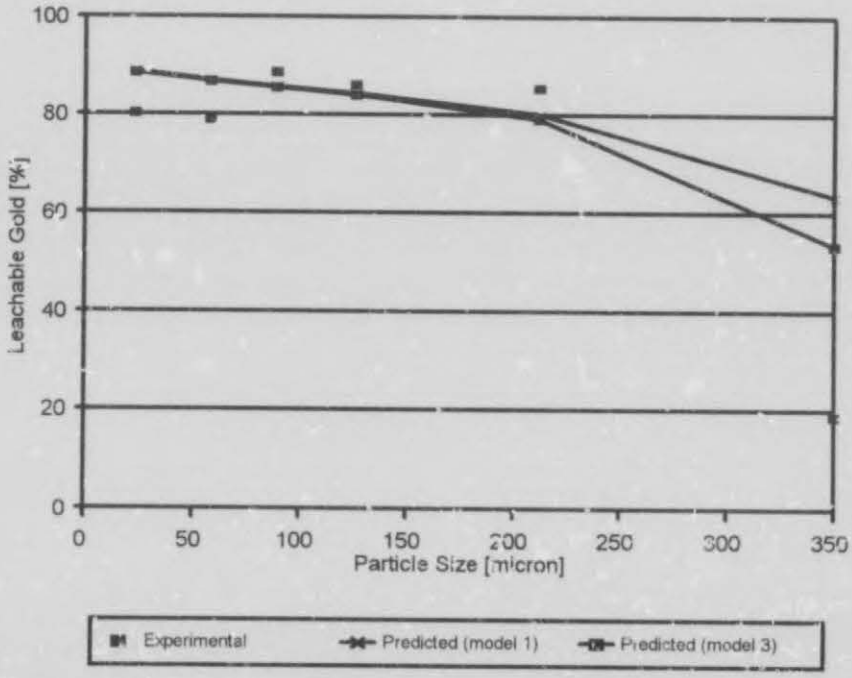

FIGURE 6.4: LEACHABLE GOLD AS A FUNCTION OF PARTICLE SIZE FOR MILLED ST. HELENA ORE WITH APPLICATION OF MODEL 1 & 3

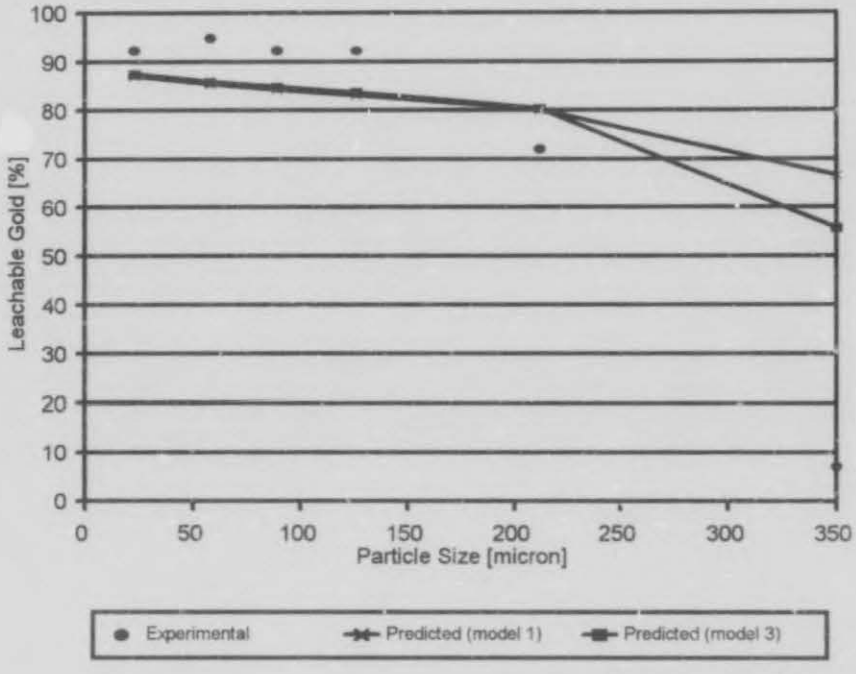

FIGURE 6.5: LEACHABLE GOLD AS A FUNCTION OF PARTICLE SIZE FOR MILLED HARMONY ORE WITH APPLICATION OF MODEL 1 & 3

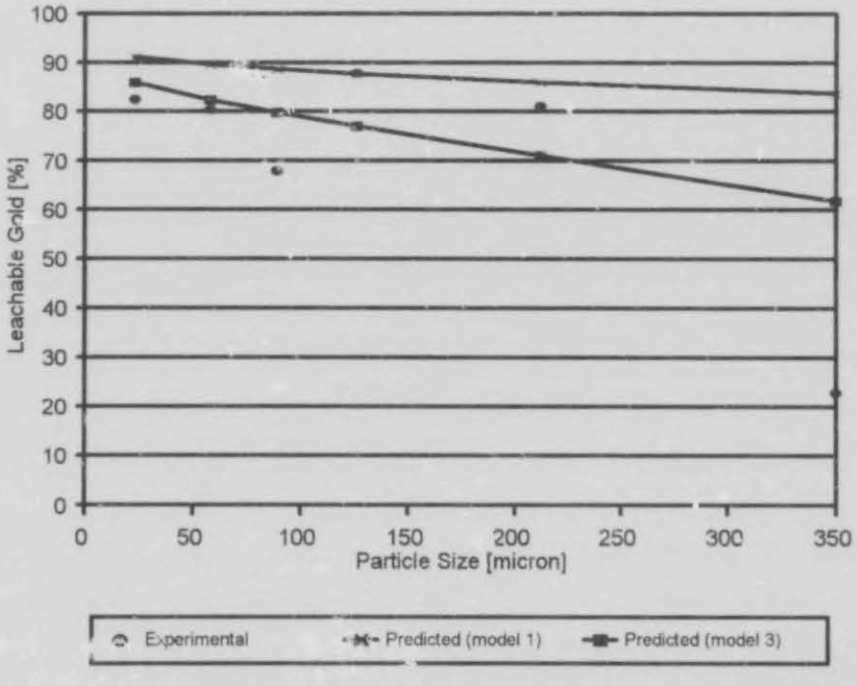

FIGURE 6.6: LEACHABLE GOLD AS A FUNCTION OF PARTICLE SIZE FOR MILLED UNISEL ORE WITH APPLICATION OF MODEL 1 & 3

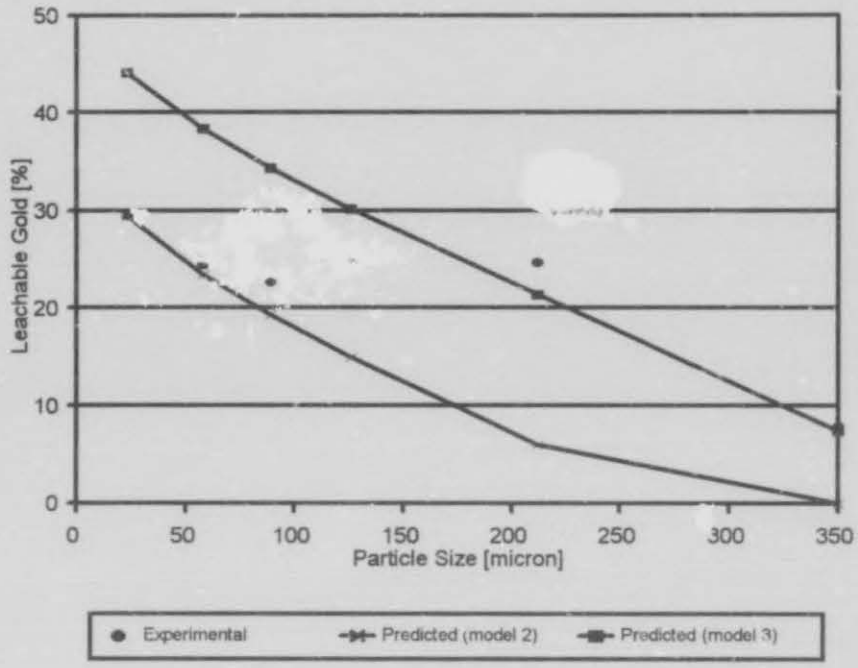

FIGURE 6.7: LEACHABLE GOLD AS A FUNCTION OF PARTICLE SIZE FOR MILLED BARBERTON ORE WITH APPLICATION OF MODEL 2&3

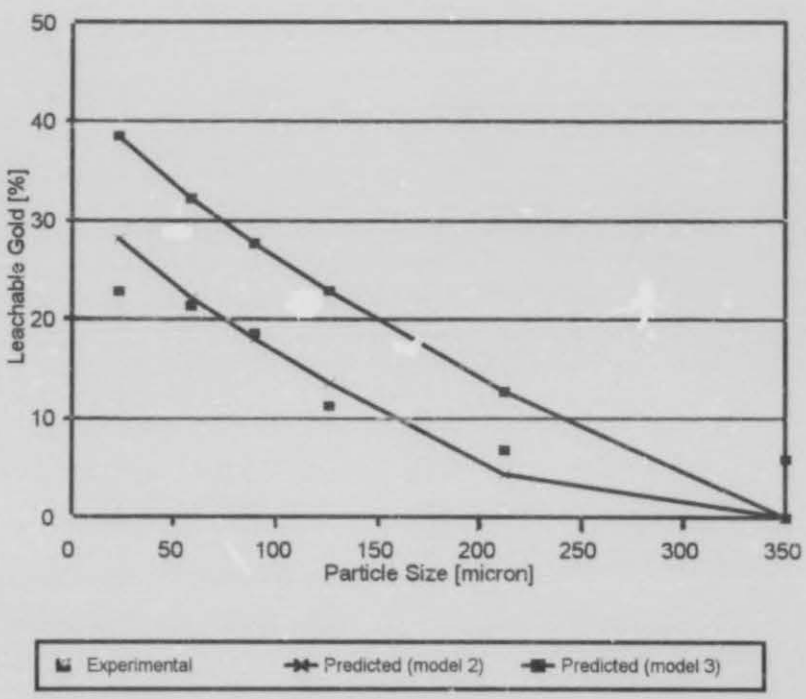

FIGURE 6.8: LEACHABLE GOLD AS A FUNCTION OF PARTICLE SIZE FOR MILLED WDL ORE WITH APPLICATION OF MODEL 2 & 3

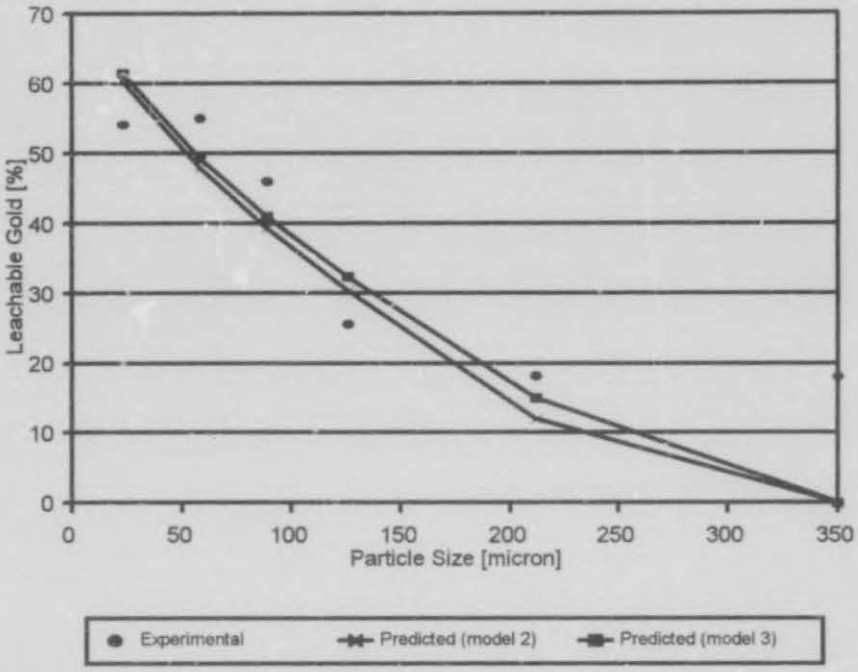

FIGURE 6.9: LEACHABLE GOLD AS A FUNCTION OF PARTICLE SIZE FOR MILLED FSG ORE WITH APPLICATION OF MODEL 2 & 3

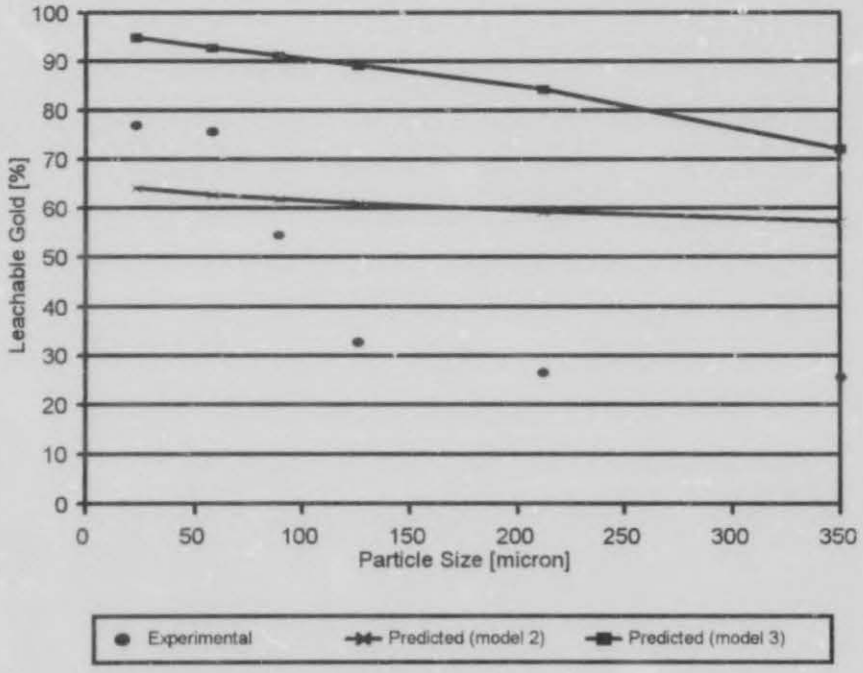

FIGURE 6.10: LEACHABLE GOLD AS A FUNCTION OF PARTICLE SIZE FOR MILLED HARTIES ORE WITH APPLICATION OF MODEL 2 & 3

CHAPTER 7

EXTENTION TO THEORETICAL LIBERATION MODELS

CHAPTER 7

EXTENSIONS TO THEORETICAL LIBERATION MODELS

In this chapter, the two theoretical liberation models selected in chapter 5, the Lorenzen-King model (Lorenzen 1992a; Lorenzen and Van Deventer 1994) and the exposure model developed by Hsih and co-workers (Wen et al, 1995) are extended, in order to predict leachable gold as a function of particle size and the mineralogy of the specific ore.

As previously stated (chapter 2), a gold particle is leachable whenever it is exposed to the leaching reagent and thus, gold particles situated in minor cracks and flaws in the ore that are not liberated as such, are, however, leachable.

Crushing and grinding are used to liberate the gold from the different minerals in the ore. According to Hsih and Wen (1994) these operations result in two types of fracture which corresponds to two types of liberation. If the interface between grains is strong, transgranular fracture will occur, with liberation induced only by size reduction. However, if the interface between the grains is weak, the fracture will be intergranular, with liberation increased by detachment. Several researchers, namely, Laslett et al (1990), Malvik (Hsih and Wen, 1994) and Kuan (Hsih and Wen, 1994) proved the detachment factor to be a real effect in liberation. It is thus necessary that when the leachable gold is calculated from these models, provision is made, not only for the gold liberated by size reduction, but also for the gold liberated by detachment and gold situated in minor cracks exposed to the leaching reagent.

7.1 ASSUMPTIONS MADE TO EXTEND THE THEORETICAL MODELS

Apart from the assumptions made by the researchers in deriving their models, one additional assumption was made in order to extend the models, namely that a specific ore is homogenous. In other words, the gold-bearing minerals break according to the same breakage pattern and thus yields a gold distribution that is the same for both the unmilled and milled (milled to 70% - 75 µm) ore samples.

It was necessary to assume homogeneity because the degree of liberation, as defined in the liberation models, is the ratio of the amount of gold liberated in a specific particle size fraction, when milled, to the amount of gold originally

contained in the same particle size fraction. Since the unmilled ore sample consists mainly of +300 µm particles, the amounts of gold originally contained in the smaller particle size fractions are thus not known.

The degree to which the gold is liberated (leachable) from mineral *i* in the particle size fraction *d* was calculated from the results in chapter 4 and is thus:

$$L_{i,d} = 1 - \frac{Au_{i,d}}{Au_{tot\,i,d}} \qquad (7.1a)$$

where $L_{i,d}$ - degree of liberation (leaching) from mineral *i* and particle size fraction *d*.

$Au_{i,d}$ - amount of gold associated with mineral *i* in the particle size fraction *d*, of the milled ore sample, [mg].

$Au_{tot,i,d}$ - amount of gold associated with mineral *i* in the particle size fraction *d*, of the unmilled ore sample [mg].

The amount of gold associated with mineral *i* in the particle size fraction *d*, of the unmilled ore sample, $Au_{tot,i,d}$, was calculated (on a basis of 1 kg ore) as follows :

$$Au_{tot\,i,d} = w_d\, Au_{tot\,i}\, HG_{tot} \qquad (7.1b)$$

where w_d - the mass fraction of the milled ore in the particle size fraction *d*.

Au_{tot} - the total fraction of gold associated with mineral *i* in the unmilled ore sample.

HG_{tot} - total head grade of the unmilled ore sample [mg/kg].

It is evident from Tables B11a to B19b (Appendix B) and Figures C1 to C9 (Appendix C) that the assumption of homogeneity is not valid for all the ores. It is noticeable that the liberation (leaching) trends for the refractory and the non-refractory ores differ quite substantially. The liberation (leaching) of gold from the non-refractory ores (Figures C1 to C9) increases with a decrease in particle size in general, while the opposite is true for the refractory ores (liberation (leaching) decreases with a decrease in particle size) (Figures C7 to C10). The latter is, however, impossible and thus the assumption of homogeneity is invalid for the refractory ores. Due to the occurrence of fluctuations in the liberation (leaching) trends of the non-refractory ores, it is clear that the assumption of homogeneity is not truly valid. It is, however,

possible to fit a general trend through the scattered liberation (leaching) data to obtain reasonable liberation (leaching) curves for further use with the theoretical liberation models.

When the liberation (leachability) of gold from the different minerals is compared to each other, the liberation (leachability) of gold from BMS, pyrite and carbonaceous material increases according to a convex exponential function with a decrease in particle size. However, the liberation (leachability) of gold from the silicates increases according to a concave exponential function, with a decrease in particle size. The latter is believed to be a real effect and is not due to experimental error or invalidity of the assumption of homogeneity, since this phenomenon (Figure C1 to C9) is true for five of the six non-refractory gold ores, except Kinross gold ore.

7.2 EXTENSIONS TO THE LORENZEN-KING LIBERATION MODEL

Lorenzen and Van Deventer (Lorenzen 1992a; Lorenzen and Van Deventer, 1994) were the first researchers to provide for the amount of leachable gold in the various size fractions that is not related to the liberation of gold due to comminution, in their extension to the King liberation model. Unfortunately, the extension made by Lorenzen was mathematically incorrect and he did not consider the different mineral species in the ores, individually (chapter 5.2.8). The proposed extensions to King liberation model presented below, rectify the shortcomings of the Lorenzen-King model. The King liberation model is as follows:

$$L(D) = 1 - \frac{1}{\mu}\int_{0}^{D_u} \{1 - N(l/D)\}\{1 - F(l)\}dl \qquad (2.7)$$

where F(*l*) - distribution of linear intercept lengths of mineral.

μ - linear intercept length.

N(*l*/*D*) - linear intercept distribution function for particles of particle size D.

D_u - the largest intercept length across any particle of particle size D.

Finch and Petruk (1984) derived from equation (2.7) three explicit solutions.

All three solutions were tested to the diagnostic leaching results by usage of a Turbo Pascal program (Appendix D). Equation (6.10), which calculates the average percentage error, was used as criterion to which the accuracy of the models was tested. It was found that equation (2.10c) is the most accurate in predicting the degree of liberation (leachability) of a gold ore.

$$L(D)= 1-\frac{D}{2\mu_m + D}[1-\exp-(\frac{2\mu_m + D}{\mu_m})] \qquad (2.10c)$$

Equation (2.10c) was applied to each mineral species in turn and the degree of liberation (leachability) of the ore was calculated by weighting the degree of liberation (leachability) of each mineral with the deportment of gold in the unmilled ore. It is obvious that the mean linear intercept lengths of gold in the various minerals can be estimated when the degree of liberation (leachability) of the ore is known. The degree of liberation of an ore is thus:

$$L(D)_{TOTAAL} = w_{BMS}L(D)_{BMS} + w_{Pyrite}L(D)_{Pyrite} + w_{Silicates}L(D)_{Silicates} + w_{\substack{Carbonaceous \\ material}}L(D)_{\substack{Carbonaceous \\ material}} + w_{\substack{Free \\ Gold}} \qquad (7.2)$$

where $L(D)_{TOTAL}$ - degree to which the gold is liberated from the ore in a specific particle size.fraction D.

$L(D)$ - degree to which the gold is liberated from the specific mineral species (B, P,.S, C) in particle size fraction D.

w - fraction of the total gold associated with the specific mineral specie in the unmilled ore sample.

B, P, S, C, F - Base Metal Sulphides (BMS), Pyrite, Silicates, Carbonaceous material and Free Gold, respectively.

It was found that equation (7.2) totally underestimates the degree of liberation (leachability) in the various size fractions, as expected. The underestimation is due to the leachabie gold in the various size fractions that is not directly related to liberation by size reduction, but to liberation by detachment and to gold situated in cracks and flaws in contact with the leaching reagent. Equation (7.2) was modified by adding a term to the right-hand side of the equation to make provision for that fraction of leachable gold.

$$L(D)_{TOTAAL} = w_{BMS}L(D)_{BMS} + w_{Pyrite}L(D)_{Pyrite} + w_{Silicates}L(D)_{Silicates} + w_{\substack{Carbonaceous \\ material}}L(D)_{\substack{Carbonaceous \\ material}} + w_{\substack{Free \\ Gold}}F(D) \qquad (7.3)$$

where $F(D)$ - factor by which leachable gold for particle size (D), not related to liberation by size reduction, is enhanced by fracture.

From equation (7.3) it is possible to determine a F(D) value for each particle size fraction (D). A linear regression analysis showed that F(D) can be written as a function of the following form:

$$F(D) = a\exp(b + cD^3) \tag{7.3a}$$

where a, b and c are coefficients for a specific ore.

The coefficients were determined for each ore and it was found that they are functions of the mean linear intercept lengths of gold in the various minerals.

Thus, the diagnostic leaching results in collaboration with the assumption of homogeneity of the ores (Tables B11a... Appendix B), were used to determine the general function, $F(D)$, which is as follows:

$$F(D) = A\exp\left(\frac{\mu_B^{1.24}\mu_C^{0.93}}{\mu_P^{1.30}\mu_S^{0.87}} + \frac{\mu_P^{0.23}}{\mu_B^{0.15}\mu_S^{2.65}\mu_C^{0.43}}D^3\right) \tag{7.4}$$

where μ - mean linear intercept length of gold in a specific mineral

D - particle size [µm]

A - empirical constant

B,P,S,C - the various minerals with which gold is associated, namely BMS, pyrite, silicates and carbonaceous material, respectively

if one of the above mentioned minerals is not present in the ore or no provision was made for the testing of gold in that mineral in the setting up of the diagnostic leaching procedure, the power of that mineral in the function $F(D)$ is summed with the power of the mineral that has the highest probability in containing the specific mineral. For example in the case of the WDL, FSG and Harties ores, gold associated with carbonaceous material was not determined, so the power of μ_C is summed with the power of μ_S. In the diagnostic leaching sequence, the determination of gold associated with carbonaceous material is followed by determination of the gold associated with silicates.

The empirical constant, A and the mean linear intercept lengths of the gold in the various minerals were determined for the different ores and are presented in Table 7.1a. Values for the function, *F(D)*, are tabulated in Table 7.1b.

7.3 DISCUSSION OF THE EXTENDED LORENZEN-KING LIBERATION MODEL

It is evident from Table 7.1a that the estimated mean linear intercept length of the gold grains enclosed by silicates is much larger than that in other minerals. It is further evident that the mean linear intercept length of the gold grains enclosed by pyrite is in many cases the second largest, followed by the mean linear intercept length of the gold grains enclosed by BMS and carbonaceous material. Approximately the same trend is evident from a report of the gold mineralisation of the Beatrix reef, where the median size of gold grains locked up in silicates, pyrite and carbonaceous material were 23 µm, 9 µm and 4.5 µm, respectively. It is noticeable that when these gold grain diameters are compared to the linear intercept lengths, calculated with the modified version of King's model, the linear intercept lengths are much larger than the gold grain diameters, especially for the gold grains associated with the silicates. This phenomenon is at first, quite unexpected, since linear intercept length and diameter are related by the following simple function:

$$\mu = \frac{4V}{S} \qquad (7.5)$$

(For example for a sphere; µ=2/3D (Underwood, 1970))

where μ - linear intercept length

V - volume of the particle

S - surface area of the particle

D - particle diameter

These relatively large linear intercept lengths are, however, not unrealistic. It must be borne in mind that the calculated linear intercept lengths of the gold grains, as defined by King, are those in the unmilled ore sample. The relatively small gold grain diameters as presented in the report from the Beatrix mine are questionable, since it is unknown how and when these values were determined. Hallbauer (G.G. Stanley, 1987) differentiated between five major types of gold in the Witwatersrand deposits.

He found that the gold size in secondary quartz veins varies from about 10 µm to several mm for large aggregates. Gold intergrown with BMS (sphalerite, chalcopyrite, etc.) varies in sizes from 10 µm to rarely 500 µm, with the average being between 50 to 100 µm. Filaments or aggregates of filaments of biochemically redistributed gold that is intergrown with carbonaceous matter range in sizes from 0.5 to 2 µm and up to 1 mm across, respectively. Primary gold is mostly intergrown with pyrite and is seldom larger than 20 µm. Recrystalized gold grows epitaxially on pyrite and ranges in size from 5 µm to 2 mm. It is thus evident that, although the calculated linear intercept lengths are in some cases very large, it still falls within the boundaries reported by Hallbauer.

Microscopic examinations (G.G. Stanley, 1987) of the Witwatersrand conglomerates indicated that gold sometimes occurs as filaments in the different minerals. It could thus happen that the volume of the gold particle is the same as the surface area, for example for a cylindrical particle, the volume would be the same as the surface area when D=4H/(H-2) where D is the diameter and H is the height of the cylinder. From equation (7.5) the mean linear intercept length will than be equal to four times the diameter. It is thus possible that the calculated mean linear intercept length could be larger than the diameter, depending on the shape of the particle.

It is evident from Figure 7.1a and 7.1b that the empirical constant A, is a function of the fraction of free gold in the unmilled ore samples. This is, however, only valid for the non-refractory gold ores and not for the refractory ores especially for the Barberton gold ore, when Figure 7.1b is considered. The reason for the irregularity is due to the different and uniqueness of the mineralogy of the Barberton gold ore (section 2.2 and chapter 4). The relationship between A and the fraction of free gold (Figure 7.1a) was expected, since both the amount of free gold in the original ore sample and A determine the position of the graph (leachable gold versus particle size) with respect to the y-axis.

It can be concluded from Figures 7.3 to 7.12 and Tables B1 to B5 (Appendix B) that the modified King model predicts the amount of leachable gold in each particle size fraction reasonably well.

7.4 EXTENSIONS TO THE HSIH et al EXPOSURE MODEL

Hsih and co-workers (Wen et al, 1995) were the first to incorporate liberation due to intergranular fracture and thus realising that random breakage does not always occur. However, in deriving their exposure model, they did not provide for the amount of leachable gold that is not directly related to liberation, but due to the gold particles positioned in minor cracks and flaws in the ore. Their exposure model, equation (2.18), was used together with the data obtained after assuming homogeneity (Tables B11a to B19b - Appendix B and Figures C1 to C9 - Appendix C) and were applied to each mineral species.

Their exposure model for gold ores is as follows:

$$L_m(K) = P\left(\frac{K^3-(K-2)^3}{K^3}\right)+(1-P)*\left(\frac{K^3-(K-1)^3}{K^3}\right) \qquad (2.18)$$

where $K=D/d$

$L_m(K)$ - degree of the liberation.

P - intergranular fracturing factor (P=1 - only fracture along grain boundaries; P=0 - only transgranular fracture).

d - grain size of the gold (μm).

D - particle size of the ore (μm).

Thus, the total degree to which the gold is leachable, is given by the following equation:

$$L_m(K)_{TOTAAL} = w_{BMS}L_m(K)_{BMS} + w_{Pyrite}L_m(K)_{Pyrite} + w_{Silicates}L_m(K)_{Silicates} + w_{\substack{Carbonaceous\\material}}L_m(K)_{\substack{Carbonaceous\\material}} + w_{\substack{Free\\Gold}} \qquad (7.6)$$

As expected, equation (7.6) underestimated the amount of leachable gold in each particle size fraction. The amount of gold situated in minor cracks was taken into account by adding a term to equation (7.6).

$$L_m(K)_{TOTAAL} = w_{BMS}L_m(K)_{BMS} + w_{Pyrite}L_m(K)_{Pyrite} + w_{Silicates}L_m(K)_{Silicates} + w_{\substack{Carbonaceous\\material}}L_m(K)_{\substack{Carbonaceous\\material}} + w_{\substack{Free\\Gold}}F(D,d) \qquad (7.7)$$

where $$F(D,d) = A_m \exp\left(-\frac{d_P^{0.65}d_S^{0.97}d_C^{0.02}}{d_B^{0.64}D}\right) \qquad (7.8)$$

$F(D,d)$ - factor by which leachable gold, not directly related to liberation, is enhanced due to fractures.

A_m - an empirical constant

d - diameter of the gold grains when P=0 [µm]

D - particle size [µm]

B,P,S,C - the various minerals with which gold is associated, namely BMS, pyrite, silicates and carbonaceous material, respectively

Function $F(D,d)$ was determined by employing the same technique that was used to derive function $F(D)$ (equation 7.4).

It must be noted that the diameter of the gold grains in the function, F(D,d), is defined as the diameter of the gold grains when P=0. When P equals any other value ($0 \leq P \leq 1$), the diameters of the gold grains will subsequently decrease, in order to yield the same degree of exposure. The gold grain diameters in the function, $F(D,d)$ is thus equal to:

$$d_{P=0} = \frac{d_{P=\text{any value}}}{e^{-0.693P}} \qquad (7.9)$$

If one of the minerals (BMS, pyrite, carbonaceous material or silicates) is not present in the ore, function $F(D,d)$ is modified according to the same principles that were used in modifying function $F(D)$ in section 7.2.

The empirical constant, A_m and the diameters of the gold grains (P=0), associated with the various minerals, are presented in Table 7.2a. The values for $F(D,d)$ are presented in Table 7.3a.

7.5 DISCUSSION OF THE EXTENDED HSIH et al EXPOSURE MODEL

It is evident from Table 7.2a that the calculated diameters are in the most cases the largest for the gold grains associated with the silicates, followed by those associated with pyrite, BMS and carbonaceous material. This trend, as well as the calculated values, is of the same order as those from the report of the gold mineralisation of the Beatrix reef (section 7.3). The gold grain diameters calculated from the modified exposure model are the average diameters of the gold grains in the various minerals in the unmilled as well as

in the milled ore sample. It thus seems that the mineralogical analysis on the Beatrix reef (report from Beatrix mine), was done on a milled ore sample (it is not believed that the size of the gold grains will stay the same throughout the crushing and grinding operations; one would expect the grains in the unmilled sample to be coarser). It is furthermore evident that the calculated diameters fall within the boundaries found by Hallbauer (G.G. Stanley, 1987).

It can be concluded from Figure 7.2a and 7.2b that the empirical constant A_m, is a function of the fraction of free gold in the unmilled non-refractory ore samples. The relationship between A_m and the fraction of free gold of the non-refractory ores was expected due to the existence of a similar relationship between A (equation (7.4)) and the fraction of free gold (section 7.3). However, the relationship between A_m and the fraction of free gold in the unmilled refractory ore samples is not clearly definable from Figure 7.2b. The reason for this phenomenon is discussed in section 7.3.

It is evident from Figures 7.13 to 7.22 and Tables B6 to B10 (Appendix B) that the modified exposure model developed by Hsin and co-workers predicts the amount of leachable gold in each particle size fraction fairly well. The accuracy with which the model, the leachable gold in each particle size fraction of the Barberton gold ore predicts is promising. It is clear from the liberation trend that the mineralogy of the Barberton gold ore differs substantially from the Witwatersrand gold ores as mentioned above (section 2.2 and chapter 4). Both the empirical models (chapter 6) and the modified King's model (section 7.2) were unsuccessful in their attempt to predict the amount of leachable gold in each size fraction, accurately.

The gradient of the exposure (predicted) curve decreases in some cases (Beatrix, Harmony, etc.) for the smaller particle size fractions. It was found that the decrease in gradient is directly related to a slight increase in the diameter of the gold grains associated mainly with the silicates. This is due to a decrease in the amount of gold not directly related to liberation. This means physically, that an increase in the coarseness of a gold particle situated in a minor crack or flaw, decreases its leachability. This phenomenon is possible whenever the duration of the leaching tests is inadequate. This effect is thus believed to be real and not due to inaccurate predictions by the modified exposure model.

7.6 GENERAL DISCUSSION

It is evident from Tables 7.3 that according to the average errors (calculated by using equation 6.10), that both models predict the leachability of gold ores fairly accurately. The only exception is the prediction of the leachability of the Barberton gold ore. The modified exposure model (Hsih and co-workers) predicts the degree to which the latter ore is leachable very well in contrast with the modified King's model which is unsuccessful in this case.

The different approaches of the models should be considered when the large linear intercept lengths of the gold grains, especially those associated with the silicates, predicted by the modified King's model, are compared to the relatively small gold grain diameters, predicted by the modified exposure model. The mean linear intercept length as defined by King, is the mean linear intercept length of the gold grains in the unbroken rock and not in the milled ore sample. The diameters of the gold grains, defined by Hsih and co-workers, are those in the milled ore samples. According to their approach the gold grains do not decrease in size when comminuted. It is thus understandable why the calculated mean linear intercept lengths and mean gold grain diameters differ quite substantially. It is believed that the gold grains decrease in size when comminuted.

It is noticeable that the modifications to the different models are of the same form, namely an exponential function. The main difference between function F(D) (modified King model) and function F(D,d) (modified exposure model) is in the number of terms present. The function, F(D), is a function of two terms to provide for the liberation of gold due to detachment and the fraction of gold not directly related to liberation. The function, F(D,d), on the other hand is a function of only one term to provide only for the fraction of gold not directly related to liberation.

It is evident from the extensions to equation 7.3 and 7.7 that the leachability of gold situated in minor cracks and flaws, is a function of particle size. A decrease in the particle size, results in a slight decrease in that fraction of gold. This supports the idea that the cracks and flaws are smaller and lesser in the smaller particle size fractions than in the coarser fractions.

It is thus concluded that the modified exposure model, developed by Hsih and co-workers, as expected (chapter 5), is valid for a broader spectrum of different ores. Unfortunately, it was not possible to test the calculated gold grain diameters and mean linear intercept lengths to experimentally determined values, since no SEM data of the specific ores were available.

TABLE 7.1a

ESTIMATES OF μ AND A (eq 7.3)

Ore Sample	A	μ_{BMS}	μ_{Pyrite}	μ_{Carbon}	$\mu_{Silicates}$
Kinross	1.05	40	40	5	700
Leslie	1.08	25	100	5	1000
Beatrix	1.27	30	35	5	1500
Harmony	1.25	60	50	200	2100
St. Helena	1.17	100	70	2	900
Unisel	1.04	30	150	60	2100
WDL	2	0.17	0.42	n.d.	140
FSG	1.25	0.9	8	n.d.	280
Harties	1.1	0.3	5	n.d.	145
Barberton	1.42	15	4.5	30	450

n.d. - not determined

TABLE 7.1b

CALCULATED F(D) (eq. 7.3) VALUES FOR EACH PARTICLE SIZE FRACTION

Ore Sample	-53 μm	+53 -75 μm	+75-106 μm	+106-150 μm	+150-300 μm
Kinross	0.86	1.00	1.02	1.03	1.04
Leslie	0.98	1.06	1.07	1.08	1.08
Beatrix	1.23	1.26	1.26	1.26	1.26
Harmony	1.05	1.05	1.05	1.05	1.05
St. Helena	1.01	1.13	1.15	1.16	1.16
Unisel	1.03	1.03	1.03	1.03	1.03
WDL	0.10	0.75	1.05	1.20	1.26
FSG	0.73	1.05	1.11	1.14	1.15
Harties	0.02	0.47	0.81	1.01	1.01
Barberton	1.25	1.36	1.38	1.39	1.39

TABLE 7.2a

ESTIMATES OF d AND A_m (eq. 7.7)

Ore Sample	A_m	d_{BMS}	d_{Pyrite}	d_{Carbon}	$d_{Silicates}$
Kinross	1.94	11.0	14.0	3.25	15.0
Leslie	2.50	8.0	11.0	7.50	16.0
Beatrix	3.96	1.6	1.7	0.68	18.0
Harmony	3.80	6.5	10.0	5.0	21.5
St. Helena	3.40	3.5	10.0	8.5	17.0
Unisel	1.80	6.5	6.0	12.0	15.0
WDL	1.10	1.0	1.0	n.d.	5.0
FSG	1.02	4.9	3.0	n.d.	0.8
Harties	1.06	25.0	2.0	n.d.	12.0
Barberton	3.15	1.0	1.5	5.0	22.0

n.d. - not determined

TABLE 7.2b

CALCULATED F(D,d) (eq. 7.7) VALUES FOR EACH PARTICLE SIZE FRACTION

Ore Sample	-53 µm	+53 -75 µm	+75-106 µm	+106-150 µm	+150-300 µm
Kinross	1.79	1.70	1.60	1.44	0.93
Leslie	2.28	2.15	2.01	1.79	1.08
Beatrix	3.65	3.45	3.26	2.94	1.88
Harmony	3.34	3.06	2.79	2.37	1.16
St. Helena	2.91	2.62	2.36	1.94	0.82
Unisel	1.68	1.61	1.54	1.41	0.98
WDL	1.07	1.06	1.04	1.01	0.89
FSG	1.02	1.02	1.01	1.01	0.99
Harties	1.05	1.04	1.03	1.02	0.96
Barberton	2.77	2.54	2.33	1.98	0.98

TABLE 7.3

AVERAGE ERRORS

Ore Sample	Average error (eq 7.3)	Average error (eq 7.7)
Kinross	4.64	2.55
Leslie	3.69	3.59
Beatrix	8.12	8.67
Harmony	5.71	5.07
St. Helena	8.27	6.73
Unisel	12.58	8.70
WDL	34.15	26.85
FSG	26.72	28.31
Harties	24.81	23.[illegible]
Barberton	17.21	3.79

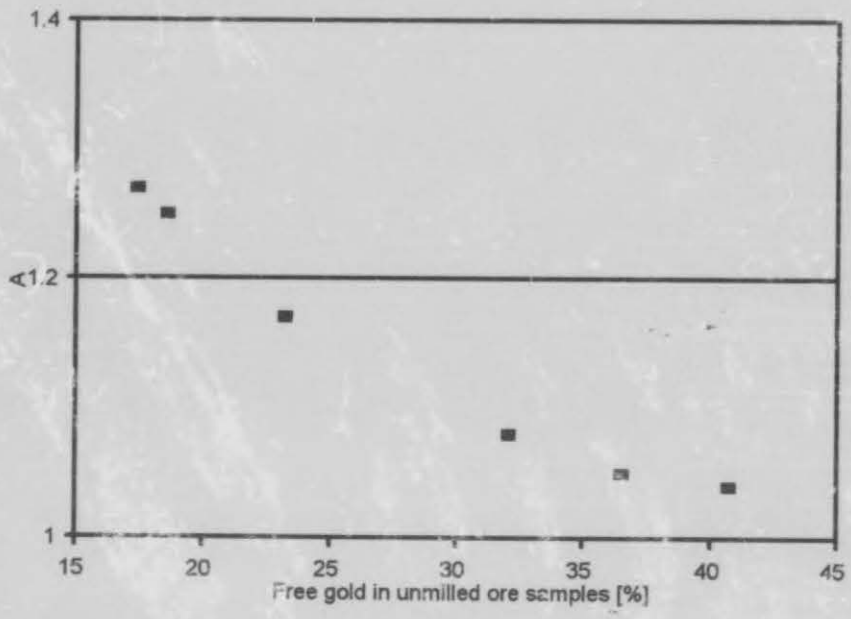

FIGURE 7.1a: EMPIRICAL CONSTANT A VERSUS THE FREE GOLD OF THE UNMILLED ORE SAMPLES (NON-REFRACTORY ORES).

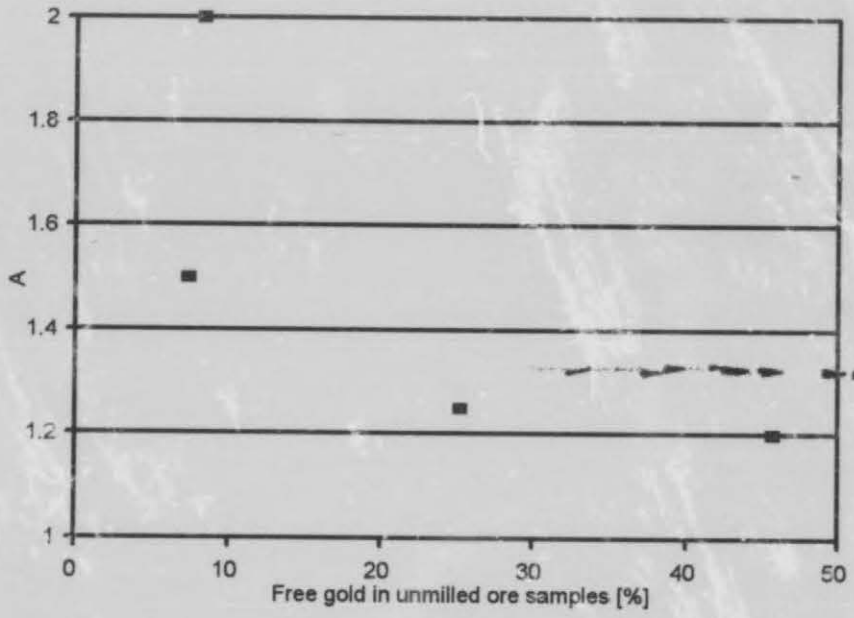

FIGURE 7.1b: EMPIRICAL CONSTANT A VERSUS THE FREE GOLD OF THE UNMILLED ORE SAMPLES (REFRACTORY ORES).

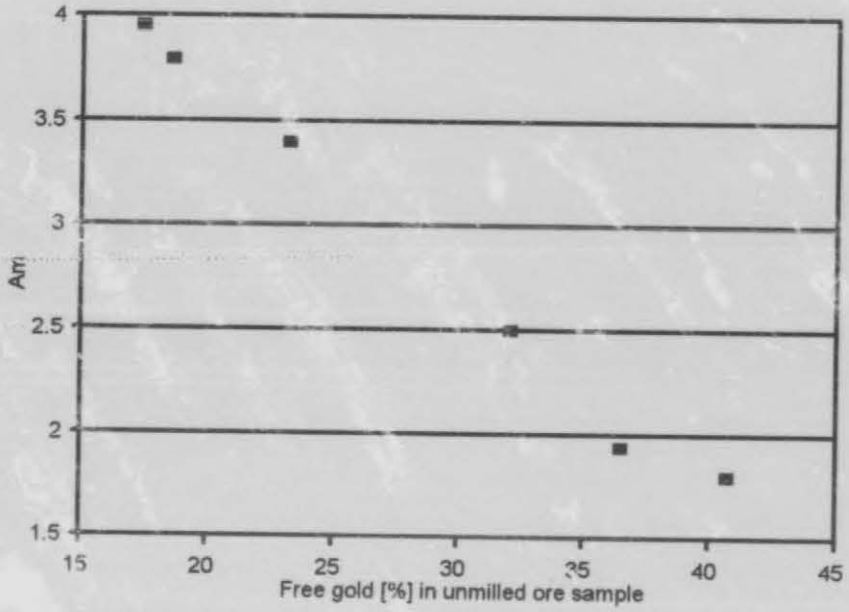

FIGURE 7.2a: EMPIRICAL CONSTANT A_m VERSUS THE FREE GOLD OF THE UNMILLED ORE SAMPLES (NON-REFRACTORY ORES).

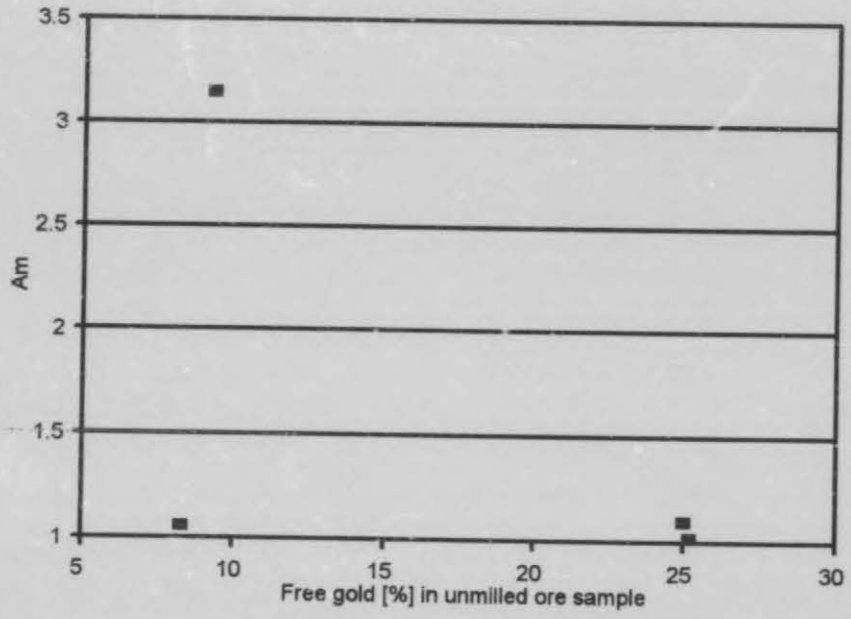

FIGURE 7.2b: EMPIRICAL CONSTANT A_m VERSUS THE FREE GOLD OF THE UNMILLED ORE SAMPLES (REFRACTORY ORES).

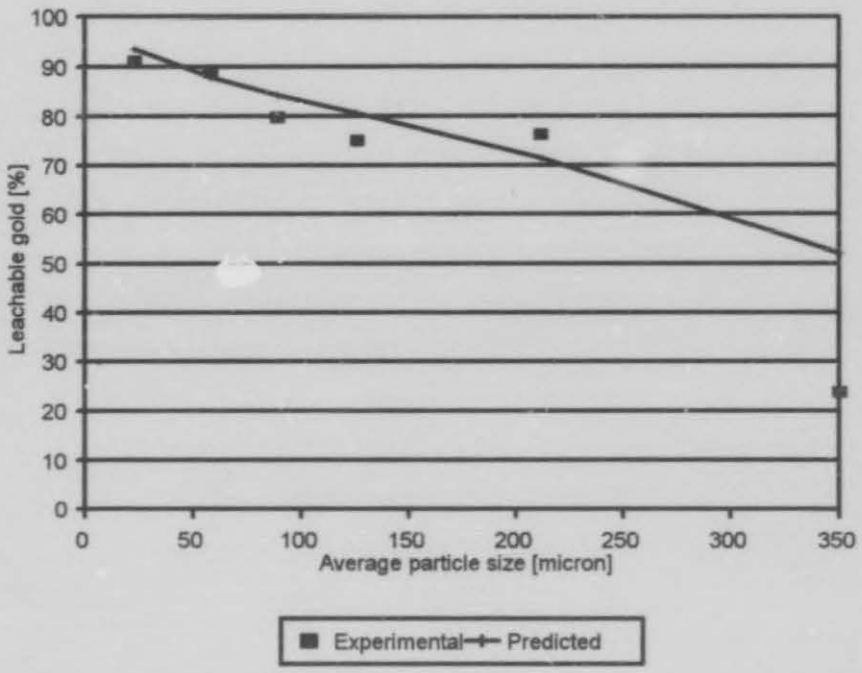

FIGURE 7.3: LEACHABLE GOLD AS A FUNCTION OF PARTICLE SIZE FOR MILLED KINROSS ORE WITH APPLICATION OF EQ. (7.3).

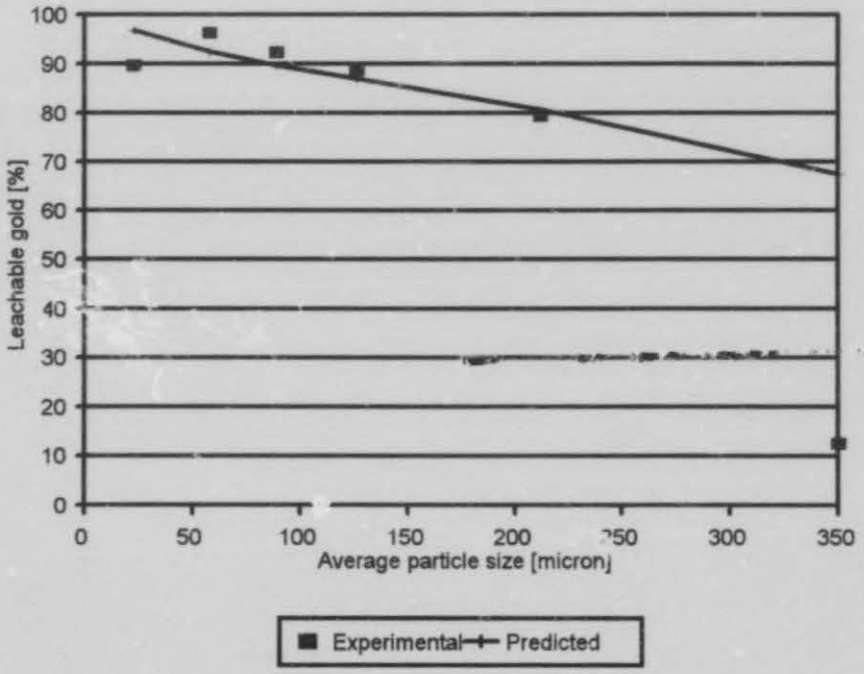

FIGURE 7.4: LEACHABLE GOLD AS A FUNCTION OF PARTICLE SIZE FOR MILLED LESLIE ORE WITH APPLICATION OF EQ. (7.3).

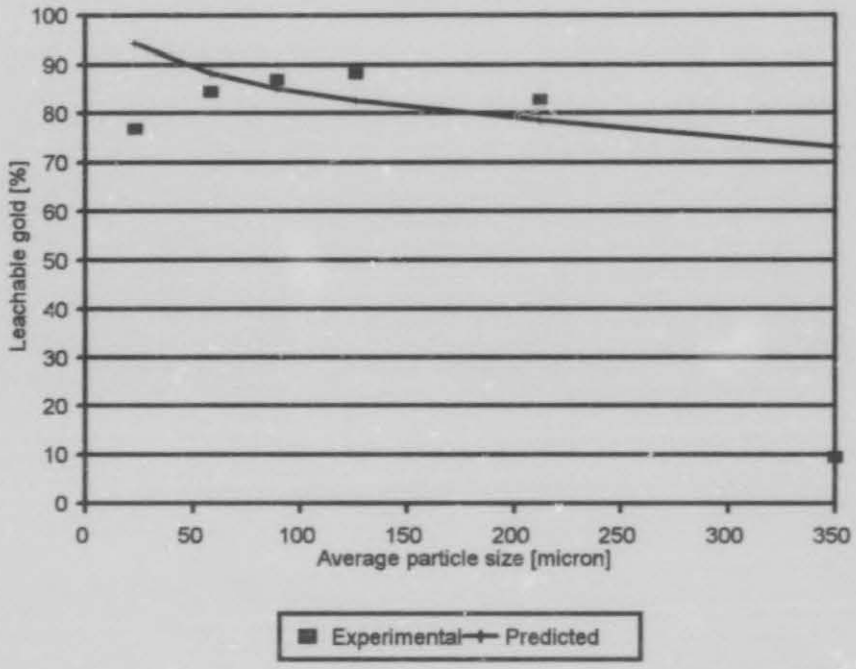

FIGURE 7.5: LEACHABLE GOLD AS A FUNCTION OF PARTICLE SIZE FOR MILLED BEATRIX ORE WITH APPLICATION OF EQ. (7.3).

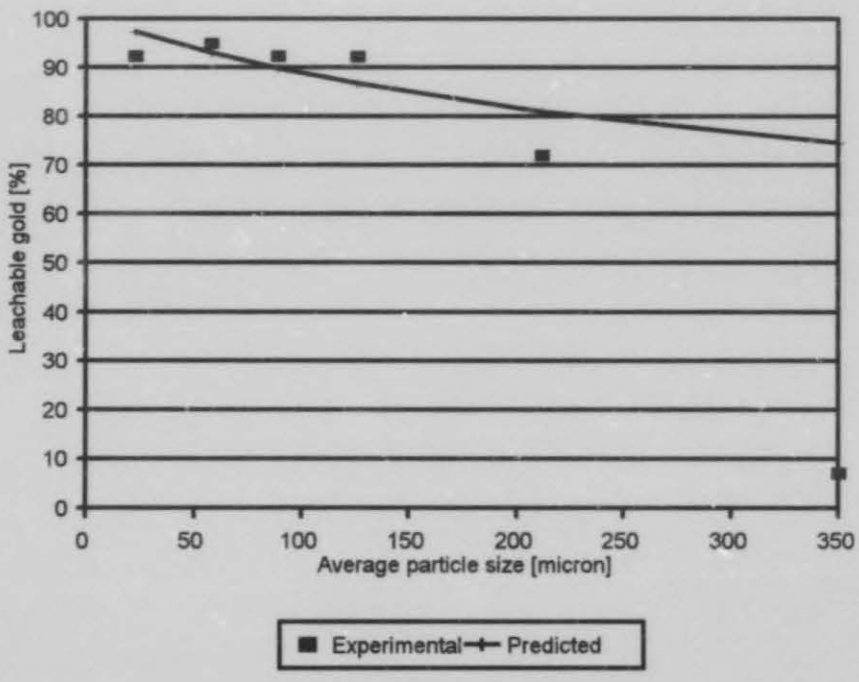

FIGURE 7.6: LEACHABLE GOLD AS A FUNCTION OF PARTICLE SIZE FOR MILLED HARMONY ORE WITH APPLICATION OF EQ. (7.3).

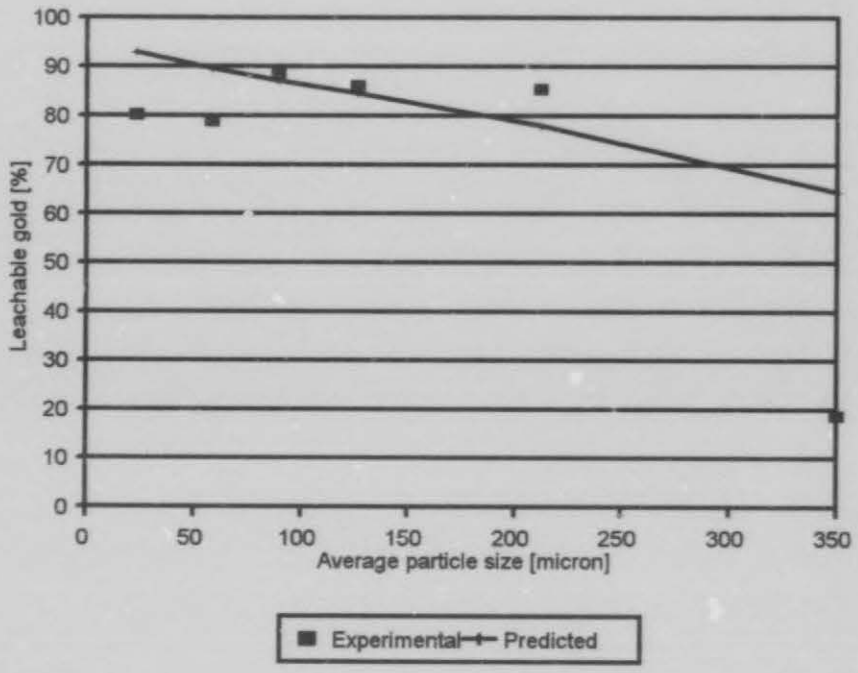

FIGURE 7.7: LEACHABLE GOLD AS A FUNCTION OF PARTICLE SIZE FOR MILLED St. HELENA ORE WITH APPLICATION OF EQ. (7.3).

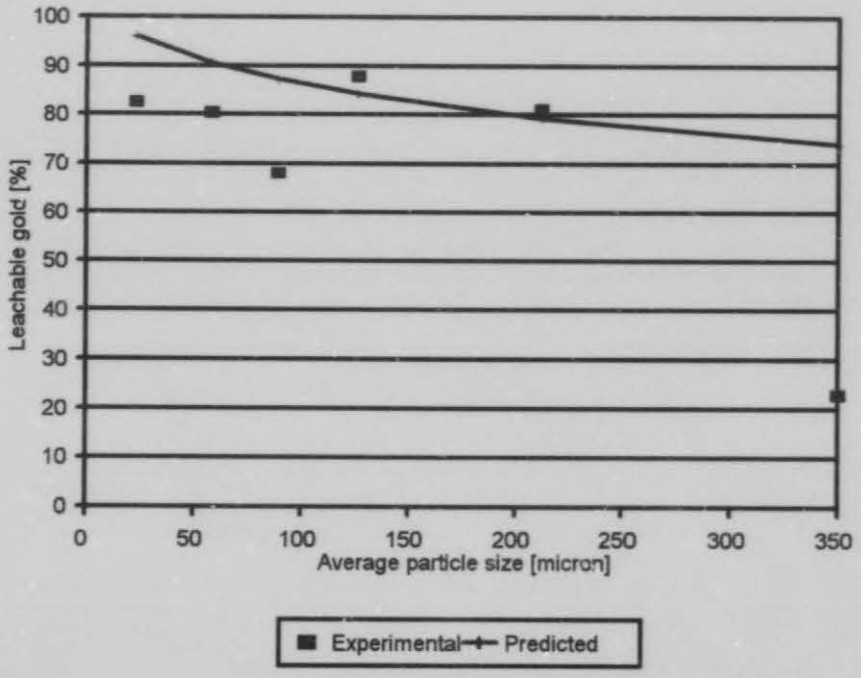

FIGURE 7.8: LEACHABLE GOLD AS A FUNCTION OF PARTICLE SIZE FOR MILLED UNISEL ORE WITH APPLICATION OF EQ. (7.3).

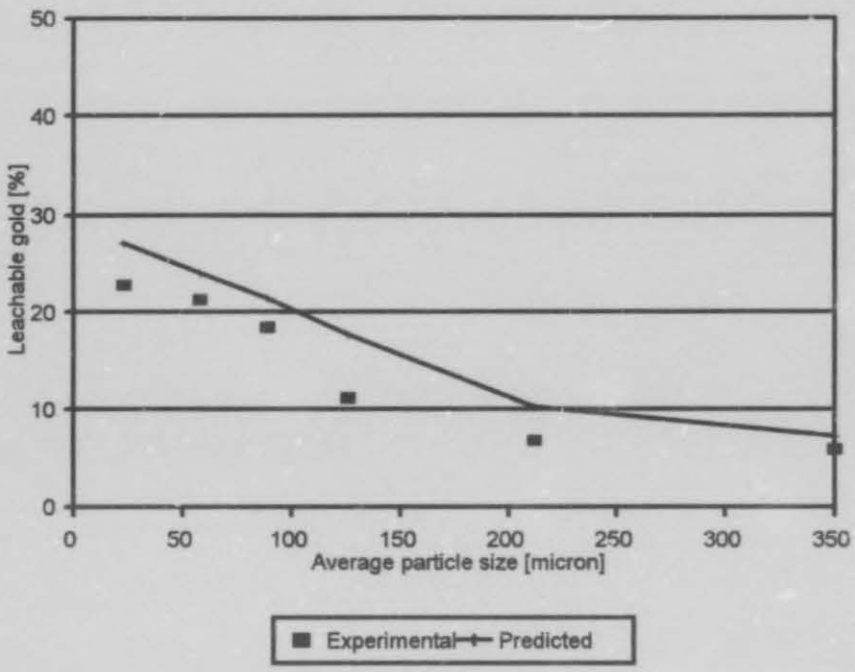

FIGURE 7.9: LEACHABLE GOLD AS A FUNCTION OF PARTICLE SIZE FOR MILLED WDL ORE WITH APPLICATION OF EQ. (7.3).

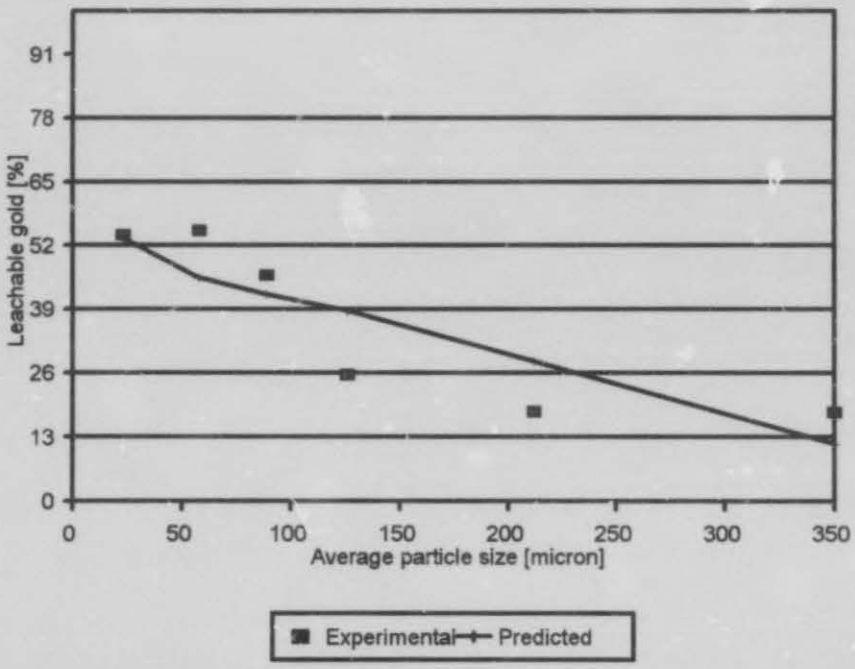

FIGURE 7.10: LEACHABLE GOLD AS A FUNCTION OF PARTICLE SIZE FOR MILLED FSG ORE WITH APPLICATION OF EQ. (7.3).

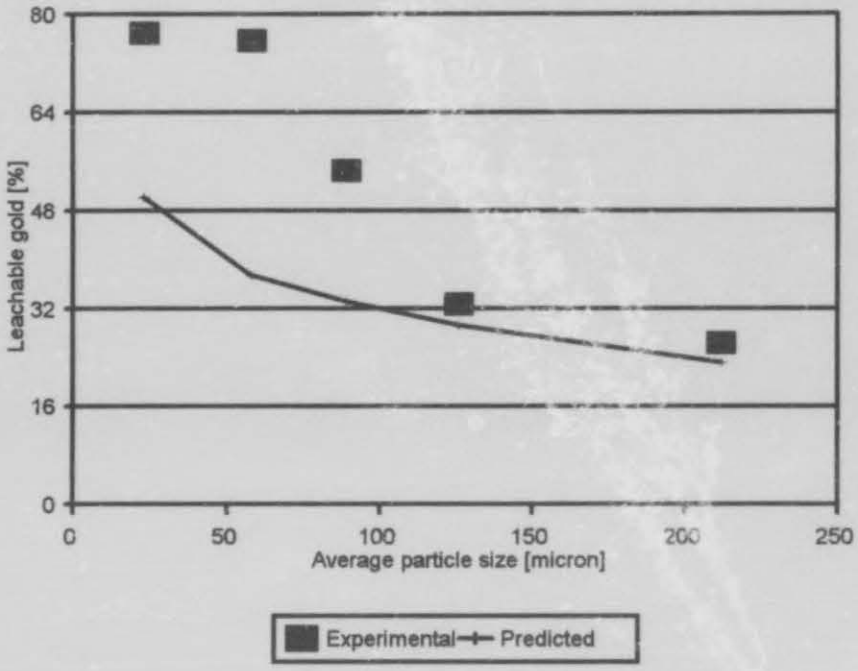

FIGURE 7.11: LEACHABLE GOLD AS A FUNCTION OF PARTICLE SIZE FOR MILLED HARTIES ORE WITH APPLICATION OF EQ. (7.3)

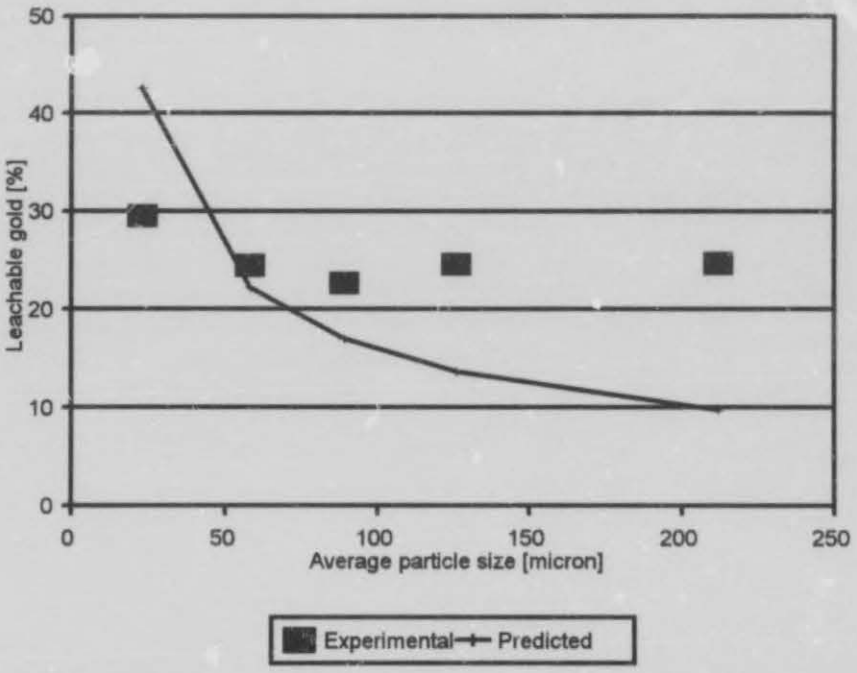

FIGURE 7.12: LEACHABLE GOLD AS A FUNCTION OF PARTICLE SIZE FOR MILLED BARBERTON ORE WITH APPLICATION OF EQ. (7.3)

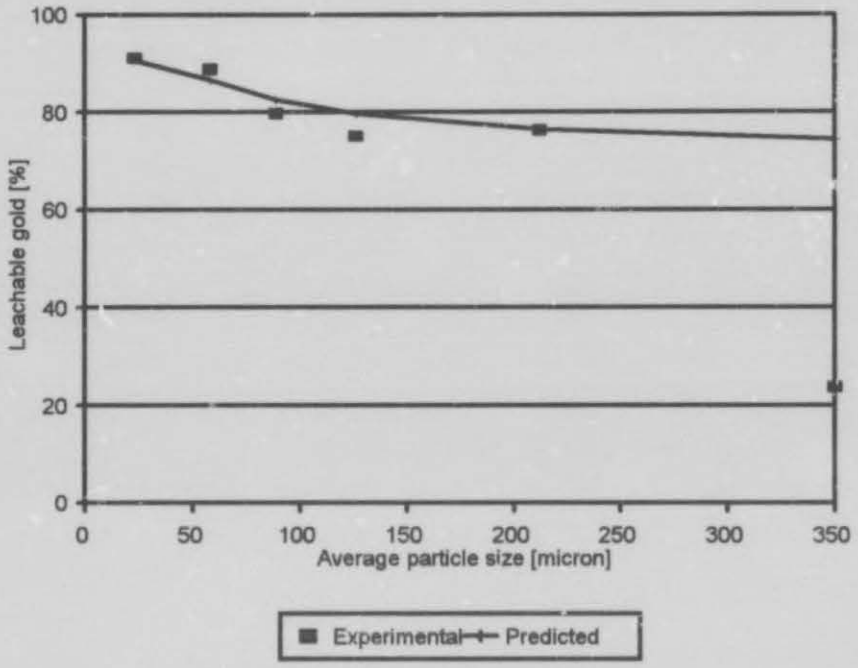

FIGURE 7.13: LEACHABLE GOLD AS A FUNCTION OF PARTICLE SIZE FOR MILLED KINROSS ORE WITH APPLICATION OF EQ. (7.7)

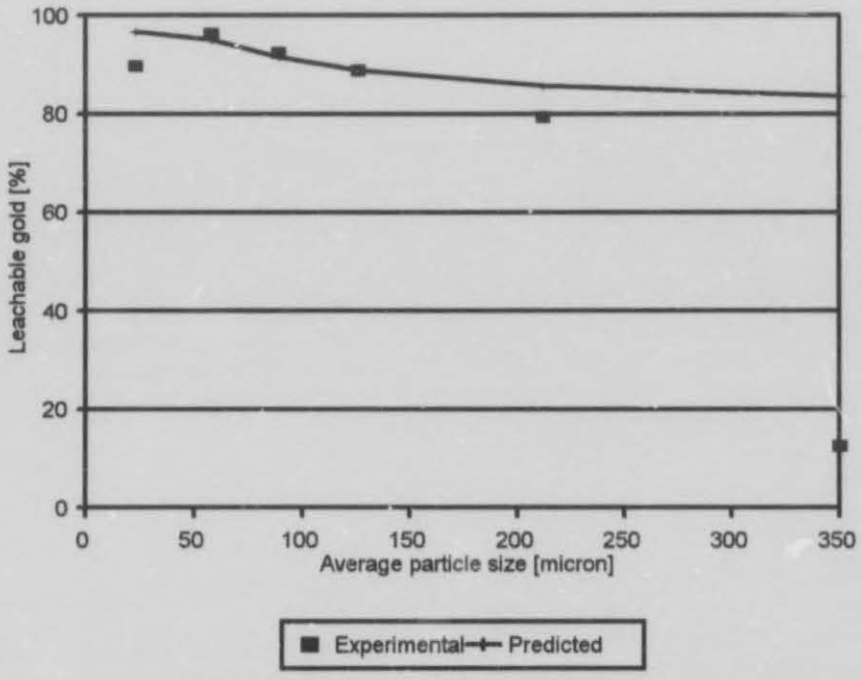

FIGURE 7.14: LEACHABLE GOLD AS A FUNCTION OF PARTICLE SIZE FOR MILLED LESLIE ORE WITH APPLICATION OF EQ. (7.7)

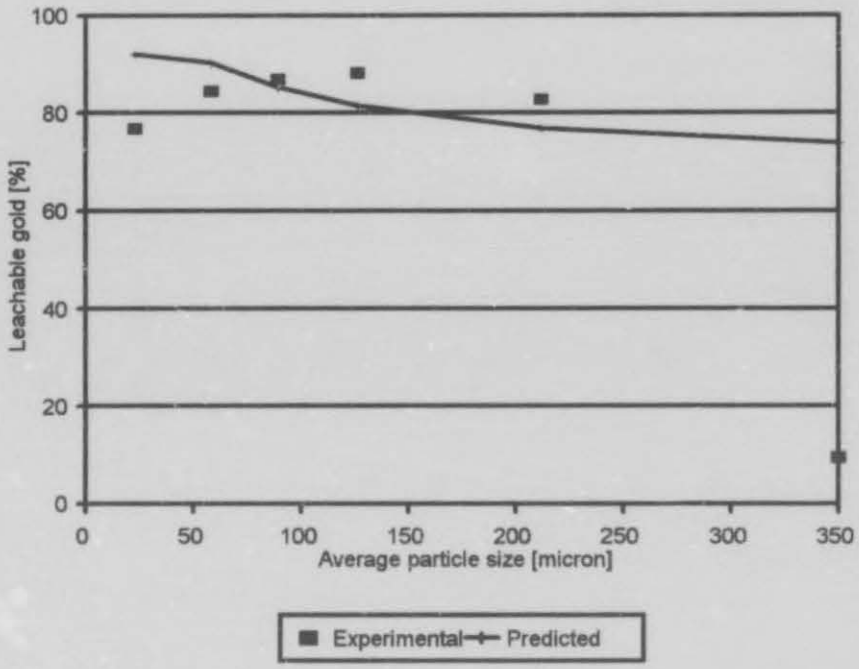

FIGURE 7.15: LEACHABLE GOLD AS A FUNCTION OF PARTICLE SIZE FOR MILLED BEATRIX ORE WITH APPLICATION OF EQ. (7.7)

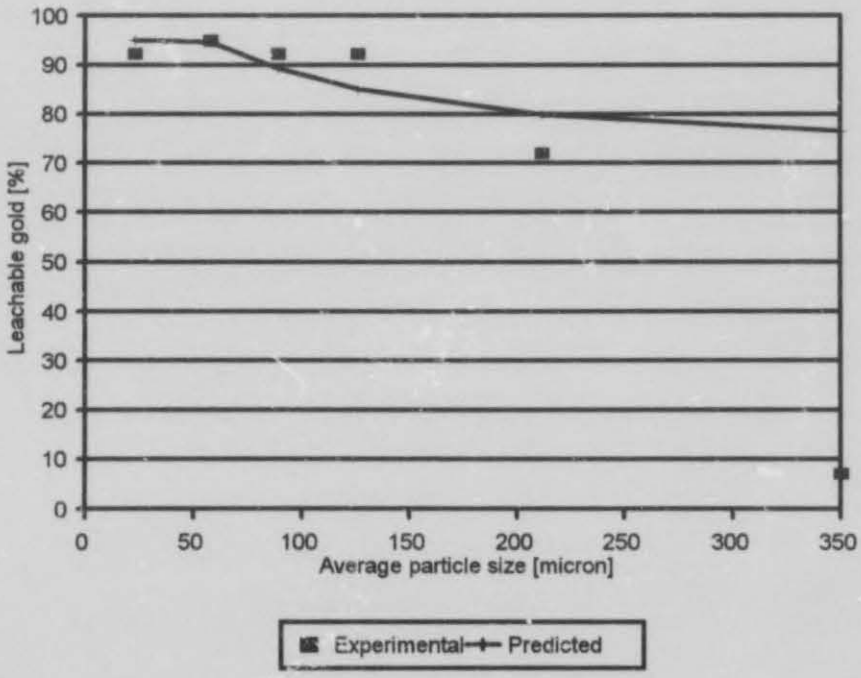

FIGURE 7.16: LEACHABLE GOLD AS A FUNCTION OF PARTICLE SIZE FOR MILLED HARMONY ORE WITH APPLICATION OF EQ. (7.7)

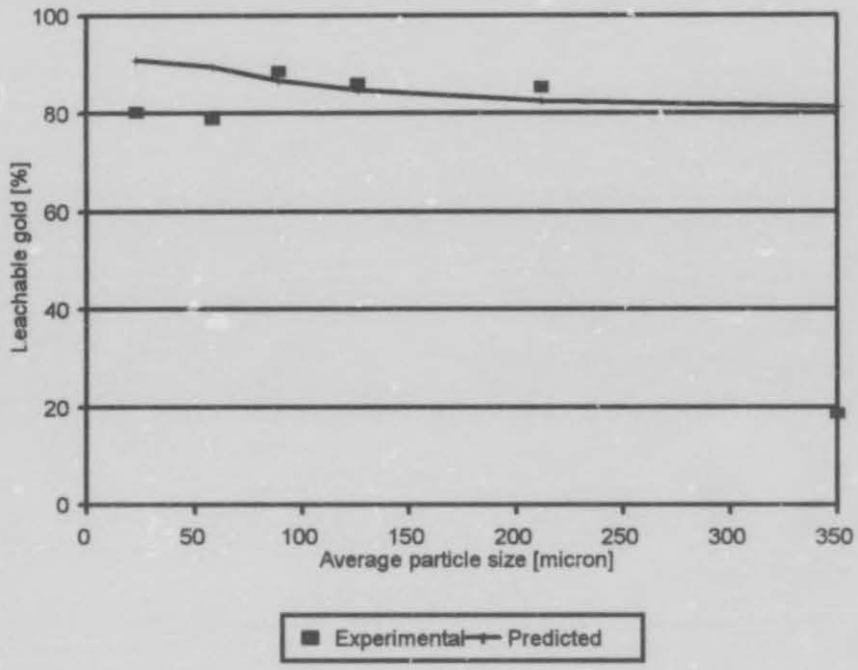

FIGURE 7.17: LEACHABLE GOLD AS A FUNCTION OF PARTICLE SIZE FOR MILLED St HELENA ORE WITH APPLICATION OF EQ. (7.7)

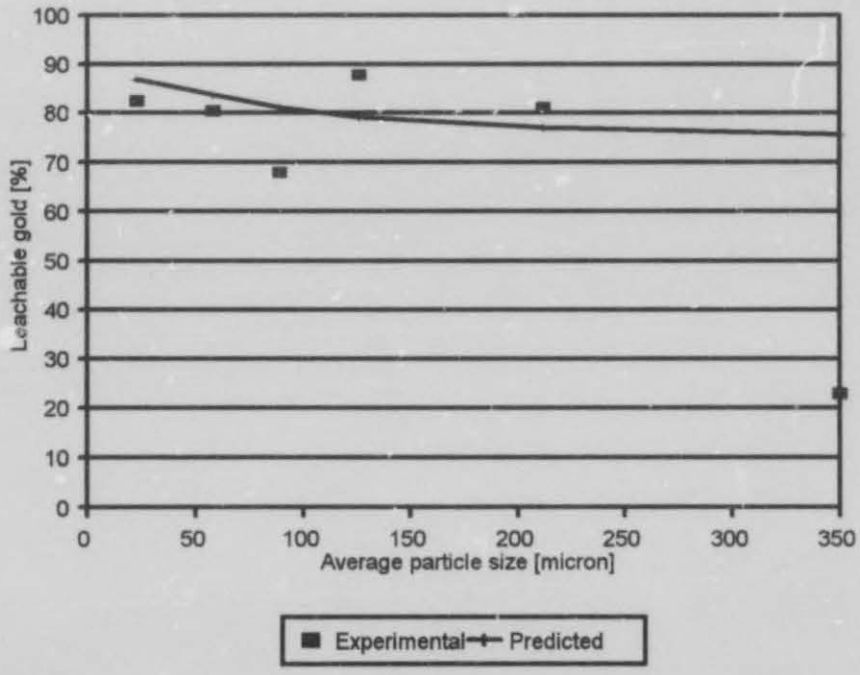

FIGURE 7.18: LEACHABLE GOLD AS A FUNCTION OF PARTICLE SIZE FOR MILLED UNISEL ORE WITH APPLICATION OF EQ. (7.7)

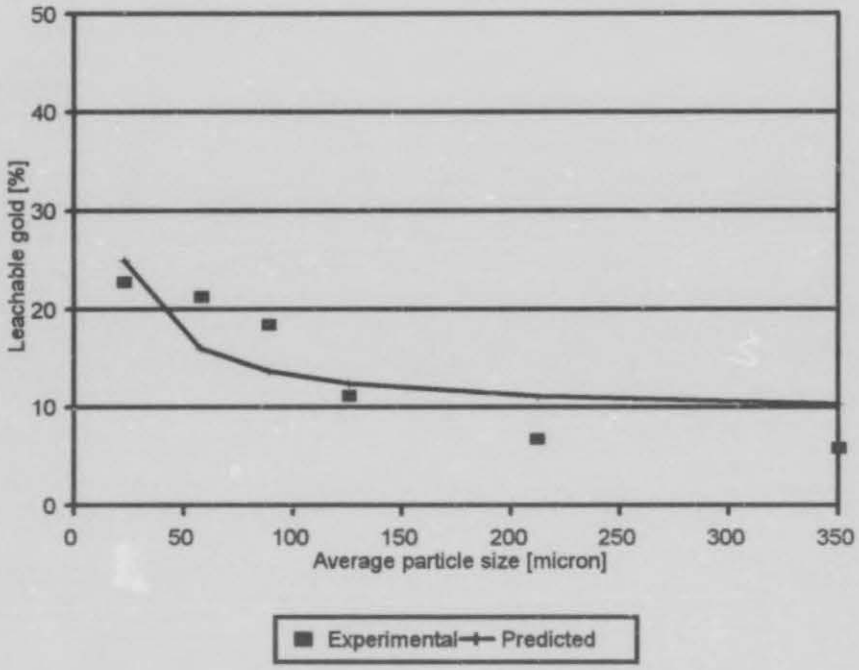

FIGURE 7.19: LEACHABLE GOLD AS A FUNCTION OF PARTICLE SIZE FOR MILLED WDL ORE WITH APPLICATION OF EQ. (7.7)

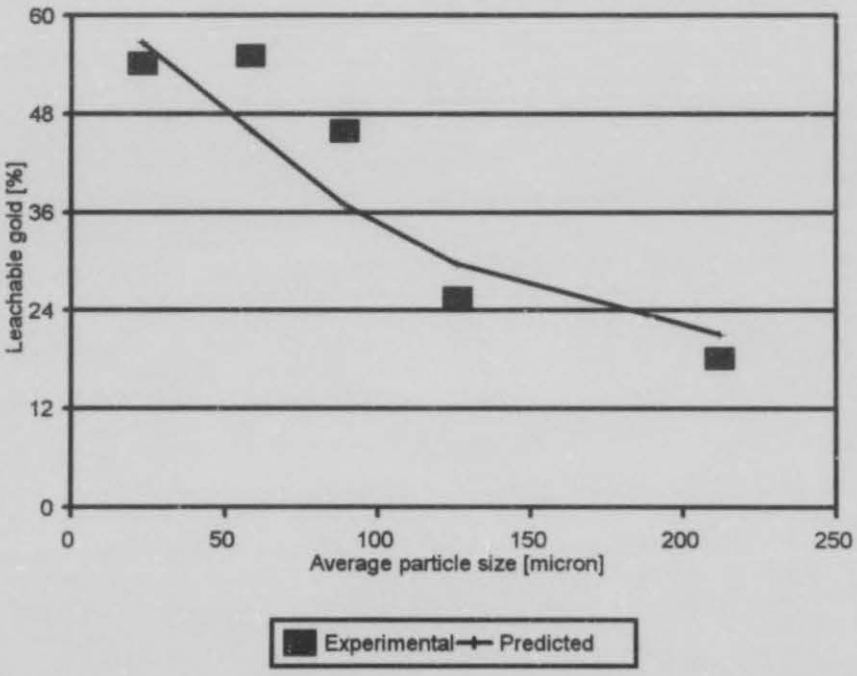

FIGURE 7.20: LEACHABLE GOLD AS A FUNCTION OF PARTICLE SIZE FOR MILLED FSG ORE WITH APPLICATION OF EQ. (7.7)

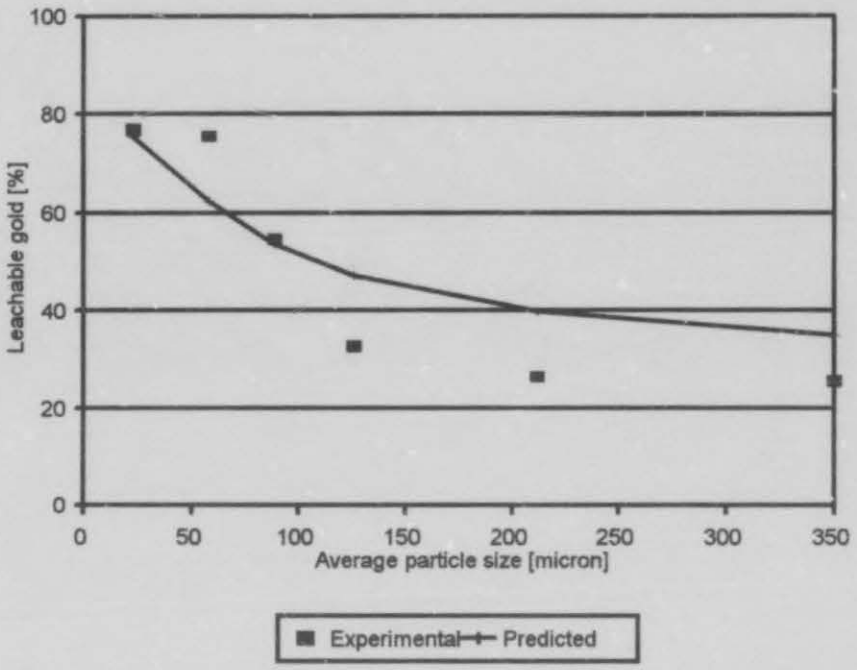

FIGURE 7.21: LEACHABLE GOLD AS A FUNCTION OF PARTICLE SIZE FOR MILLED HARTIES ORE WITH APPLICATION OF EQ. (7.7)

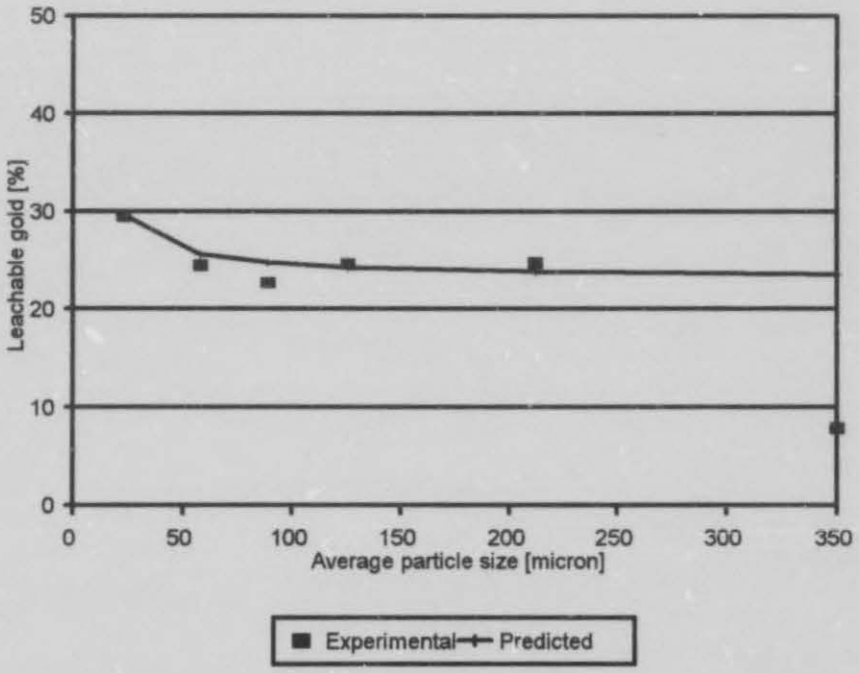

FIGURE 7.22: LEACHABLE GOLD AS A FUNCTION OF PARTICLE SIZE FOR MILLED BARBERTON ORE WITH APPLICATION OF EQ. (7.7)

CHAPTER 8

NEURAL NET ANALYSIS OF DATA

CHAPTER 8

NEURAL NETWORK ANALYSIS OF DATA

Neural net systems are widely acknowledged as one of the fastest growing computer technologies today and have attracted particular interest in the process engineering community as a framework for the representation of ill-defined processes which cannot be modelled readily by other means, such as the modelling of metal-slag equilibria (Reuter et al, 1992), generalised reaction rate kinetics (Reuter et al, 1993), etc. Although neural networks are efficient tools for the modelling and interpretation of plant and unit process data, it has not found much practical application yet in the mineral processing industry , mainly due to the lack of sufficient technology transfer and the problems associated with it. It was decided to use neural networks together with the modelling techniques discussed in previous chapters (6 and 7) to assist in the understanding of the relationship between mineral liberation and leaching behaviour. A back propagation neural network (BPNN), due to it's versatility, simpleness and effectiveness, as well as a self-organising network to perform cluster analysis were thus selected to fulfil this purpose.

8.1 NEURAL NETWORKS

Neural networks are essentially connectionist systems consisting of collections of simple, massively interconnected computational elements, and their characteristics stem from the collective behaviour of these elements, also known as (artificial) neurons, neurods, processing elements, processing nodes or processing units (Aldrich, 1994). In a back propagation neural network (BPNN) the processing elements are typically divided into disjoint subsets or layers, in which all the process units possess essentially similar computational characteristics. The layers are usually categorised as either input, hidden or output layers. Process units in these layers are attached to other units in successive layers by means of weighted connections (adjustable numeric values), as shown in Figure 8.1. The training of the net comprises essentially of the adjustment of the weight matrix of the net. It occurs by means of learning algorithms usually designed to minimise the mean square error between the desired and the actual output of the net. Information is propagated back through the net during the learning process, in order to update its weights. The net forms thus an internal representation of

the relationship between the inputs and the outputs presented to it (Aldrich, 1994).

8.1.1 Neurodynamics

The computation in back propagation nets is feedforward and synchronous, i.e. moving from the input to the output layer. The activation rules of process units are typically of the form:

$$z_i(t+1) = \phi[u_i(t)] \tag{8.1}$$

where $u_i(t)$ is the potential of a process unit (Figure 8.2) at time t; thus the difference between the weighted sum of all the inputs to the unit and the unit bias

$$u_i(t) = \sum w_{ij} z_j(t) - \theta_i \tag{8.2}$$

The transfer function $\phi(*)$ could be of a linear, step, sigmoidal or some other form, with a domain typically much smaller than that of the potential of the process unit, such as [0;1] or [1;1], for example. A back propagation neural net as earlier stated is trained by changing the weights of the net iteratively, typically by means of a gradient descent method, in order to minimise an error criterion, that is

$$w_{ij}(t+1) = w_{ij}(t) + \Delta w_{ij} \tag{8.3}$$

where

$$w_{ij} = -\tau . \partial\varepsilon / \partial w_{ij} \tag{8.4}$$

$$\varepsilon = \tfrac{1}{2}\sum (d_{o,j} - z_{o,j})^2 \tag{8.5}$$

where τ - learning rate.

ε - error criterion.

$d_{o,j}$ - desired output of the unit.

$z_{o,j}$ - actual output of the unit.

8.1.2 Scaling of data

It is usually necessary to scale the data that are presented to the net to ranges which would enable the net to learn effectively. A hyperbolic tangent transfer function produces outputs in the range lying between -1 and 1 for example and it is thus necessary to scale the outputs to the same range by mapping the minimum and the maximum values of the actual input and output data linearly to the respective minimum and maximum values of the network ranges. If an exemplar presented to the net consists of I input fields and D output fields, i.e. $[f_1, f_2,...f_I, f_{I+1},f_{I+2},..f_{I+D}]$, two sets of corresponding vectors can be defined $[m_1, m_2, ..m_I, m_{I+2}, ..m_{I+D}]$ and $[M_1, M_2, ..M_I, M_{I+1}, M_{I+2}, ..M_{I+D}]$, where m_k and M_k typically correspond to the minimum and maximum values (they can assume any values, as long as $m_k<M_k$) that f_k could assume. The mappings of the real world data to those of the network can be described as follows (Aldrich, 1994):

Input: $$i_j = [(R_i - r_i).f_j + M_j.r_i - m_j.R_i]/[M_j-m_j] \quad (8.6)$$

Output: $$d_k = [(R_D-r_D).f_k + M_k.r_D - m_k.R_D]/[M_k-m_k] \quad (8.7)$$

Mapping from network output to real world:

$$g_k = [(M_k-m_k).o_k + R_D.m_k - r_D.M_k]/[R_D-r_D] \quad (8.8)$$

Non-numeric or missing field values are usually mapped to the middle of the target range, that is $\frac{1}{2}(R_i+r_i)$ or $\frac{1}{2}(R_D+r_D)$.

where (r_i, R_i) - ranges allowed for the input layers of the net,

(r_D, R_D) - ranges allowed for the output layers of the net,

i_j - the scaled network input corresponding to f_j,

d_k - the desired scaled network output corresponding to f_k,

o_k - the actual (scaled) output of the net,

g_k - the corresponding (descaled) real world output.

The main advantage of modelling techniques based on the use of neural nets, is thus that prior assumptions with regard to the functional relationship between the inputs and the outputs are not required. The net learns this relationship on the basis of examples of typical input and output values produced by the process under investigation. Once a model has been

constructed, it is moreover possible to make use of general or special purpose Neuralware (Aldrich, 1994) to decrease computation time and thus enabling for example the use of the model in on-line control systems.

Thus, a back propagation net with an input layer, one hidden layer that comprised of three processing elements or artificial neurons and an output layer was thus used in the modelling of the deportment of gold after comminution. The input layer did not process the data, but served to distribute the data to the hidden layer. The layers were connected in a forward manner so that no layer was connected to any layer preceding it. All layers consisted of elements with hyperbolic tangent translation functions to ensure that low-valued and high valued outputs were treated equally, i.e

$$\phi(u) = (e^{+u} - e^{-u})/(e^{+u} + e^{-u}) \qquad (8.9)$$

8.2 DATA ANALYSIS

The following two techniques, namely non-linear principal component analysis (NLPCA) and self-organising maps (SOM) were used in the analysis of the data.

8.2.1 NLPCA

Non-linear principal component analysis is used as a technique to analyse multivariate data. NLPCA uncovers both linear and non-linear correlations between variables by identifying and removing correlations among problem variables as an aid to dimensionality reduction, visualisation and exploratory data analysis. It operates by training a feedforward neural network (like a BPNN) to perform the identity mapping, where the network inputs are reproduced at the output layer. The network contains an internal bottleneck layer which forces the network to develop a compact representation of the input data (Kramer, 1991).

NLPCA was performed on the gold deportment data of the unmilled and milled ores. The gold associated with pyrite , BMS , silicates and carbonaceous material of each ore in each particle size fraction was used as the inputs. These data were then reproduced by the net as the outputs.

From the results obtained, the net showed that there was a strong correlation between the gold associated with the different minerals to such an extent that only three of the four inputs are needed to perform the

analysis successfully. This phenomenon was expected, since the various gold-bearing minerals are distributed randomly in the ore and are intergrown with one another. Thus, the liberation of gold from a mineral will be influenced not only by that mineral but also by the other minerals.

8.2.2 SOM analysis

A self-organising net was used to create a two-dimensional feature map (SOM) of the input as well as the output data (see Figures 8.3 and 8.4). The maps are created in such a manner that the order of the data is preserved. This characteristic of the net makes it useful for cluster analysis and visualisation of topologies and hierarchical structures of higher dimensional input spaces (Aldrich, 1995).

A principal difference between other nets and a self organising net is that the latter learns without supervision. Such a net typically consists of an input layer that is fully connected to a two dimensional Kohonen layer (Aldrich, 1995). Each process element in the Kohonen layer measures the Euclidean distance of its weights to the input values fed to the layer. Suppose the input data consist of M-dimensional vectors of the form $x = \{x_1, x_2, x_3, ..x_M\}$, then each Kohonen element will have M weight values, that can be denoted by $w_i = \{w_{i1}, w_{i2}, w_{i3}, ..w_{iM}\}$. The Euclidean distance,

$$D_i = |x-w_i| \qquad (8.10),$$

between the input vectors and the weights of the net is then computed for each of the Kohonen elements and the winner is determined by the minimum Euclidean distance.

The weights of the element with the smallest Euclidean distance, as well as its neighbouring elements are subsequently adjusted in order to move the weights closer to the input vector, as follows:

$$w_{ij,new} = w_{ij,old} + a(x_j - w_{ij,old}) \qquad (8.11)$$

where a is an appropriate learning coefficient that is time dependent (decreases with time, typically starting at 0.4 and decreasing to 0.1 or lower).

The adjustment of the weights of the elements in the immediate vicinity of the element with the smallest Euclidean distance is important in the preservation of the order of the input space and amounts to an order preserving projection of the input space onto the two-dimensional Kohonen layer (Aldrich, 1995).

The gold deportment in the various minerals (%), the fraction of free gold (%), the head grade, the mass distribution and the geometric mean particle size in a particle size fraction of each ore in each particle size fraction of both the unmilled and milled ore samples were used as inputs to the self-organising maps. The maps of the unmilled and milled ore samples are presented in Figures 8.3 and 8.4, respectively.

The centres of gravity $c_j(X_j,Y_j)$ of each ore j on the topological maps shown in Figures 8.3 and 8.4 as well as the distance d_{ij} of each individual data point (a data point corresponds to a specific particle size fraction within the ore j) I from each of the centres of gravity c_j were calculated in order to evaluate the ability of the neural net to cluster the various data points of a specific ore. The centre of gravity and distance can be calculated as such:

$$c_j(X_j,Y_j) = (\sum_i x_{ij}/n \; ; \; \sum_i y_{ij}/n) \qquad (8.12)$$

$$d_{ij} = [(x'_j - X_j)^2 + (y'_i - Y_j)^2]^{1/2} \qquad (8.13)$$

where x_{ij} - x-coordinate of the i-th data point from the j-th ore.

y_{ij} - y-coordinate of the i-th data point from the j-th ore.

X_j - x-coordinate of the centre of gravity.

Y_j - y-coordinate of the centre of gravity.

If there is perfect separation of each of the ores, all distances d_{ij} ($i \equiv j$) can be expected to be smaller than d_{ij} ($i \neq j$). The degree of clustering, which is a measure of the sharpness of the separation, can be constructed by sorting all d_{ij} values for each ore j from small to large. Nine ranking lists, one for each ore, will thus be constructed. The measure of dispersion M_j is then calculated as follows:

$$M_j = \sum_i m_{ij}$$

where m_{ij} - the ranking order of d_{ij} if $i \equiv j$, and 0 otherwise. How lower the value of M_j, the sharper the definition of the clusters. The dispersion M_j is now normalised to enable generalised comparisons between ores.

That is:

$$M'_j = (M_j - M_{jmax})/(M_{jmin} - M_{jmax})$$

where M'_j - normalised dispersion.

M_{jmin} - the best degree of clustering possible for the system.

M_{jmax} - the worst degree of clustering possible for the system.

A value of 1 for M'_j is thus an indication of perfect clustering, while a value of 0 indicates perfect dispersion or random mapping of the various ore members.

The centres of gravity and the normalised measure of dispersion are presented in Tables 8.1a and 8.1b and Figures 8.5 and 8.6. The relative distances between the centres of gravity of the unmilled and milled ores are tabulated in Table 8.2 and are depicted graphically in Figure 8.7 (The distances were calculated from results obtained when the data of both the unmilled and milled ores were mapped by the same net).

From Figure 8.5, the measure of clustering for the unmilled Kinross, Beatrix, St. Helena and Barberton gold ores is about the same ($M'_j = 0.7$) as well as for the unmilled Harmony and Unisel gold ores (M'_j=0.92). However, when the centres of gravity of these ores (Table 8.1a) are compared with each other, it is evident that the net classifies these ores differently.

It is evident from Table 8.1a and Figure 8.5 that although the measure of clustering of the Kinross and Leslie gold ores differs with more or less 10%, the centres of gravity are very close to each other. This is probably because both ores originate from the same gold field, namely the Evander Gold Field (Figure 3.1). This phenomenon is also evident for the St. Helena and Unisel gold ores, with the variation in M'_j about 20% but with their centres of gravity close to each other. This was expected since the Unisel and St. Helena gold ores are only two separate feedstreams to the St. Helena gold mine, with the Unisel ore comprising of one third of the Basal reef, from which the St. Helena gold ore is mined, and two thirds of the Leader reef (chapter 3.1.2).

It is noticeable that not only the measure of clustering but also the centres of gravity for the milled Kinross and Leslie gold ores differ quite substantially from their unmilled counterparts as well as from one another.

This is quite different from what was found in the unmilled ores where their centres of gravity were close to each other. This shift in relative positions on the map is well illustrated by the Euclidean distances (Table 8.2) between the unmilled and milled Kinross and Leslie ores which are 0.604 and 0.241 respectively.

It can thus be concluded that although it is evident that the Kinross and Leslie gold ores are from the same goldfield (Table 8.1a), they exhibit totally different liberation characteristics when comminuted (Tables 8.1b and 8.2). This conclusion is also valid for the St. Helena and Unisel gold ores when Tables 8.1a, 8.1b and 8.2 are studied carefully. It is quite interesting to note that this conclusion was drawn qualitatively earlier in chapter 4.

From Figures 8.4 and 8.6 and Table 8.1b the measure of clustering for the milled Kinross, Beatrix, St. Helena and Barberton is again more or less the same (M'_j = 0.85). It is again, however, evident from the centres of gravity (Table 8.1b) that the ores exhibit different characteristics, mainly due to their different origins.

The unmilled as well as the milled WDL and FSG gold ores are clustered closely together and it is evident from Figures 8.3 to 8.6 that they exhibit totally different mineralogies from the non-refractory ores such as Kinross, Leslie, etc. The Barberton gold ore, as expected, differs quite substantially (centres of gravity -Table 8.1a) even from the WDL and FSG gold ores, due to the ore's unique mineral composition (chapter 3.1.5; 4.5 and 4.6). Despite these differences, the Euclidean distances between the centres of gravity of the unmilled and milled WDL and Barberton ores are more or less the same (0.46 and 0.40 respectively). This means thus that there is some resemblance in the way the ores liberate gold when comminuted.

8.3 NEURAL NET MODELS OF DIAGNOSTIC LEACHING RESULTS

As mentioned earlier, a back propagation neural network was used to model the diagnostic leaching results presented in chapter 4 (Tables 4.1 to 4.22 and Figures 4.1 to 4.20). The structures of the back propagation neural nets that were used are shown in Figure 8.8 and 8.9.

As a first approach, it was assumed that the liberation of gold from the different minerals was independent of the characteristics of the specific

minerals. It thus means thus that the breakage of the different gold-bearing minerals was assumed to be the same. This assumption was made to provide for a sufficient number of data. The geometric mean particle size in a particle size fraction (x_1) and the fraction of gold (%) associated with each of the minerals in each particle size fraction in the unmilled ore samples (x_2) were used as the input values, while the fraction of gold (%) associated with each of the minerals in each particle size fraction of the milled ore samples (y_1) were used as outputs. The set of data was randomised prior to subdivision into a test (50 vectors) and a training data (166 vectors) set. After training, the net was tested against the test data. This procedure is essential to verify the capability of the net to generalise the relationships between parameters correctly. The results (model 1) are presented in Figure 8.10.

In the second case (model 2), the following data of the unmilled ore samples were used as the inputs to the back propagation net, namely, the particle sizes (x_1); the mass distribution of the unmilled ore (x_2), the head grade (x_3), the percentage free gold (x_4), gold associated with BMS (x_5), pyrite (x_6), silicates (x_7) and carbonaceous material (x_8) in each particle size fraction. The outputs were the mass distribution of the milled ore (y_1), the head grade (y_2), the percentage free gold (y_3), percentage gold associated with BMS (y_4), pyrite (y_5), silicates (y_6) and carbonaceous material (y_7) in each particle size fraction of the milled ore samples. The net was trained with the data of eight ores (8x6=48 vectors) and the data of the ninth ore were then used to test the accuracy of the net (model 2) predictions. The sets of trained and test data that were used as inputs and outputs were thus varied nine times. The results obtained are presented in Table 8.3a to 8.3i.

In order to test the accuracy of the predictions made by the BPNN model 1, it was compared to the predictions made by a multilinear regression (MLR) model and multiquadratic regression (MQR) model which were also fitted to the experimental data. This comparison was, however, necessary since no other models were available to establish the accuracy of model 1. Only the predictions of the leachable (liberated) gold in each particle size fraction made by the BPNN model 2 was compared to the predictions that were made by the empirical models in chapter 6, since the objective of the empirical models was only to predict that fraction of leachable gold in each particle size fraction of the milled ores and not the gold deportment in the various minerals. The same criterion that was used in chapter 6, namely the average percentage error, equation 6.10, was thus used to test the

accuracy of the models. The average percentage error encountered by the different models are presented in Tables 8.4a and 8.4b. Since the neural model 2 also predicts the gold deportment, head grade and mass distribution in each particle size fraction of the milled ores, the predicted values were compared qualitatively with the experimental values. It was unfortunely not possible to obtain average percentage errors, encountered by the model that could be compared meaningfully due to large experimental errors.

It is evident from Figure 8.10 that the net performs better than the MLR and MQR models when compared to the experimental results. The average errors (Table 8.4a) for the BPNN, MLR and MQR are 62.93±48.68%, 69.56±44.56% and 91.29±85.7%, respectively. However, the predictions by the BPNN model 1 are fairly inaccurate mainly due to large experimental errors in the data (see chapter 4) and shortcomings in the assumptions. It was assumed that the liberation of the gold is independent of the characteristics of the ore. This is unfortunately not the case as illustrated with the different empirical models (equations 6.2, 6.3, 6.4 and 6.5) for the locked gold in each particle size fraction of the various gold bearing minerals in chapter 6.

In the derivation of model 2, a more accurate approach was followed. The gold deportment of the various unmilled ore samples and milled ore samples was used as inputs and outputs, respectively. Despite the small training set, the net was able to generalise the relationship between the input and output variables fairly well. It is evident from Table 8.4b that when the average errors encountered by the different models are compared, that the empirical models perform in most cases better than the net, especially with the refractory ores (Barberton, FSG and WDL). Although the net was trained on eight sets of data compared to four sets for the empirical models, the number of data were insufficient to train the net properly. It must also be noted that the predictions by the neural net model and the empirical models could not be directly compared since 31 { (8 inputs+1 bias)×3 nodes in the hidden layer + (3 nodes+1 bias)×1 output = 31} parameters were used in the neural net modelling and only 25 {8(a_1..a_4, b_1..b_4)×3 + 1 (particle size) = 25} in the modelling by the empirical models. It can thus be concluded that the empirical models predict the fraction of leachable gold in each particle size fraction slightly better.

It is evident when Table 8.3a to 8.3i are compared qualitatively to Tables 4.1 to 4.22 that the net fails to predict the gold associated with the

carbonaceous material and the head grade. This is probably due to experimental errors. Since the experimental values of the gold associated with the carbonaceous material are in most cases the smallest (Tables 4.1 to 4.22), a relatively small change (relative to the values of the other minerals, for example those of the gold associated with the silicates) in these experimental values will result in a large percentage error. Furthermore, the presence of different types of carbonaceous materials with different liberation and fracture characteristics in various quantities in the different ores will prevent the net to correlate the gold associated with carbonaceous material efficiently.

The net predicts the gold associated with the BMS only with moderate accuracy (Tables 8.3a to 8.3i). This is probably due to the fact that the base metal sulphides include various minerals, with each having its own characteristics and texture and thus liberating gold differently. This phenomenon was also found when the empirical model was derived (see chapter 6.4).

8.4 SUMMARY

Although mineral liberation is well discussed and defined in the literature by various researchers, Gaudin (1939), Wiegel (1967), King (1979), Austin (1983), Meloy (1983-1994) etc. it is still a highly complex problem. However, only very little research (Lorenzen, 1992a; Lorenzen and Van Deventer, 1994) has been done until now to understand the interrelationship between mineral liberation and leaching behaviour. Neural networks were thus used to assist in the understanding of this relationship.

From this preliminary investigation of the modelling of diagnostic leaching results of unmilled and milled ores by neural networks it can be concluded that the use of neural net methods can be a very efficient way of analysing this type of data. Although the models (model 1 and 2) only give reasonable predictions, it must be taken into account that these models are only provisional and that some refinement is still needed before they can be used to quantify the relationship between liberation and leaching behaviour satisfactory. It will thus be possible when sufficient data are obtained, not only to predict the leachable gold but also the deportment of gold in the various minerals in a milled ore when the deportment of gold in the unmilled ore is known. It is furthermore evident that although the predictions by the empirical models are at this stage more accurate than those by the neural net

models, the latter could be used more extensively and generally than the empirical models (equation 6.6) derived in chapter 6.

It is also possible that the gold deportment and liberation characteristics of a new ore could be classified by using SOM analysis

TABLE 8.1a

THE MEASURE OF CLUSTERING AND CENTRES OF GRAVITY FOR EACH UNMILLED ORE .

Symbol	Ores	Measure of clustering	Centre: x-coordinate	Centre: y-coordinate
A	Kinross	0.719	0.291	0.538
B	Leslie	0.608	0.269	0.490
C	Beatrix	0.698	0.437	0.470
D	Harmony	0.920	-0.128	0.863
E	St. Helena	0.705	-0.166	0.480
F	Unisel	0.913	-0.163	0.285
G	Barberton	0.712	-0.177	-0.862
H	WDL	1.000	0.476	-0.823
I	FSG	1.000	-0.204	-0.709

TABLE 8.1b

THE MEASURE OF CLUSTERING AND CENTRES OF GRAVITY FOR EACH M[illed] O[re]

Symbol	Ores	[illegible]	Centre: x-coordinate	Centre: y-coordinate
A	Kinross	0.851	-0.604	0.145
B	Leslie	0.375	-0.177	0.104
C	Beatrix	0.795	-0.168	0.486
D	Harmony	0.623	-0.581	-0.304
E	St. Helena	0.840	0.390	0.527
F	Unisel	0.566	0.191	0.091
G	Barberton	0.892	0.315	-0.618
H	WDL	1.000	0.380	-0.806
I	FSG	0.910	0.788	-0.472

TABLE 8.2

THE EUCLIDEAN DISTANCES BETWEEN THE CENTRES OF GRAVITY OF THE UNMILLED AND MILLED ORES.

Symbol	Ores	Euclidean distances
A	Kinross	0.604
B	Leslie	0.242
C	Beatrix	0.384
D	Harmony	0.588
E	St. Helena	0.255
F	Unisel	0.183
G	Barberton	0.465
H	WDL	0.404
I	FSG	0.097

TABLE 8.3a

BPNN-MODEL 2 PREDICTIONS FOR THE KINROSS MILLED ORE.

Particle size µm	Mass fraction	Head Grade	% Free Au	% Au in BMS	% Au in Pyrite	% Au in Carbon	% Au in Silicate
350	5.84	4.41	11.56	1.76	31.75	13.56	52.09
212	4.28	15.55	79.60	5.45	12.14	1.49	-0.27
126	4.28	15.55	79.62	5.44	12.11	1.50	-0.26
89	5.00	15.31	79.76	5.49	11.71	1.47	-0.23
58	26.57	10.67	82.60	7.09	5.71	0.83	-0.43
23	57.67	5.91	85.87	9.34	0.23	0.16	-0.60

TABLE 8.3b

BPNN-MODEL 2 PREDICTIONS FOR THE LESLIE MILLED ORE.

Particle size µm	Mass fraction	Head Grade	% Free Au	% Au in BMS	% Au in Pyrite	% Au in Carbon	% Au in Silicate
350	16.14	2.52	22.50	10.08	15.65	10.48	44.79
212	8.83	5.75	89.17	6.15	3.85	1.63	0.41
126	9.01	5.45	89.31	4.40	3.06	2.39	2.26
89	9.05	5.44	89.33	4.35	3.04	2.41	2.31
58	9.04	5.44	89.33	4.34	3.04	2.41	2.32
23	43.26	3.07	88.28	4.44	3.64	3.13	2.09

TABLE 8.3c

BPNN-MODEL 2 PREDICTIONS FOR THE BEATRIX MILLED ORE.

Particle size µm	Mass fraction	Head Grade	% Free Au	% Au in BMS	% Au in Pyrite	% Au in Carbon	% Au in Silicate
350	30.94	4.87	18.86	19.99	27.99	11.16	21.10
212	5.33	28.67	86.42	8.69	3.73	0.90	-1.53
126	5.34	28.94	87.03	8.43	3.51	0.83	-1.59
89	5.66	28.86	87.06	8.40	3.51	0.84	-1.57
58	15.24	26.36	86.39	8.03	[illegible]	0.87	-0.93
23	61.70	15.24	83.62	6.68	6.17	1.11	2.06

TABLE 8.3d

BPNN-MODEL 2 PREDICTIONS FOR THE HARMONY MILLED ORE.

Particle size µm	Mass fraction	Head Grade	% Free Au	% Au in BMS	% Au in Pyrite	% Au in Carbon	% Au in Silicate
350	46.37	3.94	15.51	15.20	20.67	12.34	42.50
212	0.41	10.56	78.79	6.37	0.72	8.34	5.31
126	0.61	10.67	80.75	6.68	0.88	2.76	3.28
89	0.37	10.80	81.51	6.24	-0.18	3.05	4.47
58	36.33	4.90	24.54	13.44	16.11	10.59	33.90
23	41.06	7.74	83.25	13.01	-2.20	2.39	2.64

TABLE 8.3e

BPNN-MODEL 2 PREDICTIONS FOR THE St. HELENA MILLED ORE.

Particle size µm	Mass fraction	Head Grade	% Free Au	% Au in BMS	% Au in Pyrite	% Au in Carbon	% Au in Silicate
350	1.66	5.77	12.33	-0.23	8.76	11.16	68.11
212	6.32	7.61	84.28	9.01	2.74	0.90	5.59
126	6.40	7.63	84.89	9.16	2.68	0.83	5.18
89	6.62	7.19	75.85	13.28	6.95	0.84	4.26
58	16.13	6.96	86.15	8.29	2.46	0.87	4.81
23	61.76	4.63	90.06	5.16	1.69	1.11	3.85

TABLE 8.3f

BPNN-MODEL 2 PREDICTIONS FOR THE UNISEL MILLED ORE.

Particle size µm	Mass fraction	Head Grade	% Free Au	% Au in BMS	% Au in Pyrite	% Au in Carbon	% Au in Silicate
350	3.09	13.36	13.45	5.66	6.60	9.47	68.37
212	3.01	29.63	84.11	8.38	1.93	1.99	3.48
126	3.01	29.75	84.50	8.34	1.86	1.97	3.30
89	3.11	29.73	84.58	8.32	1.86	1.97	3.25
58	6.54	28.48	84.74	8.23	2.14	2.08	2.81
23	61.50	14.12	86.33	5.55	3.77	3.98	0.95

TABLE 8.3g

BPNN-MODEL 2 PREDICTIONS FOR THE BARBERTON MILLED ORE.

Particle size µm	Mass fraction	Head Grade	% Free Au	% Au in BMS	% Au in Pyrite	% Au in Carbon	% Au in Silicate
350	13.07	1.51	12.51	37.97	50.89	1.04	1.97
212	13.05	15.1	12.53	37.99	50.90	1.03	1.94
126	10.01	3.10	33.12	28.12	34.85	1.33	0.99
89	7.86	4.67	54.84	18.50	21.85	1.58	0.30
58	5.37	7.34	81.76	7.24	7.70	1.95	-0.57
23	57.05	2.29	74.92	8.21	8.64	1.01	3.12

TABLE 8.3h

BPNN-MODEL 2 PREDICTIONS FOR THE WDL MILLED ORE.

Particle size µm	Mass fraction	Head Grade	% Free Au	% Au in BMS	% Au in Pyrite	% Au in Carbon	% Au in Silicate
350	-2.19	11.53	7.36	25.75	51.57	6.66	-0.91
212	4.96	14.29	28.80	27.12	42.49	3.57	-6.05
126	6.73	14.67	34.03	27.06	40.53	3.14	-6.46
89	10.24	13.89	37.40	25.65	37.83	2.91	-6.24
58	35.50	10.20	45.06	22.37	31.19	2.16	-5.67
23	61.81	6.15	58.33	15.78	19.91	1.355	-3.80

TABLE 8.3i

BPNN-MODEL 2 PREDICTIONS FOR THE FSG MILLED ORE.

Particle size µm	Mass fraction	Head Grade	% Free Au	% Au in BMS	% Au in Pyrite	% Au in Carbon	% Au in Silicate
350	5.07	8.40	6.25	26.70	63.99	6.23	1.92
212	2.75	16.57	41.74	20.55	49.24	1.22	-5.99
126	2.14	19.29	57.33	18.57	43.11	0.30	-7.03
89	1.96	20.36	63.61	17.75	40.39	-0.01	-7.35
58	4.09	19.62	66.14	17.74	38.93	-0.16	-7.43
23	57.48	3.28	34.37	26.60	48.71	1.03	-4.40

TABLE 8.4a

AVERAGE PERCENTAGE ERRORS ENCOUNTERED WITH BPNN-MODEL 1, MLR AND MQR.

	BPNN [%]	MLR [%]	MQR [%]
Model 1 -	62.93±48.68	69.56±44.56%	91.29±85.7%

TABLE 8.4b

AVERAGE PERCENTAGE ERRORS ENCOUNTERED WITH BPNN MODEL 2 AND EMPIRICAL MODELS 1, 2 AND 3 FOR THE DIFFERENT ORES.

Ores	BPNN model 2	Empirical model 1	Empirical model 2	Empirical model 3
Kinross	4.65±2.44	3.74±2.40		15.01±3.62
Leslie	5.00±4.27	3.79±1.36		3.92±1.87
Beatrix	3.33±2.98	5.72±6.54		7.06±4.52
Harmony	23.5±25.4	9.08±1.90		8.76±2.05
St. Helena	7.70±5.40	6.50±3.46		6.71±3.20
Unisel	8.32±7.98	11.63±10.13		9.70±5.58
Barberton	122.73±73.44		26.78±28.03	38.79±17.44
WDL	179.40±80.60		17.36±12.41	71.40±20.90
FSG	69.60±47.01		18.30±8.17	15.80±5.98

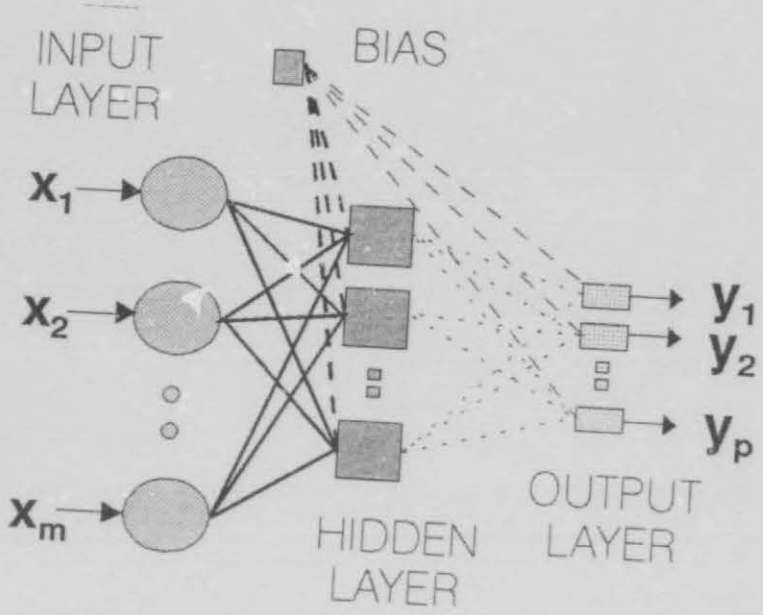

FIGURE 8.1: GENERAL STRUCTURE OF A BACK PROPAGATION NEURAL NET.

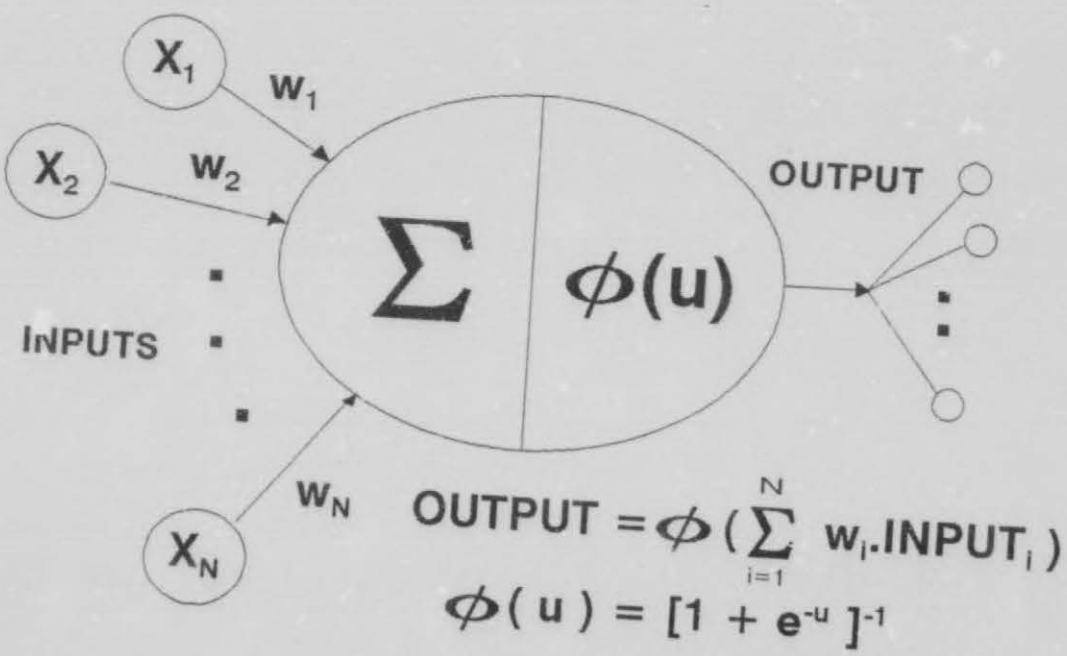

FIGURE 8.2: NEURAL NET PROCESS UNIT

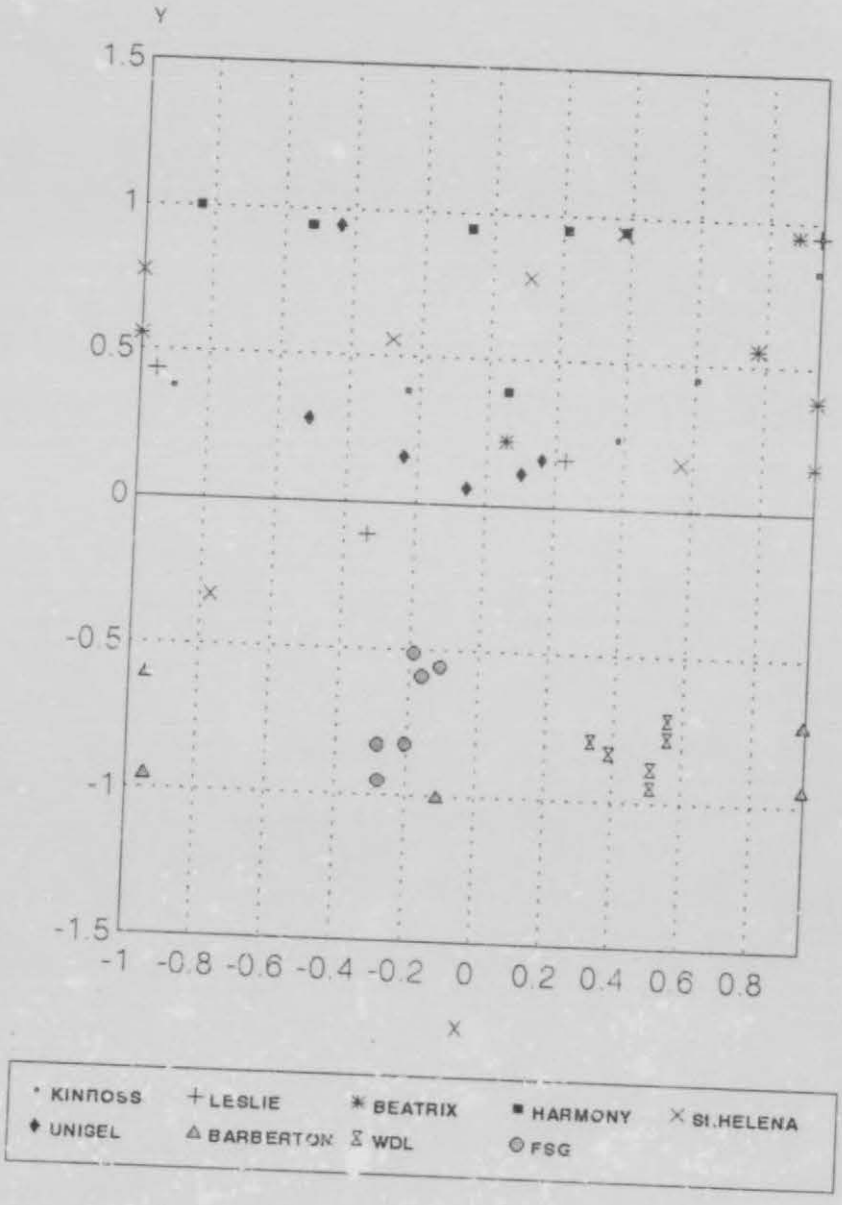

FIGURE 8.3: SOM MAPPING OF UNMILLED ORES.

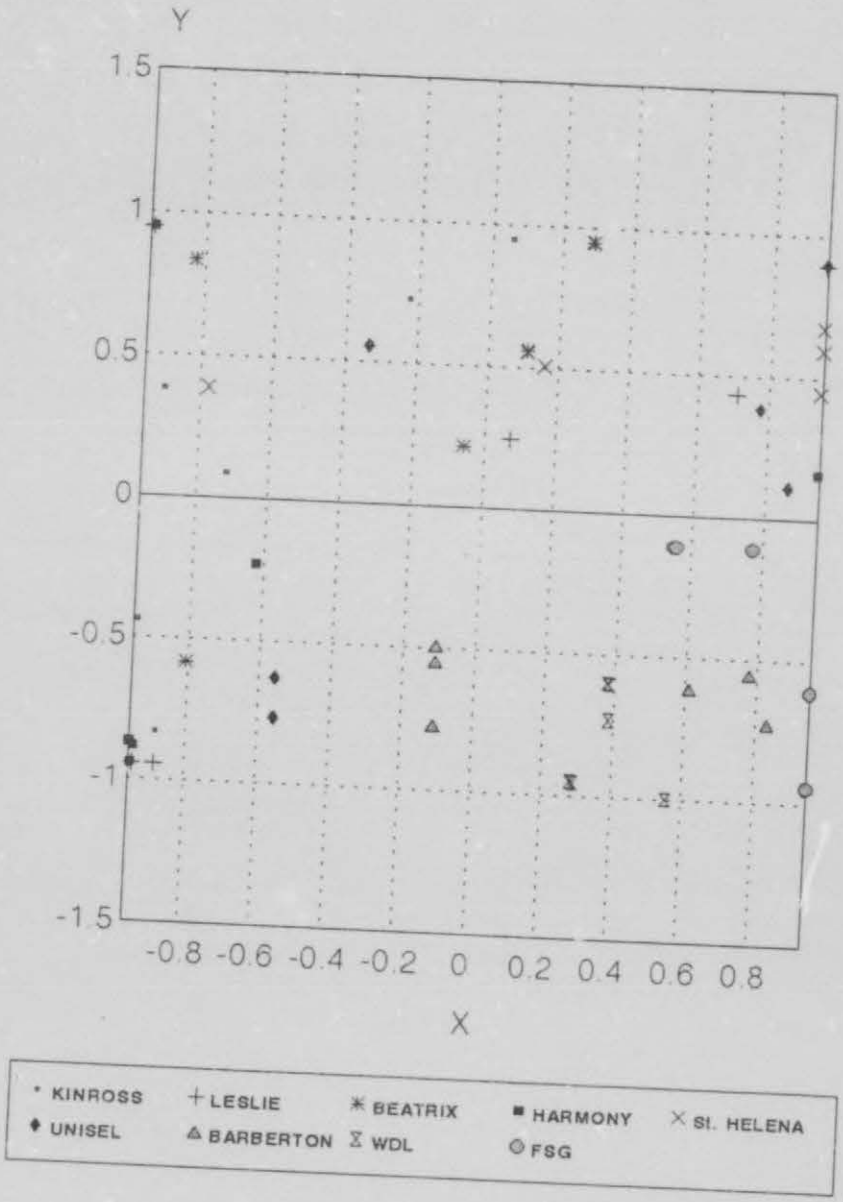

FIGURE 8.4: SOM MAPPING OF MILLED ORES.

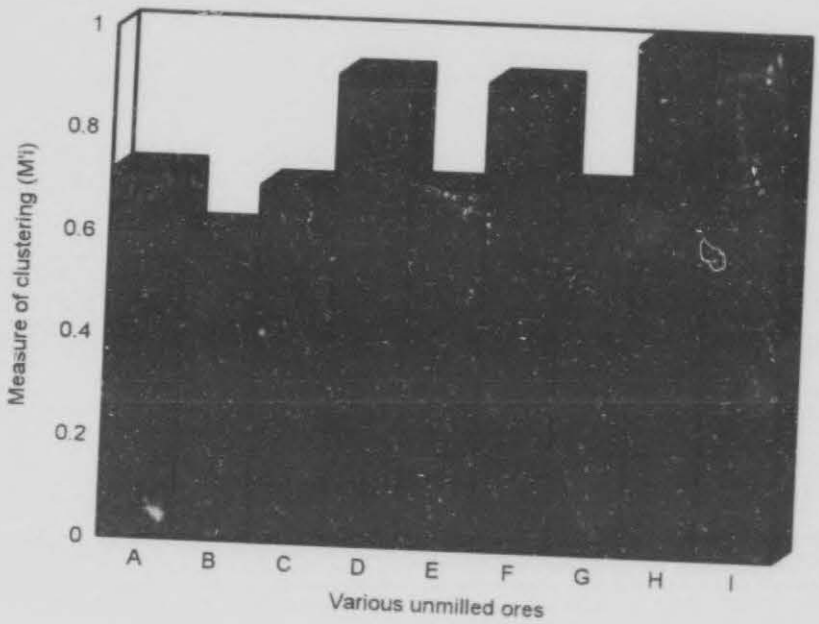

FIGURE 8.5: ANALYSIS OF CLUSTERS FORMED BY SELF-ORGANISING MAPPING OF UNMILLED ORES (A, B,... REFER TO THE ORES IN TABLE 8.1a) .

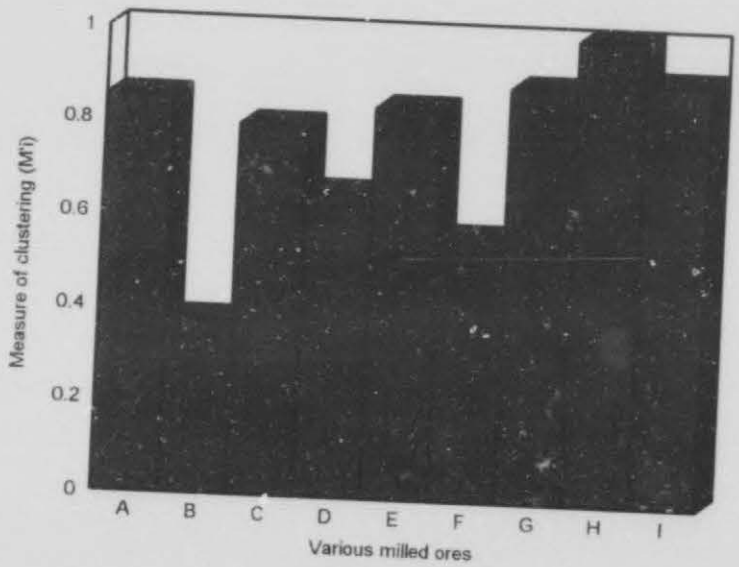

FIGURE 8.6: ANALYSIS OF CLUSTERS FORMED BY SELF-ORGANISING MAPPING OF MILLED ORES (A, B, .. REFER TO THE ORES IN TABLE 8.1b)

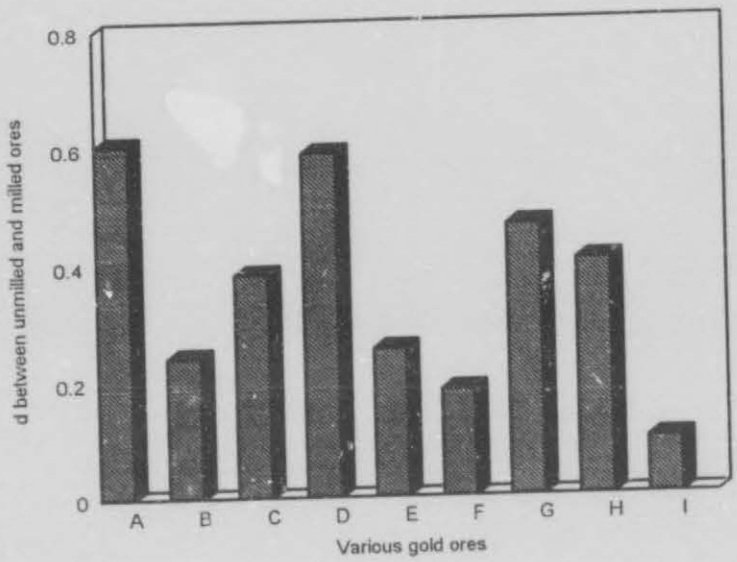

FIGURE 8.7: EUCLIDEAN DISTANCES BETWEEN THE CENTRE OF GRAVITY OF THE UNMILLED AND MILLED ORES (A, B ..I REFER TO THE ORES IN TABLES 8.2).

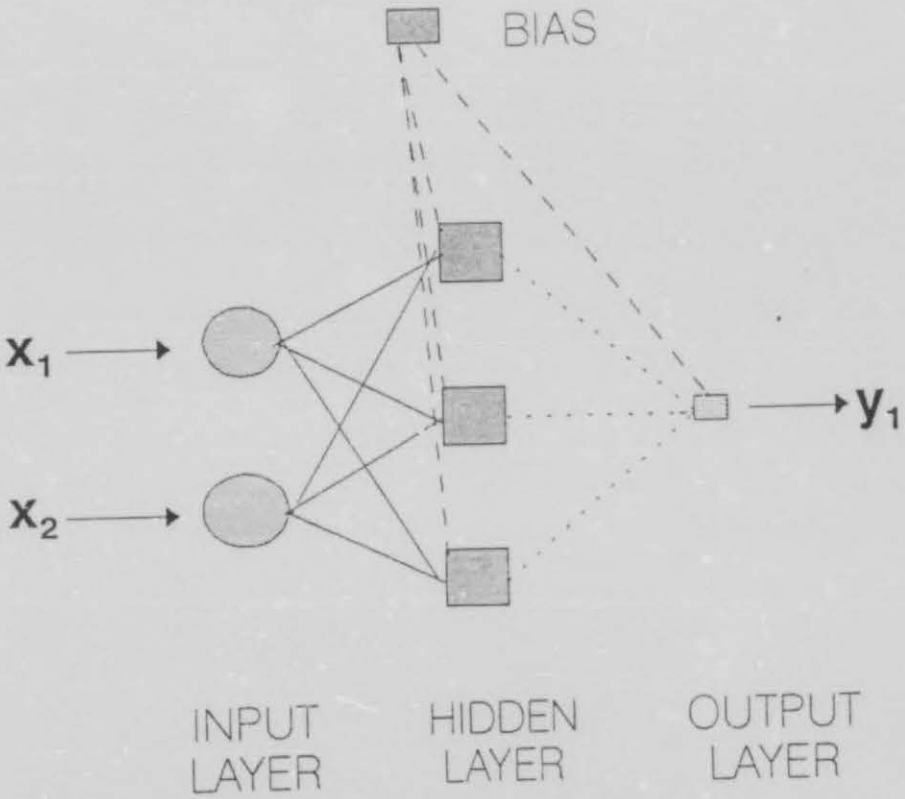

FIGURE 8.8: STRUCTURE OF THE BPNN OF MODEL 1.

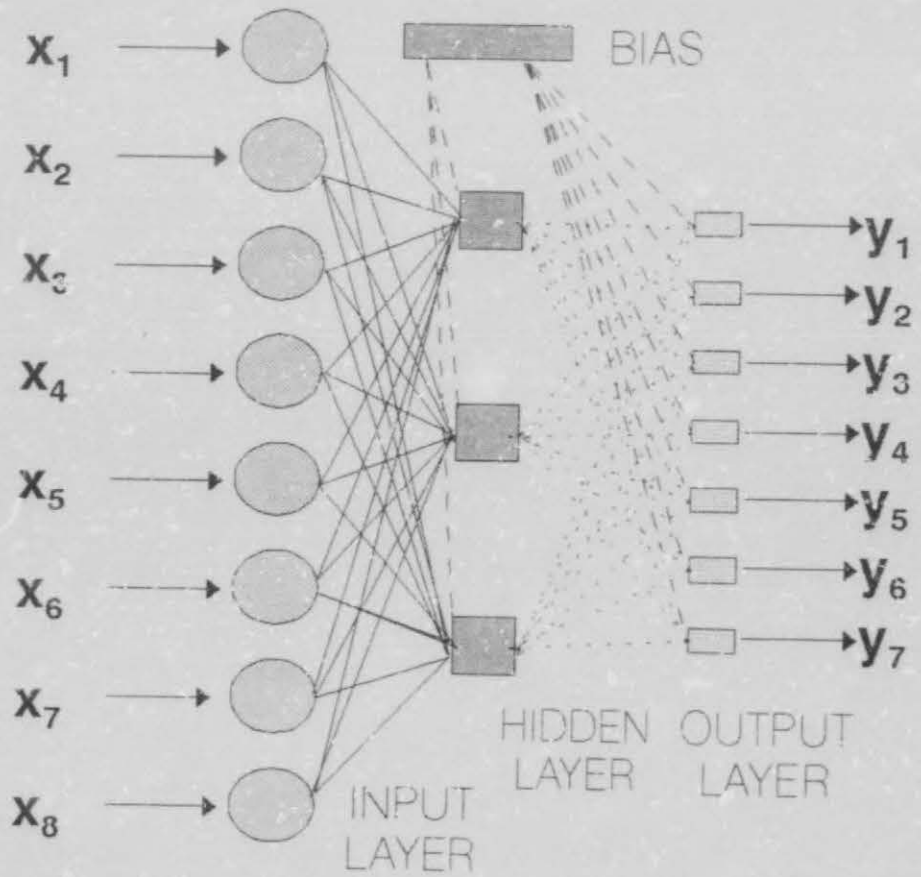

FIGURE 8.9: STRUCTURE OF THE BPNN OF MODEL 2.

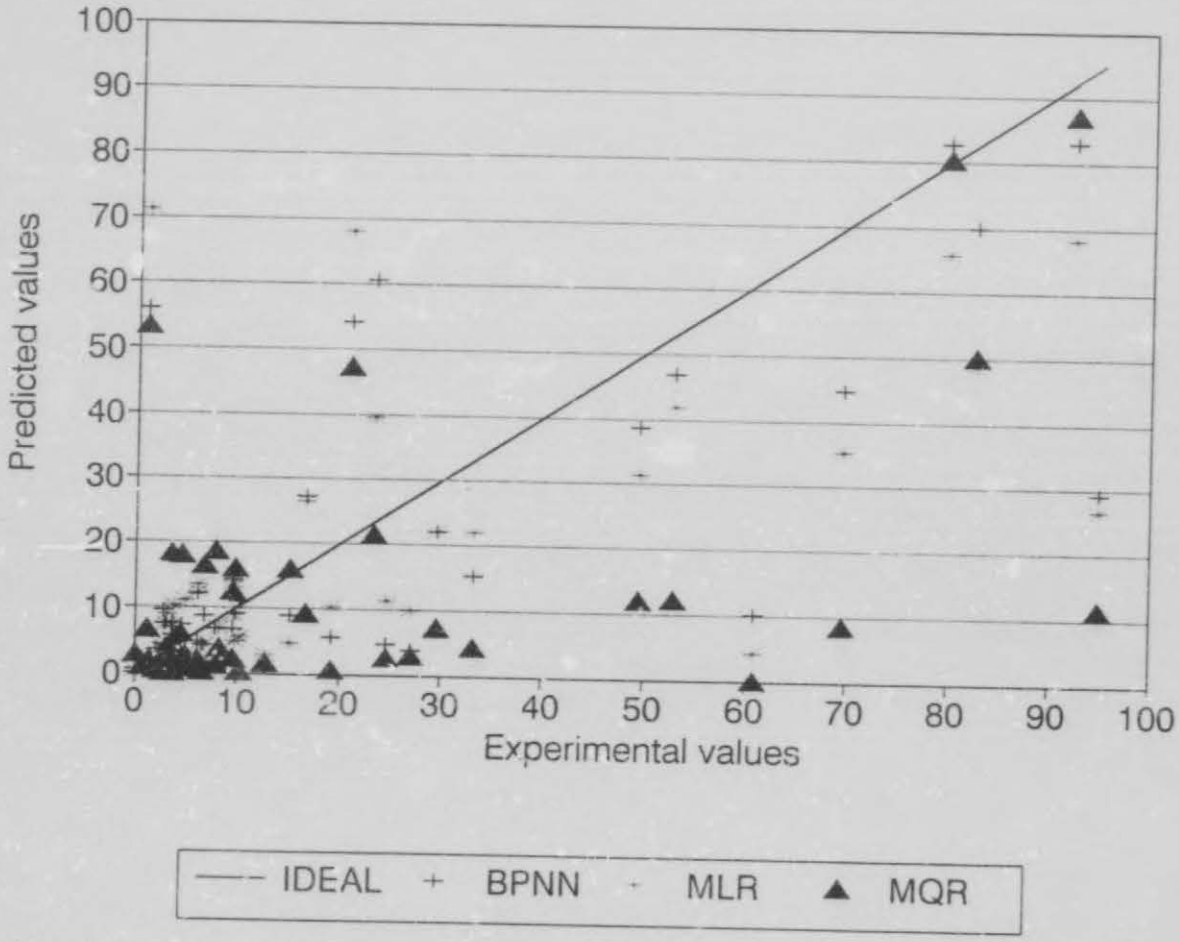

FIGURE 8.10: PREDICTION OF GOLD ASSOCIATED WITH ALL THE MINERALS IN MILLED ORE SAMPLES WITH BACK PROPAGATION NEURAL NET (BPNN-MODEL 1), MULTILINEAR REGRESSION (MLR) AND MULITQUADTRATIC REGRESSION (MQR).

CHAPTER 9

CONCLUSIONS AND SIGNIFICANCE

CHAPTER 9

CONCLUSIONS AND SIGNIFICANCE

From the results presented in this thesis it can be concluded that the leachability (that is, the degree to which a specific ore is leachable) of an ore, is not only dependent on the degree of liberation of that ore when comminuted, but that it is also very much dependent on the degree of exposure of gold grains throughout the ore. It was found that all the theoretical liberation models as well as the exposure (leaching) model of Hsih and co-workers (Wen et al, 1995) underestimated the fraction of leachable gold in each particle size fraction, mainly due to the neglect of exposed gold grains situated in minor cracks and fissures. The following specific conclusions can be drawn:

- Ores from different regions and even different locations within a specific region yield different liberation characteristics.
- It is believed that both transgranular and intergranular breakage occur when a gold ore is comminuted.
- The empirical models discussed in chapter 6 predicted the leachability of gold fairly accurately and it was found to be a function of the particle size and the deportment of gold in the unmilled ore sample.
- Liberation of gold from the silicates is quite effective compared to the other minerals because gold grains associated with silicates seem to be coarser than those associated with the other minerals.
- The liberation pattern of gold from the BMS of one ore can only be extrapolated from one ore in an approximate manner to another ore because BMS include a variety of minerals, each having its own liberation characteristics.
- It was concluded that the liberation pattern of gold from the carbonaceous material of one ore cannot be extrapolated at all to another ore due to experimental errors and different liberation and fracturing characteristics of the different carbonaceous material in the different ores.

- The liberation (leachability) pattern of the Barberton gold ore differs substantially from the other ores due to differences in mineralogical composition.

- An explicit solution to King's liberation model was modified in order to predict leachable gold in different particle size fractions. A function with two argument was added to the solution to provide for the fraction of leachable gold that cannot be attributed directly to liberation and the fraction of liberated gold that is due to fracturing along grain boundaries. It was found that the model predicts the leachability of gold from all the ores, except the Barberton gold ore, fairly accurately.

- The exposure model developed by Hsih and co-workers was extended by the addition of a function with one argument, to provide for the fraction of leachable gold that cannot be attributed directly to liberation. The leachability of gold from all the ores, including the Barberton ore, was predicted accurately.

- It was found that the fraction of leachable gold that is not directly related to liberation (due to both trans- and intergranular fracture) is a function of particle size.

- The use of neural net methods can be a very efficient way of analysing this type of data. Two back propagation neural models which use the gold deportment of unmilled ores as inputs and the gold deportment of the milled ores as outputs were constructed. Although the models are only provisional, reasonable predictions were made but some refinement and more data will still be required in order to predict leachable gold as a function of the mineralogy and particle size, accurately. It will, however, be possible to predict the leachable gold as well as the deportment of gold in the various minerals in a milled ore from the deportment of gold in the unmilled ore.

- It can be expected that the neural net models after some refinement will generally be more applicable than the empirical models.

- Self-organising neural mappings were found to be an easy and efficient way of classifying the gold deportment of an ore.

It became evident in this research that in order to model the leachability of gold fundamentally, the data obtained from diagnostic leaching tests in this thesis are insufficient. Data concerning the quantities of gold bearing minerals present in the ores as well as SEM data of the gold grains are needed along with diagnostic leaching results to model mineral liberation accurately.

Another question to be answered in future work, is: "How does the method of breakage affects the degree of liberation?".

It is evident from this thesis that liberation or the leachability of gold from a specific mineral in an ore is a highly complex phenomenon. It is clear that although many researchers have contributed to the field of liberation, much work is still needed to understand the interrelationship between liberation and leaching behaviour.

REFERENCES

REFERENCES

Aldrich C., Van Deventer J.S.J. and Reuter M.A., "The Application of Neural Nets in the Metallurgical Industry", Minerals Engineering, Vol 7, 1994, pp. 793-809.

Aldrich C., Moolman D.W., Eksteen J.J., Van Deventer J.S.J., "Characterization of Flotation Processes with Self-Organizing Neural Nets", Computers and Chemical Engineering, 1995 (in press)

Barbery G., "Liberation 1,2,3: Theoretical Analysis of the Effect of Space Dimension on Mineral Liberation by Size Reduction", Minerals Engineering, Vol 5, no 2, 1992, pp. 123-141.

Barbery G. and Le Roux, "Prediction of Particle Composition Distribution after Fragmentation of Heterogenous Materials", International Journal of Mineral Processing, Vol 22, 1988, pp. 9-24.

Davy , P.J., "Probability Models for Liberation", Journal of Applied Probability, Volume 21, 1984, pp. 260-269.

Finch J.A. and Petruk W., "Testing a Solution to the King Liberation Model", International Journal of Mineral Processing, Vol 12, 1984, pp. 305-311.

Finlayson, R.M., "The study and simulation of the Behaviour of Individual Minerals in a Grinding Circuit", Ph.D Thesis, University of Natal, 1980.

Gaudin A.M., "Principles of Mineral Dressing", McGraw-Hill Book Company, New York and London,1939, pp. 70-91.

Hsih C.S. and Wen S.B., "An Extension of Gaudin's Liberation Model for Quantitatively Representing the Effect of Detachment in Liberation", International Journal of Mineral Processing, Vol 42, 1994, pp.15-35.

Jones M.P.and Flemming M.G., Identification of Mineral Grains, 45 pages.

King R.P., "A Model for the Quantitative Estimation of Mineral Liberation by Grinding", International Journal of Mineral Processing, Vol 6, 1979, pp. 207 - 220

Kiss, L and Schonert, K., "Liberation of Two-component Material by Single Particle Compression and Impact Crushing", Aufbereitungs-Technick, Vol 5, 1980, pp. 223-230.

Klimpel R.R., "Applications of a Model for the Analysis of Liberation from a Binary System", Powder Technology, Vol 39, 1984, pp. 117-128.

Klimpel R.R. and Austin L.G., "A Preliminary Model of Liberation from a Binary System", Powder Technology, Vol 34, 1983, pp. 121-130.

Kramer M.A., "Nonlinear Principal Component Analysis Using Autoassociative Neural Networks", AIChE Journal, Vol 37, No 2, February 1991, pp. 233-243.

Laslett G.M., Sutherland D.N., Gottlieb P. and Allen N.R., "Graphical Assessment of the Random Breakage Model for Mineral Liberation", Powder Technology, Vol 60, 1990, pp. 83 - 67.

Lorenzen, L., "A Fundamental Study of the Dissolution of Gold from Refractory Ores", PhD-thesis, University of Stellenbosch, Dec 1992a, pp. 191-211.

Lorenzen L., "An Electrochemical Study of the Effect of Potential on the Selective Dissolution of Base Metal Sulphides in Sulphuric Acid", Minerals Engineering, Vol 5, 1992b, pp. 535-545.

Lorenzen L., "Some Guidelines to the Design of a Diagnostic Leaching Experiment", Minerals Engineering, Vol 8, 1995, pp. 247-256.

Lorenzen, L, Francis, P.A. & Sweeney, A.G., "A Guide to the Practise of Diagnostic Leaching for Process Control and Optimisation", Diagnostic Leaching Report No. 4, AARL, Johannesburg, Sept. 1986, 25 pages.

Lorenzen L. and Van Deventer J.S.J., "The Interrelationship between Mineral Liberation and Leaching Behaviour", International Journal of Mineral Processing, Vol 41, 1994, pp. 1 - 15.

Malvik T, "An Empirical Model to Establish the Liberation Properties of Minerals", XIV International Mineral Processing Congress, Toronto, Canada, October 17-23, 1982, 15 pages.

Meloy, T.P. and Gotoh K., "Liberation in a Homogenous Two-phase Ore", International Journal of Mineral Processing, Vol 14, 1985, pp. 45 - 55.

Puddephatt R.J. "The Chemistry of Gold", Topics in Inorganic and General Chemistry, Monograph 16, Elsevier, Third impression, 1986, pp. 9.

Reports (internal) from the Beatrix and St. Helena Gold mines.

Reuter, M.A., Van der Walt, T.J. and Van Deventer, J.S.J., "Modelling of Metal-slag equilibrium Processes using Neural Nets", Metallurgical Transactions B, Vol 23B, 1992, pp. 641-650.

Reuter, M.A., Van Deventer J.S.J. and Van der Walt, T.J., "A generalized Neural Net Kinetic Rate Equation", Chemical Engineering Science, Vol 49(6), 1993.

Stanley G.G. "The Extractive Metallurgy of Gold in South Africa", Vol 1, SAIMM Publication, Johannesburg, 1987, pp. 1-60.

Tumilty, J.A., Sweeney, A.G. and Lorenzen, L. "Diagnostic Leaching in the Development of Flow Sheets for New Ore Deposits", Proceedings of the Int. Symp. on Gold Metallurgy, Minatoba, Canada, R.S. Salter, P.M. Wyslouzil and G.W. Donald (Ed.), Pergamon Press, 1987, pp. 157-168.

Underwood E.E., Quantitative Stereology, Addison-Wesley, Reading, Mass, 1970.

Wen S.B., Hsih C.S. and Kuan C.C., "The Application of Mineral Exposure Model on Gold Leaching Operation", International Journal of Mineral Processing, 1995, 30 pages, (paper in press).

Wiegel R.L. and Li, K., "A Random Model for Mineral Liberation by Size Reduction", Transactions of the Society of Mining Engineers, June 1967, pp. 179 - 189.

APPENDICES

APPENDIX A

DIAGNOSTIC LEACHING PROCEDURE

Pergamon

Minerals Engineering, Vol. 8, No. 3, pp. 247–256, 1995

0892–6875/95 $9.50+0.00

0892–6875(94)00122–7

SOME GUIDELINES TO THE DESIGN OF A DIAGNOSTIC LEACHING EXPERIMENT

L. LORENZEN

Department of Chemical Engineering, University of Stellenbosch,
Private Bag X5018, Stellenbosch, 7600, South Africa
(Received 5 August 1994; accepted 18 October 1994)

ABSTRACT

Diagnostic leaching is an analytical tool which has been developed at the Anglo American Research Laboratories (AARL) during the mid 1980's. This technique has been used widely by various institutions during the last eight years with mixed results, mainly due to insufficient information regarding the technique or to ignorance with regard to the development of a test procedure and the analysis of results. The technique had been refined to some degree during the last few years at the Department of Chemical Engineering of the University of Stellenbosch. This paper contains all the relevant information required for implementing the technique at a laboratory successfully, and some background information to interpret results obtained from this procedure is also included. Evidently, the mineralogy of the matrix material (sample) is the main factor that determines which steps in such a technique are necessary in order to obtain optimal results.

Diagnostic leaching is only a tool to help the mineralogist or metallurgist to get a much clearer view of the deportment of gold in an ore or a sample. This will enable him or her to design new flowsheets, alter existing ones and identify problem areas in plants and unit operations.

Keywords
Mineralogy; diagnostic leaching, analytical technique

INTRODUCTION

Usually the metallurgist's first question is, "To what size do I need to grind the ore to liberate the gold?". If more accurate mineralogical data were available, the first question might be, "With which minerals is the gold associated and how will this affect the extraction route I use?".

Diagnostic leaching was developed by the Anglo American Research Laboratories [1,2] to answer the above question and in doing so, opened up the field of mineralogical analysis to the metallurgist. With diagnostic leaching, the metallurgist or scientist is able to get a much clearer view of which minerals the gold is associated with. When a mineralogist looks at the deportment of gold in an ore, he/she is usually looking for an element which is present in parts per million, so that errors in sampling are multiplied dramatically. Diagnostic leaching offers a cheap, simple, practical alternative. In order to determine with which minerals the desired precious metal is associated, a specific mineral is first eliminated using a selective oxidative leach, and cyanidation is used to extract the precious metal (in this case gold) liberated by the destruction of this mineral. The precious metal extracted can be measured in solution to give a fairly accurate record

of the amount of the precious metal associated with that mineral. Furthermore, the residue from this first stage can be subjected to another selective acid leach, and the process repeated. Interstage dilute acid and cyanide washes can also be used to destroy surface deposits. The procedure can be varied to suit the mineralogy of the matrix material. At the end of this diagnostic leach the metallurgist is left with a complete record of the deportment of the precious metal. He/She can now use this information for example to design a metallurgical flowsheet to treat the ore.

The first step in the design of a diagnostic leaching experiment should be an examination of the mineralogy of the sample to be analysed and tested. Factors affecting the extraction of gold are in many cases of a mineralogical nature. Knowledge of the mineralogy of the ore or metallurgical product to be tested, if appropriately combined with the mineralogical testwork, may help to explain various factors affecting leaching kinetics. Diagnostic leaching is thus an analytical tool which can be used by the metallurgist not only to examine new ores, but also to look at problems occurring at existing plants. The procedure is not only limited to ores and residues but in fact can deal with any type of intermediary product that occurs on a plant.

During the last seven years various papers on diagnostic leaching were published. All these papers, however, made use of diagnostic leaching to try and explain the analytical technique's various and unique applications in the development of mineral processing circuits, fault diagnosis on plants and in process streams, analysis of new deposits and the checking of balances on residue streams. However, no papers have been published on the design and set-up of such an experiment. This has caused various researchers to develop their own versions of the technique from information obtained through papers, informal reports and personal communications with people involved in the development of the technique. This has been most detrimental to the technique owing to some negative publicity it has received as a result of these pirate techniques. Some of the major mistakes made by these "researchers" and plant personnel could be related to the fact that mainly one recipe has been used for all types of experiments, irrespective of the sample's mineralogy. This has been aggravated by poor interpretation of results owing to a lack of knowledge with regard to the set-up of the experiments and logging of valuable data and parameters during the experiments. All these factors have led some people, especially plant personnel, to believe that the technique does not give the quality of results that can be trusted and believed.

This paper will attempt to provide some guidelines for the development of diagnostic leaching experiments, it will explain analytical problems and procedures in the analysis of samples obtained from steps in the procedure, and to some degree it will discuss the interpretation of results. The latter aspect has already been discussed in detail in previous papers [2–4].

EXPERIMENTAL

The concept of diagnostic leaching, as already mentioned, is very simple. The least stable mineral present in the matrix of the sample is first solubilised in aqueous acid medium. The residue is filtered, washed (water/dilute acid), cyanided to extract the gold liberated and washed with a dilute cyanide solution. The process is repeated with a more oxidative acid leach until all the non-refractory re-cyanided gold is leached by the cyanide to give an accurate record of the amount of gold associated with the various minerals. An overlap of the extent of leaching does occur [3], but is generally limited to 90% of the required mineral and 10% of the next most stable mineral. The various stages of acid pre-treatment and the minerals that it will most likely destroy are presented in Table 1 and Figure 1.

DESIGN OF AN EXPERIMENT

As explained earlier, no diagnostic leaching experiment can be designed efficiently without a mineralogical examination of the sample. The mineralogy is very important especially if the ore is regarded as refractory. Each oxidative acid leach step is designed to dissolve a specific or a combination of minerals. The destruction step, i.e. the various reagents used to destroy the minerals, depends on the refractoriness of the

minerals present, how much of the mineral/s is in the sample and at what pH and Eh will this mineral likely be destroyed, thus leached. The first part of the experiment can best be described schematically as in Figure 2.

TABLE 1 Selective pre-treatment leach stages and the minerals destroyed

	Pre-treatment stage	Minerals likely to be destroyed
1.	NaCN washes	Precipitated gold
2.	NaCN	Gold
3.	Na_2CO_3	Gypsum and Arsenates
4.	HCl	Pyrrhotite, Calcite, Dolomite, Galena, Goethite, Calcium carbonate
5.	$HCl/SnCl_2$	Calcine, Haematite, Ferrites
6.	H_2SO_4	Uraninite, Sphalerite, Labile Copper Sulphides, Labile Base Metal Sulphides, Labile Pyrite
7.	$FeCl_3$	Sphalerite, Galena, Labile Sulphides, Tetrahedrite, Sulphide Concentrates
8.	HNO_3	Pyrite, Arsenopyrite, Marcasite
9.	Oxalic Acid Washes	Oxide Coatings
10.	HF	Silicates
11.	Acetonitrile elution	Gold adsorbed on Carbon, Kerogen, Coal

Note: All the above mentioned pre-treatment stages can be varied according to the matrix of the material. Temperature, potential, concentration, treating time, etc. all play a major role in the selection of the desired pre-treatment stage.

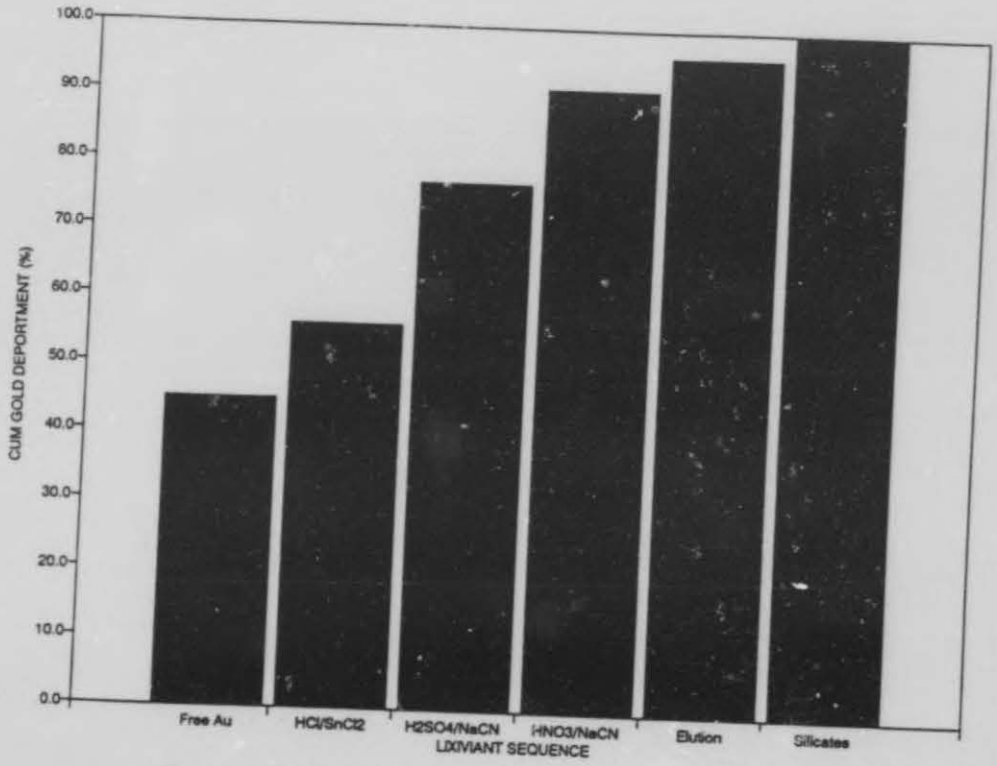

Fig.1 Typical diagnostic leach procedure for the deportment of gold

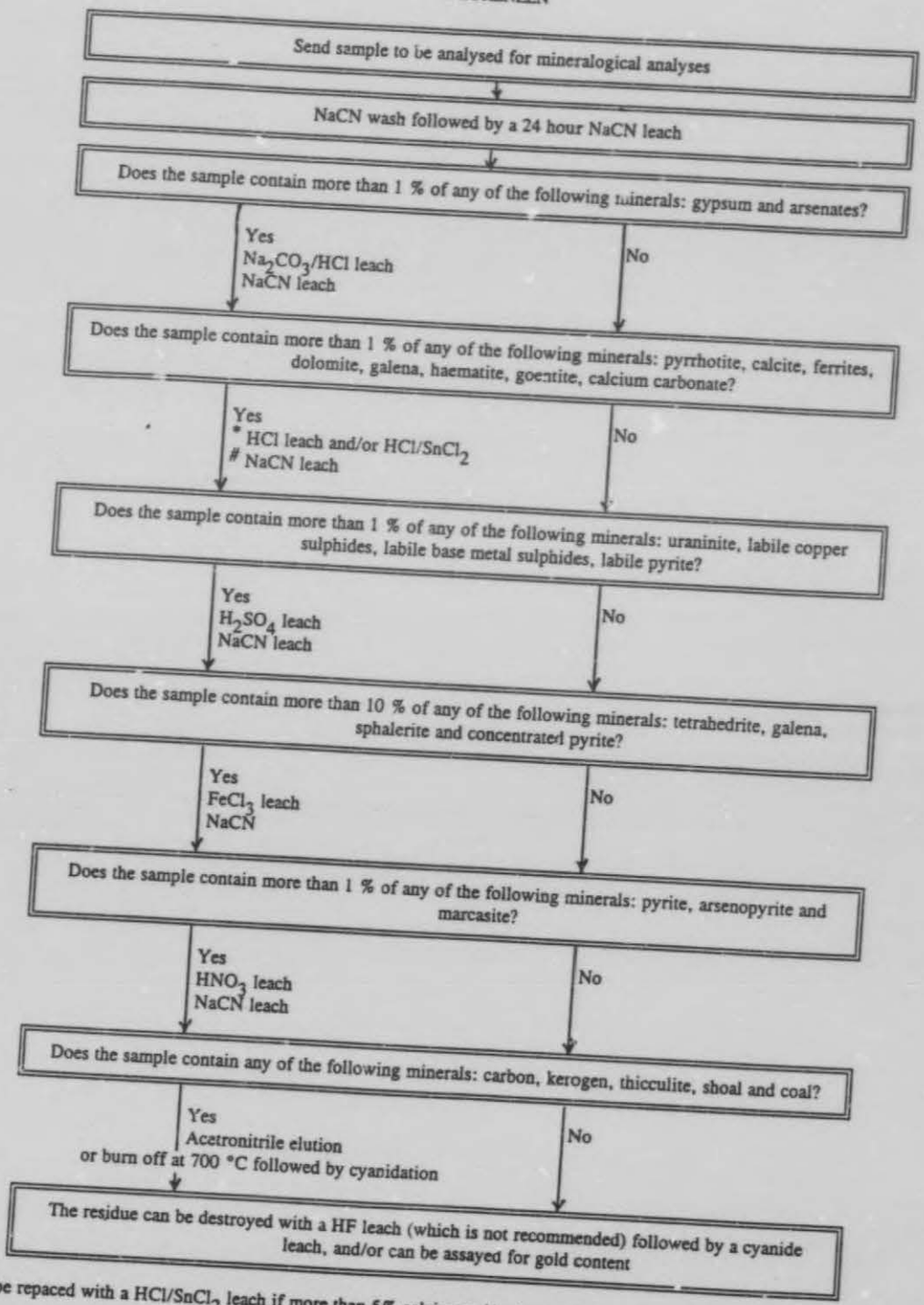

* Can be repaced with a HCl/$SnCl_2$ leach if more than 5% calcine and/or haematite is present

Can be replaced or followed by a $FeCl_3$ leach if there is significant amounts of sphalerite and tetrahedrites present with galena in the sample.

Fig.2 Detailed diagnostic leaching procedure

The minerals mentioned in Figures 1 and 2 are only the major minerals in which gold is occluded or with which gold is usually closely associated in the various South African ores. There are, however, other minerals with which gold is associated, that do not contain significant amounts of gold, and these are usually grouped with the silicates. After the mineralogical analysis is received from the laboratory, the next step is to decide on an appropriate diagnostic leaching route for the sample. This can be done with the help of Table 1 and Figure 2. It is usually better to keep the procedure as short and simple as possible, as this reduces sampling errors and time to a minimum.

Sample Preparation

The samples as received should be thoroughly blended and split into fractions of say 1 kg each. If the sample is an uncrushed or unmilled sample, the sample as received should be crushed to minus 1.65 mm before blending and splitting. After splitting the original sample, one sample should be split equally and both submitted for mineralogical examination. The remaining sample should be milled down to 70 per cent passing 74 microns. This sample should then be blended and split into fractions of 150 g each. Two samples (150 g) should be submitted for head assays (Au), one sample should be submitted for S^o, S at 1400°C after CO_3 leach (i.e. sulphides) and SO_4^{2-}, and one sample for U_3O_8 and total carbon assay (if necessary). Some of the remaining 150 g samples will be used for the diagnostic leaching procedure. The others (crushed — 1 kg and milled — 150 g) will be marked and stored in the event of a lost sample and the procedure having to be repeated.

For residue and "normal" Witwatersrand feed samples, 150 g will be sufficient for a diagnostic leaching procedure. However, for refractory samples, i.e. sulphide concentrates, calcine, arsenates, etc., 300 grams are needed for a diagnostic leaching procedure due to the mass loss of the sample during the acid leaches. All experiments should be done in duplicate to have a check on results.

The mass of the solids as well as the liquid/solids ratio should be recorded throughout the experimental procedure, especially the mass before and after each oxidative acid leaching stage.

Cyanide wash and cyanidations

To start, make up a stock solution of 0.02 g/l NaOH (CP) and 0.1 g/l NaCN. Label this solution "Cyanide wash solution". This solution will be used after each cyanidation to wash the filter cake.

Take the sample of dry solids, determine the mass and add distilled water to make up a 1:1 liquid/solid (L/S) ratio by mass. Add CaO (CP), condition for about 30 minutes at ambient temperature (25°C). 2 kg/t CaO is usually sufficient to ensure a pH of 10 or more. If the pH is 10 or more, add 1 kg/t NaCN (5 kg/t in case of sulphides, calcine and refractory material) and leach for 24 hours at ambient temperature. At the end of the leach, measure the pH, Eh, residual NaCN and dissolved O_2. If residual NaCN is below 75 ppm, repeat the test. Please note that the normal titration method for the determination of residual cyanide also determines the cyanide complexes that are present [4]. This can be avoided by analysing the samples with an ion chromatograph.

After the cyanidation, filter the pulp, collect filtrate and send in for Au analysis. Repulp the solids with the cyanide wash solution at roughly 2:1 L/S ratio and filter. Collect the filtrate and send in for Au analysis. Repulp solids with distilled water and filter. The filter cake can now be used for the second diagnostic leaching stage. Please remember to determine the mass of the wet solids after the leach. This stage is repeated throughout the diagnostic leaching procedure in between oxidative acid leaches. This stage can, however, be shortened significantly if kinetic curves are obtained during the first cyanidation. If it is found that the leaching is completed after say 4 hours, all subsequent cyanidations can be performed for only 4 hours.

Using high reagent additions, the cyanidation stages aim to leach all the free gold (or liberated gold) in the sample. Such leaches are invariably carried out in rolling bottles, but if this facility is not available, beakers in waterbaths can be used.

After the last cyanidation stage, the filter cake is dried in an oven, weighed and split into two samples for assays of the residue.

Sodium carbonate leach

The aim of the sodium carbonate leach is to solubilise calcium sulphate as sodium sulphate and then remove any calcium carbonate which may be formed. An aqueous leach solution containing the sample and 60 g/l sodium carbonate is prepared at a L/S of 10:1 and boiled for 2 hours. The sample is then filtered, washed and repulped in 0.1 M HCl solution at a L/S of 2:1 and leached at pH 1 until the acid consumption is negligible.

Oxidising hydrochloric acid leach

This leach varies, depending on the mineralogy of the ore. The concentration, temperature and duration of the leach varies from mineral to mineral. However, a standard procedure for this leach which will attack and destroy almost all the minerals as indicated in Table I [4], is as follows:

a high temperature (50 to 80°C), HCl (32 % by weight) leach at a L/S of 2:1

For samples containing large amounts of calcine, ferrites and haematite, the following procedure is recommended:

50% V/V — Concentrated HCl (30 to 32% by weight HCl)/distilled water containing 15 g/l $SnCl_2$ (stannous chloride), leach hot (80 to 98°C) at L/S of 10:1 until reddish colour disappears.

Stannous chloride is used as the reductant, and the amount added is stoichiometrically equivalent to the mass of the mineral in the sample. The end point of the leach can be identified clearly by the colour of the pulp.

Filter and wash the samples thoroughly with distilled water before subsequent cyanidation. Record mass loss (dry sample before cyanidation) and use only chemically pure (CP) grade reagents.

Oxidising sulphuric acid leach

The conditions of this leach should be optimised to give the highest extraction of labile base metal sulphides and uranium. However, if a shorter leach is required, then the time could be cut by half with only a 1% decrease in uranium extraction, which indicates that most of the gold locked by uranium minerals will be liberated. The Eh of the solution can also be manipulated to give a selective oxidative leach between the various minerals present [5].

This leach will destroy pyrrhotite, uraninite, labile base metal copper and labile base metal sulphides as well as removing coatings from the gold surfaces. The gold dissolution rate has been shown to increase dramatically after base metal sulphide removal, and therefore shorter cyanidation times can be used [6].

Add distilled water to the wet/or dry solids (weigh the sample) to make up a L/S of 1:1 by mass. Add 70 kg/t H_2SO_4 (AR) and condition for 30 minutes at 80°C. Add 5 kg/t MnO_2 (CP) or H_2O_2 until the Eh is above 500 mV (vs SCE). Allow to leach for 24 hours at 80°C and ensure that the Eh is always above 500 mV (vs SCE) (+ or − 50 mV) by addition of MnO_2 or H_2O_2 and that the pH is never higher than 2 by the addition of H_2SO_4. If lower potentials should be achieved [5], ferric sulphate (AR) can be used to reduce the potential.

Make up a stock solution of sulphuric acid at a pH of 1 and label it "Acid wash solution". At the end of the leach, filter the solids, repulp the solids in the "acid wash solution" at a L/S ratio of 2:1 and filter. Repulp the solids in distilled water and filter. The filter cake can now be dried to determine the mass loss before cyanidation.

Ferric leaching

Ferric leaching (ferric chloride) is recommended when concentrated pyrite, sphalerite and tetrahedrite samples are treated.

The ferric chloride leach is conducted at 95°C for about 6 to 24 hours at a constant Eh of 500 to 700 mV (vs SCE) using hydrogen peroxide addition. The ferric leach solution consists of 100 g/l Fe^{3+} ($FeCl_3$) and 2M HCl. A L/S ratio of 2:1 is used. After the leach, the sample is filtered and washed with distilled water. The mass loss of the solids can be determined by the drying of the sample before cyanidation.

Nitric acid leach

The nitric acid leach destroys all remaining sulphides, especially pyrite, marcasite and some arsenopyrite. The reaction of HNO_3 (AR) with sulphides is highly volatile and envolves dangerous brown fumes of NO_2. The leach must be carried out in a well ventilated fume cupboard and the nitric acid should be added slowly to the agitated slurry before heating.

Make up a stock solution of 1:1 concentrated HNO_3 (55%)/distilled water by volume and add this solution to a beaker containing the filtered wet solids to make up to roughly 10:1 L/S ratio. Boil for 6 hours or until no further reaction occurs (i.e. no brown fumes of NO_2 evolve). If brown fumes are still present after 6 hours, then allow to boil for a further 2 to 3 hours. This may require additional HNO_3 to be added to make up for evaporation losses. At the end of the leach, filter the solids, repulp the solids in distilled water to a L/S of about 2:1 and filter. Repeat this step at least two times. The filtrate of the HNO_3 leach should be sent for Au analyses (ICP), as it was found by previous researchers that this sample contains some dissolved gold. It has been noted [1] that in some cases gold is extracted during this step, possibly by total liberation of ultra fine gold from pyrite, or actual leaching due to the presence of chloride ions which form a type of aqua regia. Distilled water must thus be used throughout the leach to avoid the presence of chloride ions. Usually this loss is negligible and can be ignored. Dry the solids in an oven to determine the mass loss before cyanidation. It was found that the biggest mass loss occurs during this leaching step. Gold remaining in the residue after the nitric acid leach and subsequent cyanidation is assumed to be gold mainly associated with silicates, except where large quantities of kerogen, carbon or coal are present.

Acetonitrile elution/carbon burn off

If the sample contains significant amounts of carbonaceous material, it is suggested that either a acetonitrile elution or a burning off of the carbon followed by a cyanidation be performed to determine the amount of gold adsorbed onto the carbon material.

Acetonitrile elution

The eluate is 40% V/V acetonitrile in distilled water, 10 g/l sodium cyanide, and 2 g/l caustic. The L/S ratio is about 10:1 and the material is refluxed in a Soxhlet reactor for 16 hours. The solution analyses after the elution might be problematic but an analytic laboratory should be able to analyse the solution for gold with an ICP. The sample must be thoroughly washed with distilled water before and after the elution (acetonitrile is highly soluble in water) and these solutions must also be analysed for gold.

Burn off/cyanidation

This procedure entails the burning off of the carbonaceous material in a furnace at about 700°C for 6 hours. This will burn off all the carbon and expose the gold adsorbed for subsequent cyanidation. The recording of the mass loss during the procedure is also important.

The residue after the sample had been subjected to the entire or a part of the diagnostic leaching procedure, will now only contain siliceous material, and it is assumed that the amount of gold locked in such material is relatively small and non-extractable. An HF/aqua regia leach can be conducted to destroy these minerals

to some degree, but owing to the nasty nature of these chemicals and the safety standards applied in laboratories, this is not recommended.

Oxalic acid pre-treatment

Oxalic acid can be used for the determination of "dirty gold", thus gold coated with oxide films, especially iron oxide films and iron oxides like haematite and magnetite. This leach may, however, also dissolve base metal sulphides to some degree, depending on the severity of the leach.

Iron oxides can dissolve in oxalic acid at various concentrations (2.5 to 20%) at 80°C in less than two hours. The idea is, however, to use this step as a pre-treatment step before cyanidation to destroy all possible oxide coatings especially after HCl, H_2SO_4 and $FeCl_3$ leaches. This can be achieved by washing the residue after the above mentioned leaches with a 5% oxalic acid solution for 30 minutes in a beaker before final filtration and subsequent cyanidation.

Equipment and reagents required

Most of the cyanidations can be performed in rolling bottles on rollers in a waterbath if available. If not, leaching can be performed in beakers in a waterbath with overhead stirrers. For the oxidative acid leaches, magnetic stirrers with temperature control can be used. It is recommended that all acid leaches be performed in a fume cupboard. Due to the fact that most of these leaches have to be controlled (i.e. pH or Eh), a pH/redox potential meter with automatic titrator and valve is recommended. As most of the acid leaches entail high temperatures, strict control must be performed to ensure that there is sufficient solution in the containers at all times, i.e. L/S ratios be controlled. All chemicals used are of chemically pure (CP) grade except sulphuric acid and nitric acid which are analytically pure (AR). Manganese dioxide and ferric sulphate which can be used as oxidants or reductants are also usually of AR grade.

ANALYSIS OF RESULTS

The technician/researcher performing the work should record any abnormalities in the leaches and should have a log book of observations for this purpose. The cumulative mass loss during the leaches must be taken into account, thus the gold in the residue and gold in solution must be multiplied by the fraction of the remaining mass to give a true value related to the head of gold extracted during the leach. This is particularly important when dealing with sulphide concentrates as the mass losses here are large. When the true values of the gold in solutions and residues have been found, then a calculated head can be determined by relating the gold in solutions and in residues to the gold originally in the solids using the liquid to solids ratios. If there were no problems in the leach then the calculated head would be more accurate than the assay head due to the accuracy of gold analysis in solutions compared to solids. If the sample were thoroughly blended and split, the calculated head should be close to the assay head. If not, then the calculated head should be checked first. That is why it is very important to analyse all the filtrate streams (cyanide washes included) after cyanidation, to ensure that all the gold that might be lost in solution streams is accounted for.

Once all the figures have been obtained for a material, then the extraction (%) after each pre-treatment stage can be found. It is helpful to relate these extraction figures to others and in such a way obtain a picture of the gold deportment for a sample (see Figure 3 as an example). If available, "normal" deportments for such an ore, i.e. plant figures, etc., should be used for comparison. The following paragraphs are just a short explanation with the help of one or two case studies of how results should be interpreted.

Ores

The deportment of gold in any sample is essentially related to the degree to which the sample has been ground or milled. The cyanidation step in diagnostic leaching gives the maximum amount of gold which is possible to extract under ideal conditions, i.e. ultimate residue. Normally the plant extraction should come close to this although a substantial variation in the head assay could mean a big difference in the deportment

of free gold. A better means of analysing plant efficiency would be to test whether there is still free gold remaining in the plant residue. Diagnostic leaching of ores is useful at the stage before they are combined and fed into a plant, especially if the ores originate from different plants and thus ore bodies. Using diagnostic leaching, it may be possible to see if a particular ore is causing problems at the plant. For example, if an ore is isolated and milled to the plant grind, it may be found that it has a much higher gold in sulphide value than the others, and should thus be treated separately. It is also important to note that the grind practised on plants might not be the most efficient and cost effective grind. Diagnostic leaching analysis of ore samples milled to various size fractions, can help to answer the above scenario.

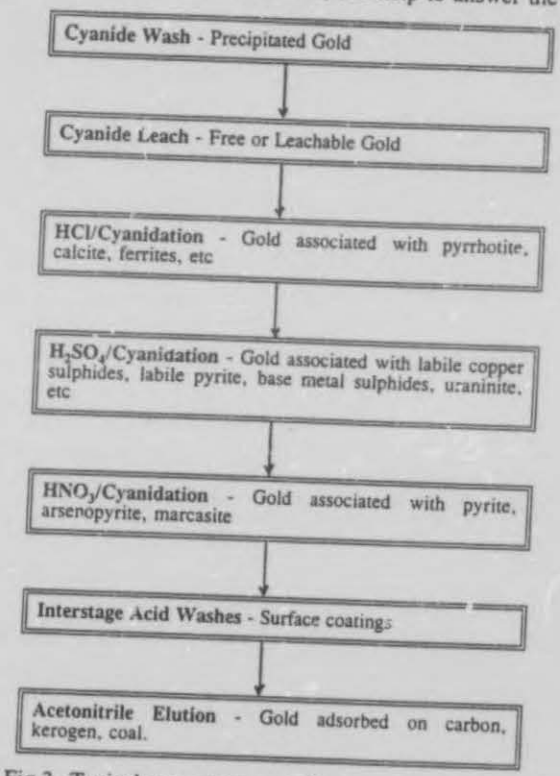

Fig.3 Typical presentation of diagnostic leaching data

Sulphide Concentrates

The deportment of gold in sulphide concentrates is dependent on which minerals were present in the float plant feed and with what efficiency they are floated. A high sulphide recovery should indicate that the gold recovery in sulphides will be high. Precipitated gold will not float unless it is precipitated in pyrite or pyropyllite which are the main constituent minerals of the concentrate. In a good float, the free gold recovery should be high, unless the material is abnormally coarse. The way to find the gold flotation recovery from each mineral phase is to find the gold deportment in the feed and tails of the flotation plant and compare this to the gold deportment in the concentrate. In a good float the gold recovery from pyrite should be high too and should match the pyrite recovery. Gold recovered from the base metal sulphides and uraninite phases may be low or high depending on whether these minerals are floated with pyrite or not. Gold associated with silicates should not be recovered unless it is mostly associated with pyrophyllite and not quartz during flotation.

Calcines

These minerals are the most complicated to deal with as most of the minerals present have undergone a physical change. Diagnostic leaching conditions for the roaster product have not been optimised yet. It is

suggested that the sample be cyanided first, followed by a $HCl/SnCl_2$ leach and a subsequent cyanidation. A more accurate method for analysing problems in a calcine product is to do a diagnostic leach on the pyrite feed to the roaster. This together with a $HCl/SnCl_2$ leach will enable one to make more meaningful conclusions of possible problems, i.e. an increase in gold associated with base metal sulphides could mean an increase in gold lock up in arsenates and ferrites.

Residues

These have already been mentioned as being the most effective way of monitoring plant performance. By finding changes in the gold deportment it will indicate where problems are possibly occurring. A high residual gold value in silicates may be due to the fact that the plant grind had coarsened too much, or that a change in mineralogy did occur due to the fact that mining has moved into a different area. Analysis of a plant residue together with the feed and some intermediate stream samples are still the best options for analysing problems on a plant.

CONCLUSIONS

Diagnostic leaching consists of a set of relatively simple experiments which can determine the deportment of gold accurately in various mineral matrices. The metallurgist, chemist or scientist can use this information to design metallurgical flowsheets, solve problems occurring at an existing plant and/or evaluate the effect of various reagents on the performance of an existing plant. The technique can cope with any plant problem caused by a (i) change in operation, (ii) change in reagents used, (iii) change in the mineralogy and/or gold deportment of the feed to the plant or (iv) a combination of the above mentioned.

It can also deal with new ore deposits, refractory minerals, i.e. calcines, roaster clinker, sulphide minerals, etc. The method is flexible and depends on the sample to be analysed. The data obtained from a modest amount of testwork enable the derivation of possible process routes for treatment of the ore-body/refractory minerals for gold recovery. The routes chosen depend on such factors as the economics of the project, location of the ore-body/refractory minerals and the relative amount of the latter.

It is important that the procedure should be applied as accurately as possible, and that the development of a diagnostic leaching treatment route should be conducted in collaboration with a geologist and/or mineralogist. The technique is very powerful if used correctly, and care should be taken especially with the analysis and interpretation of results.

REFERENCES

1. Lorenzen, L., Francis, P.A. & Sweeney, A.G., A guide to the practice of diagnostic leaching for process control and optimisation, *Diagnostic Leaching Report No. 4, AARL*, 25 pages, (1986)
2. Lorenzen, L. & Tumilty, J.A., Diagnostic leaching as an analytical tool for evaluating the effect of reagents on the performance of a gold plant, *Minerals Engineering*, **5**,Nos 3–5, 503–512 (1992).
3. Tumilty, J.A., Sweeney, A.G. & Lorenzen, L., Diagnostic leaching in the development of flowsheets for new ore deposits, *Proceedings of the International Symposium on Gold Metallurgy*, Eds: R.S. Salter, D.M. Wyslouzil and G.W. McDonald, Pergamon Press, 157–168 (1987).
4. Lorenzen, L. & Van Deventer, J.S.J., The mechanism of leaching of gold from refractory ores, *Minerals Engineering*, **5**,Nos 10–12, 1377–1383 (1992).
5. Lorenzen, L., An electrochemical study of the effect of potential on the selective dissolution of base metal sulphides in sulphuric acid, *Minerals Engineering*, **5**,Nos 3–5, 534–544 (1992).
6. Tumilty, J.A. & Schmidt, C.G., Deportment of gold in the Witwatersrand System, *Gold 100, Proceedings of the International Conference on Gold*, **2**. Extractive Metallurgy of Gold, Johannesburg, SAIMM, 541–553 (1986).

APPENDIX B

ADDISIONAL TABLES

APPENDIX B

ADDISIONAL TABLES

TABLE B1

THE LEACHABILITY (EXPERIMENTAL AND PREDICTIONS BY THE MODIFIED KING MODEL - EQ. 7.3) OF THE KINROSS AND LESLIE GOLD ORES VS PARTICLE SIZE.

Average particle size [µm]	Kinross			Leslie		
	Exp	Predicted	%error	Exp	Predicted	%error
212	76.46	69.86	8.63	79.48	80.04	0.70
126	75.20	78.93	4.96	88.85	86.36	2.80
89	79.90	82.56	3.32	92.44	89.09	3.62
58	89.00	86.08	3.28	96.36	91.78	4.75
23	91.25	91.77	0.57	89.74	96.12	7.11
Average			4.15			3.80

TABLE B2

THE LEACHABILITY (EXPERIMENTAL AND PREDICTIONS BY THE MODIFIED KING MODEL - EQ. 7.3) OF THE BEATRIX AND HARMONY GOLD ORES VS PARTICLE SIZE.

Average particle size [µm]	Beatrix			Harmony		
	Exp	Predicted	%error	Exp	Predicted	%error
212	82.88	78.56	5.22	72.11	80.43	11.54
126	88.31	82.62	6.44	92.28	86.47	6.30
89	86.96	85.17	2.06	92.35	89.63	2.95
58	84.54	88.26	4.40	94.99	92.78	2.32
23	76.97	94.31	22.53	92.37	97.65	5.72
Average			8.13			5.76

TABLE B3

THE LEACHABILITY (EXPERIMENTAL AND PREDICTIONS BY THE MODIFIED KING MODEL - EQ. 7.3) OF THE St HELENA AND UNISEL GOLD ORES VS PARTICLE SIZE.

Average particle size [µm]	St. Helena			Unisel		
	Exp	Predicted	%error	Exp	Predicted	%error
212	85.49	83.62	2.19	81.16	73.52	9.42
126	86.14	86.41	0.32	87.93	77.81	11.51
89	88.71	87.87	0.95	68.08	80.37	18.05
58	78.98	89.36	13.14	80.51	83.19	3.33
23	80.36	92.05	14.55	82.55	88.18	6.82
Average			6.23			9.82

TABLE B4

THE LEACHABILITY (EXPERIMENTAL AND PREDICTIONS BY THE MODIFIED KING MODEL - EQ. 7.3) OF THE WDL AND FSG GOLD ORES VS PARTICLE SIZE.

Average particle size [µm]	WDL			FSG		
	Exp	Predicted	%error	Exp	Predicted	%error
212	6.8	7.9	15.78	18.2	17.7	2.54
126	11.2	11.7	4.40	25.6	35.8	39.99
89	18.5	16.6	10.06	46.0	43.5	5.53
58	21.3	21.3	0.19	55.1	49.5	10.09
23	22.8	25.9	13.49	54.2	59.7	10.10
Average			8.78			13.65

TABLE B5

THE LEACHABILITY (EXPERIMENTAL AND PREDICTIONS BY THE MODIFIED KING MODEL - EQ. 7.3) OF THE HARTIES AND BARBERTON GOLD ORES VS PARTICLE SIZE.

Average particle size [µm]	Harties			Barberton		
	Exp	Predicted	%error	Exp	Predicted	%error
212	26.5	23.29	12.12	24.67	9.76	60.42
126	32.8	38.75	18.13	24.62	13.64	44.62
89	54.6	54.65	0.09	22.68	16.99	25.08
58	75.8	67.11	11.46	24 46	22.14	9.50
23	77.0	77.83	1.08	29.51	37.21	26.08
Average			8.58			33.14

TABLE B6

THE LEACHABILITY (EXPERIMENTAL AND PREDICTIONS BY THE MODIFIED EXPOSURE MODEL - EQ 7.7) OF THE KINROSS AND LESLIE GOLD ORES VS PARTICLE SIZE.

Average particle size [µm]	Kinross			Leslie		
	Exp	Predicted	%error	Exp	Predicted	%error
212	76.46	76.48	0.02	79.48	85.69	7.81
126	75.20	79.75	6.06	88.85	88.80	0.06
89	79.90	82.63	3.42	92.44	91.47	1.05
58	89.00	86.70	2.58	96.36	95.11	1.30
23	91.25	90.64	0.67	89.74	96.70	7.75
Average			2.55			3.59

TABLE B7

THE LEACHABILITY (EXPERIMENTAL AND PREDICTIONS BY THE MODIFIED EXPOSURE MODEL - EQ 7.7) OF THE BEATRIX AND HARMONY GOLD ORES VS PARTICLE SIZE.

Average particle size [µm]	Beatrix			Harmony		
	Exp	Predicted	%error	Exp	Predicted	%error
212	82.88	76.94	7.17	72.11	79.83	10.85
126	88.31	81.45	7.77	92.28	85.05	7.84
89	86.96	85.26	1.95	92.35	89.28	3.32
58	84.54	90.31	6.83	94.99	94.63	0.38
23	76.97	92.08	19.53	92.37	95.12	2.97
Average			8.67			5.07

TABLE B8

THE LEACHABILITY (EXPERIMENTAL AND PREDICTIONS BY THE MODIFIED EXPOSURE MODEL - EQ 7.7) OF THE St HELENA AND UNISEL GOLD ORES VS PARTICLE SIZE.

Average particle size [µm]	St. Helena			Unisel		
	Exp	Predicted	%error	Exp	Predicted	%error
212	85.49	82.58	3.41	81.16	77.02	5.10
126	86.14	84.76	1.60	87.93	79.17	9.96
89	88.71	86.70	2.26	68.08	81.08	19.09
58	78.98	89.46	13.26	80.51	83.81	4.10
23	80.36	90.89	13.10	82.55	86.88	5.24
Average			6.73			8.70

TABLE B9

THE LEACHABILITY (EXPERIMENTAL AND PREDICTIONS BY THE MODIFIED EXPOSURE MODEL - EQ 7.7) OF THE WDL AND FSG GOLD ORES VS PARTICLE SIZE.

Average particle size [µm]	WDL			FSG		
	Exp	Predicted	%error	Exp	licted	%error
212	6.8	8.7	27.9	18.2	21.1	15.8
126	11.2	12.1	8.2	25.6	29.7	16.2
89	18.5	15.0	18.8	46.0	36.9	19.8
58	21.3	19.0	11.0	55.1	46.2	16.2
23	22.8	26.1	14.6	54.2	56.7	4.7
Average			16.1			14.5

TABLE B10

THE LEACHABILITY (EXPERIMENTAL AND PREDICTIONS BY THE MODIFIED EXPOSURE MODEL - EQ 7.7) OF THE HARTIES AND BARBERTON GOLD ORES VS PARTICLE SIZE.

Average particle size [µm]	Harties			Barberton		
	Exp	Predicted	%error	Exp	Predicted	%error
212	26.5	29.7	12.22	24.67	23.81	3.50
126	32.8	43.0	31.06	24.62	24.25	1.52
89	54.6	53.7	1.59	22.68	24.71	8.93
58	75.8	67.0	11.58	24.46	25.56	4.49
23	77.0	77.0	0.05	29.51	29.65	0.49
Total			11.30			3.79

TABLE B11a

THE AMOUNT OF GOLD IN EACH PARTICLE SIZE FRACTION ASSOCIATED WITH BMS AND PYRITE FOR A HOMOGENOUS KINROSS ORE

Average particle size [µm]	BMS			Pyrite		
	Unmilled ore [µg]	Milled ore [µg]	%unliberated	Unmilled ore [µg]	Milled ore [µg]	%unliberated
350	18.09	14.51	80.22	29.61	35.76	100.00
212	9.57	5.60	58.55	15.66	3.67	23.47
126	34.80	19.68	56.56	56.96	10.16	17.84
89	63.00	28.81	45.73	103.12	24.26	23.53
58	59.45	19.18	32.26	97.31	11.11	11.42
23	251.37	44.94	17.88	411.45	58.19	14.14
Total	436.28	132.72		714.10	260.43	

TABLE B.11b

THE AMOUNT OF GOLD IN EACH PARTICLE SIZE FRACTION ASSOCIATED WITH CARBONACEOUS MATERIAL AND SILICATES FOR A HOMOGENOUS KINROSS ORE

Average particle size [µm]	Carbonaceous material			Silicates		
	Unmilled ore [µg]	Milled ore [µg]	%unliberated	Unmilled ore [µg]	Milled ore [µg]	%unliberated
350	5.66	9.12	100.00	94.10	73.14	77.72
212	3.00	4.30	100.00	49.77	5.82	11.70
126	10.90	10.15	93.12	181.02	22.94	12.67
89	19.72	39.17	100.00	327.72	21.67	6.61
58	18.61	11.84	63.58	309.27	13.75	4.44
23	78.70	14.58	18.52	1307.65	59.89	4.58
Total	136.60	89.15		2269.54	197.22	

TABLE B12a

THE AMOUNT OF GOLD IN EACH PARTICLE SIZE FRACTION ASSOCIATED WITH BMS AND PYRITE FOR A HOMOGENOUS LESLIE ORE

Average particle size [µm]	BMS			Pyrite		
	Unmilled ore [µg]	Milled ore [µg]	%unliberated	Unmilled ore [µg]	Milled ore [µg]	%unliberated
350	131.92	86.45	65.53	169.39	83.50	49.30
212	14.29	14.56	100.0	18.35	8.59	46.84
126	25.93	24.83	95.78	33.29	9.65	29.00
89	54.15	37.89	69.97	69.53	3.86	5.55
58	71.01	35.21	49.59	91.18	8.95	9.81
23	400.98	142.99	35.66	514.87	89.06	17.30
Total	698.27	341.93		896.61	203.63	

TABLE B12b

THE AMOUNT OF GOLD IN EACH PARTICLE SIZE FRACTION ASSOCIATED WITH CARBONACEOUS MATERIAL AND SILICATES FOR A HOMOGENOUS LESLIE ORE

Average particle size [µm]	Carbonaceous material			Silicates		
	Unmilled ore [µg]	Milled ore [µg]	%unliberated	Unmilled ore [µg]	Milled ore [µg]	%unliberated
350	40.58	68.35	100.00	701.39	936.29	100.00
212	4.39	2.18	49.61	75.97	5.58	7.34
126	7.97	2.03	25.52	137.84	7.09	5.14
89	16.66	4.86	29.19	287.92	8.97	3.12
58	21.84	3.58	16.39	377.55	9.44	2.50
23	123.33	48.52	39.34	2131.94	19.50	0.91
Total	214.77	129.53		3712.61	986.86	

TABLE B13a

THE AMOUNT OF GOLD IN EACH PARTICLE SIZE FRACTION ASSOCIATED WITH BMS AND PYRITE FOR A HOMOGENOUS BEATRIX ORE

Average particle size [µm]	BMS			Pyrite		
	Unmilled ore [µg]	Milled ore [µg]	%unliberated	Unmilled ore [µg]	Milled ore [µg]	%unliberated
350	155.62	113.81	73.14	151.81	209.36	100.00
212	3.20	2.50	77.88	3.13	3.81	100.00
126	7.94	10.76	100.00	7.74	9.19	100.00
89	30.79	30.10	97.78	30.03	26.42	87.97
58	59.69	44.95	75.30	58.23	53.10	91.18
23	486.45	378.33	77.78	474.55	320.51	67.54
Total	743.68	580.45		725.50	622.38	

TABLE B13b

THE AMOUNT OF GOLD IN EACH PARTICLE SIZE FRACTION ASSOCIATED WITH CARBONACEOUS MATERIAL AND SILICATES FOR A HOMOGENOUS BEATRIX ORE

Average particle size [µm]	Carbonaceous material			Silicates		
	Unmilled ore [µg]	Milled ore [µg]	%unliberated	Unmilled ore [µg]	Milled ore [µg]	%unliberated
350	106.19	219.46	100.00	813.72	768.42	94.43
212	2.19	1.60	72.97	16.75	0.87	5.20
126	5.42	4.41	81.50	41.50	4.84	11.67
89	21.01	34.28	100.00	160.98	2.87	1.78
58	40.73	41.80	100.00	312.14	3.11	1.00
23	331.93	271.58	81.82	2543.64	19.96	0.78
Total	507.46	573.14		3888.74	800.08	

TABLE B14a

THE AMOUNT OF GOLD IN EACH PARTICLE SIZE FRACTION ASSOCIATED WITH BMS AND PYRITE FOR A HOMOGENOUS St. HELENA ORE

Average particle size [µm]	BMS			Pyrite		
	Unmilled ore [µg]	Milled ore [µg]	%unliberated	Unmilled ore [µg]	Milled ore [µg]	%unliberated
350	161.18	93.62	58.08	166.32	275.44	100.00
212	13.07	71.88	100.00	13.49	6.76	50.13
126	23.29	89.00	100.00	24.03	20.20	84.03
89	47.11	76.60	100.00	48.62	16.22	33.37
58	73.47	98.81	100.00	75.81	20.59	27.15
23	493.80	370.39	100.00	509.54	101.75	19.97
Total	811.93	800.30	75.01	337.80	440.96	

TABLE B14b

THE AMOUNT OF GOLD IN EACH PARTICLE SIZE FRACTION ASSOCIATED WITH CARBONACEOUS MATERIAL AND SILICATES FOR A HOMOGENOUS St. HELENA ORE

Average particle size [µm]	Carbonaceous material			Silicates		
	Unmilled ore [µg]	Milled ore [µg]	%unliberated	Unmilled ore [µg]	Milled ore [µg]	%unliberated
350	264.07	95.29	36.08	1375.02	380.66	27.68
212	21.41	4.75	22.21	111.49	2.42	2.17
126	38.16	7.21	18.88	198.70	3.47	1.75
89	77.19	7.98	10.34	401.93	7.57	1.88
58	120.37	58.91	48.94	626.74	8.13	1.30
23	809.03	200.70	24.81	4212.60	37.55	0.89
Total	1330.23	374.84		6926.48	439.81	

TABLE B15a

THE AMOUNT OF GOLD IN EACH PARTICLE SIZE FRACTION ASSOCIATED WITH BMS AND PYRITE FOR A HOMOGENOUS HARMONY ORE

Average particle size [µm]	BMS			Pyrite		
	Unmilled ore [µg]	Milled ore [µg]	%unliberated	Unmilled ore [µg]	Milled ore [µg]	%unliberated
350	3.42	0.69	20.08	2.41	1.62	67.10
212	12.30	86.95	100.00	8.67	18.78	100.00
126	20.67	19.92	96.33	14.56	4.87	33.41
89	14.69	11.60	78.95	10.35	0.10	0.99
58	20.16	14.30	70.94	14.20	2.61	18.39
23	99.61	36.52	36.66	70.17	12.74	18.16
Total	170.87	169.98		120.35	40.72	

TABLE B15b

THE AMOUNT OF GOLD IN EACH PARTICLE SIZE FRACTION ASSOCIATED WITH CARBONACEOUS MATERIAL AND SILICATES FOR A HOMOGENOUS HARMONY ORE

Average particle size [µm]	Carbonaceous material			Silicates		
	Unmilled ore [µg]	Milled ore [µg]	%unliberated	Unmilled ore [µg]	Milled ore [µg]	%unliberated
350	17.55	4.40	25.07	19.39	34.83	100.00
212	63.20	4.50	7.12	69.81	5.67	8.12
126	106.20	7.26	6.84	117.31	4.59	3.91
89	75.48	10.32	13.67	83.38	3.07	3.68
58	103.57	7.08	6.84	114.41	2.72	2.38
23	511.71	11.66	2.28	565.24	14.32	2.53
Total	877.71	15.09		969.54	65.20	

TABLE B16a

THE AMOUNT OF GOLD IN EACH PARTICLE SIZE FRACTION ASSOCIATED WITH BMS AND PYRITE FOR A HOMOGENOUS UNISEL ORE

Average particle size [µm]	BMS			Pyrite		
	Unmilled ore [µg]	Milled ore [µg]	%unliberated	Unmilled ore [µg]	Milled ore [µg]	%unliberated
350	94.44	215.68	100.00	158.79	306.14	100.00
212	25.54	98.61	100.00	42.95	42.25	98.37
126	44.42	53.41	100.00	74.69	43.02	57.60
89	62.23	239.56	100.00	104.63	124.31	100.00
58	78.59	62.82	79.93	132.15	95.13	71.99
23	461.07	230.97	50.09	775.22	318.89	41.14
Total	766.31	901.04		1288.43	929.74	

TABLE B16b

THE AMOUNT OF GOLD IN EACH PARTICLE SIZE FRACTION ASSOCIATED WITH CARBONACEOUS MATERIAL AND SILICATES FOR A HOMOGENOUS UNISEL ORE

Average particle size [µm]	Carbonaceous material			Silicates		
	Unmilled ore [µg]	Milled ore [µg]	%unliberated	Unmilled ore [µg]	Milled ore [µg]	%unliberated
350	107.28	222.55	100.00	217.08	197.41	90.94
212	29.02	8.71	30.00	58.71	20.82	35.47
126	50.46	1.55	3.07	102.10	10.17	9.96
89	70.69	20.71	29.29	143.04	11.98	8.38
58	89.28	11.02	12.34	180.65	18.74	10.38
23	523.75	61.37	11.72	1059.77	81.72	7.71
Total	870.47	325.90		1761.35	340.85	

TABLE B17a

THE AMOUNT OF GOLD IN EACH PARTICLE SIZE FRACTION ASSOCIATED WITH BMS AND PYRITE FOR A HOMOGENOUS BARBERTON ORE

Average particle size [µm]	BMS			Pyrite		
	Unmilled ore [µg]	Milled ore [µg]	%unliberated	Unmilled ore [µg]	Milled ore [µg]	%unliberated
350	149.70	46.61	31.14	584.95	388.04	66.34
212	54.74	86.09	100.00	213.88	83.97	39.26
126	81.32	119.54	100.00	317.77	248.22	78.11
89	126.55	215.23	100.00	494.47	731.53	100.00
58	137.78	678.89	100.00	538.35	797.63	100.00
23	963.72	2085.57	100.00	3765.00	2098.40	55.72
Total	1513.81	3231.94		5915.10	4347.80	

TABLE 7.17b

THE AMOUNT OF GOLD IN EACH PARTICLE SIZE FRACTION ASSOCIATED WITH CARBONACEOUS MATERIAL AND SILICATES FOR A HOMOGENOUS BARBERTON ORE

Average particle size [µm]	Carbonaceous material			Silicates		
	Unmilled ore [µg]	Milled ore [µg]	%unliberated	Unmilled ore [µg]	Milled ore [µg]	%unliberated
350	71.73	62.43	87.03	38.44	26.79	69.70
212	26.23	2.83	10.79	14.05	3.00	21.33
126	38.97	14.78	37.93	20.88	3.35	16.03
89	60.64	37.52	61.88	32.49	6.75	20.79
58	66.02	90.98	100.00	35.38	8.23	23.26
23	461.78	174.18	37.72	247.45	56.19	22.71
Total	725.36	382.72		388.69	104.31	

TABLE B18a

THE AMOUNT OF GOLD IN EACH PARTICLE SIZE FRACTION ASSOCIATED WITH BMS AND PYRITE FOR A HOMOGENOUS FSG ORE

Average particle size [µm]	BMS			Pyrite		
	Unmilled ore [µg]	Milled ore [µg]	%unliberated	Unmilled ore [µg]	Milled ore [µg]	%unliberated
350	12.48	7.46	59.72	10.50	5.95	56.69
212	141.43	83.65	59.13	119.03	67.79	56.95
126	251.74	152.88	60.73	211.81	134.67	63.58
89	218.46	109.20	49.99	183.80	120.67	65.65
58	201.81	112.40	55.70	169.80	123.88	72.96
23	1254.56	770.15	61.39	1055.56	874.83	82.88
Total	2080.53	1235.74		1750.51	1327.80	

TABLE B18b

THE AMOUNT OF GOLD IN EACH PARTICLE SIZE FRACTION ASSOCIATED WITH CARBONACEOUS MATERIAL AND SILICATES FOR A HOMOGENOUS FSG ORE

Average particle size [µm]	Silicates		
	Unmilled ore [µg]	Milled ore [µg]	%unliberated
350	3.57	0.89	24.94
212	40.46	17.10	42.26
126	72.00	34.30	47.64
89	62.48	60.61	97.00
58	57.72	35.05	60.73
23	358.81	67.29	18.76
Total	595.04	215.25	

T[illegible]

THE AMOUNT OF GOLD IN EACH PARTICLE SIZE FRACTION ASSOCIATED WITH BMS AND PYRITE FOR A HOMOGENOUS WDL ORE

Average particle size [µm]	BMS			Pyrite		
	Unmilled ore [µg]	Milled ore [µg]	%unliberated	Unmilled ore [µg]	Milled ore [µg]	%unliberated
350	13.58	8.77	64.57	20.96	10.92	52.11
212	59.98	40.34	67.26	92.58	62.50	67.51
126	144.86	110.16	76.04	223.58	165.07	73.83
89	109.78	106.84	97.32	169.43	142.56	84.14
58	102.99	126.60	100.00	158.95	170.22	100.00
23	700.55	779.88	100.00	1081.23	1077.99	99.70
Total	1131.75	1172.59		1746.74	1629.26	

TABLE B19b

THE AMOUNT OF GOLD IN EACH PARTICLE SIZE FRACTION ASSOCIATED WITH CARBONACEOUS MATERIAL AND SILICATES FOR A HOMOGENOUS WDL ORE

Average particle size [µm]	Silicates		
	Unmilled ore [µg]	Milled ore [µg]	%unliberated
350	7.15	1.20	16.77
212	31.58	5.83	18.46
126	76.27	20.63	27.05
89	57.80	20 51	35.48
58	54.22	40.20	74.15
23	368.83	196.97	53.40
Total	595.84	285.34	

APPENDIX C

ADDISIONAL GRAPHS

APPENDIX C

ADDISIONAL GRAPHS

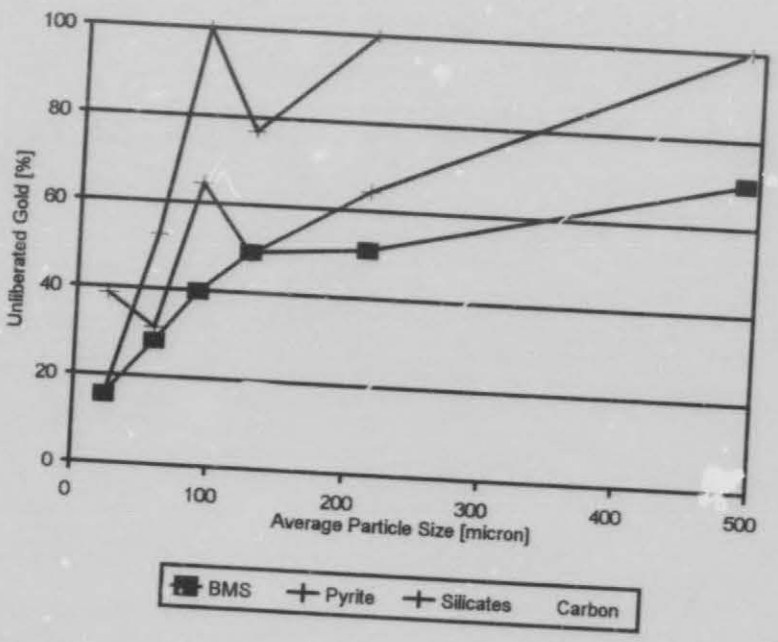

FIGURE C1: THE FRACTION OF GOLD IN EACH PARTICLE SIZE FRACTION ASSOCIATED WITH DIFFERENT MINERALS FOR A HOMOGENOUS KINROSS ORE.

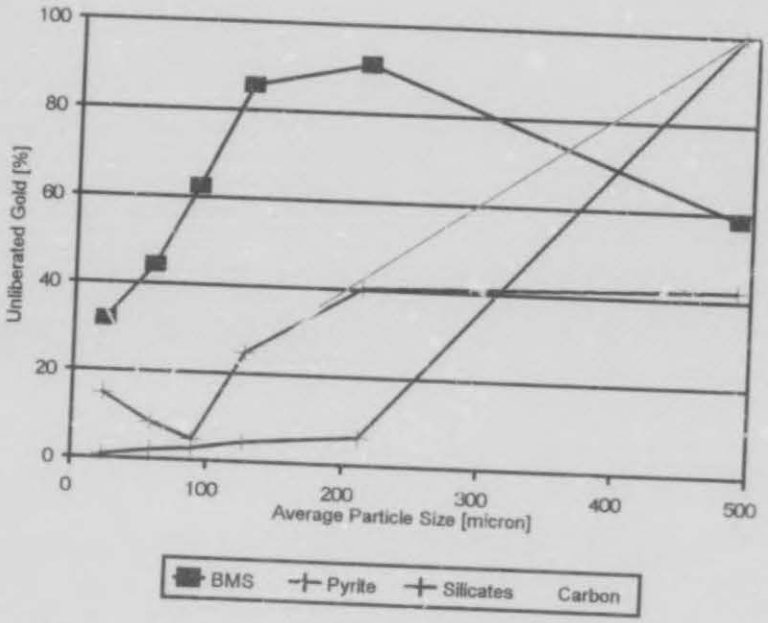

FIGURE C2: THE FRACTION OF GOLD IN EACH PARTICLE SIZE FRACTION ASSOCIATED WITH DIFFERENT MINERALS FOR A HOMOGENOUS LESLIE ORE.

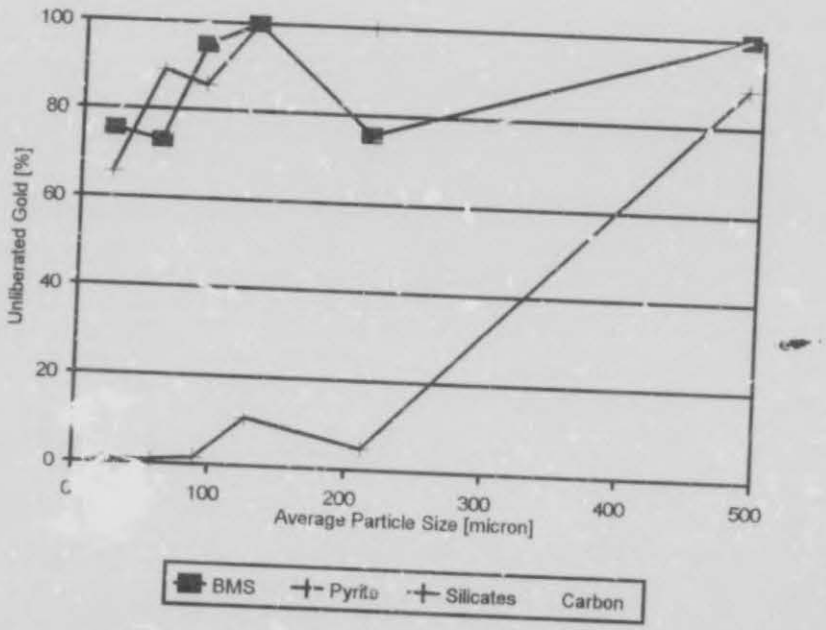

FIGURE C3: THE FRACTION OF GOLD IN EACH PARTICLE SIZE FRACTION ASSOCIATED WITH DIFFERENT MINERALS FOR A HOMOGENOUS BEATRIX ORE.

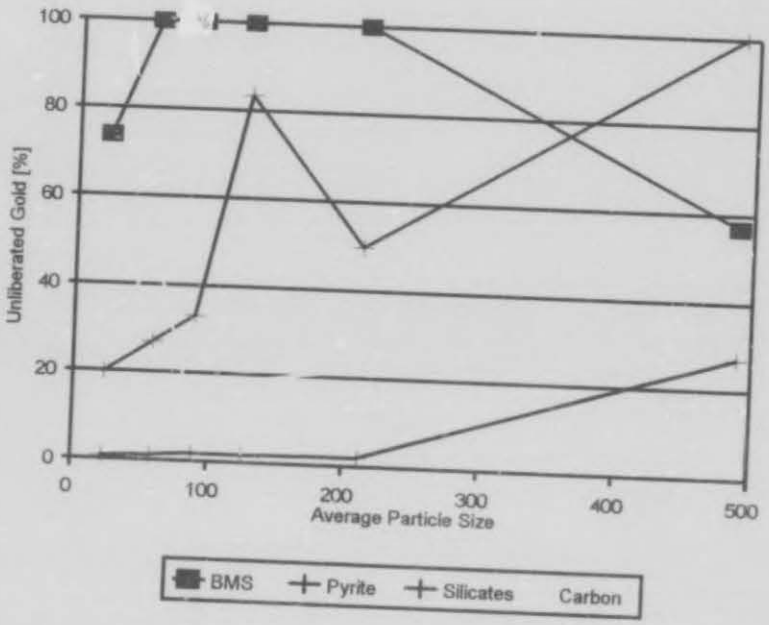

FIGURE C4: THE FRACTION OF GOLD IN EACH PARTICLE SIZE FRACTION ASSOCIATED WITH DIFFERENT MINERALS FOR A HOMOGENOUS St. HELENA ORE.

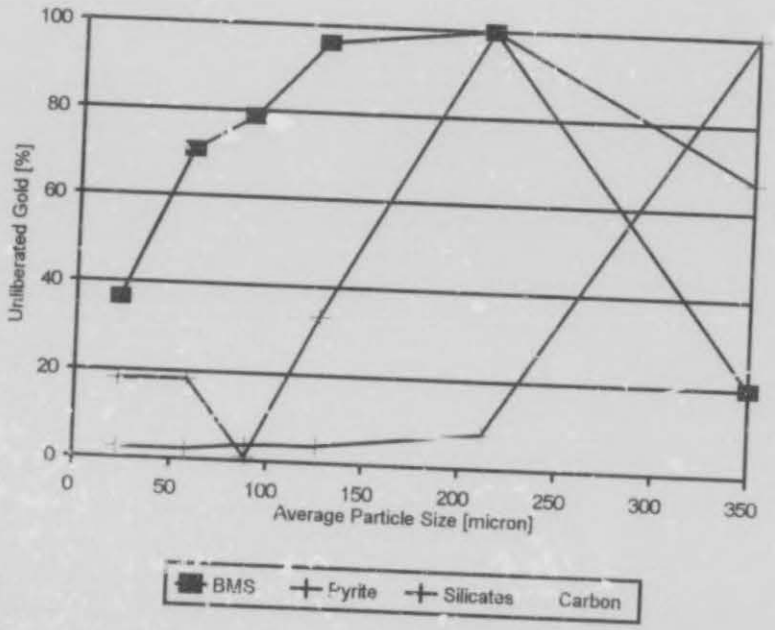

FIGURE C5: THE FRACTION OF GOLD IN EACH PARTICLE SIZE FRACTION ASSOCIATED WITH DIFFERENT MINERALS FOR A HOMOGENOUS HARMONY ORE.

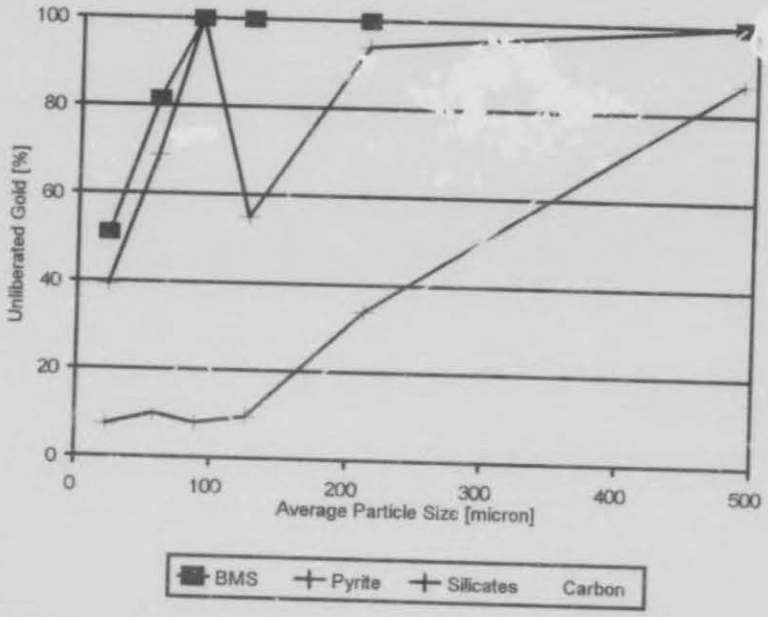

FIGURE C6: THE FRACTION OF GOLD IN EACH PARTICLE SIZE FRACTION ASSOCIATED WITH DIFFERENT MINERALS FOR A HOMOGENOUS UNISEL ORE.

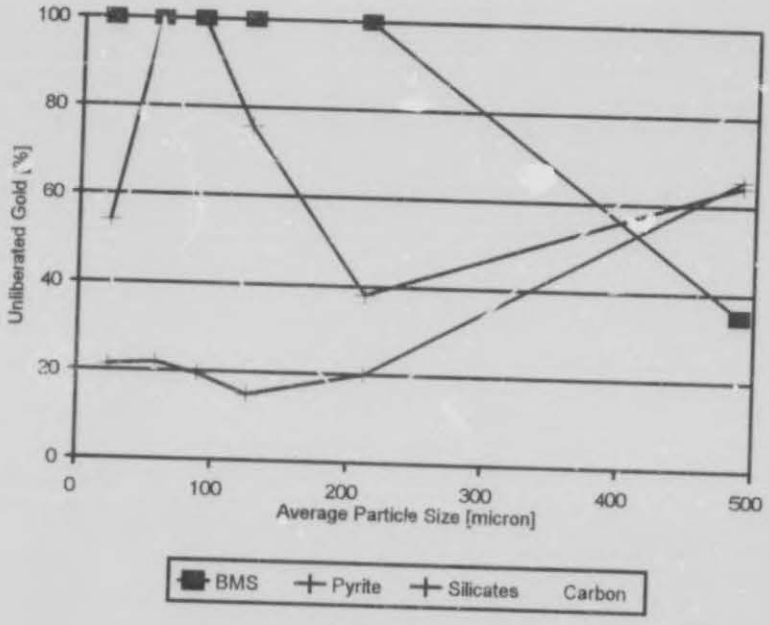

FIGURE C7: THE FRACTION OF GOLD IN EACH PARTICLE SIZE FRACTION ASSOCIATED WITH DIFFERENT MINERALS FOR A HOMOGENOUS BARBERTON ORE.

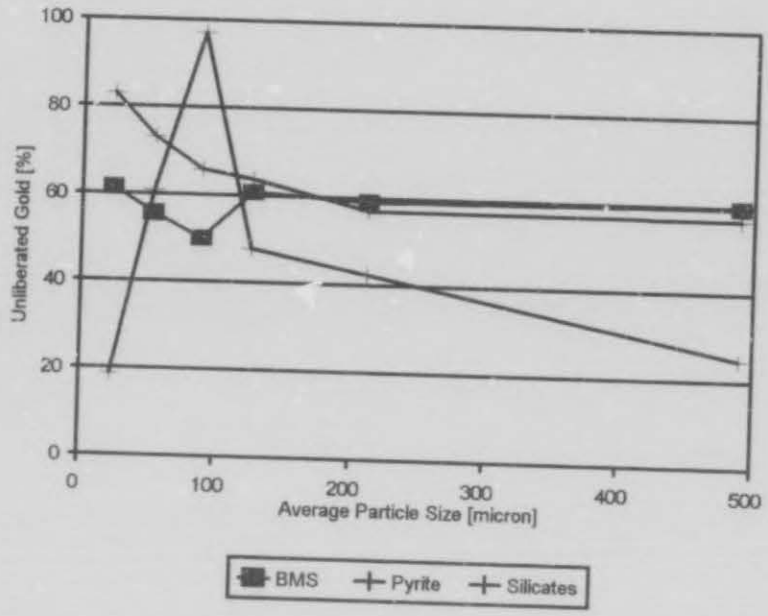

FIGURE C8: THE FRACTION OF GOLD IN EACH PARTICLE SIZE FRACTION ASSOCIATED WITH THEN DIFFERENT MINERALS FOR A HOMOGENOUS FSG ORE.

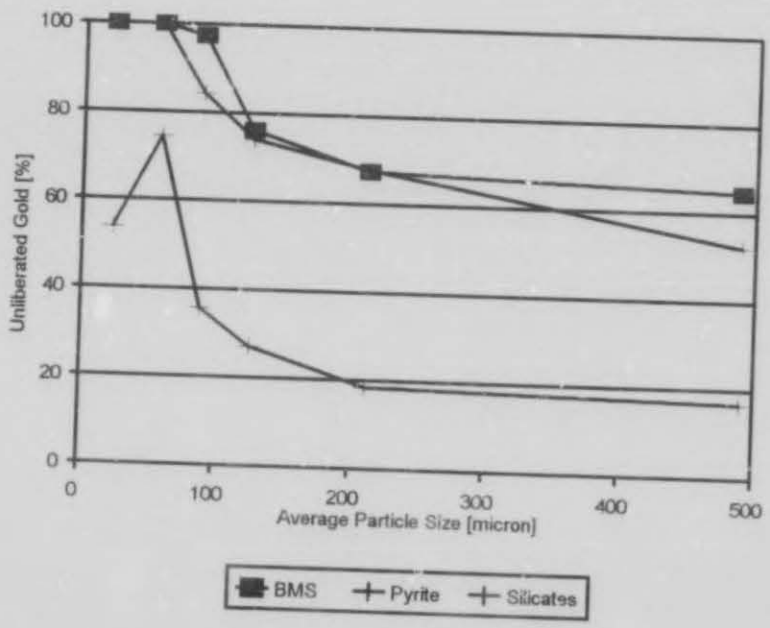

FIGURE C9: THE AMOUNT OF GOLD IN EACH PARTICLE SIZE FRACTION ASSOCIATED WITH DIFFERENT MINERALS FOR A HOMOGENOUS WDL ORE.

APPENDIX D

TURBO PASCAL PROGRAMMES

```
Program Kingmodel;
uses crt;

   var
     x,dp,Vt,B,mhum1,mhum2,mhum3,mhum4,ave1,ave2,
     ave3,ave4,z,sum,k,m                                  :real;
     V,D,L                                                :array [1..6] of real;
     LL                                                   :array [1..6] of real;
     Fmel,xx,Fm                                           :array [1..6] of real;
     P1,P2,P3,P4,P,mhu1,mhu2,mhu3,mhu4,R,
     av1,av2,av3,av4                                      :array [1..6] of real;
     Du                                                   :array [1..6] of real;
     a                                                    :integer;


   Procedure Invoer;

     Begin
       d[1]:=490;
       d[2]:=212;
       d[3]:=126;
       d[4]:=89;
       d[5]:=58;
       d[6]:=23;

       Du[1]:=800;
       Du[2]:=300;
       Du[3]:=150;
       Du[4]:=106;
       Du[5]:=75;
       Du[6]:=53;

       R[1]:=800/300;
       R[2]:=300/150;
       R[3]:=150/106;
       R[4]:=106/75;
       R[5]:=75/53;
       R[6]:=53/45;

       z:=0.01;
       k:=2;
       m:=2;
       {PP:=1;}
       LL[1]:=94.43;
       LL[2]:=5.200;
       LL[3]:=3.500;
       LL[4]:=1.780;
       LL[5]:=1.000;
       LL[6]:=0.780;

       end;


   Procedure Bereken;
    Begin

       {Sum:=LL[1]+LL[2]+LL[3]+LL[4]+LL[5]+LL[6];

       L[5]:=1-LL[6]/sum;
       L[4]:=-LL[5]/sum+L[5];
       L[3]:=-LL[4]/sum+L[4];
       L[2]:=-LL[3]/sum+L[3];
       L[1]:=-LL[2]/sum+L[2];}
```

```
   L[1]:=(100-LL[1])/100;
   L[2]:=(100-LL[2])/100;
   L[3]:=(100-LL[3])/100;
   L[4]:=(100-LL[4])/100;
   L[5]:=(100-LL[5])/100;
   L[6]:=(100-LL[6])/100;

end;

Procedure King;
 Begin

   For a:=1 to 6 do
   Begin
    mhu1[a]:=50;
    mhu2[a]:=10;
    mhu3[a]:=0.1;
    mhu4[a]:=800;

    Repeat
      P1[a]:=2*mhu1[a]/D[a]/D[a]*(mhu1[a]-(mhu1[a]+D[a])*exp(-D[a]/mhu1[a
      mhu1[a]:=mhu1[a]+z;
     {writeln(mhu1[a]:8:4,'    ',P1[a]:8:4,'    ',L[a]:8:4,'  ',a);}

    Until abs(P1[a]-L[a])<=0.001;
      mhu2[a]:=mhu2[a]-z;

    Repeat
     P2[a]:=1-D[a]/(2*mhu2[a]+D[a])*(1-exp(-2-D[a]/mhu2[a])){+10*exp(-3*D
     mhu2[a]:=mhu2[a]+z;
     {writeln(mhu2[a]:8:4,'    ',P2[a]:8:4,'    ',L[a]:8:4,'  ',a);}
    Until abs(P2[a]-L[a])<=0.001;
     mhu1[a]:=mhu1[a]-z;

    Repeat
     B:=R[a]*R[a]+sqrt(2)*Du[a]/mhu3[a];
     P3[a]:=1+sqrt(2)*Du[a]*(1-B-exp(-B))/(mhu3[a]*B*B);
     mhu3[a]:=mhu3[a]+z;
    {writeln(mhu3[a]:8:4,'    ',P3[a]:8:4,'    ',L[a]:8:4,'  ',a);}
    Until abs(P3[a]-L[a])<=0.001;
     mhu3[a]:=mhu3[a]-z;

    Repeat

     {P4[a]:=1-0.865*D[a]/mhu4[a]+D[a]/(2*mhu4[a]+k*D[a])*(-1+exp(-2-k*D[
     mhu4[a]:=mhu4[a]+z;}
     P4[a]:=1-4*D[a]/mhu4[a]-2*D[a]/(k*mhu4[a])*(exp(-k)-1)-2/m*(exp(-m*D
     *(-1+exp(-k-m*D[a]/mhu4[a]));
     mhu4[a]:=mhu4[a]+z;
     {writeln(mhu4[a]:8:4,'    ',P4[a]:8:4,'    ',L[a]:8:4,'  ',a);}
    Until abs(P4[a]-L[a])<=0.001;
     mhu4[a]:=mhu4[a]-z;


 end;

mhum1:=(mhu1[1]+mhu1[2]+mhu1[3]+mhu1[4]+mhu1[5]+mhu1[6])/6;
mhum2:=(mhu2[1]+mhu2[2]+mhu2[3]+mhu2[4]+mhu2[5]+mhu2[6])/6;
mhum3:=(mhu3[1]+mhu3[2]+mhu3[3]+mhu3[4]+mhu3[5]+mhu3[6])/6;
```

```
        mhum4:=(mhu4[1]+mhu4[2]+mhu4[3]+mhu4[4]+mhu4[5]+mhu4[6])/6;

        For a:=1 to 6 do
         begin
          av1[a]:=(-mhum1+mhu1[a])/mhum1*100;
          av2[a]:=(-mhum2+mhu2[a])/mhum2*100;
          av3[a]:=(-mhum3+mhu3[a])/mhum3*100;
          av4[a]:=(-mhum4+mhu4[a])/mhum4*100;
          P[a]:=1-D[a]/(2*mhum2+D[a])*(1-exp(-2-D[a]/mhum2));

         end;
        ave1:=(abs(av1[1])+abs(av1[2])+abs(av1[3])+abs(av1[4])+abs(av1[5])+abs
        ave2:=(abs(av2[1])+abs(av2[2])+abs(av2[3])+abs(av2[4])+abs(av2[5])+abs
        ave3:=(abs(av3[1])+abs(av3[2])+abs(av3[3])+abs(av3[4])+abs(av3[5])+abs
        ave4:=(abs(av4[1])+abs(av4[2])+abs(av4[3])+abs(av4[4])+abs(av4[5])+abs
        end;

    Procedure Afvoer;

    begin
     writeln('King Model');
     writeln('');
     writeln('mhu1':8,'ave1 %':8,'mhu2':8,'ave2 %':8,'mhu3':8,'ave3 %':8,'mhu
     writeln('');
     For a:=1 to 6 do
     writeln(mhu1[a]:8:2,av1[a]:8:2,mhu2[a]:8:2,av2[a]:8:2,mhu3[a]:8:2,av3[a]
     writeln('');
     writeln(mhum1:8:2,ave1:8:2,mhum2:8:2,ave2:8:2,mhum3:8:2,ave3:8:2,mhum4:8
     writeln('');
     writeln('');
    end;


Begin
  clrscr;
  Invoer;
  Bereken;
  King;
  Afvoer;
  Readln;
End.
```

```
Program HsihWenmodel;
uses crt;

   var

     LL,L,Fk,P,dd,D,K,Fk2,dd2,k2,P2,dev,dev2          :array [1..6] of real;
     Du,R                                             :array [1..7] of real;
     a                                                :integer;
     ave,ave2,devm,devm2                              :real;


   Procedure Invoer;
     Begin

       d[1]:=490;
       d[2]:=212;
       d[3]:=126;
       d[4]:=89;
       d[5]:=58;
       d[6]:=23;

       Du[1]:=800;
       Du[2]:=300;
       Du[3]:=150;
       Du[4]:=106;
       Du[5]:=75;
       Du[6]:=53;
       Du[7]:=10;

       R[1]:=800/300;
       R[2]:=300/150;
       R[4]:=150/106;
       R[5]:=106/75;
       R[6]:=75/53;
       R[7]:=53/10;


       LL[1]:=90.94;
       LL[2]:=35.47;
       LL[3]:=9.960;
       LL[4]:=8.380;
       LL[5]:=8.000;
       LL[6]:=7.710;


      end;


   Procedure Bewerking;
    Begin

      L[1]:=(100-LL[1])/100;
      L[2]:=(100-LL[2])/100;
      L[3]:=(100-LL[3])/100;
      L[4]:=(100-LL[4])/100;
      L[5]:=(100-LL[5])/100;
      L[6]:=(100-LL[6])/100;

    end;


   Procedure Wen1;
      Begin
```

```
      For a:=1 to 6 do
       begin
        dd[a]:=0.1;
        k[a]:=D[a]/dd[a];
        P[a]:=0;
         Repeat
          FK[a]:=P[a]*(K[a]*K[a]*K[a]-(K[a]-2)*(K[a]-2)*(K[a]-2))/(K[a]*K[a]
          (1-P[a])*(K[a]*K[a]*K[a]-(K[a]-1)*(K[a]-1)*(K[a]-1))/(K[a]*K[a]*K[
          dd[a]:=dd[a]+0.01;
          k[a]:=D[a]/dd[a];
          {writeln(dd[a]:4:4, '    ',FK[a]:8:6,'    ',L[a]:8:4,'    ',a:2);}

         Until abs(FK[a]-L[a])<=0.001;
          dd[a]:=dd[a]-0.01;
        end;

     ave:=(dd[1]+dd[2]+dd[3]+dd[4]+dd[5]+dd[6])/6;
     devm:=0;
     For a:=1 to 6 do
      begin
      dev[a]:=(ave-dd[a])/ave*100;
      devm:=abs(dev[a])+devm;
      end;
     devm:=devm/6;
    End;

  Procedure Wen2;
     Begin

      For a:=1 to 6 do
       begin
        dd2[a]:=0.1;
        k2[a]:=D[a]/dd2[a];
        P2[a]:=1;
         Repeat
          FK2[a]:=P2[a]*(K2[a]*K2[a]*K2[a]-(K2[a]-2)*(K2[a]-2)*(K2[a]-2))/(K
          (1-P2[a])*(K2[a]*K2[a]*K2[a]-(K2[a]-1)*(K2[a]-1)*(K2[a]-1))/(K2[a]
          dd2[a]:=dd2[a]+0.01;
          k2[a]:=D[a]/dd2[a];
          {writeln(dd[a]:4:4, '    ',FK[a]:8:6,'    ',L[a]:8:4,'    ',a:2);}

         Until abs(FK2[a]-L[a])<=0.001;
          dd2[a]:=dd2[a]-0.01;
        end;

     ave2:=(dd2[1]+dd2[2]+dd2[3]+dd2[4]+dd2[5]+dd2[6])/6;
     devm2:=0;
     For a:=1 to 6 do
      begin
      dev2[a]:=(ave2-dd2[a])/ave2*100;
      devm2:=abs(dev2[a])+devm2;
      end;
     devm2:=devm2/6;
    End;


Procedure Afvoer;
 Begin
  writeln('');
  writeln('Fk':8,'L':8,'P':8,'dd':8,'dev %':8);
  writeln('');
  For a:=1 to 6 do
```

```
    writeln(Fk[a]:8:4,L[a]:8:4,P[a]:8:2,dd[a]:8:2,dev[a]:8:2);
   writeln('');
   writeln(ave:32:2,devm:8:2);
   writeln('');
   For a:=1 to 6 do
    writeln(Fk2[a]:8:4,L[a]:8:4,P2[a]:8:2,dd2[a]:8:2,dev2[a]:8:2);
   writeln('');
   writeln(ave2:32:2,devm2:8:2);
   writeln('');



  End;


BEGIN
  clrscr;
  Invoer;
  Bewerking;
  Wen1;
  Wen2;
  Afvoer;
  Readln;
END.
```

END OF ROLL

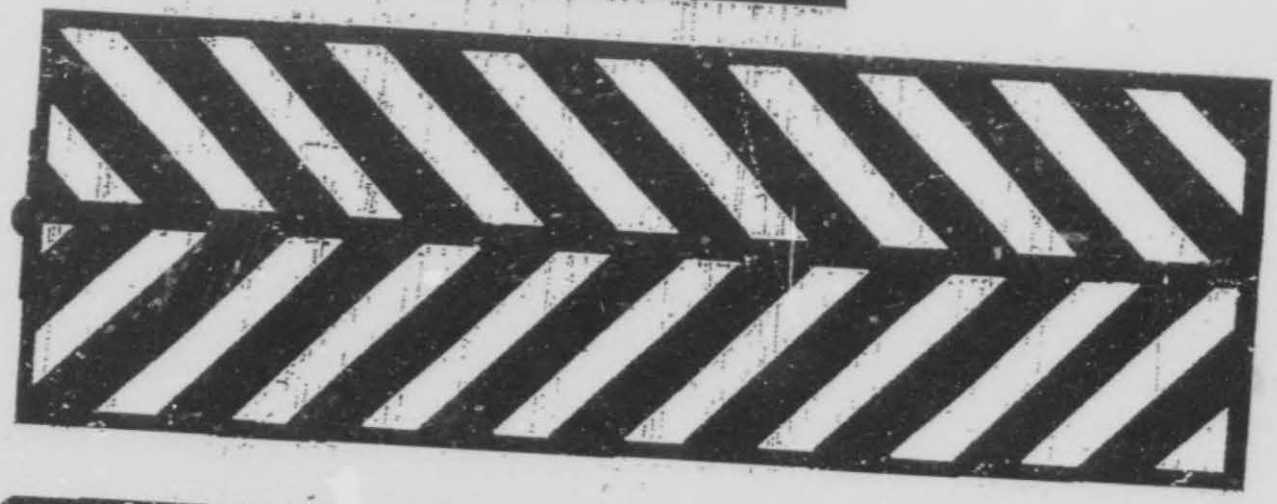

M.G.X.

ROLL NO.